



universidad
de león

FACULTAD DE CIENCIAS BIOLÓGICAS Y AMBIENTALES
INSTITUTO DE INVESTIGACIÓN DE LA VIÑA Y EL VINO
INSTITUTO DE BIOTECNOLOGÍA DE LEÓN (INBIOTEC)

**DEVELOPMENT OF MICROBIAL TECHNOLOGIES FOR THE SOLUBLE
PHOSPHORUS PRODUCTION BY PHOSPHATE ROCK SOLUBILIZATION**

DESARROLLO DE TECNOLOGÍAS MICROBIANAS PARA LA
PRODUCCIÓN DE FÓSFORO SOLUBLE POR SOLUBILIZACIÓN DE ROCA
FOSFÓRICA

ANA MARÍA IBÁÑEZ SÁNCHEZ

LEÓN 2021

Memoria presentada por **Ana Ibáñez Sánchez**
para optar al grado de Doctor en Biología Molecular y Biotecnología



universidad
de león



esDule
Escuela de Doctorado
de la Universidad de León

INFORME DE LOS DIRECTORES DE LA TESIS

Los Doctores D. Juan José Rubio Coque, y el Dr. D. Carlos Barreiro Méndez, como Directores de la Tesis Doctoral titulada **“Development of microbial technologies for the soluble phosphorus production by phosphate rock solubilization” / “Desarrollo de tecnologías microbianas para la producción de fósforo soluble por solubilización de roca fosfórica”** realizada por **Dña. Ana María Ibáñez Sánchez** en el programa de doctorado Biología Molecular y Biotecnología, informa favorablemente el depósito de la misma, dado que reúne las condiciones necesarias para su defensa.

Lo que firmo, en León a 31 de mayo de 2021.

Fdo. Dr. Juan José Rubio Coque

Fdo. Dr. Carlos Barreiro Méndez

Por conducirme hasta el día de hoy.

Por ser parte de quién soy.

A mi familia.

Decía Quilón en uno de sus discursos que “*si confieres un beneficio, nunca lo recuerdes; si lo recibes, nunca lo olvidas*”. En mi caso, son tantas las personas a la que agradecer haberme traído hasta el día de hoy, que espero no olvidar a ninguna.

En primer lugar, quiero expresar mi agradecimiento a la **Junta de Castilla y León**, por otorgarme una ayuda para contratos predoctorales 2017 (orden EDU/529/017), adscrita al proyecto de investigación “Desarrollo de Tecnologías Microbianas para la producción de fósforo soluble por solubilización de roca fosfórica), financiado por la empresa Agroquimes S.A. Gracias, también, a la **Universidad de León**, por su “ayuda a la movilidad para la realización de estancias breves en otro centro de investigación”, así como al departamento de Microbiología, por el apoyo administrativo y por permitirme colaborar con labores de docencia a lo largo de todo el periodo de Tesis Doctoral. Me gustaría, también, agradecer al **Instituto de la Viña y el Vino** por recibirme y ofrecerme la oportunidad de desarrollar este trabajo durante estos años. Además, me gustaría dar las gracias al Instituto de Biotecnología de León (**INBIOTEC**) por la colaboración durante la Tesis Doctoral, permitiéndome realizar todos los ensayos de proteómica, así como cualquier apoyo que he necesitado.

Al Dr. Juan José Rubio Coque, tutor y director de esta Tesis, me gustaría agradecerle, en primer lugar, la oportunidad de realizar un Doctorado e incorporarme a su grupo de investigación. **Juanjo**, muchas gracias por tu ayuda y enseñanzas durante todo este tiempo. Gracias por dar siempre lo mejor de ti, y por compartir conmigo tu parte más humana y tu parte más profesional.

Al Dr. Carlos Barreiro Méndez, codirector de esta Tesis, porque si alguien me condujo a este proyecto fuiste tú. Gracias, **Carlos**, por tenerme en cuenta, por exigirme siempre, por hacerme trabajar más, trabajar mejor. Gracias por las risas y por poner la banda sonora a mis largas horas de laboratorio, tu buen gusto musical compensa tu pésimo criterio cinematográfico.

Gracias de corazón, a los dos, por confiar en mí y por darme la oportunidad de aprender de vosotros durante todo este tiempo. Sé que no podría haber estado en mejores manos. Seguí dejándome boquiabierto con todo lo que sabéis, con toda vuestra pasión por la ciencia (que ojalá no perdáis nunca, a pesar de que este país os empuje a ello) y con toda vuestra humanidad. No tengo más que palabras de agradecimiento y admiración hacia ambos, y espero que nuestros caminos vuelvan a juntarse en algún momento.

No puedo olvidarme de todos mis compañeros del **Instituto de Investigación de la Viña y el Vino**, los que siguen y los que se fueron. Gracias Rebeca y Carla, por esos cafés en el laboratorio y esas cañas fuera de él. Gracias Jose, Sandra y Ana. Gracias a todos los que pasasteis (más o menos tiempo) en laboratorio conmigo: Olego, Jesús, Mario, Jorge, Jaime, “desca”, Dani, Marina... Un gracias muy especial a mi queridísima Alba. Gracias por esas risas, por estar como una regadera y hacer que cada día de mierda se convirtiese en una fiesta,

que 12 horas trabajando no pesaran, que trabajar fuera divertido. Gracias por las cenas, por las cervezas, por el terraceo... gracias incluso por traer a Raquel a mi vida, que aún con sus malas pulgas, se hace querer.

Gracias a toda la familia de **INBIOTEC**, por sembrar en mí el amor por la microbiología hace unos años. Gracias a todos por ayudarme en todo lo que he necesitado hasta el día de hoy, y por hacerlo siempre con una sonrisa en la cara: a Rosma, por ser mi tutora de TFG y permitirme iniciar este viaje, a Carlos (lo siento, paso de lo de Charly), por acogerme bajo tu ala desde el minuto cero y estar disponible 24/7 (excepto cuando juegas al escondite por el edificio), a Antonio, por compartir conmigo una pequeña parte de todos tus conocimientos de bioinformática. Gracias Clara, por toda tu ayuda con el HPLC. Gracias Josefina y Berna, os culpo de mis altas expectativas en cuanto a la opinión de lo que un técnico debe ser. Gracias a todo el equipo y a los que ya no están en él: Alex, Laura, Inés, Alexia, Esmeralda, Óscar, Mariana, Eva, Ana... y todos los demás, ¡que sois muchos!

Along my PhD, I had the opportunity to carry out a scientific international stay. I would like to thank the host institution **UMCG** (University Medical Center Groningen) for having me and for their assistance throughout the stay. I am particularly grateful to Professor Jan Maarten van Dijl, professor of the Department of Medical Microbiology. Thanks to the labmates who made that experience one of the happiest in my life. Gracias Rocío por tu supervisión dentro del laboratorio y por tu amistad fuera de él. Gracias Marina, por ser casa cuando más lo necesitaba, y por seguir siendo risas después de todos estos meses. Thanks to Aysegül, for becoming a real friend in Groningen, thanks for the dinners and the dances, and thanks for the company every weekend in the lab. Thanks, Bimal and Praygi, for always being kind to me in a foreign land. Thanks to all of you: Sjouke, Jolanda, Mafalda, Elisa, Rita, Marines, YanYan, Francis, Alisa, Iris... you all are amazing, and I'll be waiting for you in Spain!

Quiero dar las gracias a todos los que, desde siempre, me han apoyado y han creído en mí. Porque soy lo que ellos han hecho de mí: lo que me han enseñado y lo que me han dado.

Gracias **Alba e Inés**, por todo. Porque no tengo recuerdos de antes de vosotras. Porque, aunque nos hallamos separado, seguís conmigo, celebrando y poniendo el hombro cuando hace falta. A **Facu y Rober**, porque fuisteis el mejor apoyo en la tesis fuera del labo (o al menos lo intentasteis). De nuevo a **Alba**, porque eres compañera, vecina, amiga... ¡porque eres familia! A **Laura**, por tus podcasts por WhatsApp que siempre me hacen reír hasta llorar, por toda tu ayuda en INBI y por todos los recuerdos vividos juntas. Gracias a los fichajes que llegasteis más tarde, pero sois incondicionales. Gracias **Vir, Virgi, Diego y Julio** por esas comidas y cenas de fin de semana que hacen que la semana se pase volando pensando en juntarnos. Y un gracias especial, Julio, por cederme esa magnífica foto para la portada de mi tesis.

Gracias a mis mayores apoyos: los telerines. Gracias a todos y cada uno de vosotros, porque, para bien o para mal, os debo todo lo que soy. Gracias **papá y mamá** por ser increíbles. Gracias por enseñarme el valor del

esfuerzo, por ponernos siempre a Vega y a mí por delante de todo, y por hacernos creer capaces de cualquier cosa. Gracias por dejarme equivocarme, por enseñarme a soñar, por ayudarme a levantarme. Nunca podré agradeceros todo lo que os debo. Gracias papá por enseñarme a reírme de todo en la vida, por muy dura que sea la situación. Gracias mamá por estar siempre pendiente de todo, por llamarme todo el día (tanto que a veces ni te conteste), por hacer que llegara hasta aquí. Gracias, **Vega**. Por todo. Por ser el lado artístico que nunca tuve, por ser siempre ejemplo de generosidad, de amor y de sensibilidad. Porque si hoy estoy aquí te lo debo a ti más que a nadie, aunque a estas alturas a lo mejor te planteas que hubiera molado más el perro que la hermana. Gracias por ayudarme a entender cómo quiero ser y cómo no quiero ser (aunque a veces me cueste). No olvides que, aunque me cueste decírtelo, y aunque no siempre estemos de acuerdo, eres la persona más importante de mi vida. Gracias **Tiana y Tio Luismi**, por toda vuestra ayuda en esta Tesis y en cada cosa que os he pedido (que han sido muchas). Gracias por ser uno de mis mayores apoyos. Gracias por enseñarme mi lado más racional y por ser dos de mis grandes ejemplos a seguir. Gracias **abu**, simplemente por ser como eres. Siento darte estos disgustos y siempre querer saber más, estudiar más, trabajar más. Pero si puedo hacerlo es gracias a esos platos que siempre tenías preparados en la mesa cuando salía del cole y esos tupperes ya en la universidad. ¡Menos mal de ellos! Si no, “¡qué sería de mí ahora!” , como siempre dices tú. Gracias a todos los telerines por hacer de mí lo que soy hoy. Espero que algún día podáis estar la mitad de orgullosos de mí de lo que yo lo estoy de cada uno de vosotros.

Gracias a todos mis catalanes. Gracias **avi**, por darme tu cabezonería (aunque no siempre sea algo bueno), y gracias **yaya**, por darme tu humor andaluz.

Y, por último, a mi otro gran apoyo: **Suso**. Gracias por todo tu amor y comprensión. Gracias por creer en mí incluso cuando ni siquiera yo lo hacía. Gracias por todo lo vivido, porque después de tantos años, sigues enseñándome lo mejor y lo peor de mí (y sigues a mi lado a pesar de ello). Gracias por tu paciencia, por soportarme en mis peores momentos, por hacerme reír, por ser mi amigo, mi compañero y mi familia. Gracias por ponerme tan fácil quererte.

A todos, gracias por ser parte de mí.

*“If I have seen farther than others, it is because
I have stood on the shoulders of giants”*

*“Si he logrado ver más lejos ha sido porque he
subido a hombros de gigantes”*

Isaac Newton (1643 – 1727)

Table of Contents

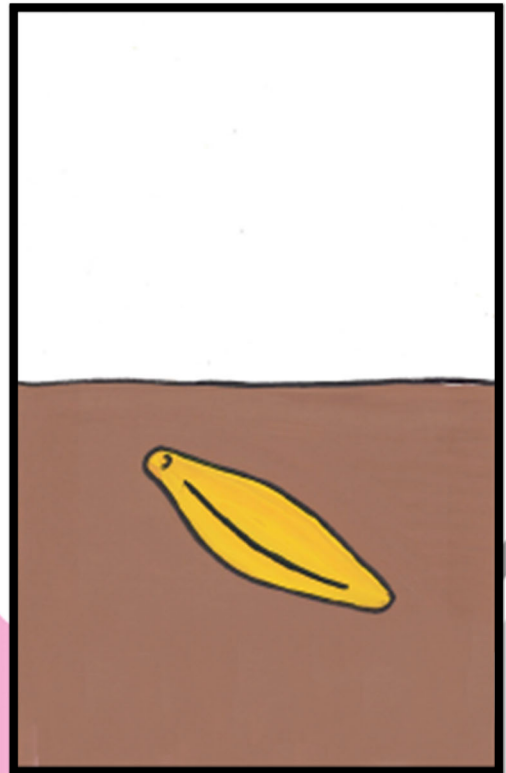
| | |
|---|-----------|
| Summary / Resumen | 1 |
| Introduction | 9 |
| I. Phosphorus's natural cycle. Why phosphorus? | 11 |
| II. Phosphorus: the big problem | 12 |
| III. Phosphorus in plants | 13 |
| IV. Phosphorus's industrial cycle | 15 |
| IV.I. Phosphorus mining from phosphate rock | 16 |
| IV.I.I. Biomining, bioleaching and sulphur-oxidizing bacteria (SOB) | 17 |
| IV.I.II. <i>Acidithiobacillus</i> spp. and biomining: what is known and what is not | 20 |
| IV.II. Phosphorus in agriculture: P-based fertilizer production and their application in crops | 22 |
| IV.II.I. Bio-fertilizers and plant growth-promoting rhizobacteria | 24 |
| V. Sulphur: commodity or waste? | 28 |
| Objectives | 31 |
| Chapter 1. Isolation, identification and selection of sulphur-oxidizing bacteria for phosphorus solubilization from phosphate rock schlams | 35 |
| 1. Introduction | 37 |
| 2. Material and methods | 38 |
| 2.1 Isolation and selection of sulphur-oxidizing bacteria | 38 |
| 2.2 Identification of SOBs | 38 |
| 2.3 Analysis of schlams from phosphate rock (PR) | 40 |
| 2.4 Phosphate solubilization in liquid medium | 40 |
| 2.5 Bioleaching experiments of phosphate rock schlams at lab-scale | 42 |
| 2.5.1 Mini-dump in-vitro assays | 42 |
| 2.5.2. P recovery from phosphate rock schlams in trays assay | 43 |
| 2.6. <i>A. thiooxidans</i> P-solubilization in dump assay..... | 43 |
| 3. Results and discussion | 45 |
| 3.1. Isolation and selection of SOB | 45 |
| 3.2 Identification of SOB | 45 |
| 3.3. Determination of P-content of phosphate rock schlams | 46 |

| | |
|---|-----------|
| 3.4. P solubilization from schlams in liquid medium | 48 |
| 3.5. Bioleaching experiments of phosphate rock schlams at lab-scale | 50 |
| 3.5.1. Mini-dump in-vitro assays | 50 |
| 3.5.2. Solubilization of phosphate rock schlams in trays | 56 |
| Chapter 2. Molecular study of <i>Acidithiobacillus thiooxidans</i> SOB3 | 59 |
| 1. Introduction | 61 |
| 2. Material and methods | 62 |
| 2.1. <i>A. thiooxidans</i> 16S rRNA gene copies quantification..... | 62 |
| 2.1.1. DNA isolation | 62 |
| 2.1.2. 16S rRNA gene copies quantification by Southern Blotting | 63 |
| 2.2. <i>A. thiooxidans</i> growth determination by quantitative PCR (q-PCR) | 66 |
| 2.3. <i>A. thiooxidans</i> genome sequencing | 67 |
| 2.4. Determination of the pH stress conditions in <i>A. thiooxidans</i> by reverse transcription PCR (RT-PCR) | 67 |
| 2.5. <i>A. thiooxidans</i> SOB3 proteome analysis under pH stress by 2-D DIGE analysis | 71 |
| 2.5.1. Preparation of <i>A. thiooxidans</i> protein extracts | 71 |
| 2.5.2. Protein concentration quantification by Bradford assay | 72 |
| 2.5.3. 1D: SDS-PAGE (sodium dodecyl sulphate-polyacrylamide gel electrophoresis) | 73 |
| 2.5.4. Colloidal Coomassie staining method | 75 |
| 2.5.5. 2D protein electrophoresis | 75 |
| 2.5.6 2D DIGE analysis | 77 |
| 3. Results and discussion | 82 |
| 3.1. <i>A. thiooxidans</i> growth determination by qPCR | 82 |
| 3.1.1. Standard curve | 83 |
| 3.1.2. <i>A. thiooxidans</i> growth curve | 84 |
| 3.2. <i>A. thiooxidans</i> SOB3 genome analysis | 88 |
| 3.3. <i>A. thiooxidans</i> protein extraction optimization | 91 |
| 3.4. Determination of the conditions for the 2D DIGE proteome analysis | 92 |
| 3.4.1. Stress detection by gene differential expression by RT-PCR | 92 |
| 3.4.2. 1D: SDS-PAGE (sodium dodecyl sulphate polyacrylamide gel electrophoresis) | 93 |
| 3.4.3. 2D electrophoresis optimization | 95 |
| 3.5. 2D DIGE analysis | 96 |

| | |
|--|------------|
| Chapter 3. Isolation, identification and selection of phosphate solubilizing bacteria and their application to barley crops | 107 |
| 1. Introduction | 109 |
| 2. Material and methods | 111 |
| 2.1. Isolation and selection of phosphate solubilizer bacteria (PSB) | 111 |
| 2.2. Endospores detection | 111 |
| 2.3. Determination of P solubilization in solid media | 112 |
| 2.4. Identification of PSB | 112 |
| 2.5. Determination of phosphate solubilization in liquid medium | 114 |
| 2.6. Determination of P solubilization mechanisms | 114 |
| 2.6.1. Phosphatase activity quantification | 114 |
| 2.6.2. Phytase activity determination | 115 |
| 2.6.3. Organic acid biosynthesis | 116 |
| 2.6.4. Siderophore production | 117 |
| 2.6.5. HCN production | 118 |
| 2.7. Miscellaneous plant growth promoting characters | 118 |
| 2.7.1. Indoleacetic acid synthesis | 118 |
| 2.7.2. Zn solubilization | 119 |
| 2.7.3. K solubilization | 120 |
| 2.8. Greenhouse pot experiments | 120 |
| 2.8.1. Phosphorus determination in root and shoot samples | 121 |
| 2.8.2. Starch determination in barley grains samples | 122 |
| 2.8.3. Statistical analysis | 124 |
| 2.9. In vitro germination assay | 124 |
| 2.10. In vitro antifungal activity on agar plates | 125 |
| 3. Results and Discussion | 126 |
| 3.1. Isolation and selection of PSB | 126 |
| 3.2. Identification of PSB | 129 |
| 3.3. Endospores formation | 132 |
| 3.4. Analysis of the phosphate solubilization capabilities in liquid medium | 132 |
| 3.5. Analysis of different P solubilization mechanisms | 135 |
| 3.5.1. Acidic and alkaline phosphatase activity determination | 135 |
| 3.5.2. Phytase production | 136 |

| | |
|---|------------|
| 3.5.3. Organic acid biosynthesis | 137 |
| 3.5.4. Siderophore production | 143 |
| 3.5.5. HCN production | 143 |
| 3.6. Miscellaneous plant growth-promoting traits | 144 |
| 3.6.1. Indoleacetic acid production | 144 |
| 3.6.2. Zn solubilization | 145 |
| 3.6.3. K solubilization | 145 |
| 3.7. Greenhouse pot experiment | 146 |
| 3.8. In vitro germination assay | 152 |
| 3.9. In vitro antifungal activity on agar plates | 153 |
| General discussion | 157 |
| I. Improving the phosphorus recovery: biomining with <i>A. thiooxidans</i> | 159 |
| II. Improving the phosphorus performance in soils | 161 |
| Future perspectives | 165 |
| Conclusions | 169 |
| Bibliography | 173 |
| Appendix | 195 |
| I. Abbreviations | 197 |
| II. Culture media | 198 |

SUMMARY & RESUMEN



CONFIDENTIAL

INTRODUCTION



I. Phosphorus's natural cycle. Why phosphorus?

It is said that nature is capricious, and in the case of phosphorus (P), it seems to be true. **Phosphorus is an essential element for life**, since it is involved in numerous biological processes. It plays an important role in most of the metabolic pathways and biochemical reactions taking place in all biological systems: the synthesis of genetic material (DNA and RNA). P is present at the "molecular currency" of intracellular energy transfer (ATP), and also in the structural elements for cells (membrane phospholipids), as well in vertebrate's bones and teeth (hydroxyapatite) (Ruttenberg, 2003). However, despite its relevance, P constitutes a low percent of Earth crust [just 0.09% (w/v)], compared to oxygen (46.6%) or silica (27.7%) (Lutgens & Tarbuck, 2014).

It is also interesting to note that P has no stable atmospheric gas phase, so unlike other essential nutrients for life, such as oxygen or nitrogen, ecosystems depends entirely on its transport through an aqueous phase (both superficial and subterranean), making it costlier to spread over the Earth's surface (Falkowski, 2001; Filippelli, 2008).

Phosphorus is mainly deposited in big sediments of **phosphate rock (PR)**, which is **not directly assimilable by most organisms**. PR is a sedimentary rock that contains high amounts of phosphate minerals, mostly precipitated as insoluble salt compounds (apatites) combined with chemical elements like calcium, fluor or chlorine ($\text{Ca}_{10}(\text{PO}_4)_6(\text{OH},\text{F},\text{Cl})_2$). Actually, it is estimated that only 0.1% of the total P is in soluble forms, being available for plant uptake (Ruttenberg, 2003; Sharma *et al.*, 2013). These large PR deposits are mainly located in the Rocky Mountains (North America), in the Andes Mountains and the Brazilian Highlands (South America), in some parts of Africa (such as Morocco and Algeria), in India and Russia. China also has their own reserves in some points of the country (Figure 1) (Yang *et al.*, 2012; Zangarini *et al.*, 2020; Zhu *et al.*, 2018).

Apatites can be slowly dissolved in the natural environment thanks to a combination of prolonged exposure to climatic processes and the microbiological activity of soil. They can be also transported as particles, or dissolved into superficial or subterranean water flows, until they reach the sea. While transported, they can be deposited, reacting with some metals such as iron [$\text{Fe}_2(\text{PO}_4)_3$], calcium [$\text{Ca}(\text{PO}_4)_2$] or aluminium [$\text{Al}_2(\text{PO}_4)_3$], to generate non-soluble salts. **This phosphorus-mineralization process is one of the main problems for the agricultural industry**, since it also occurs during fertilizer addition into crop soils, preventing that added phosphorus can be easily assimilated by plants (Filippelli, 2008; Li & Marschner, 2019; Ruttenberg, 2003; Zhu *et al.*, 2018).

So, why nature has chosen phosphorus at the heart of all biological systems on Earth? There are several reasons for that. P is very stable at intracellular pH, but it is fast hydrolysed by some enzymes. Despite its low mobility under environmental conditions, it is readily available within organisms. Besides, in intracellular conditions, P is found as phosphate, which has a friendly dissolution and precipitation behaviour, allowing it to be quickly stored or used for the cells. Finally, P is the essential element in bones and teeth's vertebrates, contributing to the hydroxylapatite/organic scaffold giving them strength, some flexibility (preventing their easy breakdown), and an open structure to allow

the exchange of nutrients. Thus, despite its low natural abundance, the chemical behaviour of P makes it the most likely candidate to build with biological systems, contrary to what it might seem at first (Filippelli, 2008; Ruttens, 2003).

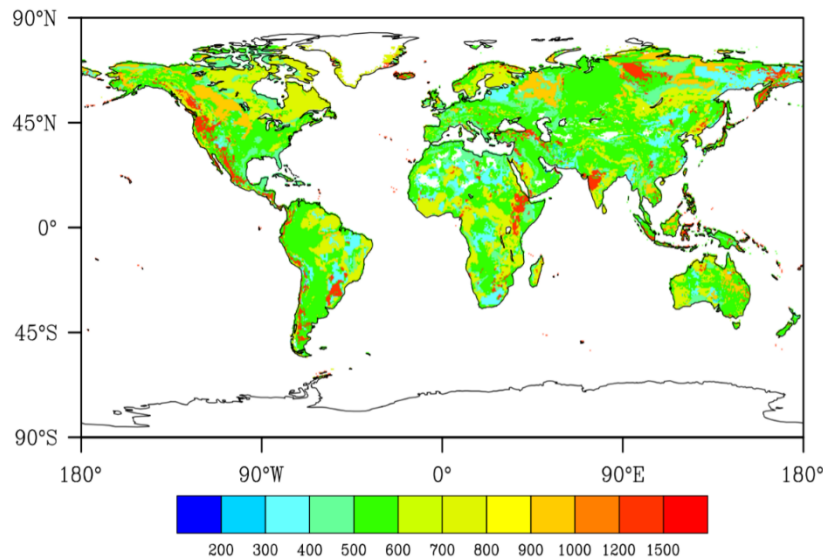


Figure 1. The distribution of phosphorus concentration in soil parent material (unit: ppm) (Yang *et al.*, 2012).

II. Phosphorus: the big problem

The exponential growth of human population (at present, around 8 billion people annually), demands a concurrent production and supply of food. So far, a highly productive agricultural system has mainly been accomplished by intensifying the use of chemical fertilizers. **Agricultural productivity worldwide is mainly limited by nitrogen (N) and phosphorus (P)**, being them the main elements in the chemical fertilizers along with potassium (K). Nevertheless, P resources are finite, in contrast to nitrogen (N) and potassium (K), which can be considered as infinite (Steiner *et al.*, 2015).

So, P is a non-negotiable requirement for life. It is abundant in the soil as mineral salts, or incorporated into organic compounds (values ranging between 400 and 1,200 mg/kg of soil). Thus, the scientific world has its eye on P yield in crops. The reason is twofold: first, as soon as P hits the soil, a big portion of it reacts with other elements, forming **insoluble compounds** that are unavailable for plant uptake. Thus, for centuries, P has been added in extra amounts to the fields to boost harvest, consuming more resources than necessary. Second, there is no P to waste, since it is a non-renewable resource (Glick, 2012).

In 2018, the P market (phosphate rock, DAP, fertilizers...) moved around 650 million dollars, being India and Germany the largest importers, and Vietnam and Kazakhstan the bigger exporters (OEC: Observatory of Economic Complexity; <https://oec.world/en/profile/hs92/phosphorus>). More than 46,500 tons of P (P_2O_5) were used in the fertilizer production that year, and its consumption increased by around 2% annually. Besides, it is a finite resource, whose world reserves are estimated around 61 million tons (FAO, 2020). So, knowing all this, some experts have estimated that the world's phosphorus reserves could be depleted over the next two centuries (more alarmist ones claim that even in the next 50 years) (Fang *et al.*, 2020).

According to the World Bank Group database, 1.5 thousand billion hectares of land worldwide were dedicated to intensive crops in 2016, and, in average, 140 kg of fertilizer were used for each of them. This is mainly due to the low P yield after fertilizers addition to soils. In general, it is estimated that only between 10 to 15% of artificially added P is actually consumed by crops, while the rest is precipitated and accumulated forming compounds that cannot be assimilated by plants, constituting what we know as "**legacy phosphorus**". For this reason, the amounts of P added to soil are much higher than crops actually require, making the process economically more expensive and ecologically much more damaging. It is estimated that the P accumulated in agricultural soils could supply crops for about 100 years at the current rate of production if it were available to plants. Thus, this process is unsustainable in the long term. Furthermore, this accumulation of P generally ends in water contamination (rivers, aquifers or even seas), in a process known as water eutrophication, and in the acidification of agricultural soils (Carstensen *et al.*, 2018; Khan *et al.*, 2007; Lu & Tian, 2017; Zhu *et al.*, 2018).

III. Phosphorus in plants

P is an essential macronutrient for plants. Not only due to its structural role, but also by playing a key role in numerous plant processes such as photosynthesis, the intracellular transference of energy, the transport of nutrients inside the plant, or the transformation of sugars. As reported above, despite the high phosphorus concentration in soils, most of this element is present in unavailable forms, which makes it the second most limiting plant nutrient after nitrogen (Sharma *et al.*, 2013; Thuynsma *et al.*, 2016).

P deficiency alters the photosynthesis process mainly at the photosystem I (PSI) level. This is due to the fact that the concentration of orthophosphate inside the chloroplast stroma is reduced, inhibiting ATP synthase activity. Consequently, electrons are accumulated in the thylakoids, causing acidification of the lumen, which stops the electron transport chain. Thus, in P-deficient conditions, NADH levels increase, while ATP synthesis remains inhibited, which reduces the CO_2 fixation in the plant (Carstensen *et al.*, 2018).

Apart from stunted growth and reduced crop yields, P deficiency symptoms in plants first appear in the older leaves. The first symptom is the appearance of a purple or reddish colour at the stem

and leaves, due to the accumulation of anthocyanins (Figure 2). If **phosphorus deficiency** persists for the whole growth cycle, it could be observed **severe stunting, thin stems, poor leaf** development and **reduced seed production**. Phosphorus lack also affects to root development, showing a spindly and reddish appearance (Fageria, 2008).

Giving the key role of P in plant nutrition, deficiency problems result into big problems for industrial crop production. However, nature has endowed plants with different systems to cope with this problem. First, the morphological development of the roots, maximizing the surface/volume ratio through the production of numerous absorbent hairs, formed from the trichoblasts of the rhizodermis, which can constitute up to 70% of the total surface of the root. This is conducive to improve the contact with larger surfaces of soil and, therefore, to solubilise P in higher amounts. Second, the symbiosis that take place between rhizosphere microorganisms and some plants is also interesting, since, in many cases, these **microorganisms are able to solubilize the precipitated P** to assimilable forms for them. Finally, there are numerous plants with a root system adapted to P deficiency, developing phosphorus solubilization mechanisms through the exudation of certain organic acids (oxalic, malic, citric ...), or humic acids (a complex mixture of many different organic acids) to the soil, the synthesis of chelating ions of certain metals that react with P, or the secretion of enzymes (phytases and phosphatases) to allow its solubilization. (Bucher *et al.*, 2001; Carstensen *et al.*, 2018; Schachtman *et al.*, 1998; Zhu *et al.*, 2018).



Figure 2. Phosphorus deficiency symptoms in five months barley plants from a greenhouse pot assay. Stems turned purple from the bottom to the top, showing more purple colour on the older leaves and stems from the bottom of the plant.

Plants mainly take P from soil by diffusion (as HPO_4^{2-} and H_2PO_4^- forms) towards the root cells. This is a relatively slow process and highly dependent on the extracellular concentration of available P and the rhizosphere microorganisms present in the soil. After that, P transport through plant membranes is mediated by a number of families of transporter proteins. This fact implies that large electrochemical gradients must be generated, due to the negative charge of both the phosphate and the interior of the plasmalemma (the cytoplasmic membrane). Once inside the plant, P travels through the vascular tissues without the need to cross any other membrane (Brito *et al.*, 2020; Maçik *et al.*, 2020; Smith, 2002; Zhu *et al.*, 2018).

IV. Phosphorus's industrial cycle

P used to produce both fertilizers and additives for animal feed is mainly obtained from the mining of phosphate rock reserves (in fact, **more than 85 percent of mined PR is used to produce fertilizer**).

However, 90% of the countries of the world do not have any P mineral reserves in sufficient quantity and quality to be processed, and they depend on its import (Ohtake & Tsuneda, 2019). This, added to the fact that numerous studies estimate that P reserves will be depleted in the next two centuries, has resulted in an increase of the P export taxes in countries like China (i.e. in 2008 imposed an export tariff of 135% higher than the previous year), in order to ensure their autonomy and subsistence in the future (IFADATA, <http://ifadata.fertilizer.org/ucSearch.aspx>, International Fertilizer Industry Association). This fact causes prices to be higher and higher for fertilizers and feed supplements.

Therefore, given the **phosphate rock depletion**, numerous ways of P saving and recycling from very diverse sources have been under study in recent years, such as: **i)** phosphorus recovery from sewage sludge (Fang *et al.*, 2020; Ye *et al.*, 2017), **ii)** its extraction from farm animal bones like chickens and pigs (Du *et al.*, 2020), or **iii)** its recovery from human urine and faeces (Mihelcic *et al.*, 2011).

The science writer, Isaac Asimov, suggested, "*Life can multiply until all the phosphorus has gone, and then there is an inexorable halt which nothing can prevent*" (Barreiro & Martínez-Castro, 2019). So, if P is irreplaceable, how will we deal with the end of global reserves? It is impossible. For this reason, it is essential to understand the industrial cycle of P (Figure 3), how it is obtained and how is used. In this way, it can be analysed how to improve the performance of the process before reaching that point. Thus, the main points in the cycle are set out below: phosphorus mining, fertilizer production and its application; followed by some alternatives exposed in this dissertation: biomining and biofertilization.

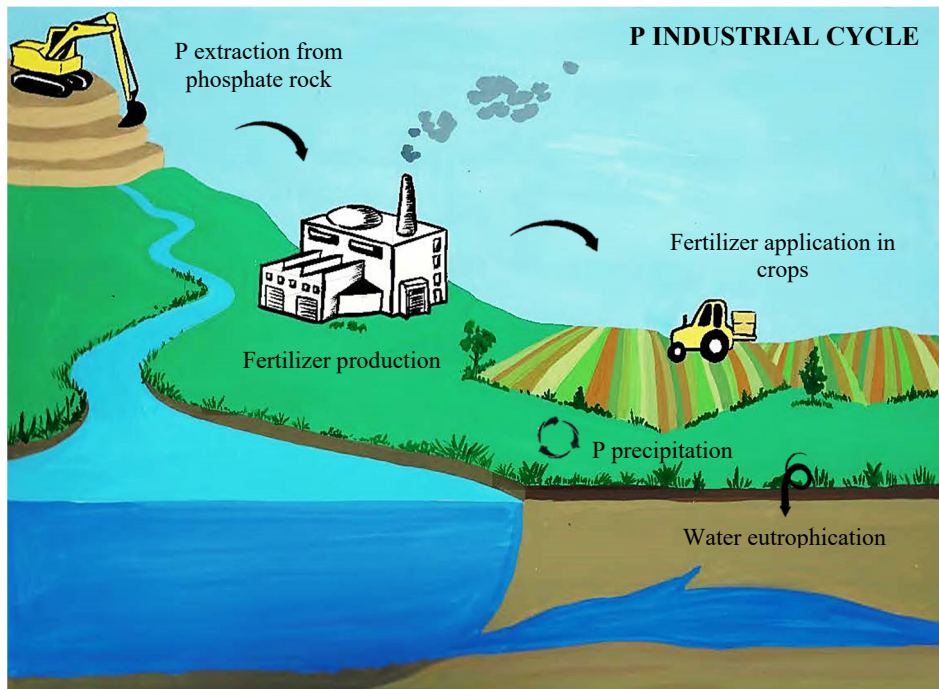


Figure 3. Diagram of the industrial P cycle, starting with the P extraction by mining for fertilizer production and their application into crops. P precipitates in the soil after reacts with minerals as Al, Ca or Fe, building up and contaminating soils and waters in the process known as eutrophication.

IV.I. Phosphorus mining from phosphate rock

P is mainly obtained from three sources: sedimentary deposits sources (75%), igneous sources (15-20%), and animal sources such as bird and bat guano (2-3%). Thus, P is mostly mined from rock deposits, and this mining process can be classified in two types based on the depth and deposit geometry: the surface (strip) mining method (for deposit up to 100 m of depth), and the underground mining method (for deposits at a depth greater than 100 m) (Reta *et al.*, 2018).

By way of introduction, the cycle starts in the phosphate rock mines, where the rock is extracted and processed to obtain intermediary products, such as phosphoric acid and white phosphorus (P_4), which are the base of the P chemical industry. Then, white phosphorus is used to obtain phosphate, which is mainly used in the food and industrial sectors; while phosphoric acid is used in the so-called wet route to obtain the different products used in intensive agriculture as fertilizers (Ohtake & Tsuneda, 2019).

Nowadays, the process begins with a dragline bucket, a large bucket suspended from a boom, which is big enough to hold a truck. This bucket scoops up the initial 4.5 to 9 m of earth, called "overburden," and dumps it in piles on the side of the mine pit. The dragline bucket then digs out

the ore-bearing layer, called matrix. This layer is made up of phosphate rock, clay and sand. The rock is then mixed with water using high-pressure water guns to create a slurry. It is then pumped to the beneficiary plant, where the phosphate rock is separated from the sand and clay, in a process called beneficiation, whose objective is the removing of the unnecessary minerals to increase the grade of mining product (concentrate). Phosphate ores can be beneficiated using one or a combination of different methods. The most common ones are: flotation, crushing, des-liming, separation, grinding and washing (Reta *et al.*, 2018).

Nevertheless, **in none of these concentration steps recovery performance reaches 100%, and some percentage of the phosphate rock is lost as wastes called schlams**. Most of the times, these schlams could have more than 20% (w/w) of P. However, P extraction from the schlams for mining techniques is hard and no cost-effective, so they are simply piled up in large dumps, being all their P content wasted (de Boer *et al.*, 2019; Haneklaus *et al.*, 2017). However, “losses” concept is not a static concept; what is considered a loss today, may differ from what would be considered a loss in the future. For example, in the copper industry, when the average ore-grade was around 2.5% Cu, more than 100 years ago, nobody would have predicted the mining of ore grades at 0.4% Cu or even below (Steiner *et al.*, 2015). **Thus, our concept is born from this precept: P recovery from phosphate rock wastes (schlams).**

IV.1.1. Biomining, bioleaching and sulphur-oxidizing bacteria (SOB)

Biomining is a technology that uses biological systems to facilitate the extraction and recovery of metals, and other substances, with industrial interest from a low-grade source. Occasionally the term is used as synonymous of bioleaching, although strictly the latter one refers to situations where the target metal(s) is/are solubilized during bio-processing. In some other cases, for example, gold biomining and some other precious metals, microorganisms are used to remove minerals that occlude target metals, that are solubilized in a second process (Jerez, 2017b; Johnson, 2014).

Biomining is generally perceived as an eco-friendly process, since the microorganisms involved in mineral oxidation processes are usually autotrophs and fix carbon dioxide, which contrasts with traditional mining and smelting operations that emit large amounts of CO₂. The most interesting skill of these microorganisms is their capability to oxidize intermediate sulphur compounds to sulphate and protons (sulphuric acid), creating an acidic environment which is able to dissolve metal sulphides. The most relevant is the **oxidation of elemental sulphur to sulphuric acid**, since elemental sulphur can only be biologically oxidized under bioleaching conditions (Jerez, 2017b; Johnson, 2014; Schippers *et al.*, 2013).

The naturally occurring ores of copper, zinc, and nickel exist largely in the form of metal sulphides, and they all are currently processed by biomining all around the world (Johnson, 2014; Schippers *et al.*, 2013). Thus, biomining and bioleaching processes have been deeply studied for substances like gold (Liu *et al.*, 2017; Wang *et al.*, 2015), arsenic (Deng *et al.*, 2017), chromium (Zeng *et al.*, 2016),

copper, iron, nickel (Chen *et al.*, 2020; Wang *et al.*, 2020), and the treatment of wastes containing heavy metals (Chang *et al.*, 2019; Wei *et al.*, 2018). It has been also applied for elements such as manganese (Han *et al.*, 2013), or lithium from discarded lithium-ion batteries (Horeh *et al.*, 2016; Wu *et al.*, 2019), although in these cases the leaching ratio is fairly high, and they are expensive and heavily-polluting processes.

Nowadays, biomining is applied using three different engineered methods: dump bioleaching, heap bioleaching and stirred tank bioleaching. The first to be commercially applied was the dump bioleaching for copper extraction 50 years ago. Interestingly, the same biological process had been, unknowingly, used to extract metals for several hundred years at mine sites from, for example, Spain, UK and China. Basically, dumps contain millions of tonnes of run-of-mine ore, and they are often more than 60 m deep. Acidified water is applied to the top surface of the dump using sprinklers or drippers. As the solution percolates through the dump, favourable conditions develop for the growth of naturally-occurring microorganisms, which catalyse the oxidation of the sulphide minerals. The ores are dissolved in the leach solution and percolates to the base of the dump, where the mineral-containing leach solution is collected and directed to a solvent extraction process. Dump bioleaching is the cheapest process and does not require human intervention for long time. For example, The Escondida dump bioleach (Chile) is expected to produce 180,000 - 200,000 tonnes of cathode copper per year over the next 40 years, making Escondida the largest dump bioleach operation in the world (Brierley, 2008; Johnson, 2014).

Heap bioleaching is widely practiced around the world for the extraction of sulphide ores and to “pre-treat” gold ores in which the gold is occluded in sulphide minerals. The ore is crushed to particles about 19 mm or less, and agglomerated in rotating drums with acidified water, to condition the ore for the microorganisms, and also to affix fine particles to the larger rock particles. The ore is conveyed to specially engineered pads where it is stacked. The pads are lined with high-density polyethylene and perforated plastic drain lines are placed on the pad to improve the drainage of mineral-containing solution from the bottom of the ore heap. Air is forced through the air lines and directed to the microorganisms in the heap by blowers external to the heap. The ores are dissolved in the leach solution and percolates to the base of the dump where the mineral-containing leach solution is collected and directed to a solvent extraction process. It is a faster process, since the microorganisms which intervene throughout the process are selected and inoculated in the dump. Besides, their growth conditions are carefully considered since pH, aeration or temperature are controlled (Brierley, 2008; Johnson, 2014).

Finally, aerated continuous stirred-tank reactor is usually applied to mineral concentrates, because of the capital and operating costs associated with this technology. Tanks are equipped with agitators that keep the acidified finely-ground gold concentrate in suspension and ensure that oxygen and carbon dioxide are efficiently transferred to the microorganisms into the solution. It is the most expensive process, but also the faster, since the time required for the biooxidation of the

concentrate is 3 to 5 days, and it can be used for a wide range of metals. For example, the plant at Kasese Cobalt Company Limited in Uganda recovers cobalt, nickel, copper and zinc (Brierley, 2008).

All these bioleaching and biomining processes, as applied to mineral ores and concentrates, operate using essentially the same principles and similar consortia of microorganisms. These microorganisms are the so-called acidophilic **sulphur-oxidizing bacteria (SOB)**, many of which are considered as extremophiles.

Extremophiles are living organisms that have the ability to grow under conditions where normal organisms are not able to survive. These extremophilic organisms are always attracted towards conditions like extremely high and low temperature, extreme pH, high salinity, low and high pressure, growth in presence of heavy metals, and other habitats which are harsh for normal survival. According to the growth conditions, extremophiles are categorized into extremophilic and extremotolerant organisms. **Extremophilic** includes organisms which usually grow under an extreme environmental condition, whereas **extremotolerant** includes organisms that normally grow under common conditions, but can also survive on exposure to extreme environmental conditions (Salwan & Sharma, 2020).

Acidophiles are those microorganisms that can grow at, or below, pH 3 - 4. Various microorganisms such as *Thiobacillus thioparus* have capacity to oxidize reduced sulphur to harmless state, and hence play important role in the biogeochemical cycling of sulphur. They are the so-called SOB, and they have countless applications, such as bioleaching, bioremediation, biofertilizer, biofilters, biosensors, and biodeodorizers and rubber recycling (Rana *et al.*, 2020).

The first extreme acidophile microorganism to be isolated and characterized was the SOB ***Acidithiobacillus thiooxidans*** (formerly *Thiobacillus thiooxidans*) by Waksman and Joffe in 1921. It is an autotrophic chemolithotroph which uses inorganic electrons donors to fix CO₂ as carbon source, with an optimum pH growth of 2.0 - 4.0 (Johnson, 2009).

The most studied SOB strains for biomining are: *Acidithiobacillus ferrooxidans*, *A. thiooxidans*, *Leptospirillum ferrooxidans*, *Thiobacillus thioparus* and *Sulfobacillus thermosulfidooxidans*. These strains are widely distributed in acidic sulphur-containing environments in soil and water, where they participate in the global cycles of sulphur and iron. Based on their metabolic function, they are classified into two types: chemolithotrophs and photoautotrophs. **Chemolithotrophs**, such as *Thiobacillus neapolitanus* or *A. thiooxidans*, are the ones that grow on supplement of oxidizable sulphur compounds. **Photoautotrophic** are the ones that require light as energy source and includes *Thiobacillus aquaesulis* or *Thiomicrospira thvasirae* among others. Both groups of bacteria use inorganic compounds (specially compounds containing sulphur and Fe²⁺) as electron donors to solubilize metals and other compounds, mainly by producing ions (Fe³⁺) or acids (sulphuric acid) (Jerez, 2017b; Rana *et al.*, 2020).

Therefore, we can speculate that the inoculation of dumps made with schlams of phosphate rock dumps and sulphur with some of these SOB could result into sulphuric acid production, and the consequent solubilization of P contained in the schlams in an ecofriendly and cost-efficient process.

IV.I.II. *Acidithiobacillus* spp. and biomining: what is known and what is not

Elemental sulphur (S_0), mainly present in the form of insoluble homocyclic S_8 , is hydrophobic, metastable, and almost insoluble in water. Elemental sulphur oxidation activity was first detected in *Acidithiobacillus thiooxidans* as early as 1959. Since then, three species of *Acidithiobacillus* genus (*A. ferrooxidans*, *A. thiooxidans*, and *Acidithiobacillus caldus*) have been studied and widely applied not only in bioleaching and biomining industry, but also in solving environmental pollution problems caused by heavy metals and inorganic sulphur compounds (Wang *et al.*, 2019).

Acidithiobacillus is a strictly aerobic, Gram-negative, γ -proteobacteria, obligately acidophilic and sulphur-oxidizing chemolithotropic bacteria. It belongs to the class *Acidithiobacillia* (formerly known as *Thiobacillus*) and it grows around 30°C. They have an **optimum growth at pH below 4.0** by using some reduced inorganic sulphur compounds (RISCs), such as S_0 , thiosulphate or tetrathionate, to obtain electrons for carbon dioxide fixation. Thus, they are prevalent in acid mines due to their capabilities of utilizing sulphur, and their adaptation to extremely acidic environments. In fact, this is its most important skill. The outcome of a long and winding metabolic process is the production of SO_4^{2-} , which ends up **generating sulphuric acid** (H_2SO_4), and its release to the medium. This environment acidification offers an inexpensive way to numerous industries to solubilize metals from important minerals (Garrity *et al.*, 2005b; Wang *et al.*, 2019).

However, **sulphur metabolism pathways are complex and diverse**. Several pathways have been described, involving a big number of enzymes such as the Sulphur Oxygenase Reductase (SOR), the Sulphur Dioxygenase (SDO), a Rhodanese (Rhd), the Thiosulfate Dehydrogenase (TSD), the Sulphur oxidase complex (Sox), and the Heterodisulfide Reductase (Hdr)-Like System. There have also been described sulphur carriers (as TusA) and intermediates (such as tetrathionate, S_4I ; or sulphide, S^{2-}) (Wang *et al.*, 2019). Nevertheless, **a definitive sulphur (oxidizing) pathway is not fully known** yet. Many possible pieces of the puzzle have been described that can be used to outline the complex metabolism of these bacteria in the near future.

In fact, this is a complex issue since not much is known about *Acidithiobacillus* at molecular level. Genome sequences for some *Acidithiobacillus* spp. have become available in public databases since 2008 (Nuñez *et al.*, 2017). Since then, 13 different genomes have been published, and just one of them with less than 40 scaffolds. On the contrary, 416 genomes of *Bacillus subtilis* and 5,718 genomes of *Pseudomonas aeruginosa* have been reported in NCBI database in the same period of time.

Besides, it must be noted that multiprotein phylogeny and genetic phylogeny studies have already proved the uniqueness of this genus in the past. Although it is classified in the γ -proteobacteria class, there is really no relation between *Acidithiobacillus* and the rest of genus from this class. It also shows no relation to the rest of the proteobacteria classes. So, according to some authors, ***Acidithiobacillus* could take part of a new class within proteobacteria phylum**, becoming the seven class of the phylum together with the α -, beta-, γ -, delta-, epsilon- and zeta-proteobacteria (Williams *et al.*, 2010; Williams & Kelly, 2013).

To make matters more difficult, the evolutionary relationships among members of this group remain poorly understood yet. Besides, knowledge on the taxonomic structure of the *Acidithiobacillus* species complex has relied on classifications achieved on the basis of morphological and physiological characteristics for many years. Thus, acidophilic rods catalysing the dissimilatory oxidation of both iron and sulphur have mainly been classified as strains of *A. ferrooxidans*, while those that only oxidizing sulphur have been assigned to *A. thiooxidans* or *A. caldus* species, depending on the optimal temperature of growth of the isolate. According to 16S rRNA gene oligotyping results, 35.6% of the isolates, which presumably have been experimentally diagnosed before being assigned to a particular taxon, were actually incorrectly classified. In fact, new species have been proposed just five years ago to try to classify those strains that do not fit in the rest of the clades (Falagán & Johnson, 2016). Finally, several

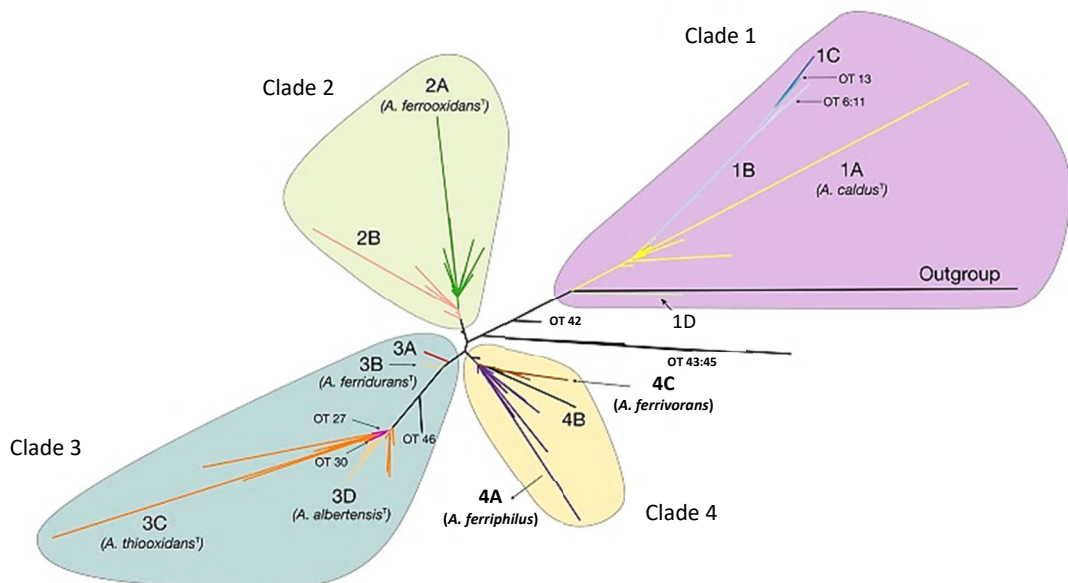


Figure 4. *Acidithiobacillus* species complex consensus phylogenetic tree. Picture taken from Nuñez *et al.* (2017). Clade's affiliation are as follows: clade 1 (purple, *A. caldus*), clade 2 (green, *A. ferrooxidans*), clade 3 (turquoise, *A. ferridurans*, *A. thiooxidans*, and *A. albertensis*), and clade 4 (yellow, *A. ferriphilus* and *A. ferrivorans*).

differences in the genome of the same *Acidithiobacillus* species due to econiche-driven divergence have been detected (Figure 4), becoming even more complicated their molecular analysis not having other genomes to compare (Nuñez *et al.*, 2017).

IV.II. Phosphorus in agriculture: P-based fertilizer production and their application in crops

Fertilizers are defined as natural or man-made chemicals, that can supplement natural soil nutrients to improve crop productivity and soil fertility (Giri *et al.*, 2019). P-based fertilizer production starts with the **phosphate rock extraction** in enormous mines, mainly using explosives and industrial machinery. Once the phosphate rock is extracted, it is treated with **strong mineral acids** (mainly hydrochloric acid ⁽¹⁾, nitric acid ⁽²⁾ and sulphuric acid ⁽³⁾, Figure 5) following the so-called wet route of the phosphoric acid. This route is the most used in P-based fertilizer production, and generally the sulphuric acid is the one used, since the calcium sulphate generated during the process is more insoluble - and therefore easier to separate and eliminate - than calcium nitrate and calcium chloride.

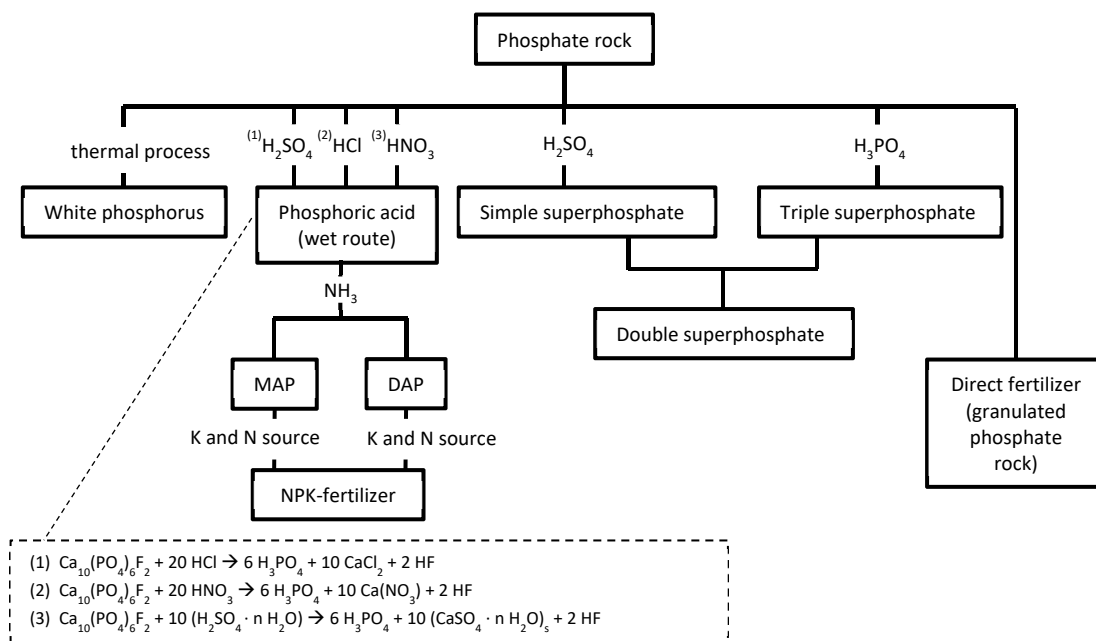


Figure 5. An overview of the P-based fertilizers production processes. Based on de Boer *et al.* (2019).

The process basically consists of two steps: **i)** the digestion of phosphate rock in a reactor and, **ii)** filtration of the gypsum (calcium sulphate, CaSO_4) formed. Sometimes a third step of final product concentration and purification is added (de Boer *et al.*, 2019; Haneklaus *et al.*, 2017).

In the first place, the rock is ground to a suitable grain size. Later, during the digestion of phosphate rock, the present fluorapatite [$\text{Ca}_5(\text{PO}_4)_3\text{F}$] reacts with the sulphuric acid, producing phosphoric acid (H_3PO_4), hydrogen fluoride (HF), and calcium sulphate. Then, everything is extracted from the reactor and filtered under partial vacuum, by flocculation and subsequent decantation, or, more commonly, by flotation using surfactants, obtaining a product with a P_2O_5 (phosphorus pentoxide) richness between 28% and 32% (w/v). However, this concentration is too low to be used in fertilizers, so it is needed a concentrate step mainly by evaporation, reaching concentrations of phosphoric acid higher than 70% (de Boer *et al.*, 2019; Huang *et al.*, 2019).

Finally, the resulting phosphoric acid is neutralized with ammonia to obtain MAP (monoammonium phosphate) or DAP (diammonium phosphate). When they are supplemented with a nitrogen (N) and potassium (K) source, NPK fertilizers are obtained. Sulphuric and phosphoric acids can also be added directly to the phosphate rock to obtain simple (SSP) or triple superphosphate (TSP) to be used as fertilizers. Superphosphate sources mainly contain non-purified monocalcium phosphate [$\text{Ca}(\text{H}_2\text{PO}_4)_2$], mixed with the gypsum from the phosphate rock (Figure 5) (de Boer *et al.*, 2019; Giri *et al.*, 2019).

Once these fertilizers are produced, they are used in the field as a nutritional supplement for crops. Nevertheless, **P rapidly precipitates in soils** when reacting with cations of aluminium⁽¹⁾ and iron⁽²⁾ (in acidic soils), or calcium⁽³⁾ (in calcareous soils), being 4.5 and 6.5 the best pHs for the availability of phosphorus for plants (Figure 6) (Penn & Camberato, 2019). The term P fixation is commonly used to describe reactions that remove available P from the soil (Barber, 1995).

Thus, the P pollution problem runs alongside the rising demand for phosphatic mineral fertilizers, being the most important ones the eutrophication and hypoxia in lakes and estuaries due to phosphorus precipitation, and the increase of the emission of greenhouse gases due to fertilizer production (Giri *et al.*, 2019; Ngatia & Taylor, 2019; FAO, 2020, Zangarini *et al.*, 2020).

Because of these drawbacks, the concepts of sustainable agriculture and mitigation of environmental impacts are growing in significance. Thus, microbial inoculants - mostly denominated as bio-fertilizers - are gaining prominence in the framework of agriculture (Giri *et al.*, 2019; Santos *et al.*, 2019).

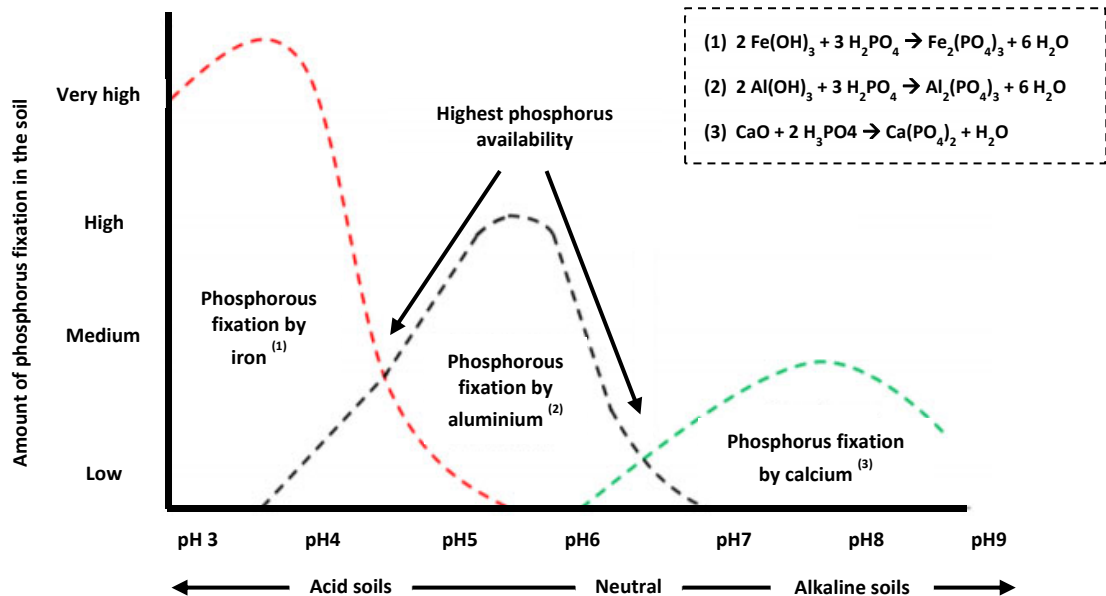


Figure 6. General qualitative representation of soil phosphorus availability as impacted by pH, and its reaction with the main chemical element present in each range of pH. Redrawn from Penn & Camberato, 2019.

IV.II.I. Bio-fertilizers and plant growth-promoting rhizobacteria

Bio-fertilizers are defined as “a substance that contains living microorganisms which, when applied to seed, plant surface or soil, colonise the rhizosphere or the interior of the plant, and promote growth by increasing the supply or availability of primary nutrients to the host plant” (Basu *et al.*, 2021; Chatzipavlidis *et al.*, 2013). Bio-fertilizers transform nutritionally important elements from non-usable to highly assimilable forms through natural processes of nitrogen fixation, solubilization of phosphorus or potassium, and plant growth-regulators production, among others (Chatzipavlidis *et al.*, 2013).

Plant growth-promoting rhizobacteria (PGPR) are defined as “that rhizosphere bacteria which can enhance plant growth by a wide variety of mechanisms” like mineral solubilization (for example P, K or Zn), nitrogen fixation, phytohormone production [auxins like indol-3-acetic acid (indoleacetic acid), ethylene or gibberellins as gibberellic acid], synthesis of molecules with antibiotic activity [mycotoxins, cell-wall-degrading enzymes...], or volatile organic compounds production (Figure 7). Like chemical substances, PGPR’s nature can be very diverse and their category is defined on the basis of its agricultural/horticultural outputs. ‘Biofertilizers’ and ‘biocontrol agents’ are also used for describing PGPRs. They play an important role in crops health and soil fertility as they enhance plant

growth by producing growth-promoting chemicals or antimicrobial compounds, and inducing tolerance to some abiotic stress. PGPR can be divided into two groups: extracellular PGPR (living in the rhizosphere of the plant), and intracellular PGPR (located inside of root cells forming nodules). This groups of PGPR commonly includes *Bacillus*, *Burkholderia*, *Enterobacter*, *Rhizobacteria*, *Serratia* or *Pseudomonas* (Giri *et al.*, 2019; Maçik *et al.*, 2020; Mukhtar *et al.*, 2017; Saxena *et al.*, 2019; Zhang *et al.*, 2020).

Despite there is a limited understanding of PGPR-plant interactions, there are several cases of these bacteria being currently commercially used as adjuncts to agricultural practice. Commercialized PGPR strains include *Agrobacterium radiobacter*, *Azospirillum brasilense*, *Azospirillum lipoferum*, *Azotobacter chroococcum*, *Bacillus firmus*, *Bacillus licheniformis*, *Bacillus megaterium*, *Bacillus mucilaginosus*, *Bacillus pumilus*, *Bacillus spp.*, *Bacillus subtilis*, *Bacillus subtilis*

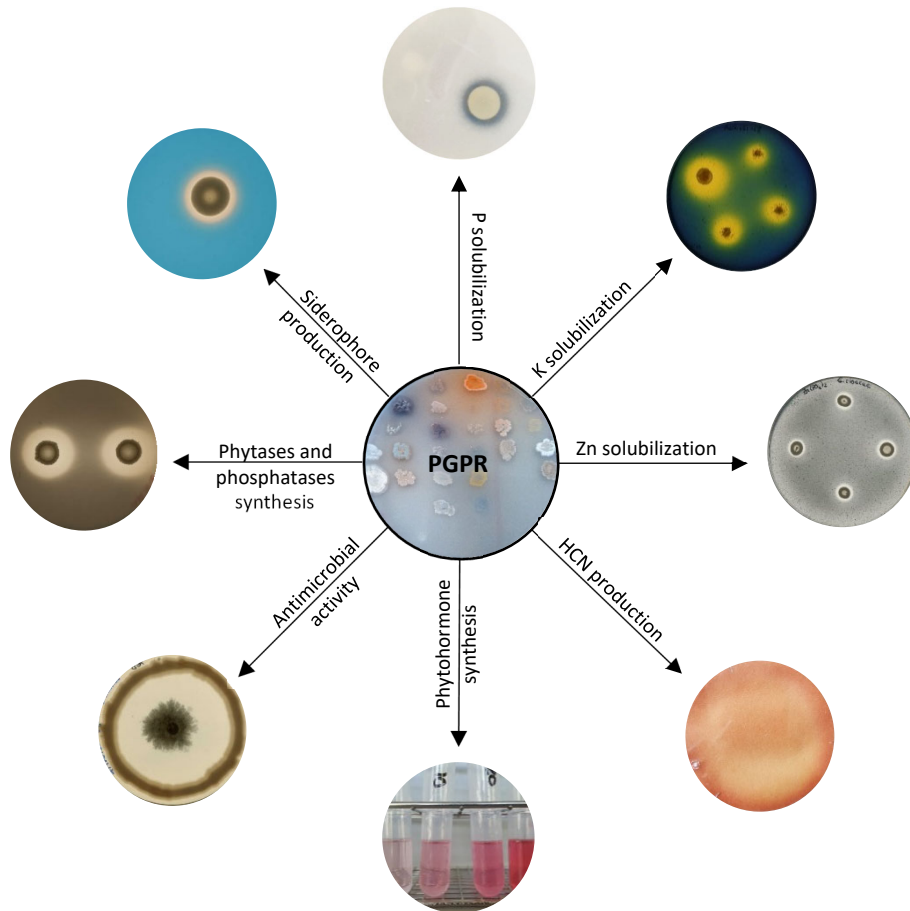


Figure 7. Overview of different plant growth-promoting traits exerted by the isolates.

var. amyloliquefaciens, *Burkholderia cepacia*, *Delftia acidovorans*, *Paenobacillus macerans*, *Pantoea agglomerans*, *Pseudomonas aureofaciens*, *Pseudomonas chlororaphis*, *Pseudomonas fluorescens*, *Pseudomonas solanacearum*, *Pseudomonas spp.*, *Pseudomonas syringae*, *Serratia entomophila*, *Streptomyces griseoviridis*, *Streptomyces spp.*, *Streptomyces lydicus* and various *Rhizobia spp.* However, PGPR inoculated crops represent only a small fraction of current worldwide agricultural practice (Backer *et al.*, 2018; Glick, 2012).

Nitrogen-fixing microorganisms is the most studied and used group in bio-fertilizers. Despite nitrogen is the most abundant chemical element in the air, becomes a limiting nutrient in soils due to its difficulty to be fixed and uptaken by plants. Some α -proteobacteria, especially some members of the family *Rhizobiaceae* are widely used in bio-fertilizers. For example, *Rhizobium* sp. is already commercialized for leguminous plants. Besides, the actinobacteria *Frankia* is also a well-known bio-fertilizer for rice, whereas *Azospirillum* is used in biofertilizers for non-legume plants as sugarcane, cotton or coffee (Abdallah *et al.*, 2009; Giri *et al.*, 2019; Mączik *et al.*, 2020).

Nevertheless, with the change of century, the eyes of the scientific world have turned to the challenge of phosphorus’s solubilization in soils, so this problem have reached a prominent position in the bio-fertilizers market in recent years (Figure 8). In this way, the first studies about phosphorus-solubilizing microorganisms (PSM) began, by analysing both fungi (such as *Penicillium*, *Aspergillus*, *Curvularia* and *Trichoderma*), and bacteria (especially *Pseudomonas* and *Bacillus*) (Brito *et al.*, 2020; Giri *et al.*, 2019; Li *et al.*, 2019; Mączik *et al.*, 2020).

These initial studies confirmed that phosphorus solubilization takes place mainly through two different mechanisms: **i)** secretion of P-solubilizing enzymes (mainly phosphatases and phytases), able to extract P from the soil organic matter **ii)** secretion of low molecular weight organic acids (malic, oxalic, acetic, succinic, fumaric, citric, gluconic...), and mineral chelating compounds (like siderophores), to dissolve the inorganic P present in soil (Figure 9) (Aeron *et al.*, 2019; Chen *et al.*, 2016; Mączik *et al.*, 2020; Wei *et al.*, 2018).

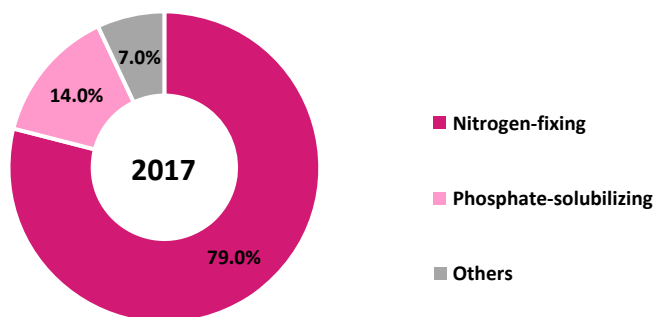


Figure 8. Global fertilizer market share by product typology (nitrogen-fixing, phosphate-solubilizing and others microbe-based biofertilizers. Marked date of 2017. Picture taken from Basu *et al.* (2021).

i) **Secretion of P-solubilizing enzymes to recover P from the organic soil matter.** Some microorganisms are able to produce enzymes to recover P from the organic soil matter. One of the most common and known are phytases. P is commonly stored in seeds and pollen as phytate. Once in soil, if they do not germinate, some microorganisms can release their P by synthesizing phytases. Another strategy, used by both plants and microorganisms, is the secretion of phosphatase enzymes. These phosphatases induce the release of phosphorus from precipitated organic compounds in soil or fertilizers by dephosphorylating phospho-ester or phosphoanhydride bonds. This hydrolysis removes a phosphate ion, generating a molecule with a free hydroxyl group and soluble phosphate (Alori *et al.*, 2017; Sharma *et al.*, 2013; Zhu *et al.*, 2018).

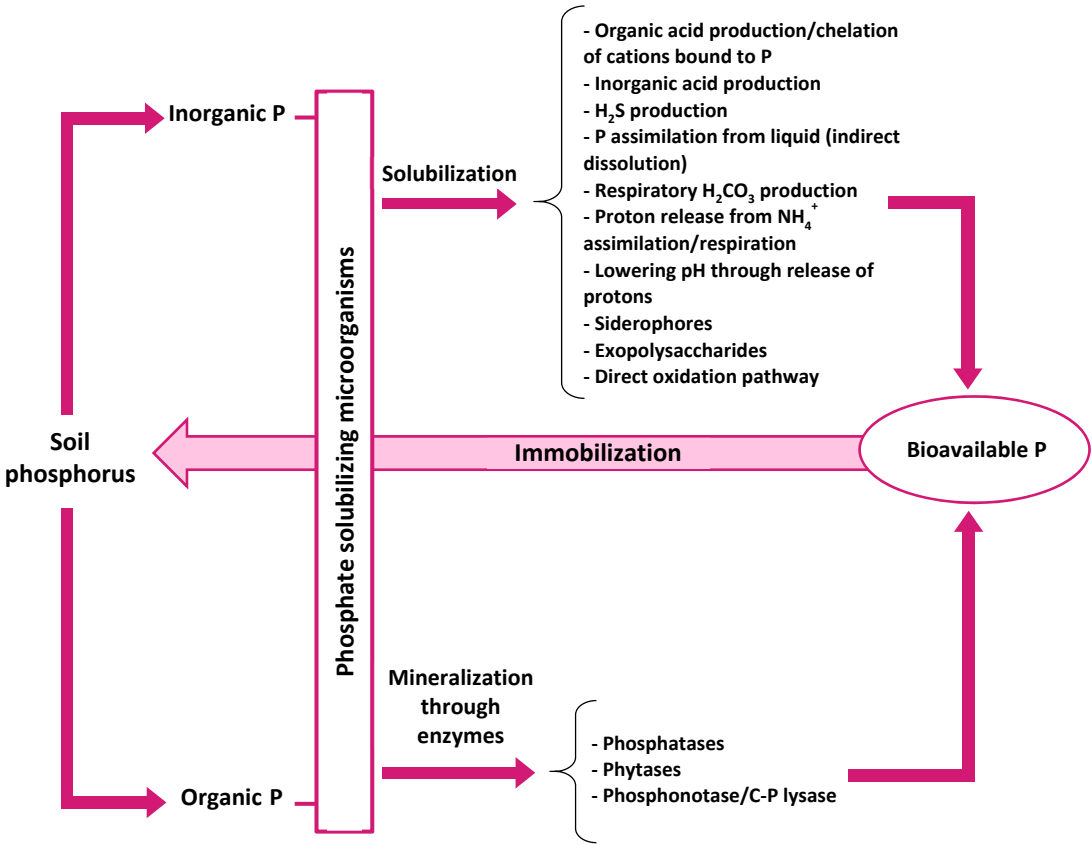


Figure 9. Schematic representation of mechanism of soil P solubilization/mineralization and immobilization by PSM. Based on Sharma *et al.*, 2013.

ii) **Secretion of compounds to dissolve the inorganic P present in soil.** Most of the rhizobacteria strains produce a wide variety of organic acids due to its intrinsic metabolism, which has been related with mineral phosphate solubilization. They are also able to chelate cations as Ca^{2+} , Fe^{3+} , Fe^{2+} or Al^{3+} , which react with soluble phosphorus from soil. Besides, some mineral phosphorus sources such as TCP (tricalcium phosphate) or hydroxyapatite are dissolved in acid environments like those generated by these acids (Chen *et al.*, 2016; Wei *et al.*, 2018).

On the other hand, iron is an essential nutrient for all rhizobacteria, because it is present in the redox centre of many enzymes from respiratory chain. Thus, they produce high concentrations of siderophores to capture the Fe^{2+} present in soil, decreasing the iron concentration which is able to react with the phosphorus, allowing its solubilization in this way (Aeron *et al.*, 2019; Alori *et al.*, 2017).

Besides, even those microorganisms that are not able to solubilize phosphorus extracellularly, are able to improve soluble phosphorus availability for the plant. This is due to the fact that many microorganisms are able to use some mineral, or precipitated, phosphorus sources so that they assimilate and incorporate into their cellular metabolism. Once the cell is lysed, phosphorus is released in assimilable forms for the plant (Aeron *et al.*, 2019).

V. Sulphur: commodity or waste?

Turning to the matter of biomining process, the development of a mining activity with SOB's raises another concern: to secure large amounts of sulphur supply, which is an expensive product. However, **given the role of sulphur in biomining activities** (to provide to SOB with a source of energy) **a high purity is not required.** Thus, S can be obtained from cheaper sources.

Sulphur occurs in nature combined with other elements forming sulphides, sulphates and organic compounds. It exists in various oxidation states ranging from -2 to +6, which results in a variety of reduced inorganic sulphur compounds (RISCs) including tetrathionate ($\text{S}_4\text{O}_6^{2-}$), thiosulfate ($\text{S}_2\text{O}_3^{2-}$), sulphite (SO_3^{2-}), sulphide (S^{2-}), and elemental sulphur (S^0) (Wang *et al.*, 2019). Thus, we can find S in sedimentary, metamorphic, and igneous rocks, as well as in all fossil fuels. Nevertheless, only a small portion of the global S sources occurs in enough concentrated quantities to make cost-effective its commercial extraction by mining.

Sulphur is one of the most important elements utilized by mankind as a fundamental industrial and chemical raw material. The history of S dates back to immemorial time: Egyptians used sulphur in bleaching linen textiles. In the Odyssey, Homer refers to its use as a fumigant. Romans used it to produce the first incendiary weapons, and China used it in pyrotechnic around the 10th century (Ceccotti *et al.*, 1998; Kogel *et al.*, 2009; Warren, 2016).

Early civilizations obtained their scanty requirements from deposits around volcanoes. However, the discovery in the 19th century that insoluble phosphates can become more available for plants by

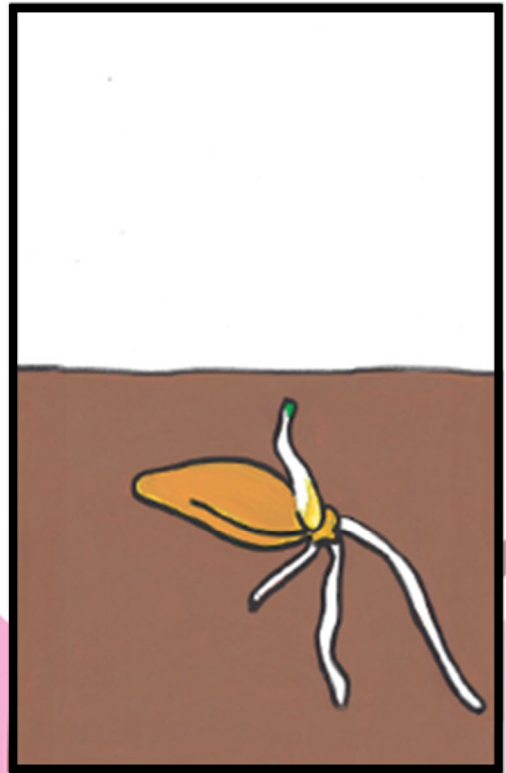
reacting with sulphuric acid, the phosphate fertilizer industry started, turning it into an important component of every sector of the world's fertilizer industry. Fertilizers are the ultimate use of about 50% of the world's S production, but other key uses include rubber processing, cosmetics, and pharmaceutical applications (Ceccotti *et al.*, 1998) (<https://ihsmarket.com>).

As we said before, we can find S as a component of fossil fuels, like petroleum, in a wide range of concentrations. Thus, in the petroleum refining, a high proportion of S is removed and recovered in its elemental form. In this way, nowadays, a new form of producing very cheap elemental S exists.

Currently, most vehicles' fuels are derived from natural petroleum, which is converted in oil refineries into a wide range of fuels and petrochemical feedstocks. This natural **petroleum** composition is significantly varied, but **usually contains sulphur compounds** (such as benzothiophene, dibenzothiophene and alkylated derivatives) **from about 1 to 4 percent** (although it can even reach 8% in some cases). These compounds are one of the main problems of pollution, because they became sulphur oxides when subjected to combustion which give rise to the formation of oxyacids in the atmosphere, causing the phenomenon known as acid rain. Actually, from now on, sulphur removal from petroleum feedstocks and products is expected to become increasingly important [the global sulphur limit for marine fuels was reduced from 3.5% to 0.5% (w/w) in January 2020] (Jönander & Dahllöf, 2020; Keckler *et al.*, 2009).

Between 6,000 and 7,000 tonnes of S are generated per million barrels of SCO (Synthetic Crude Oil) produced, which are close to 7 million tonnes per year in 2020. The sulphur price decreased throughout last year and reached about \$46 per ton in early October 2020, the lowest price since 2009. Besides, sulphur has no import tax. All this information makes us think that **it may be a very cheap sulphur source for a biomining process with SOBs** (Marsulex Environmental Technologies, 2010; U.S. Geological Survey, 2020).

OBJECTIVES



The **main objective** of this work **faces the problem of the progressive disappearance and consumption of phosphorus (P) reserves by providing biological solutions**. The major problem with P arises from its high reactivity in soil after the fertilization process, precipitating in the form of insoluble salts, that are not assimilated by crops. For this reason, fertilizer addition to the soils is much higher than necessary, causing the phosphate rock reserves (its main source of obtaining) to be depleted in the near future. In addition, this excessive addition of phosphorus causes huge contamination problems of soils and aquifers, without being useful for agricultural productions. In order to shed light on these problems, different types of phosphate solubilizing bacteria (PSB) were isolated, selected and characterized. These PSBs should be able to solubilize the precipitated P from soils, making it available for crops. **CONFIDENTIAL**

The **specific objectives** established to reach this purpose were:

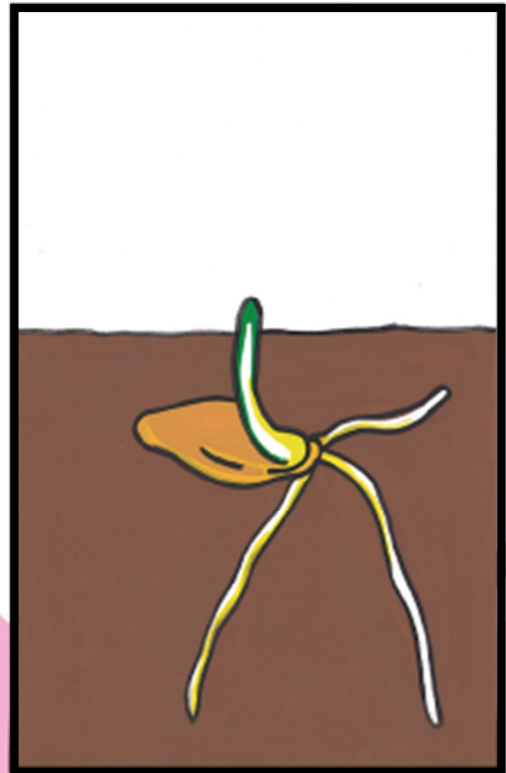
- **CONFIDENTIAL**

- The analysis of the proteome of the sulphur-oxidizing bacteria *Acidithiobacillus thiooxidans* under different pH conditions, in order to determine its response to extreme acid pHs and its possible adaptation to hyper-extreme environments.

- The isolation and characterization of different phosphorus solubilizing bacteria and their application to barley crops to analyze their possible application as biofertilizers.

CHAPTER 1

Isolation, identification and selection of sulphur-oxidizing bacteria for phosphorus solubilization from phosphate rock schlams

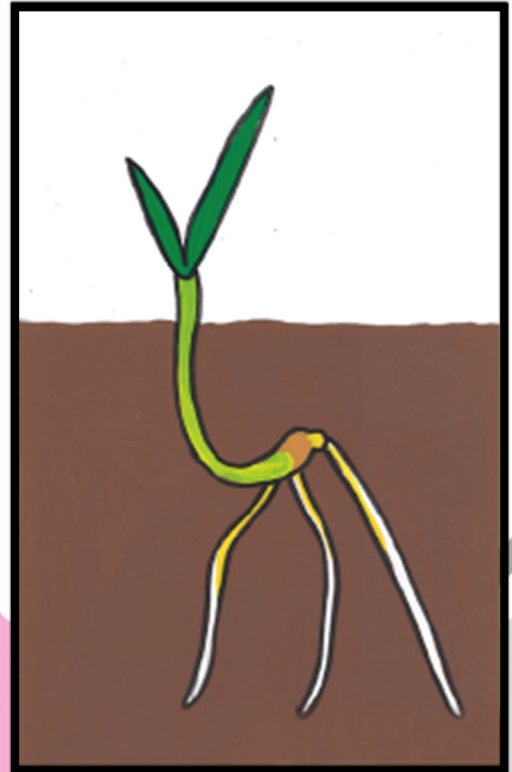


The work described in this chapter has been financed by Agroquimes S.L. (Madrid, Spain) through a Research Contract (Art. 83) entitled "Desarrollo de tecnologías microbianas para la producción de fósforo soluble por solubilización de roca fosfórica" and date of signature May (8th/2015).

CONFIDENTIAL

CHAPTER 2

Molecular study of
Acidithiobacillus thiooxidans SOB3



1. Introduction

***A. thiooxidans* is a mesophilic, chemolithotroph, autotroph, aerobic and Gram-negative γ -proteobacteria.** It is motile by one polar flagellum and is widely distributed in acidic environments with sulphur compounds, like sulphur springs and acid mine drainage waters (Garrity *et al.*, 2005b).

It was first isolated in 1921 by Waksman and Joffe (1922). Nevertheless, during these almost 100 years, it has been barely studied, due to its extreme conditions of growth. *A. thiooxidans* needs a pH close to 3 and none organic carbon source is required. In fact, even a minimal glucose contamination in the flask can prevent its growth. There is no formal definition of what constitutes an extreme acidophile, but it has been propose as “those that have an optimum pH at 3 or below” (Johnson & Quatrini, 2016). **Thus, *A. thiooxidans* is traditionally described as an obligately extreme acidophilic bacteria.**

Nevertheless, all the microorganisms, even the extreme acidophiles as *A. thiooxidans*, require a near-neutral intracellular pH (~ 6.5) to survive. Thus, acidophiles face a tough task, because they are exposed to high pH gradients. They leverage this gradient to obtain energy from the proton movement across membranes downhill the electrochemical potential, with the consequent conversion of ADP to ATP, via membrane-bound ATPases or proton-pumping respiratory chain complexes. However, the influx of protons increases intracellular protonation, that would affect molecular processes such as DNA replication, transcription, protein synthesis and enzyme activity. Thus, **these acidophiles shows diverse mechanisms to maintain the intracellular pH homeostasis.** The mechanisms of these processes are no well-known, since some of which were postulated in the 1980s and early 1990s, but they were not rigorously supported (Booth, 1985; Matin, 1990).

One of the most studied mechanisms is the **impermeability of the cell membrane**, which restricts the influx of protons into the cytoplasm. Thus, acidophiles present a complex cell wall structure, incorporating fatty acids with greater chain length, saturation and cyclization, at low pH. In fact, *A. thiooxidans* is able to synthesize unsaturated acids, such as oleic acid, linoleic and, specially, cyclopropane, under extreme acid stress, to maintain the intracellular homeostasis (Feng *et al.*, 2015). Besides, they can change the lipid surface charge by the ionization of their membrane lipids, changing by this way their permeability. Besides, it has been reported that some strains of extreme acidophiles, as *A. ferrooxidans*, are able to modify the pore size of their membrane channels. Thus, they prevent protons from entering the cells (Baker-Austin & Dopson, 2007; Mirete *et al.*, 2017; Mykytczuk *et al.*, 2010).

Besides, some acidophiles are able to generate a transmembrane electric potential with the diffusion of ions (specially Na^+ and K^+) through the membrane by cations transporters. Thus, they create a **chemiosmotic barrier** with these positive charges. In fact, it has been reported that the maintenance of the electric potential in *A. thiooxidans* is mainly due to the potassium up-take, probably through an energy dependent cation pump. Besides, the F_0F_1 -ATPase pump promotes

proton extrusion through the pump with energy consumption (Krulwich *et al.*, 2011; Mirete *et al.*, 2017; Mykytczuk *et al.*, 2010).

Once the protons manage to penetrate the cell membrane, a range of intracellular mechanisms help to reduce the biological damage. First, the cells try to sequester or **release protons** with cytoplasmic buffer molecules, such as basic amino acids (lysine, histidine or arginine) (Baker-Austin & Dopson, 2007). Other strategy is the **proton uncoupling** by organic acids. Thus, active mechanisms of organic acid degradation might be a pH homeostatic mechanism used by heterotrophic acidophiles, since the proton dissociation from the organic acid results in the acidification of the cytoplasm and loss of proton motive force (Baker-Austin & Dopson, 2007; Lehtovirta-Morley *et al.*, 2014; Mirete *et al.*, 2017).

Finally, if DNA and proteins are damaged because of the low intracellular pH, they can be repaired by **chaperones**. Several protein repair genes have been found in extreme acidophiles genome sequences, which can be related to problems associated with this pH homeostasis. In fact, DnaK, DnaJ and GrpE increased their transcriptional levels when *A. thiooxidans* was grown under super acid pH (0.4) conditions (Baker-Austin & Dopson, 2007; Feng *et al.*, 2015; Mirete *et al.*, 2017).

However, there is still much that is unknown about all these mechanisms to prevent cell damage under extreme acid environments. There are two main problems for the research in these strains: **i)** the lack of genetic tools to construct mutants, which would help to understand the genetic and biochemical basis of these mechanisms; and **ii)** the hard conditions to grow some of these strains under lab conditions (some of these acidophiles are even uncultured, and can only be studied using culture-independent techniques, like metagenomics or metatranscriptomics) (Mirete *et al.*, 2017).

Throughout this chapter, the study of the *Acidithiobacillus thiooxidans* proteome is addressed to try to identify the keys to its survival in extremely acidic environments.

2. Material and methods

2.1. *A. thiooxidans* 16S rRNA gene copies quantification

2.1.1. DNA isolation

A. thiooxidans DNA isolation was carried out from a liquid culture grown in AT medium at pH 3.0 at 30°C and 200 rpm for 7 days, as described by Bergamo *et al.* (2004). DNA was purified with phenol-chloroform method, which is based on the solubility of the biomolecules. DNA is a polar molecule with a negative charge, while proteins are non-polar. Thus, DNA dissolves in water but not in phenol, which remains at the bottom of the tube due to its higher density, while proteins settle into the phenol phase. On the other hand, chloroform increases the efficiency of protein denaturalization by phenol, and improves the organic and aqueous phases separation. Thus, a last step with chloroform : isoamyl alcohol gets rid of the phenol of the samples.

Protocol development

- Grow a 200-mL culture for 7 days at 30°C and 200 rpm in ATT medium.
- Centrifuge the culture at 10,700 $\times g$ for 1 min.
- Discard the supernatant.
- Wash the pellet twice with 5 mL of TE buffer¹¹.
- Centrifuge 10 min at 10,700 $\times g$.
- Wash the pellet with 1 mL of TAS buffer¹².
- Centrifuge 10 min at 10,700 $\times g$.
- Resuspend the pellet in 500 μL of the breaking mix buffer¹³.
- Incubate samples 1 h at 50°C.
- Centrifuge 5 min at 17,000 $\times g$. Transfer the supernatant to a new tube.
- Wash the DNA twice with 1 volume of phenol-CIA¹⁴ and mix thoroughly by inversion.
- Centrifuge 5 min at 17,000 $\times g$.
- Transfer the aqueous phase (upper phase) to a new tube. Add 1 volume of CIA¹⁵ and mix thoroughly by immersion (~ 30 s). Centrifuge 2 min at 17,000 $\times g$.
- Transfer the aqueous phase to a new tube. Add 2.5 volumes of ethanol and 1/10 volume of 3 M sodium acetate. Incubate at -20°C for at least 2 hours or at -80°C for at least 30 min.
- Centrifuge 15 min at 17,000 $\times g$ and 4°C.
- Discard the supernatant.
- Wash the DNA adding carefully 50 μL of 70% ethanol (v/v) over the pellet. Centrifuge 10 min at 17,000 $\times g$ and 4°C.
- Discard the supernatant.
- Let the pellet dry and re-suspend in 50 μL of TE buffer¹¹.

2.1.2. *16S rRNA* gene copies quantification by Southern Blotting

Southern blotting (Southern, 1975) was carried out to quantify the number of copies of *16S rRNA* gene. Southern blotting is a method used for detection of a specific DNA sequence, which allow us to detect the number of copies of some specific sequence. It combines the DNA electrophoresis with its transference on a nylon membrane, and subsequent fragment detection by labelled probe hybridization.

¹¹ **TE buffer:** 10 mM Tris-HCl; 1 mM EDTA; pH 8.0.

¹² **TAS buffer:** 50 mM Tris-HCl; 50 mM EDTA; 150 mM NaCl; pH 8.0.

¹³ **Breaking mix buffer:** 50 μL of 10% SDS; 150 μL 20 mg/mL Proteinase K (Fermentas); 300 μL TAS buffer.

¹⁴ **Phenol-CIA:** 50% neutral phenol; 50% CIA.

¹⁵ **CIA:** chloroform : isoamyl alcohol [24:1 (v/v)].

a. Probe labelling

Label sequences were amplified from *A. thiooxidans* total DNA by using specific designed primers: 16S-thiooxF (5' GCTAATATCGCCTGCTGTTG 3') and 16S-thiooxR (5' GTTCCACCGCCATTCCC 3'). They amplify a 182 bp sequence from the 16S *rRNA* gene. Probe labelling reaction was performed following the protocol of Barreiro *et al.* (2004)

Protocol development

- Amplify and purify 1 µg of DNA by phenol-CIA (see section 2.1.1).
- Denaturalize by heating at 95°C for 10 min. Cool quickly on ice to avoid DNA re-naturalization.
- Mix 1x DIG-DNA labelling mix (Roche), 1x hexanucleotides mix (Roche), 1x reaction buffer for Klenow fragment (Fermentas), 1U Klenow polymerase (Fermentas) and 30 ng of DNA in a final volume of 20 µL.
- Incubate the sample at 37°C at least 60 min (preferably between 16 and 24 h).
- Stop the reaction by adding 2 µL of 0.25 mM EDTA pH 8.0.
- Store at -20°C in the dark until use.

To check the label process, seven 5-fold serial dilutions were carried out, and analysed as follows: 1 µL of each dilution was applied over a nylon membrane [*HybondTM-N+ membrane optimised for nucleic acid transfer* (GE Healthcare)] and DNA was fixed into the membrane by the application of three pulses of 120,000 µJ of UV light using a *UV-Stratalinker 2400* (Stratagene). Thus, membrane verification was performed following a modified protocol of Godio (2007).

Protocol development

- Place the membrane in a hybridization bag or in a tray.
- Equilibrate the membrane with 30 mL of buffer I¹⁶ for 1 min under constant agitation at RT.
- Replace the buffer I by 50 mL of buffer II¹⁷ and incubate for 30 min under the same conditions.
- Place the membrane into a new hybridization bag containing 15 mL of antibody solution¹⁸ and incubated for at least 30 min under constant agitation.
- Wash the membrane twice with buffer I for 15 min under constant agitation.
- Replace by 40 mL of buffer III¹⁹ and incubate for 2 min under the same conditions.
- Place the membrane into a new bag hybridization containing 10 mL of detection solution²⁰ and incubate for 20 - 30 min under constant agitation at RT, protected from light.

¹⁶ **Buffer I:** 100 mM maleic acid; 50 mM NaCl; pH 7.5.

¹⁷ **Buffer II:** Buffer I supplemented with 1% blocking reagent (Roche).

¹⁸ **Antibody solution:** Buffer II supplemented with a 1:15,000 diluted solution of Anti-Digoxigenin antibodies (*Anti-Digoxigenin-AP Fab fragments*, Roche)

¹⁹ **Buffer III:** 0.1 M Tris-HCl, pH 9.5; 0.1 M NaCl; 0.5 M MgCl₂ · 6 H₂O.

²⁰ **Detection solution:** Buffer III supplemented with 350 µg/mL NTB (Roche) and 175 µg/mL BCIP (Roche).

- Stop the reaction by washing the membrane with dH₂O.

Dark spots appeared on the membrane with lower intensity in serial dilutions.

b. DNA transfer to a nylon membrane

Total genomic DNA from *A. thiooxidans* was digested with four different restriction enzymes: BamHI (Fermentas), EcoRV, HindIII and XhoI (EURx), which did not cut inside the labelled probe. To determine the restriction enzymes that should be used, SeqBuilder v 7.1 software (DNASTAR, Lasergene) was used.

Protocol development

- Separate the digested DNA by electrophoresis in a 0.6% (w/v) agarose gel. Stain the gel by immersion in 2.0 µg/mL ethidium bromide. 1 µL of the PCR fragment without labelling was used as control.
- Wash the agarose gel with transfer solution²¹ (also called 20x SSC solution).
- Cut a nylon membrane (Hybond™-N+ membrane, GE Healthcare) 1 cm larger in each side than the gel and wet it with 20x SSC solution.
- Place the membrane into the transfer system according to the manufacturer's instructions. Mark the position of the wells into the membrane and connect the vacuum system (until reach 50 mbar).
- Cover the gel with depurination solution²² for 15 - 20 min.
- Remove the depurination solution and cover the gel with denaturation solution²³ for 15 - 20 min.
- Replace the denaturation solution by neutralizing solution²⁴ and incubate for 20 - 25 min.
- Then, remove neutralizing solution and cover the gel with transfer solution²¹ and incubate for 1 h.
- Remove the solution and fix the membrane by the application of three pulses of 120,000 µJ of UV light [*UV-Stratalinker 2400* (Stratagene)].
- Wash the nylon membrane with 2x SSC and let it dry.

In order to check the success of the transfer process, the agarose gel was recovered and visualised by staining again with ethidium bromide. No bands should appear on the gel.

²¹ **Transfer solution (20x SSC):** 3 M NaCl; 0.3 M sodium citrate; pH 7.0.

²² **Depurination solution:** 0.25 M HCl.

²³ **Denaturation solution:** 1.5 M NaCl; 0.5 N NaOH.

²⁴ **Neutralizing solution:** 1.5 M NaCl; 0.05 M Tris-HCl, pH 7.2; 1 mM EDTA.

c. DNA hybridization and detection

Protocol development

- Wet the membrane with 20x SSC²¹ solution and place it into a hybridization bag containing 0.2 mL/cm² of pre-hybridization solution²⁵. Incubate it in a water bath at 42°C for 1 - 4 h under constant agitation.
- Meanwhile, boil the labelled probe at 95°C for 10 min in order to denaturalize the DNA. Quickly, cool it on ice to avoid re-naturalization.
- Replace pre-hybridization solution by 0.2 mL/cm² of the hybridization solution²⁶ and incubate at least for 8 h under the same conditions (at 42°C and constant agitation).
- Wash the nylon membrane twice with 15 mL of wash buffer I²⁷ for 15 min under constant agitation at RT.
- Wash twice the membrane with 15 mL of wash buffer II²⁸ for 25 min under the same conditions.
- Equilibrate the membrane with 30 mL of buffer I for 1 min under constant agitation at RT.
- Replace the buffer I by 50 mL of buffer II and incubate for 30 min under the same conditions.
- Place the membrane into a new bag hybridization containing 15 mL of antibody solution¹⁸ and incubated for at least 30 min under constant agitation.
- Wash the membrane twice with buffer I¹⁶ for 15 min under constant agitation.
- Replace by 40 mL of buffer III¹⁹ and incubate for 2 min under the same conditions.
- Place the membrane into a new bag hybridization containing 10 mL of detection solution²⁰ and incubate for 20 - 30 min under constant agitation at RT protected from light.
- Stop the reaction by washing the membrane with dH₂O.

2.2. *A. thiooxidans* growth determination by quantitative PCR (q-PCR)

A 500-mL Erlenmeyer flasks containing 200 mL of AT medium were inoculated with 1 mL of a 7-days pre-grown culture, and incubated at 30°C and 200 rpm for 11 days. 1.5 mL samples were taken daily and filter through sterile filter paper. 1 mL of the sample was then centrifuged at 17,000 $\times g$ for 10 min and pellets were washed with 100 μ L of ddH₂O. Pellets were resuspended in 20 μ L of sterile ddH₂O. Samples were storage at -20°C until use. At the end of the fermentation, cell suspensions were quantified by q-PCR.

The q-PCR reactions were performed in the *Mx3005P qPCR System* (Stratagene) using the *SYBR TB Green Premix Ex Taq* (Takara). q-PCR reactions were carried out in triplicate in 96-well plates in a 20 μ l final volume containing 1 \times *TB Green Premix Ex Taq* (Takara), 200 nM of each primer and 5 μ L

²⁵ **Pre-hybridization solution:** 5x SSC; 30% formamide; 0.1% laurosylsarcosine; 0.02% SDS; 1% blocking reagent (Roche)

²⁶ **Hybridization solution:** Pre-hybridization solution supplemented with the labelled probe.

²⁷ **Wash buffer I:** 2x SSC; 0.1% SDS.

²⁸ **Wash buffer II:** 0.1x SSC; 0.1% SDS.

of a 1:10 diluted culture. Cells were disrupted by heat during the initial denaturation step. The cycling protocol was as follows: initial denaturation for 2 min, at 95°C; followed by 40 cycles of 20 s, at 95°C; 20 s, at 62°C; and a final extension of 1 min at 72°C. Melting curve assays were performed from 55 to 95 °C. Specific amplification was confirmed by a single peak in the melting curve. A standard curve of the C_T values vs initial DNA concentration was calculated using total DNA with a concentration from 2.5 fg to 25 ng, and it was used to determine the concentration of the unknown samples, based on their C_T values (Wilhelm *et al.*, 2003). Nuclease-free water was used as non-template control (NTC). Next, the amount of DNA in the unknown sample (fg) is split into the number of copies of the *16S rRNA* gene that exists in the initial sample, and is transformed by the length of the template (in bp) by the following formula:

$$\text{copies} = \frac{\text{fg (DNA)} \cdot N_A}{\text{length (bp)} \cdot M_{BP}}$$

Where N_A is Avogadro's Number ($6.022 \cdot 10^{23}$ molecules/mol), M_{BP} is the average weight of a base pair (bp) which is 660 g/mol, fg (DNA) is the amount of DNA based on its C_T , and length is the length of the template (in bp), which was 182 bp.

2.3. *A. thiooxidans* genome sequencing

A. thiooxidans total DNA was extracted as described by Bergamo *et al.* (2004) (see section 2.1.1), and sent to Macrogen (Humanizing Genomics Macrogen, Korea) for Pacbio and Illumina sequencing, *de novo* assembly and annotation.

Functional analysis of *A. thiooxidans* genome was carried out using RAST server (Rapid Annotation using Subsystem Technology) (www.rast.theseed.org/FIG/rast.cgi) (Aziz *et al.*, 2008; Overbeek *et al.*, 2014).

2.4. Determination of the pH stress conditions in *A. thiooxidans* by reverse transcription PCR (RT-PCR)

RT-PCR (reverse transcription polymerase chain reaction) is a molecular biology technique based on the PCR, which monitor the amplification of a targeted DNA molecule. In our case, the two-step RT-PCR was used, since the reverse transcription of the RNA to cDNA and the PCR steps were performed in separate tubes. Besides, a non-specific detection was carried out, using SYBR Green as dye. SYBR Green binds to all double-stranded DNA (including primer dimers), so it is important to verify the specificity of amplification with the melting peaks.

In order to determine the pH conditions for the *A. thiooxidans* proteome analysis, five different pHs were tested: 0.5, 1.5, 3.0, 5.5 and 6.0; at two different times: 30 and 60 min. Thus, differential

expression of four well-known stress genes was checked. Besides, *sdoA* expression was used as control.

Table 5. Oligonucleotides used for the RT-PCR assay.

| <i>Primer name</i> | <i>Primer sequence (5'-3')</i> |
|------------------------|------------------------------------|
| F_ <i>dnaJ</i> | TCGAAGTCAAAGTGCCGGCCGGAGTAGATA |
| R_ <i>dnaJ</i> | GCCGCGTCCCCAGCTCCCCTTACCATTAGAC |
| F_ <i>dnaK</i> | GGAAGGCGACAAGGTCAAGG |
| R_ <i>dnaK</i> | CGCGCACTTCCACCAGG |
| F_ <i>groEL</i> | ACTGCGGTATCTGTCGTCCTA |
| R_ <i>groEL</i> | GATCTGGCCGCTCCTCTA |
| F_ <i>rpoH</i> | TTGCGCAACTGGCGTATTGTCAAAGTGGCTACCA |
| R_ <i>rpoH</i> | CTTCAGCAATGGCCGCACTTCTCACCCTCAAC |
| F_ <i>sdoA</i> | CGAGGAAAATCTGCAGGTTGAGTGG |
| R_ <i>sdoA</i> | CGTTATAGATCTGGGCGAAAGTT |

The first step towards differential expression quantification by RT-PCR is the RNA extraction from the samples. Thus, six 500-mL Erlenmeyer flasks containing 200 mL of AT medium supplemented with 1% (w/v) elemental S were inoculated with 1 mL of a 7-days pre-grown culture, and incubated at 30°C and 200 rpm for 5 days. Cultures were then collected by centrifugation at 9,600 $\times g$ for 10 min into 50-mL tubes, and pellets were resuspended in 50 mL of AT medium at pH 3.0. Each 50-mL sample was spread out into 5 different tubes containing 10 mL each one. Samples were centrifuged at 9,600 $\times g$ for 10 min and each pellet was resuspended in 50 mL of AT medium at the defined pH (0.5, 1.5, 3.0, 5.5 or 6.0) (Figure 21). Samples were incubated at 30°C and 200 rpm, and three tubes per pH condition were incubated for 30 min and the other three for 60 min.

Protocol development

- Centrifuge the samples at 9,600 $\times g$ for 10 min after the incubation at the corresponding pH for 30 or 60 min.
- Add 1 mL of TRIzol reagent (Invitrogen) and resuspend the pellet mixing by pipetting.
- Incubate at RT for 5 min.
- Add 0.3 mL of chloroform and incubate 2 - 3 min at RT.
- Centrifuge 15 min at 17,000 $\times g$ and 4°C.
- Transfer the upper phase (aqueous phase) to a new 1.5-mL microtube.
- Add 0.55 volumes of isopropanol and incubate at RT for 15 min.
- Centrifuge 10 min at 17,000 $\times g$ and 4°C.
- Discard the supernatant and wash the pellet with 1 mL of 70% (v/v) ethanol. Centrifuge at 17,000 $\times g$ and 4°C for 5 min and discard the supernatant.

- Resuspend the RNA with 50 μL of ddH₂O (RNase free) and quantify with *NanoDrop 2000 Spectrophotometer* (Thermo Scientific).

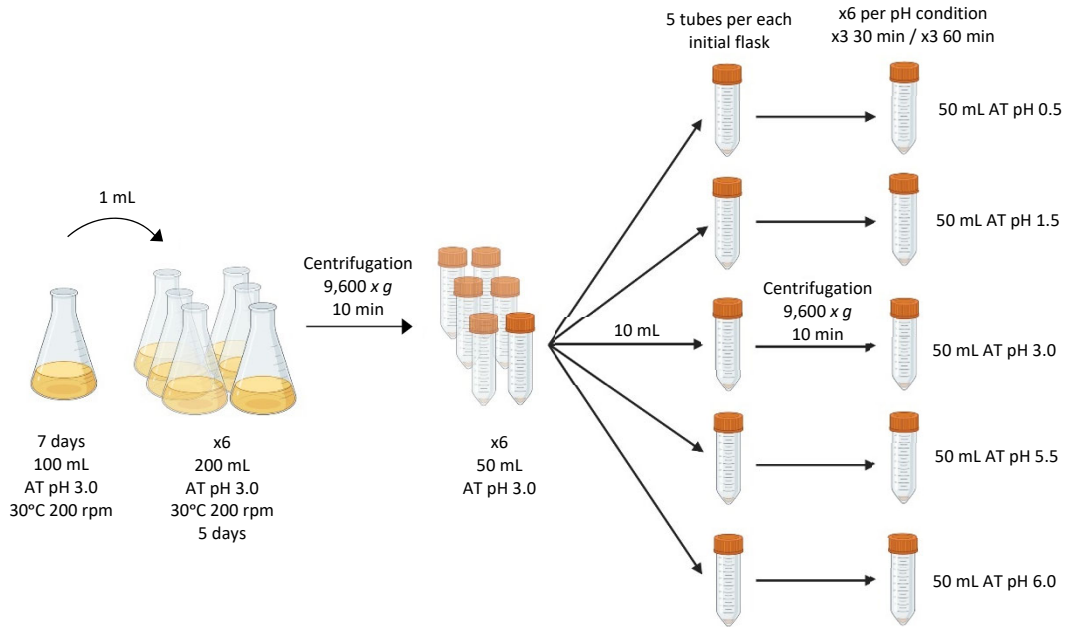


Figure 21. Diagram explaining the sample collection for the RT-PCR assay. Six flasks containing 200 mL cultures were collected by centrifugation and pellets were resuspended in 50 mL of AT medium at pH 3.0. Each sample was then spread out in 5 different tubes, which were centrifuged and resuspended in the corresponding pH. Thus, one pH condition was obtained from each flask, with a total of 6 samples per pH condition. Three of them were incubated for 30 min and the other three for 60 min at 30°C and 200 rpm.

Once the RNA is extracted, cDNA was synthesized via reverse transcription:

Protocol development

Step one:

- Place 1 μg of RNA in a new microtube.
- Add 1 μL of DNase I, RNase free (Thermo Scientific) and 1 μL of 10x Reaction buffer supplemented with MgCl₂ and RNase free H₂O (Takara) up to 10 μL .
- Incubate at 37°C for 30 min.
- Stop the reaction by adding 1 μL of 25 mM EDTA and incubate 10 min at 65°C. Quantify with *NanoDrop 2000 Spectrophotometer* (Thermo Scientific).

Step two:

- Place 500 ng of RNA in a new microtube and add 2 μ L of 5x *PrimeScript RT Master Mix* (Takara) and ddH₂O RNAse free up to 10 μ L.
- Incubate the reaction at 37°C for 15 min and stop the reaction by incubating the samples at 85°C for 5 s. Store the samples at 4°C until use.

Transcript levels of the selected genes were determined by quantitative reverse transcription PCR (RT-PCR). RT-PCR reactions were carried out in triplicate in 96-well plates in a final volume of 20 μ L containing 1x *TB Green Premix Ex Taq* (Takara), and 100 nM forward and reverse primers (Table 5). Cycling parameters were the following:

Table 6. Cycling parameters of the RT-PCR for the six selected genes.

| Cycles | <i>groEL2</i> | <i>dnaJ</i> | <i>rpoH</i> | <i>dnaK</i> | <i>sdoA</i> |
|--------|---------------|-------------|----------------------------|-------------|-------------|
| x1 | | | 95°C ; 2 min | | |
| x40 | 60°C ; 20 s | 62°C ; 20 s | 95°C ; 20 s 62°C ; 20 s | 60°C ; 20 s | 58°C ; 20 s |
| x1 | | | 72°C ; 1 min | | |

Melting peaks were visualized to check the specificity of the amplification. The results obtained for each gene of interest were normalized to the expression of *sdoA* gene. Three biological, with three technical replicates, were used. Relative gene expression was determined with the formula fold induction: $2^{-\Delta\Delta Ct}$, where:

$$\Delta\Delta Ct = \Delta Ct (EC) - \Delta Ct (CC)$$

$$\Delta Ct = Ct_{TG} - Ct_{RG}$$

Ct (cycle threshold) value is based on the threshold crossing point of individual fluorescence traces of each sample. CC is the control condition (pH 3.0 in our case) and EC are the experimental conditions (the rest of the conditions). On the other hand, TG are the target genes (*groEL*, *dnaJ*, *dnaK* and *rpoH*) and RG are the reference genes (*sdoA*). The genes analysed were considered significantly up- or downregulated when differences of expression ratio were higher than 2 or lower than 0.5, respectively.

2.5. *A. thiooxidans* SOB3 proteome analysis under pH stress by 2D DIGE analysis

2.5.1. Preparation of *A. thiooxidans* protein extracts

Without prior information in this regard, one would expect that the strain could have a complex and thick cell membrane due to the extreme conditions to grow, so it should be considered to use vigorous lysis methods, such as sonication or glass bead homogenization.

a. *A. thiooxidans* protein extraction by glass beads homogenization

A. thiooxidans protein extracts were prepared from cells grown to the mid-exponential growth phase in AT liquid medium. Thus, 10 L of AT medium supplemented with 0.1% elemental sulphur were inoculated at 0.25% (v/v) with a 5-days grown pre-culture. The culture was grown for 65 h and centrifugated at 10,700 $\times g$ for 10 min. The pellet was resuspended into 30 mL of AT medium at pH 3.0 and separated into 3 tubes containing 10 mL of the sample. They were centrifugated at 10,700 $\times g$ for 10 min and each tube was resuspended in 50 mL of AT medium at the corresponding pH: 0.7, 3.0 or 6.0. Flasks containing 50 mL of AT medium at the corresponding pH were inoculated with 10 mL of the sample and they were incubated at 30°C and 200 rpm for 90 min. Samples were centrifugated at 10,700 $\times g$ for 10 min and pellets were washed with 1 mL of cold and sterile ddH₂O. After removal of the supernatant, protein extraction was carried out by following Barreiro *et al.* (2005) protocol:

Protocol development

- Resuspend the pellet in 800 μ L of washing buffer²⁹ containing a protease inhibitor mix (COMPLETE, Roche) and add the sample into a *FastProtein BLUE tube BIO 101* (MP Biomedicals) containing a silica-ceramic matrix of 0.1 mm of diameter.
- Cell disruption was carried out in a *Savant Bio 101 FastPrep FP120 cell disruption system* Fastprep (MP Biomedicals) machine at a speed ratio of 6.5 m/s for three-time intervals of 30 s, and 1 min resting on ice.
- Centrifuge the samples at 16,168 $\times g$ for 10 min to remove cell debris and silica matrix.
- Transfer the supernatant to a new tube and add 1 μ L of Benzonase³⁰ (Merck). Incubate the samples for 30 min at 37°C.

b. *A. thiooxidans* protein extraction by sonication

A. thiooxidans protein extracts were prepared from cells grown to the mid-exponential growth phase in AT liquid medium. Thus, 200 mL of AT medium supplemented with 1% elemental sulphur were inoculated at 0.25% (v/v) with a 5-days grown pre-culture. The culture was grown for 65 h and

²⁹ **Washing buffer:** 50 mM Tris-HCl; pH 7.2.

³⁰ **Benzonase:** Mix of RNase I and DNase I (Merck).

centrifugated at 10,700 x g for 10 min. After removal of the supernatant, protein extraction was carried out by sonication with an *Ultrasonic Processor XL* sonicator (Misonix):

Protocol development

- Resuspend the pellet in 800 µL of washing buffer²⁹ containing a protease inhibitor mix (COMPLETE, Roche).
- Sonicate the samples for five-time intervals of 10 s, and 1 min resting on ice.
- Centrifuge the samples at 16,168 x g for 30 min.
- Transfer the supernatant to new tube and add 1 µL of Benzonase³⁰ (Merck). Incubate the sample for 30 min at 37°C.

c. Protein precipitation with acetone

After protein extraction, the proteins are present in a wide dynamic range of concentrations in the whole cell lysates. Thus, precipitation of the proteins in the sample and removal of interfering substances are optional steps, but recommended, and depends on the nature of the sample and the experiment goal. So, for a 2-D DIGE analysis, both steps are crucial to assure the quantity and quality needed of protein sample. The precipitation step was carried out using acetone, since proteins are insoluble in acetone (specially at low temperatures), while other molecules such as hydrocarbons are soluble. Thus, this method allows to wash and concentrate the protein from a culture sample (Barreiro *et al.*, 2017).

Protocol development

- Add 4-9 volumes of cold acetone and incubate the sample at -20°C O/N.
- Centrifuge the sample at 3,220 x g and 4°C for 5 min.
- Wash the pellet with acetone 80% (v/v) and centrifuge the samples at 3,220 x g and 4°C for 5 min.
- Let the pellet air-dry and resuspend in 100 µL of rehydration buffer³¹.
- Quantify the crude extract protein by the Bradford assay (see section 2.5.2) and store at -20°C until use.

2.5.2. Protein concentration quantification by Bradford assay

Protein quantification was carried out by Bradford assay (Bradford, 1976), by mixing the samples with *Bio-Rad Protein Assay Dye Reagent Concentrate* (BioRad), following manufacturer's instruction. This method is based on the absorption change from 465 nm to 595 nm of the Coomassie blue when

³¹ **Rehydration buffer:** 8 M urea; 2% (w/v) CHAPS [3-[(3-cholamidopropyl) dimethylammonio]-1-propanesulfonate]; 0.01% bromophenol blue.

mixed with proteins. The standard curve was carried out with bovine serum albumin (BSA, Fermentas) from a stock solution at 0.25 mg/mL as follow:

Table 7. Preparation of the standard curve of BSA for the protein quantification by Bradford method.

| | | | | | | | | | | |
|--|-----|-----|------|-----|------|-----|------|-----|------|-----|
| Total protein (μg) | 0 | 0.5 | 1.25 | 2.5 | 3.75 | 5 | 6.25 | 7.5 | 8.75 | 10 |
| V (stock) (μL) | 0 | 2 | 5 | 10 | 15 | 20 | 25 | 30 | 35 | 40 |
| V (ddH ₂ O) (μL) | 800 | 798 | 795 | 790 | 785 | 780 | 775 | 770 | 765 | 760 |

Protocol development

- Transfer 1 μL of protein samples to a new 1.5-mL microtube and add dH₂O until a final volume of 800 μL .
- Add 200 μL of Bradford reactive (*Bio-Rad Protein Assay Dye Reagent Concentrate*, BioRad). Mix gently and incubate in the dark for 5 min.
- Mix the samples and measure absorbance at 595 nm.

2.5.3. 1D: SDS-PAGE (sodium dodecyl sulphate-polyacrylamide gel electrophoresis)

SDS is an anionic detergent that dissociate the proteins into their monomers and break non-covalent forces (hydrogen-bonding, hydrophobic and ionic interactions), which are partially responsible for the three-dimensional structure of a native protein. Thus, it masks the charge of the proteins themselves and the formed anionic complexes have a roughly constant net negative charge per unit mass. SDS-PAGE was carried out by following Laemmli protocol (1970). So, acrylamide gels have two different phases: upper phase is the stacking gel (which concentrate the proteins, making them start from the same point) (Table 8) and the lower phase is the separating gel, which separate the proteins on the basis of molecular weight (Table 9). Both phases have the same compounds but different concentrations, so they have different characteristics, such as pH or ionic strength. Besides, both gels have TEMED (N,N,N',N'-Tetramethylethylenediamine), which acts as catalyst, and APS (ammonium persulphate), which is the radical initiator of the polymerization process.

Protocol development

- Assembly the glass-plates with the *Mini-Protean II* system (BioRad) for 8 cm gels following manufacturer's instructions, with 0.75 mm spacers.
- Prepare the mix for the separating gel (Table 9), being PSA the last compound to be added.
- Add the mix between the glass-plates without creating bubbles. Cover the mix with isopropanol and let the gel polymerize.
- Remove the isopropanol and wash the surface of the gels with ddH₂O.
- Prepare the mix for the stacking gel (Table 8).

- Put the comb between the glass-plates and add the mix of the stacking gel. Let the gel polymerize.
- Mix 20 µg of total protein (in a final volume of 10 µL) with 10 µL of denaturalizing buffer³² and boil the samples for 5 min. Immediately, place the samples on ice.
- Run the gels into an electrophoresis chamber with electrophoresis buffer³³ at 100 - 150 V.

Table 8. Composition of the stacking phase for SDS-PAGE for a final volume of 10 mL.

| | |
|--|---------|
| Acrylamide / bis-acrylamide 37.5:1 ³⁴ | 1.3 mL |
| Tris-HCl 0.5 M pH 6.8 | 2.5 mL |
| SDS 20% (w/v) | 50.0 µL |
| APS 10% (w/v) | 50.0 µL |
| TEMED | 10.0 µL |
| ddH ₂ O | 6.1 mL |

Table 9. Composition of the separating phase for SDS-PAGE for a final volume of 10 mL and a final concentration of acrylamide/bis-acrylamide of 12% (w/v).

| | |
|--|---------|
| Acrylamide / bis-acrylamide 37.5:1 ³² | 4.0 mL |
| Tris-HCl 1.5 M pH 8.8 | 2.5 mL |
| SDS 20% (w/v) | 50.0 µL |
| APS 10% (w/v) | 50.0 µL |
| TEMED | 5.0 µL |
| ddH ₂ O | 3.4 mL |

5 µL of *Precision Plus Protein Standards* (Bio-Rad) was used as molecular weight marker. Gels were stained following the “blue silver” Colloidal Coomassie staining method (see section 2.5.4) (Jami *et al.*, 2010).

³² **Denaturalizing buffer:** 350 mM Tris-HCl, pH 6.8; 2% SDS; 30% glycerol; 0.02 % (w/v) bromophenol blue; 0.6 M DTT.

³³ **Electrophoresis buffer:** 250 mM Tris base; 2 M glycine; 1% (p/v) SDS; pH 8.3.

³⁴ **Acrylamide/bis-acrylamide:** commercial solution (Protogel, National Diagnostics) containing 30% (w/v) acrylamide : 0.8 (w/v) bis-acrylamide (37.5 :1).

2.5.4. Colloidal Coomassie staining method

The staining protocols mainly consist on: **i)** fixation, to immobilize the proteins on the gel and eliminate SDS, buffers and other contaminants, **ii)** staining of the gel with organic dyes such as Coomassie blue, or formulations for the deposition of metals like silver, and, **iii)** a final stage to carry out the staining reaction when using metals, or the washes to reduce the background of the organic dyes (Candiano *et al.*, 2004; Steinberg, 2009).

In our case, a colloidal Coomassie blue staining was carried out. Colloidal Coomassie can be formulated to effectively stain proteins within 1 hour and requires only water (no methanol or acetic acid) for fading. This protocol has numerous advantages: it is quick, simple and reversible, among others. Because no chemical modification occurs, excised protein bands can be completely faded and the proteins recovered for analysis by mass spectrometry or sequencing.

Protocol development

- Incubate the gel in 50 mL of fixation buffer³⁵ for 30 min.
- Wash the gel three times by incubating it in 50 mL of ddH₂O for 10 min each.
- Place the gel in a Coomassie solution³⁶ and stain O/N.
- Place the gel in ddH₂O to de-stain the gel, to visualize the separated protein molecules as bands.

2.5.5. 2D protein electrophoresis

a. First-dimension: isoelectric focusing (IEF).

Proteins are amphoteric molecules: they can present either positive, negative or zero net charge, depending on the pH of their surroundings. The net charge of a protein is the sum of all the negative and positive charges of its amino acid side chains, and amino- and carboxyl-termini. The isoelectric point (pI) is the specific pH at which the net charge of the protein is zero. Thus, proteins are positively charged at pH values below their pI and negatively charged at pH values above their pI. In a pH gradient, and under the influence of an electric field, a protein will move to the gradient position where its net charge is zero (Gorg, 2004).

Thus, the IEF was carried out with the *IPGphor Isoelectric Focusing System* (Amersham Biosciences), with a 7 cm IPG strips (*Immobiline DryStrips gels*, GE Healthcare) nonlinear (NL) gradient pH from 3 to 10 and linear gradient pH from 4 to 7.

³⁵ **Fixation buffer:** 7% (v/v) acetic acid; 7% (v/v) methanol.

³⁶ **Coomassie brilliant blue G250 dye solution:** 10% (v/v) phosphoric acid; 10% (w/v) ammonium sulphate; 0.12% (w/v) Coomassie brilliant blue G250 dye; 20% (v/v) methanol. Filter through a filter paper (Candiano *et al.*, 2004).

Protocol development

- Place 80 - 100 µg of protein in a new microtube. Add rehydration buffer (RB)³⁷, supplemented with 1% IPG buffer³⁸ and 65 mM DTT (dithiothreitol), to a final volume of 125 µL.
- Place the mix into the holder for 7 cm IPG strips.
- Place the strip in the holder, over the mix. Avoid air bubbles trapped between the sample and the strip.
- Cover the strip with 1 mL of *DryStrips Cover Fluid* (GE Healthcare).
- Run the electrophoresis at 50 µA/strip and 20°C: 1 h 0 V (rehydration); 12 h 30 V; 30 min 60 V; 30 min 300 V; 30 min 1,000 V; 30 min (gradient) until 5,000 V; and 5,000 V up to reach a total of 10,000 Vh (2 h approx.).
- Store the strips at -80°C until use.

b. Second-dimension: SDS-PAGE

As described above for 1-D gels, SDS denatures proteins masking their net charge. Besides, the DTT from the IEF step is a reducing agent which reduces disulphide bonds from the proteins, preserving the fully reduced state of denatured, unalkylated proteins. Both together, make the proteins run through the acrylamide just by their molecular weight. Finally, before second dimension running, samples are incubated with iodoacetamide (IAM), which alkylates thiol groups of proteins to avoid the re-oxidation during the electrophoresis.

Protocol development

- Assemble the glass-plates with the *Mini-Protean II* system (BioRad) for 7 cm gels, following manufacturer's instructions, with 1.50 mm spacers.
- Prepare the mix for the separating gel (Table _), being PSA the last compound to be mixed.
- Add the mix between the glass-plates without creating bubbles. Cover the mix with isopropanol and let the gel polymerize.
- Remove the isopropanol and wash the surface of the gels with ddH₂O.
- Incubate each IEF strips with 5 mL of equilibration buffer³⁹ supplemented with 1% DTT for 15 min in constant agitation.
- Remove the buffer and replace it for 5 mL of equilibration buffer supplemented with 4% IAM in constant agitation.

³⁷ **Rehydration buffer (RB):** 8 M urea; 2% (w/v) CHAPS (3-[[3-cholamidopropyl] dimetilamonio]-1-propanesulfonate); 0.002% (w/v) bromophenol blue. Filter through 0.45 µM membrane (Millipore). Store at -20°C.

³⁸ **IPG buffer:** commercial mix (Cytiva, formerly GE Healthcare) of ampholytes to improve protein migration and produce more uniform conductivity along the Immobiline DryStrip during focusing.

³⁹ **Equilibration buffer:** 2% (w/v) SDS; 50 mM Tris-HCl, pH 8.8; 6 M urea; 30% (v/v) glycerol; 0.002% bromophenol blue.

- Wash the IEF strips with ddH₂O and place them into the glass-plates.
- Run the gels into an electrophoresis chamber with electrophoresis buffer⁴⁰ at 100 - 150 V.
- Stain the gel by the colloidal Coomassie staining method (see section 2.5.4).

5 µL of *Precision Plus Protein Standards* (Bio-Rad) was used as molecular weight marker.

2.5.6. 2-D DIGE analysis

2-D Fluorescence Difference Gel Electrophoresis (2-D DIGE) is a method that labels protein samples prior to 2-D electrophoresis, enabling accurate analysis of differences in protein abundance between experimental groups. Thus, labelling samples with up to three fluorescent dyes (*CyDye DIGE Fluor dyes*) during 2-D DIGE offers a quantitative analysis of protein expression. This ability to separate more than one sample in a single gel permits the inclusion of up to two samples and an internal standard (internal reference) in every gel. The internal standard is prepared by mixing equal amounts of each sample and replicates in the experiment and including this mixture on each gel (Gorg, 2004).

a. 2-D Clean-up

Protein extraction and sample clean-up are the main steps to ensure an optimal resolution and reduce variability of 2-D gels. Clean-up is designed to prepare samples for an optimal 2-D DIGE labelling, removing salts, detergents, denaturants or organic solvents. Thus, *Clean-Up Kit* (GE Healthcare) was used following manufacturer's instructions.

Protocol development

- Transfer 200 µg of protein in a maximum volume of 100 µL to a 1.5-mL microtube.
- Add 300 µL of precipitant. Mix by vortexing and incubate on ice for 15 min.
- Add 300 µL of co-precipitant to the mixture and mix by vortexing.
- Centrifuge at 16,168 x g and 4°C for 5 min.
- Remove the supernatant by pipetting. Centrifuge the tubes to bring any remaining liquid to the bottom of the tubes.
- Without disturbing the pellet, layer 40 µL of co-precipitant on the pellet. Incubate on ice for 5 min.
- Remove the supernatant by pipetting. Centrifuge the tubes to bring any remaining liquid to the bottom of the tubes.
- Resuspend the pellet in 100 µL of ddH₂O by pipetting or vortexing.
- Add 1 mL of prechilled wash buffer (-20°C) and 5 µL of wash additive. Mix by vortexing or pipetting until the pellet is fully dispersed.
- Incubate at least 30 min at -20°C.

⁴⁰ **Electrophoresis buffer:** 250 mM Tris base; 2 M glycine; 1% (p/v) SDS; pH 8.3.

- Centrifuge at 16,168 x g and 4°C for 5 min.
- Totally remove the supernatant by pipetting. Centrifuge the tubes to bring any remaining liquid to the bottom of the tubes. Ensure supernatant elimination.
- Resuspend the pellet in 20 µL of resuspension buffer⁴¹ supplemented with 30 mM Tris.
- Centrifuge at 16,168 x g for 30 seg to remove any insoluble material and reduce any foam.
- Adjust the pH of the sample to 8 – 8.5 with 100 mM NaOH.
- Measure final pH by means of pH indicator strips.
- Quantify the protein samples by Bradford protocol (see section 2.5.2).

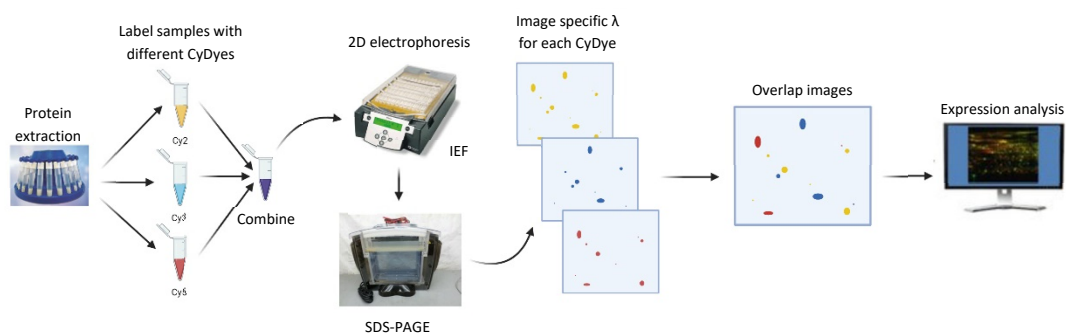


Figure 22. 2-D DIGE analysis scheme from the protein extraction by FastPrep to the analysis of the differential expression by DeCyder™ Image Analysis Software (GE Healthcare).

b. Minimal labeling proteins with CyDye DIGE Fluor minimal dyes

CyDye DIGE Fluor minimal dyes consist of three bright, spectrally resolvable fluors (Cy2, Cy3, and Cy5). The dyes contain an N-hydroxysuccinimidyl ester reactive group, which forms a covalent bond with the lateral amino group of lysine residues. To assure minimal labelling, the concentration of dye present in a protein labelling is limiting, to lead the labelling of 1 - 2% of lysine residues (Gorg, 2004).

Protocol development

- Keep the dyes at RT at least 10 min to avoid water condensation.
- Reconstitute CyDye DIGE Fluor minimal dyes with 99% anhydrous N,N-dimethylformamide (DMF) to a final concentration of 1 nmol/µL. This is the called stock dye solution and is stable for two months at -20°C.

⁴¹ **Resuspension buffer (RB2):** 8 M urea; 4% (w/v) CHAPS (3-[[3-cholamidopropyl] dimetilamonio]-1-propanesulfonate. Filter through 0.45 µM membrane (Millipore). Store at -20°C.

- Dilute the stock dye solution to 0.4 nmol/ μL (working dye solution) with DMF. This solution is stable for one week at -20°C .
- Add 1 μL of Cy3 or Cy5 working solution to a sample containing 50 μg of protein. Mix by vortexing and centrifuge at $16,168 \times g$ for 30 seg. Label replicates of the same condition with different dyes (dye swap).
- For internal standard dye, add 25 μg of each sample to a microtube and add $x \mu\text{L}$ of Cy2 (when x is half the number of total gels).
- Incubate samples 30 min on ice in the dark.
- Stop the labelling reaction by adding 1 μL of 10 mM lysine and incubate for 10 min on ice and in the dark.

c. First dimension IEF

Soluble proteins in sample buffer were isoelectrofocussed on an IPGphor apparatus, by means of 3-10 NL Immobiline™ 18-cm IPG strips (GE Healthcare).

Protocol development

- Pair samples labelled with Cy3 and Cy5 and add the internal standard.
- Add RB³⁷ supplemented with 1% IPG buffer³⁸ and 80 mM DTT to a final volume of 350 μL .
- Place the mix into the holder for 18 cm IPG strips.
- Place the strip in the holder, over the mix. Avoid air bubbles between the sample and the strip.
- Cover the strip with 2 – 2.5 mL of *DryStrips Cover Fluid* (Amersham Biosciences).
- Run the electrophoresis at 100 $\mu\text{A}/\text{strip}$ and 20°C : 1 h 0 V; 12 h 30 V (rehydration); 2h 60 V; 1 h 500 V; 1 h 1,000 V; 30 min gradient until 8,000 V; and 8,000 V until 50,000 kWh (6 - 7 h approx.).
- Store the samples at -80°C until use.

d. Second dimension SDS-PAGE

Protocol development

- Assembly the *Ettan DALT six* gel casting cassettes (GE Healthcare) for 24 cm gels, following manufacturer's instructions with 1 mm spacers.
- Prepare the mix for the separating gel (Table 10) and degas it by continuous stirring for 30 min.
- Add the PSA to the mixture and place it between the glass-plates avoiding bubbles. Cover the mix with isopropanol and let the gel polymerize (1 h approx.).
- Remove the isopropanol and wash the surface of the gels with ddH₂O. Cover the gels with lower electrophoresis buffer⁴² 1x and storage them at 4°O/N .

⁴² **Lower electrophoresis buffer 5x:** 15.2 g/L of Tris; 72 g/L of glycine; 5 g/L of SDS.

- Incubate each IEF strips with 10 mL of equilibration buffer⁴³ supplemented with 1% DTT for 15 min in constant agitation. Remove the buffer and replace it for 10 mL of equilibration buffer supplemented with 4% IAA in constant agitation.
- Wash the IEF strips with ddH₂O.
- Insert the gels into the *Ettan DALT electrophoresis unit* and add 5 L of 1x lower electrophoresis buffer and 1 L of upper electrophoresis buffer⁴⁴.
- Place the strips on the top pf each gel.
- Run the electrophoresis at 3 W per gel for 45 min and 1.3 W per gel until 100 W (12 h approx.).

5 μ L of *Precision Plus Protein Standards* (Bio-Rad) was used as molecular weight marker. Gels were scanned by *Ettan Dige Imager Software 1.0* (GE Healthcare) and stained following the “blue silver” Colloidal Coomassie staining method as described above (see section 2.5.4).

Table 10. Composition of the protein denaturalizing acrylamide gels for the second dimension for a final volume of 400 mL (6 gels of *Ettan DALT Six*, Amersham Bioscience) and a final concentration of 12.5% (w/v) acrylamide/bis-acrylamide.

| | |
|--|---------------|
| Acrylamide / bis-acrylamide 37.5:1 ³² | 166.8 mL |
| Tris-HCl 1.5 M pH 8.8 | 100.0 mL |
| SDS 20% (w/v) | 4.0 mL |
| APS 10% (w/v) | 2.0 mL |
| TEMED | 132.0 μ L |
| ddH ₂ O | 129.2 mL |

e. Image analysis with DeCyder 2-D Differential Analysis Software

The software consists of an automated image analysis software suite that enables the detection, quantitation, matching, and study of gel spots used with Ettan DIGE system. The co-detection algorithm in *DeCyder 2-D software* co-detects overlaid image pairs and produces identical spot boundaries for each pair. This allows direct spot volume ratio measurements and therefore produces an accurate comparison of every protein with its representative in-gel internal standard (Gorg, 2004).

In this case, difference protein expression was analysed with: **i)** *p*-value less than 0.05, **ii)** difference of expression ratio higher than 2 and lower than -2, **iii)** at least appeared in 70% of gel images, and **iv)** with a minimal volume higher than 4,000. False Discovery Rate (FDR) was applied.

⁴³ **Equilibration buffer:** 2% (w/v) SDS; 50 mM Tris-HCl, pH 8.8; 6 M urea; 30% (v/v) glycerol; 0.002% bromophenol blue.

⁴⁴ **Upper electrophoresis buffer:** 8.5 g/L of Tris; 40.3 g/L of glycine; 2.8 g/L of SDS.

f. Protein digestion and MALDI-ToF/ToF detection

Mass spectrometry is a technique for analyzing molecular weights based on the motion of ionized samples in an electrical field. Briefly, to proceed with the identification of the proteins and the analysis of the difference in protein expression, spots are picked and digested. The picked spots are digested with trypsin, the resultant peptides are mixed with matrix (α -hydroxycinnamic acid), and spotted onto MALDI-ToF MS well insert (Applied Biosystem) and analysed by MALDI-ToF/ToF (mod. 4800, Applied Biosystem) (Havliš *et al.*, 2003).

Protocol development

- Pick the spots with a tip and place them into a microtube with 50 μ L of ddH₂O. Take special care with keratin contaminations, which can mask the protein identification.
- Replace the ddH₂O with 50 μ L of acetonitrile (ACN) and incubate in agitation at 25°C and 1,400 rpm for 5 min. Remove the ACN and add 50 μ L of ddH₂O. Incubate in thermoblock at 21°C and 300 rpm for 10 min. Repeat three times the ACN-H₂O wash-step.
- Replace the ddH₂O with 50 μ L of ACN and incubate in thermoblock at 25°C and 1,400 rpm for 5 min. Remove the ACN.
- Dry the spots by speed-vac (30 min approx.).
- Add 50 μ L of 25 mM ammonium bicarbonate (AMBI) supplemented with 10 mM DTT. Incubate the samples at 56°C and 300 rpm for 30 min in thermoblock.
- Replace the AMBI with 50 μ L of ACN and incubate at RT for 1 min.
- Remove the ACN and add 50 μ L of 10 mg/mL iodoacetamide (IAM). Incubate 15 min at RT in the dark.
- Replace the IAM with 50 μ L of ACN and incubate 5 min at RT. Remove the ACN.
- Add 50 μ L of AMBI and incubate 5 min at RT. Add 50 μ L of ACN and incubate 15 min at RT. Remove the supernatant.
- Dry the spot by speed-vac (30 min approx.).
- Add 5 μ L of AMBI supplemented with 10 ng/ μ L trypsin (Promega) and incubate 45 min on ice.
- Remove the supernatant and add 50 μ L of AMBI.
- Incubate at 37°C at least 6 h (it could be O/N).
- Transfer the supernatant to a new tube. The supernatant from the next extractions will be also placed in this tube.
- Add to the tube containing the spot, 0.5% trifluoroacetic acid (TFA) and 50% ACN and sonicate 10 min. Transfer the supernatant to the previous tube.
- Add 10 μ L of ACN to the tube containing the spot and incubate 10 min at RT and sonicate 5 min. Transfer the supernatant to the previous tube.
- Dry the tube with the three extraction supernatants by speed-vac (at least 2 h).
- Resuspend the digested protein with 4 μ L of 0.1% TFA and 50% ACN by sonication in a bath for 5 min.
- Store samples at 4°C until use.

- Spot 1 μL of the sample onto a MALDI-ToF well insert (Applied Biosystem). Let it dry. Spot 0.5 μL of MALDI-ToF matrix (LaserBio Labs).

Samples were analysed with 4800 Proteomics Analyser (MALDI-ToF/ToF, AB Sciex). A 4700 Proteomics analyser calibration mixture (Cal Mix 5, AB Sciex) was used as external calibration. All MS spectra were internally calibrated using peptides from the auto-digested trypsin. The analysis by MALDI-ToF/ToF mass spectrometry produced peptide mass fingerprints (PMF), and the peptides observed (up to 65 peptides per spot) were collected and represented as a list of monoisotopic molecular weights with signal to noise (S/N) ratio > 20 , using the 4000 Series Explorer V3.5.3 software (AB Sciex). All known contaminant ions (trypsin- and keratin-derived peptides) were excluded from later MS/MS analyses. From each MS spectra, the 10 most intensive precursors with an S/N > 20 were selected for MS/MS analyses with CID (atmospheric gas was used) in 2-kVion reflector mode and precursor mass windows of ± 7 Da. For protein identification, Mascot Generic Files combining MS (PMF) and tandem MS (MS/MS) spectra were automatically created and used to query a non-redundant protein database using a local license of Mascot v 2.2 from Matrix Science through the Global Protein Server v 3.6 (Applied Biosystems). Search parameters for peptide mass fingerprints and tandem MS spectra obtained were as follows: **i)** Uniprot γ -proteobacteria (date 2021.03.07), *A. thiooxidans* SOB3 FASTA proteome sequence and every *Acidithiobacillus* strain FASTA proteome sequences (date 2021.03.12) were used as database (950,740 sequences, 311,457,478 residues); **ii)** fixed and variable modifications were considered (Cys as S-carbami-domethyl derivative and Met as oxidized methionine); **iii)** one missed cleavage site was allowed; **iv)** precursor tolerance was 150 ppm and MS/MS fragment tolerance was 0.3 Da; **v)** peptide charge: 1+; **vi)** the algorithm was set to use trypsin as the enzyme (García-Calvo *et al.*, 2018).

3. Results and discussion

3.1. *A. thiooxidans* growth determination by qPCR

The first problem that can be found when working with *A. thiooxidans* is the difficulty in effectively determining its growth. Despite some manuscripts have described the measure of *Acidithiobacillus* growth by optical density (OD) (X. Li *et al.*, 2014; Nguyen *et al.*, 2016), or with an haemocytometer (Méndez-Tovar *et al.*, 2019; Negishi *et al.*, 2005), in our hands it was impossible to obtain a real growth curve following these methods.

Thus, it has been described that the absorbance of an *A. thiooxidans* curve range from 0.05 to 0.1, reaching maximum absorbance around 10 - 15 days, during the stationary phase when they have up to 10^8 cells/mL of concentration (Konishi *et al.*, 1995). Nevertheless, other groups claim that elemental sulphur presence in the media misrepresent the measures. In our culture conditions, the cultures showed absorbances from 0.02 to 0.05, with high deviations.

So, another option is to use a cell counter cytometer with a Live/Death marker (Camacho *et al.*, 2020). According Camacho's group, stationary phase is reached after 4 - 5 days into minimal medium supplemented with elemental sulphur. Nevertheless, this method was not an option for us, since we did not have the needed equipment.

On the other hand, there is another group that have used an haemocytometer under the phase-contrast microscope, getting higher magnification with fixed cells (Naseri *et al.*, 2019). Any case, again, this was not an option for us.

Other of the most common options, is the ufc count on agar plates. However, it was impossible to reach a real curve from liquid cultures, since inconsistent results were found: **i)** no correct relation between the dilutions, and **ii)** huge differences between concentrations estimated in days in a row. As a result, it is not surprising that some of the authors working with *A. thiooxidans* does not quantify its growth (Calle-Castañeda *et al.*, 2018b). Nevertheless, it is important to know how *A. thiooxidans* grows for performing any molecular study. Thus, a growth curve was carried out by using q-PCR. q-PCR is a method to measure the amplification of a target sequence, through a standard curve previously made with a sample of known concentration of this target sequence. The standard curve is made by relating the C_t to the number of copies of the amplified sequence, by using the following formula:

$$\text{copies} = \frac{fg(DNA) \cdot N_A}{\text{length}(bp) \cdot M_{BP}}$$

However, when the growth curve is made with culture samples, *A. thiooxidans* cells could have more than one copy of the sequence of study. Then, once the initial number of copies of the target sequence is determined, it must be divided among the copies of each cell to determine the initial number of cells in the sample.

In this case, *16S rRNA* gene was selected as target gene, and its number of copies was determined by Southern Blotting (data not shown), and by genome sequencing (see section 3.2, Figure 29). **In both cases, the copy number was two.**

3.1.1. Standard curve

A calibration curve from 2.5 fg to 25 ng was first performed by relating DNA template concentration to signal emitted (C_T). Thus, the standard curve of DNA will allow us to convert the cycle threshold (C_t) values into amount of DNA using the linear regression equation $y = -3.173x + 35.26$, where "x" is the logarithm of the DNA quantity (fg) and "y" is C_t value. The regression coefficient obtained was $R^2 = 0.993$, and the amplification efficiency was 106.6% (Figure 23). Next, the amount of DNA in the unknown sample (fg) is split into the number of copies of the *16S rRNA* gene that exists in the initial sample.

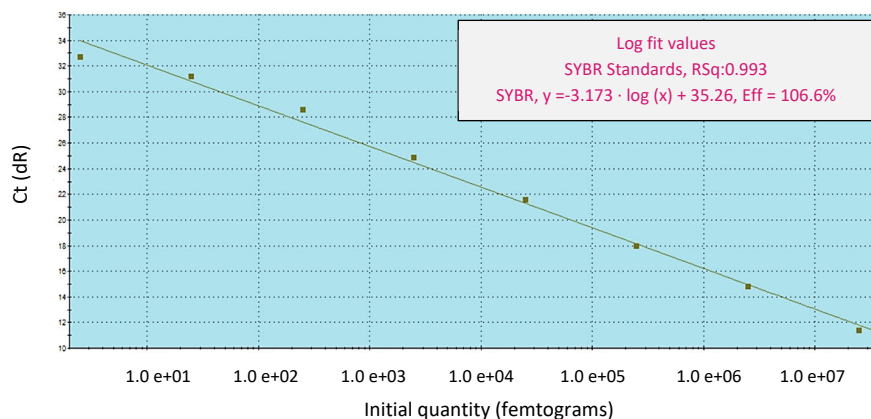


Figure 23. Standard curve for DNA quantity (femtograms) related with Ct from RT-PCR.

3.1.2. *A. thiooxidans* growth curve

To transform the C_T from the qPCR to number of cells, the number of copies obtained by amplification were divided by two. With the results obtained, the graph of the Figure 24 was sketched.

It could be observed a faster growth than those determined by spectrophotometry (Nguyen *et al.*, 2016), reaching the stationary phase after 3 - 4 days in every flask instead of 12 – 14 days, with more than 10^7 cells/mL on average (Figure 24). This may be due to the low absorbance of *A. thiooxidans* cells, since there was hardly any turbidity when growing in AT medium. In addition, a sudden pH decrease was observed during the first 3 days of incubation, and then it was maintained over time with small variations, staying close to 1.5 during the whole fermentation.

In 1995, the way to grow of *A. thiooxidans* was described for the first time, showing that it grows by alternating a cycle of growth in suspension, and then on the surface of sulphur particles present in the medium. In addition, the growth curve was described using a hemocytometer for the free cells in suspension and the cells on the surface. However, in that case, an exponential phase of growth that lasted until day 14 of culture was observed, while in our case, the cells in suspension had reached the stationary phase after 3 days (Figure 24). In both cases, the maximum growth obtained was closed to 10^8 cells/mL (Konishi *et al.*, 1995).

In order to determine the optimum conditions for the analysis of *A. thiooxidans* proteome under extreme acid growth conditions, we analysed the growth kinetic with different concentrations of S. We also tested the effect of the concentration of the initial inoculum, and the growth kinetic in 10 L of AT media.

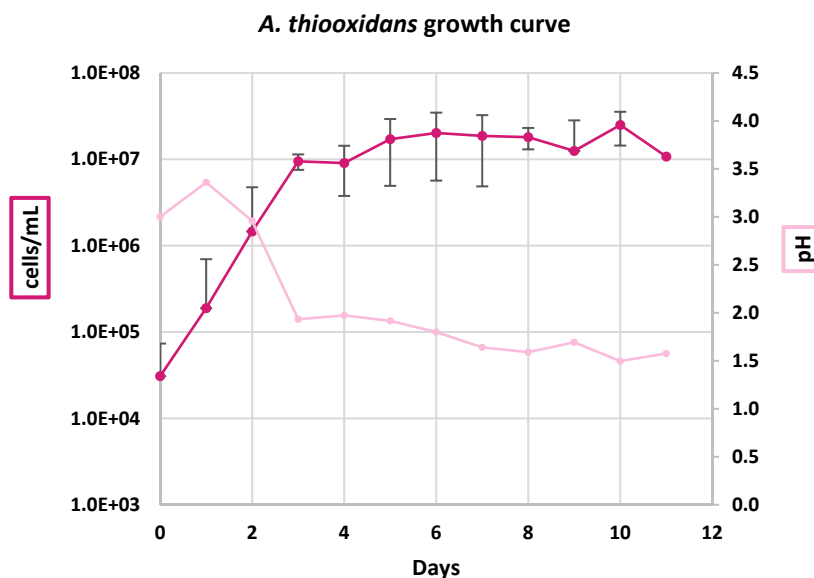


Figure 24. Growth curve for *A. thiooxidans* in AT medium at 30°C and 200 rpm for 11 days by qPCR determination. On the secondary axis it can be observed the pH of the supernatant during the whole fermentation. Data shown (with SD) are the average of three independent experiments.

a. Minimum sulphur concentration

A. thiooxidans uses elemental sulphur and other RISCs as sulphur source for growth. Nevertheless, most of the described media are supplemented with elemental sulphur or sodium thiosulphate, which are insoluble and soluble in water, respectively. The main problem with S could be found during the protein extraction by mechanical processes, because *A. thiooxidans* grows over the sulphur particles surface. Thus, sulphur could prevent that glass bead crash with cells to disrupt them. However, at a pH lower than 4.0, thiosulphate is decomposed to sulphite and colloidal sulphur, that cannot be used by *Acidithiobacillus* spp. (Wang *et al.*, 2019). Thus, it could not be used as S source in the proteomic analysis, since most of the pH analysed were below 3.0.

Therefore, to avoid problems with sulphur during future steps of the protein extraction, it was determined the minimal sulphur concentration needed for the process. So, *A. thiooxidans* was grown into 200 mL of AT medium at initial pH 3.0, at 30°C and 200 rpm for 8 days supplemented with different concentrations of elemental sulphur: 1%, 0.5%, 0.25% and 0.1%.

It could be observed that the growth was uniform for the first 2-3 days (Figure 25). After this period, the growth of samples supplemented with 0.25% sulphur sharply decreased. Nevertheless, for 0.1% sulphur samples, growth continued increasing until day 5, and started to hardly decrease afterwards. Every condition reached a final pH close to 1.5 (data not showed).

To analyse the effect of an extremely acid or neutral pH in the proteome expression of *A. thiooxidans*, it is very important to take the samples during the mid-exponential growth phase. Thus, it was important to reach an enough number of cells with the minimum S as possible. This optimum point in *A. thiooxidans* growth is after 72 h of incubation in AT medium pH 3.0 supplemented with 0.1% sulphur.

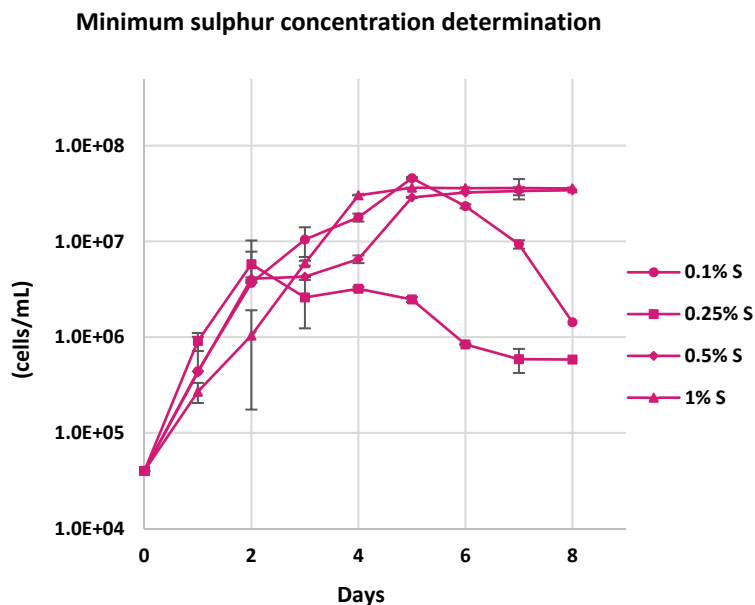


Figure 25. Growth curve of *A. thiooxidans* in AT medium supplemented with elemental sulphur (S) at different concentrations (w/v): 0.1%, 0.25%, 0.5% and 1%. Fermentations were carried out at 30°C and 200 rpm for 8 days and *A. thiooxidans* growth was determined by qPCR analysis. Data shown (with SD) are the average of three independent experiments.

b. Minimum inoculum concentration

Another important point to keep in mind when analysing a bacterial proteome is the protocol for sample collection. Thus, to compare the effect of pH in the bacterial cultures is important to analyse the cells in the mid-exponential growth phase, to avoid the cellular lysis, which is so common once the culture reach the stationary phase. In that case, an intracellular protein could be located in the secretome sample, causing a misinterpretation of the results.

Thus, in an attempt to reach a longer exponential growth phase, to assure that samples were taken during the mid-exponential growth phase, but the culture were grown as much as possible, we analysed the growth curve with different initial amounts of inoculum. So, 500-mL Erlenmeyer flasks containing 200 mL of AT medium at initial pH 3.0, and supplemented with 0.1% elemental sulphur, were inoculated with 1 mL, 500 μ L or 250 μ L of a 7-days pre-grown culture of *A. thiooxidans*.

It could be observed that stationary phase was reached at day 4 when inoculated at 1%, and at day 5 for 0.25% (v/v) (Figure 26). These results suggested that the best condition for the final assay was to inoculate at 0.25% and incubate at 30°C and 200 rpm for 72 - 96 h.

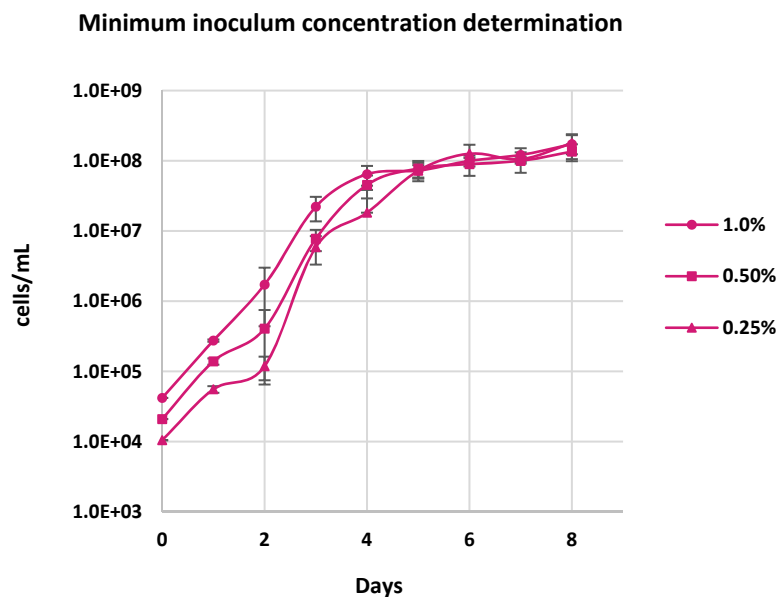


Figure 26. Growth curve for *A. thiooxidans* in AT medium supplemented with 0.1% (w/v) elemental S and inoculated with different initial concentration of inoculum (v/v): 1%, 0.5% and 0.25%. Fermentations were carried out at 30°C and 200 rpm for 8 days. *A. thiooxidans* growth was determined by qPCR analysis. Data shown (with SD) are the average of three independent experiments.

c. Final growth curve

In the light of the result obtained, the final growth curve for *A. thiooxidans* was analysed in 10 L of AT medium supplemented with 0.1% (w/v) elemental sulphur and inoculated at 0.25% (v/v). Again, it could be observed that the exponential phase finished between days 3 and 4 (Figure 27). Thus, it could be better to take the sample before finish the 72 first hours, to assure the samples were in the exponential phase. The pH in that moment would be between 2 and 3. Thus, the control pH selected for the assay was 3.0 (the same as the initial pH for the fermentation, since it can be observed that *A. thiooxidans* could grow at that pH at a good rate).

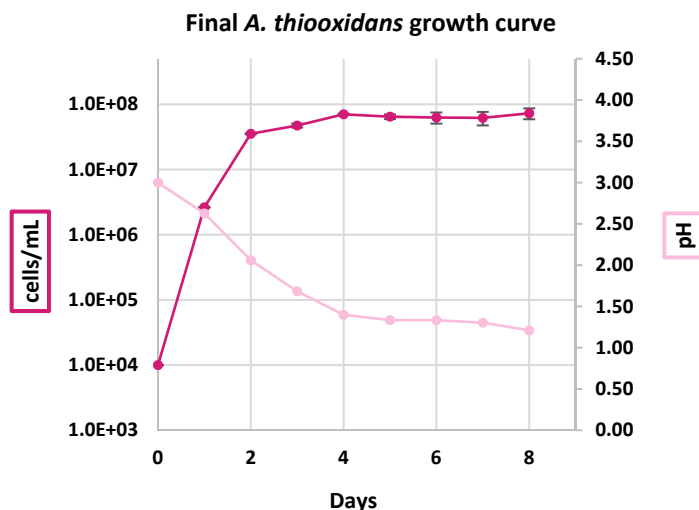


Figure 27. Growth curve for *A. thiooxidans* in 10 L of AT medium supplemented with 0.1% (w/v) elemental S, inoculated at 0.25% (v/v) and incubated at 30°C and 200 rpm for 8 days. *A. thiooxidans* growth was determined by qPCR analysis. On the secondary shaft it can be observed the pH of the supernatant during the whole fermentation. Data shown (with SD) are the average of three independent experiments.

3.2. *A. thiooxidans* SOB3 genome analysis

In order to get the maximum information possible for the further proteomic analysis, we decided to sequence the genome of *A. thiooxidans* SOB3 strain.

The genome size of *A. thiooxidans* SOB3 strain is 3,239,842 bp with a GC content of 52.92%. Moreover, it contained 18 tRNAs, 6 rRNAs and 3300 CDS, but 1525 of these were described as hypothetical proteins (46.21% of the total genome) (Figure 29). These results were in accordance with other *A. thiooxidans* genome analysis, as those obtained for the strains A01, ATCC 19377 and ZBY (Travisany *et al.*, 2014; X. Zhang *et al.*, 2018). Thus, after the RAST analysis, 1108 proteins were classified by the subsystem category distribution (Figure 28), and the other 2192 proteins could not be classified. Functional classification by subsystem database revealed the predominance of protein metabolism subsystem (14.29%), followed by amino acids and derivatives (12.45%), respiration (10.62%) and DNA metabolism (9.34%). It is interesting to remark that no known gene could be included into the acid stress subsystem, even when survival at extreme acid environment is one of the most important skills in this strain. A total of 12 genes which could be related with sulphur oxidation (the ones from the *sox* cluster) were detected.

It was not strange to get these results, since up to 13 different genome sequences are deposited in databases (date 2021.03.12) [3 of them are from the same strain (*A. thiooxidans* ATCC 19377)], with different assembly levels (NCBI). Besides, just one of the 13 genomes (ATCC 19377 strain) is complete, and even this one shows almost 50% of the detected CDS annotated as hypothetical proteins.

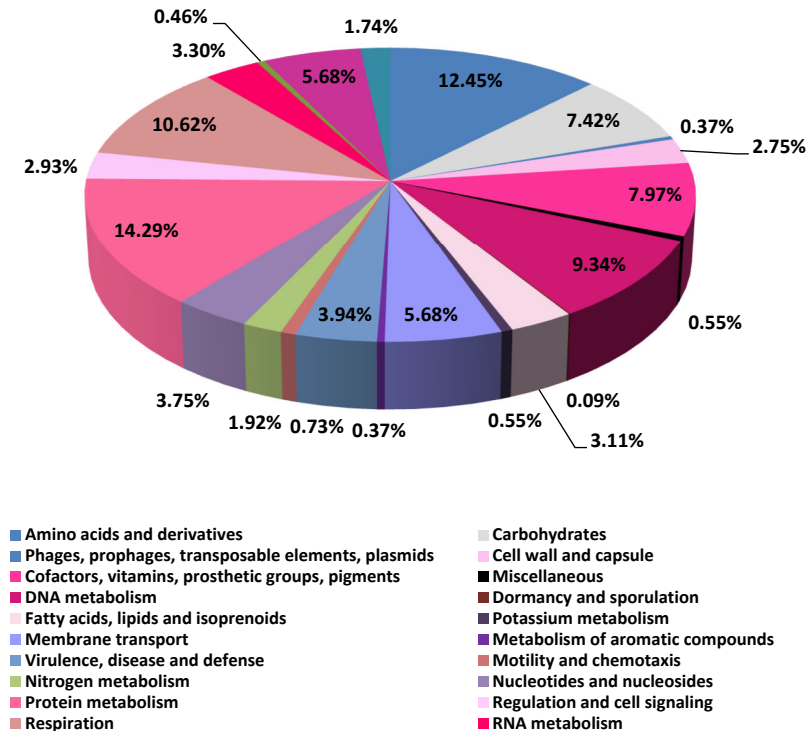


Figure 28. Distribution of functional categories for subsystem database in *A. thiooxidans* SOB3 strain. Each slice represents the percentage of genes that match into a particular category. Hypothetical proteins represent 46.21% of the total amount of proteins, and they are not represented on the graph.

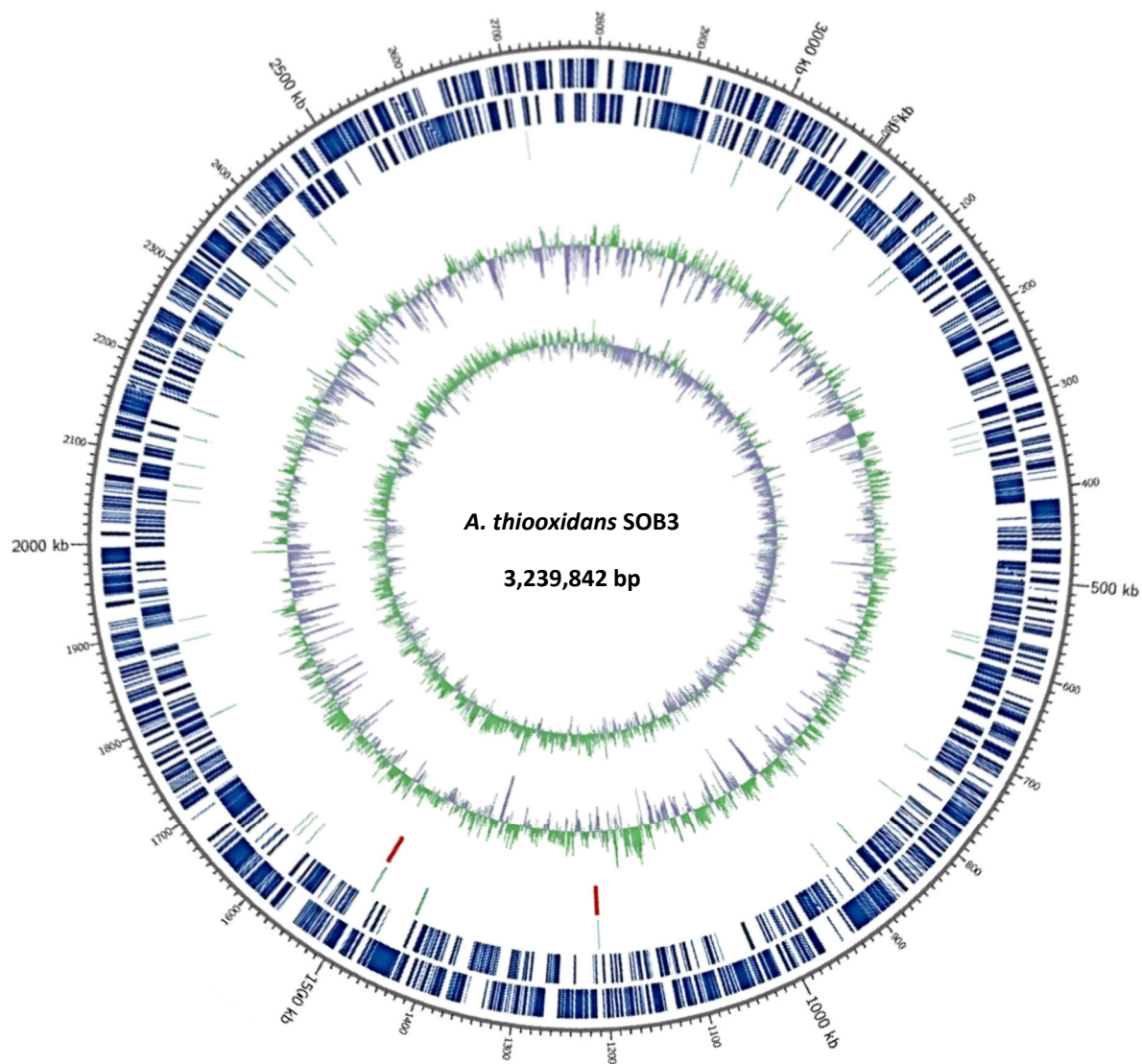


Figure 29. Circular map of the *A. thiooxidans* SOB3 genome: 3,239,842 bp with 3300 CDS. Marked characteristics are shown from outside to the centre: CDS on forward strands (blue), CDS on reverse strand (blue), tRNA (green), rRNA (two copies of rRNA genes: 16S, 23S and 5S; red colour), GC content and GC skew.

3.3. *A. thiooxidans* protein extraction optimization

In order to fully analyse intracellular proteins, the cells must be effectively disrupted. There are numerous mechanical and chemical lysing methods that can be applied. However, and due to the extreme conditions to grow, it should be considered the use of vigorous breaking procedures, such as sonication or glass bead homogenization. Nevertheless, as described above, *A. thiooxidans* grows on the sulphur particles surface. Thus, it is important to keep in mind that glass bead extraction could not work in sulphur presence, since sulphur particles could prevent bead crash with the cells. On the other hand, to remove the sulphur could go hand in hand with cell removing.

Thus, three different protocols were analysed: sonication, glass beads after filtering through paper filter, and glass beads without filtration. In all cases, 200 mL of AT liquid medium were inoculated with 3 mL of a 7-days seed culture and incubated at 30°C and 200 rpm for 72 h. Two flasks were filter through sterile paper filter and the rest flasks were untreated. Then, sonication and glass beads breaking protocols were carried out, and protein extracts were visualized in a 1D acrylamide gel.

Under normal conditions, 20 µg of total protein can be easily visualized in a 1D SDS-PAGE. It allows us to analyse, not only the quantity and quality of the protein extraction protocol, but the accuracy of its quantification. However, the visual quantification of the protein concentration showed that the volume needed to run 20 µg of total protein in the 1D SDS-PAGE was higher than the maximum volume of the gel wells. Thus, 10 µL of each sample were run in the gel (Figure 30).

As it can be deduced from Figure 30 (lanes 5 and 6), sonication was not an effective method for *A. thiooxidans* protein extraction, since a very small amount of proteins could be detected in the gel. On the other hand, the breaking with glass beads and the FastPrep apparatus showed clean samples

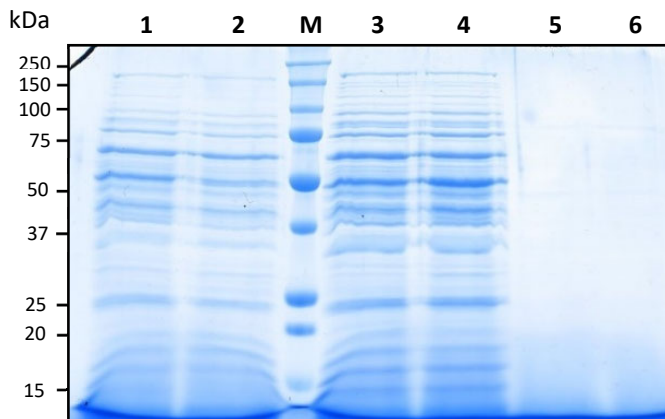


Figure 30. 1D SDS-PAGE gel with 10 µL of each sample of protein extracted from optimization (left to right): two replicates from filtered and glass beads extraction samples (lanes 1 and 2), protein ladder (M) (*Precision Plus Protein Standards*, Bio-Rad), two replicates from glass beads extraction (lanes 3 and 4) and two replicates from sonication extraction (lanes 5 and 6).

without degradation (no smear appeared in the gel) (lanes 1 to 4) and good extraction (enough amount of sample with uniform band distribution). Nevertheless, the quantification by Bradford method showed that a lower amount of proteins had been extracted after filtration through the filter paper (as it can be noticed in lanes 1 and 2). Thus, **the best method for the protein extraction was the cell breaking using FastPrep with beads without previous filtration.**

3.4. Determination of the conditions for the 2D DIGE proteome analysis

A. thiooxidans has a growth pH range between 0.5 and 5.5, with an optimum pH range of 2.0-3.0 (Garrity *et al.*, 2005b). Thus, the control pH condition for the proteome analysis should be 3.0, and pHs close to 0.5 (such as 0.5, 0.7 or even 1.5) should be analysed as stress in acid pH. On the other hand, pHs close to 5.5 (such as 5.5 and 6.0) should be analysed as “alkaline” stress for *A. thiooxidans*. Initially, optimum pHs and sample collection time for the 2-D proteome analysis of *A. thiooxidans* under acid and “alkaline” stress conditions were analysed. In second place, it was optimized the best range of pH for the 2D acrylamide gel electrophoresis before the DIGE analysis, to reach the maximum protein separation.

3.4.1. Stress detection by gene differential expression using RT-PCR

In order to determine the optimum pH and time conditions for the sampling, a RT-PCR was carried out, analysing the differential expression of four well-known genes related with stress: *groEL*, *dnaJ*, *dnaK* and *rpoH*. A fifth gene was used as reference gene: *sdoA*. This gene encodes for the sulphur dioxygenase enzyme, involved in the sulphur metabolism of *A. thiooxidans*, and it is essential for the microorganism (Jing Zhang *et al.*, 2020).

The first three genes (*groEL*, *dnaJ* and *dnaK*) are well-known chaperones from the called heat-shock proteins (Hsps), whose function is to protect proteins against protein aggregation, related with protein folding in adaptive cellular response to many stress conditions. On the other hand, *rpoH* gene encodes the σ^{32} factor, which is involved in the regulation of the expression of heat-shock and other stresses genes (Roncarati & Scarlato, 2017).

Nevertheless, none of these genes was up-regulated under acid stress conditions (Table 11). A small over expression of *rpoH* at pH 1.5 after 30 min of incubation could be observed, but its expression decreased to normal levels after 60 min of incubation (Table 11). A similar pattern was observed for the pH 1.5 condition, since a down-regulation could be observed at 30 min of incubation, but the expression increased to normal levels after 60 min of incubation (Table 11).

It was especially interesting to observe that the expression of the four genes decreased to undetectable levels for the pH 0.5 condition after 60 min of incubation. Cell lysis was not observed under the microscope, although cell mobility was reduced. Thus, it was decided that pH 0.5 could be too harsh for the cells, and pH 0.7 would be assayed for the 1D acrylamide gel analysis.

Table 11. Relative transcript levels of the selected genes, which were determined by RT-PCR using *sdoA* as reference gene. Samples were recovered at 30 and 60 min of incubation at pH 0.5, 1.5, 3.0 (control condition), 5.5 and 6.0. Data shown represent the average (with SD) from three independent experiments. The analysed genes were considered significantly up- or down-regulated when changes in their expression were higher than 2 or lower than 0.5, respectively.

| Time | pH | $2^{-\Delta\Delta Ct}$ | | | |
|--------|-----|------------------------|-------------|-------------|-------------|
| | | <i>groEL</i> | <i>dnaJ</i> | <i>rpoH</i> | <i>dnaK</i> |
| 30 min | 0,5 | 0,00 ± 0.01 | 0,31 ± 0.52 | No Ct | No Ct |
| | 1,5 | 0,00 ± 0.00 | 0,00 ± 0.00 | 2,09 ± 4.46 | No Ct |
| | 3 | 1,00 ± 0.00 | 1,00 ± 0.00 | 1,00 ± 0.00 | 1,00 ± 0.00 |
| | 5,5 | 0,50 ± 0.063 | 0,41 ± 0.02 | 0,18 ± 0.00 | 0,37 ± 0.01 |
| | 6 | 0,52 ± 0.09 | 0,78 ± 0.05 | 0,48 ± 0.09 | 0,60 ± 0.08 |
| 60 min | 0,5 | No Ct | No Ct | No Ct | No Ct |
| | 1,5 | 0,00 ± 0.05 | 0,71 ± 0.51 | 0,94 ± 1.00 | No Ct |
| | 3 | 1,00 ± 0.00 | 1,00 ± 0.00 | 1,00 ± 0.00 | 1,00 ± 0.00 |
| | 5,5 | 1,59 ± 0.45 | 1,67 ± 1.09 | 1.26 ± 1.14 | 0,23 ± 0.01 |
| | 6 | 0,92 ± 0.43 | 2,34 ± 1.34 | 4.70 ± 2.93 | 0,54 ± 0.06 |

Besides, an up-regulation of *dnaJ* and *rpoH* genes was observed after 60 min of incubation. Thus, if mRNA expression was detected after 60 min of incubation, at least 1.5 h could be necessary to observe differential expression in the proteome.

3.4.2. 1D: SDS-PAGE (sodium dodecyl sulphate polyacrylamide gel electrophoresis)

Two of the main uses of one-dimensional protein gels are: **i)** to confirm that the quantification by the Bradford method is real and has not been biased by pigments or other compounds present in the medium, and, **ii)** to verify the integrity of the extracted proteins (a smear along the gel should not be observed).

Thus, in the view of the previous results, a first 1D assay was carried out to determine the optimum time for sample collection. Three different times of incubation were analysed for pH 6.0, which was the pH that showed the lowest differential expression in the RT-PCR assay: 1.5 h, 3.0 h and 7.0 h. The gel showed changes in protein quantity, but not in the bands pattern, so no difference expression could be observed between these three times of incubation at pH 6.0 in a 1D SDS-PAGE assay (Figure 31). However, changes were observed in the analysis of differential expression by RT-PCR after 60 min of incubation. For this reason, it was decided to carry out the definitive assay after 1.5 h of incubation.

Therefore, six different conditions of pH were tested in a 1D acrylamide gel: 0.5, 0.7, 1.0, 1.3, 3.0 and 6.0 after 1.5 h of incubation. First of all, the analysis of the gels indicated that the quantification carried out was correct (Figure 31). The protein quantification showed that the samples corresponding to pH 0.5, 1.0 and 1.3 were much less concentrated than the rest. For this reason, and for these samples, 20 µg of total protein could not be loaded into the wells, and 10 µL of sample were loaded instead. On the contrary, the samples corresponding to pH 0.7, 3.0 and 6.0 were loaded with 20 µg of total protein as usual. Second, we observed that the samples were not degraded after

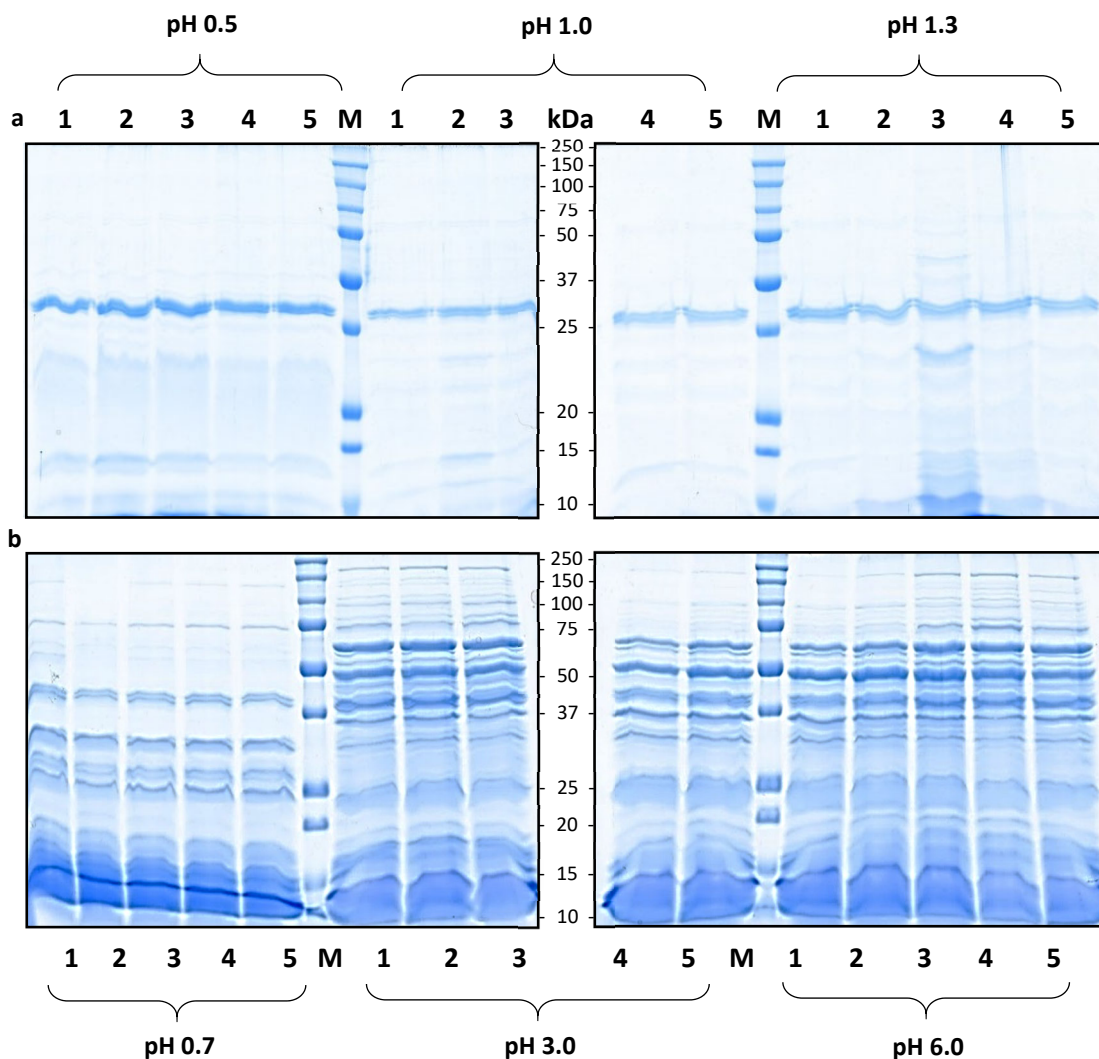


Figure 31. (a) 1D Acrylamide gels with 10 µL of each sample of protein extraction from samples incubated 1.5 h at pHs: 0.5, 1.0 and 1.3 (left to right) with five replicates of each pH condition. (b) 1D Acrylamide gels with 20 µg of extracted protein from samples incubated 1.5 h at pHs: 0.7, 3.0 and 6.0 (left to right) with five replicates of each pH condition. 5 µL of *Precision Plus Protein Standards* (Bio-Rad) were used as standard.

extraction. However, we could observe that the samples corresponding to pH 0.5, 1.0 and 1.3 showed a low protein concentration and besides exhibited a biased pattern: some protein bands were much more concentrated than in the rest of the samples. This may be due to the fact that in excessively acidic pH environments, the cellular breakdown undergoes some type of alteration and not all the proteins are equally extracted. It is also possible that some proteins are degraded under these conditions. Nevertheless, samples corresponding to pH 0.7 were properly extracted (good concentration and numerous bands). In conclusion, pHs 0.7, 3.0 and 6.0 were chosen for the final *A. thiooxidans* proteome analysis.

3.4.3. 2-D electrophoresis optimization

The main objective of a DIGE analysis is the detection of individual proteins that show differential expression under different conditions. For this reason, it is essential to find the right conditions in which the protein spots exhibit a good physical separation in the gel that allow their optimal resolution.

For this reason, we analysed two different ranges of pH gradients for the IEF: 3-10 and 4-7. Precipitated proteins were found at pH 7.0 in the pH range 4-7, because they had not reached their real pI, and they were accumulated at the right end of the gel (Figure 32). Thus, to our purposes, the optimum condition would be the non-linear pH range 3-10. Besides, the same optimum pH range had been previously observed for the *A. ferrooxidans* proteome analysis (Chi *et al.*, 2007).

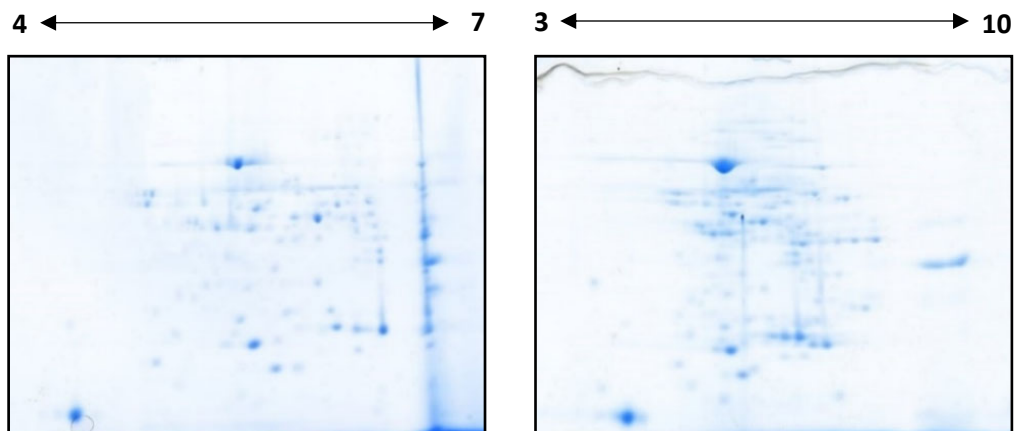


Figure 32. Effect of IEF pH range on 2D resolution gels for *A. thiooxidans* cytoplasmatic proteins. 80 μ g of protein extracted from flasks inoculated with *A. thiooxidans* in AT medium at pH 6.0, incubated at 30°C and 200 rpm for 1.5 h, focused on a 7 cm *Immobiline DryStrip* pH 4 - 7 NL and 3 - 10 NL (left to right).

3.5. 2-D DIGE analysis

A proteomic approach was used to reinforce our knowledge of the growth of *A. thiooxidans* SOB3 under extreme acid stress. It conditions had been previously studied the response of *Acidithiobacillus* strains to pH stress on cytoplasmic membrane composition (Mykytczuk *et al.*, 2010, 2011). Nevertheless, the interest on the proteome and transcriptomic analysis of this kind of microorganism is very recent (Bellenberg *et al.*, 2019; Yin *et al.*, 2019).

In our case, 573 proteins showed differential expression between pH 0.7 vs 3.0 and 0.7 vs 6.0, but just 201 were really picked from the gel, since the rest of them were poorly visualized after Coomassie staining (Figures 33 and 34). It could seem a huge expression difference for a DIGE analysis, but keep up with the *A. thiooxidans* CCTCC M 2012104 transcriptome analysis between pH 1.6 and 0.8 conditions, that detected 630 differentially expressed genes (Yin *et al.*, 2019).

After trypsin digestion, all of the 201 proteins were analysed with a database created after merge γ -proteobacteria database from Uniprot (<https://www.uniprot.org>) with the proteins from *A. thiooxidans* SOB3 genome and all the *Acidithiobacillus* strains with an annotated genome from NCBI database (date 2021.03.12). To reach a better identification, keratins were identified with the NCBI database. In addition, the peptide tolerance values were increased (the error window for the ionic mass values of the MS / MS fragment) trying to identify the proteins by similarity with the proteomes of other strains. Besides, a new database was created with every ORF from *A. thiooxidans* SOB3 genome by RanSEPS software. A total of 170,197 ORFs were created from both DNA strands and the three-reading frame of each one. Finally, those non-confirmed proteins after Mascot database search were trying to identify by *de novo* sequencing and BLAST similarity search, following the procedure described by Liska and Shevchenko (2003). All MS/MS spectra for a sample were sequenced *de novo* using ProBLAST software (Applied Biosystems). The best fragmented ions were manually selected and the top six candidate peptide sequences for each MS/MS were combined into a single text-format search string by means of the DeNovo Explorer software (Version 3.6) included in GPS Explorer Software (Applied Biosystems). This search string was used for similarity searches using the BLASTP algorithm against an in-house protein sequence database containing the database created before under the following parameters: **i)** fixed modifications: Cys as S carbamidomethyl derivative; **ii)** mass tolerance: 0.3 Da **iii)** E-value threshold: 20; **iv)** scoring matrix: PAM30MS; **v)** algorithm enzyme: trypsin. Protein identification significance was judged using the BLASTP scoring algorithm. Only those proteins matched by a minimum of two peptide sequences with a score higher than 52 according to DeNovo Explorer software were included in the results list, providing more stringent criteria for the identification (Cobos *et al.*, 2010). After all these processing, 53 digested proteins were identified, showing 38 different identifications (Table 12).

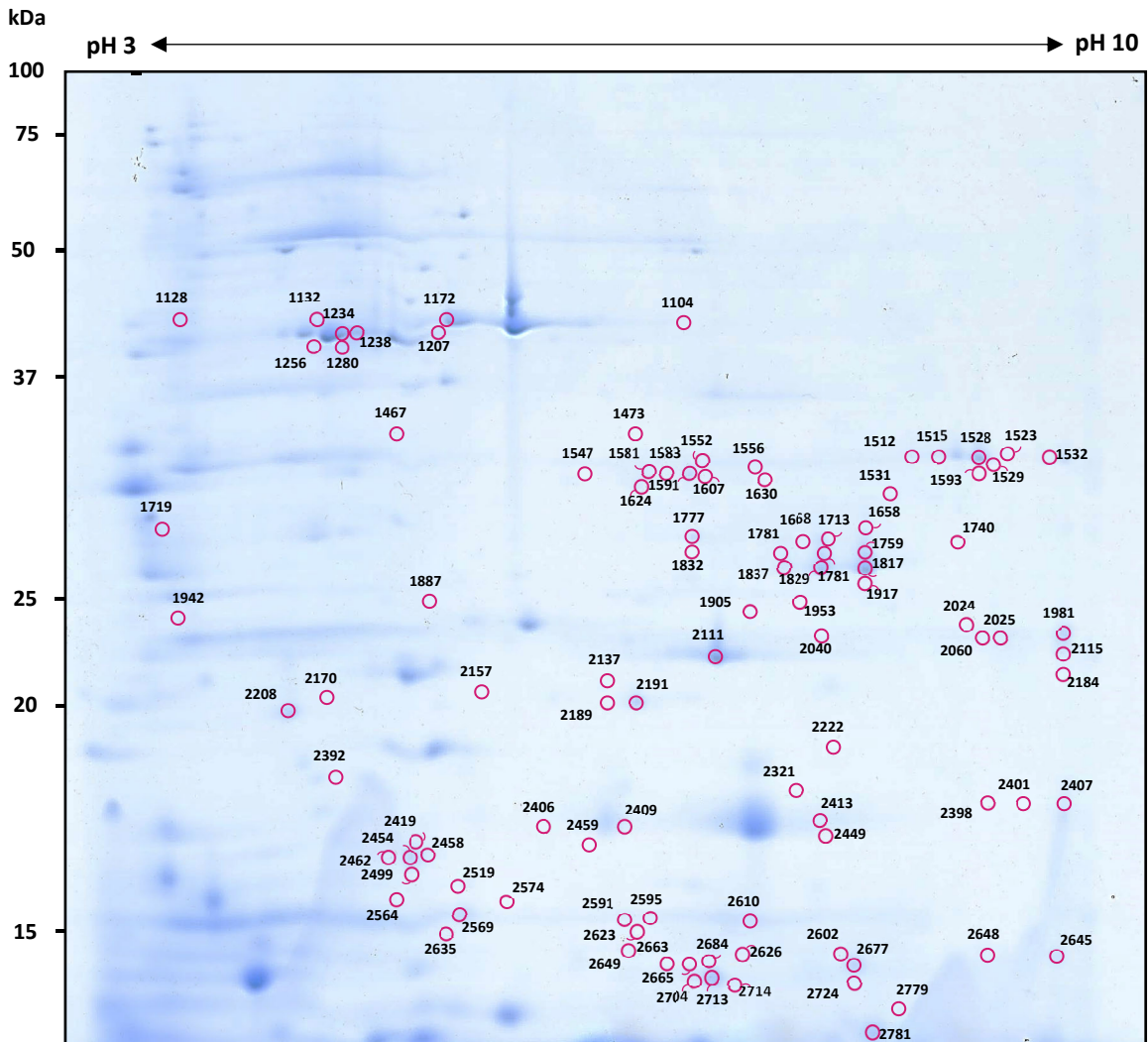


Figure 33. Mix of *A. thiooxidans* SOB3 intracellular proteome incubated at pH 0.7 + pH 3.0, stained with Coomassie after DIGE analysis. A total of 573 protein spots were visualized in a 3.0 – 10.0 pH range, 201 of which showed differential expression between conditions and were successfully localized and extracted from the gel. Molecular weights are marked on the left and the assigned numbers correspond to those proteins identified in Table 12.

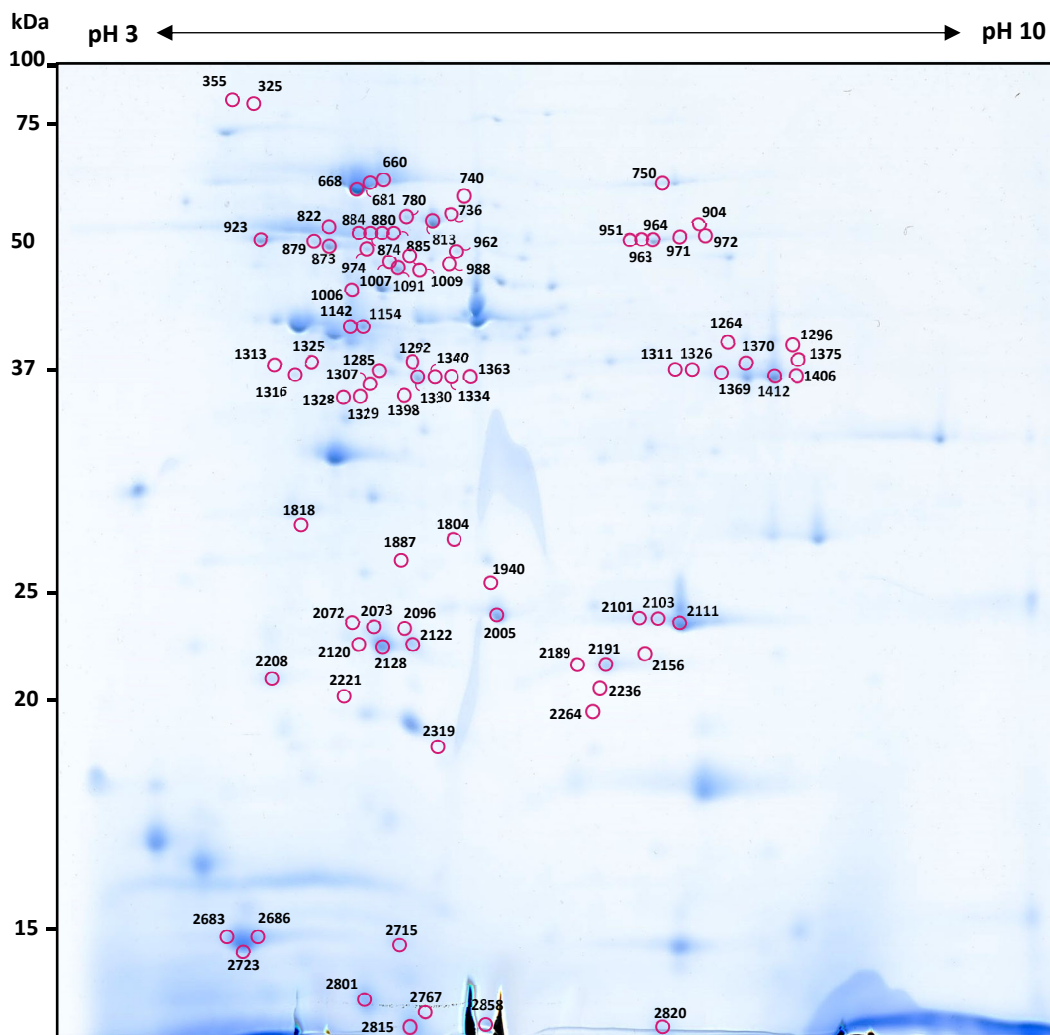


Figure 34. Mix of *A. thiooxidans* SOB3 intracellular proteome incubated at pH 6.0 + pH 3.0, stained with Coomassie after DIGE analysis. A total of 573 protein spots were visualized in a 3.0 – 10.0 pH range, 201 of which showed differential expression between conditions and were successfully localized and extracted from the gel. The assigned numbers correspond to those proteins identified in Table 12.

Some of the identified **down-regulated** proteins are involved in **central carbon metabolism and CO₂ fixation**. The fixation of CO₂ is closely related to the central carbon metabolism in chemoautotroph bacteria, since they use it as carbon source for cell growth. Thus, the carbon-fixing key enzymes carboxysome shell protein and ribulose-1,5-bisphosphate carboxylase (Rubisco) were detected in this study. Both are involved in the Calvin cycle for the CO₂ fixation. Also were down-regulated some enzymes from the pentose phosphate pathway and glycolysis, such as the enolase, the Fructose-1,6-bisphosphatase, and the Ribulose-phosphate-3-epimerase (Figure 35).

Also, the **energy metabolism** was down-regulated at extreme acid conditions. Thus, the sulphur oxidation protein SoxB (from the *sox* gene family) was down-regulated. This enzyme is related with the sulphur metabolism in chemolithotrophs, since is a thiosulfohydrolase involved in the step of the oxidation of the thiosulphate (Wang *et al.*, 2019).

Moreover, the **nitrogen fixation** pathway could be also down-regulated, since the enzyme glutamate synthase was detected in the analysis. This enzyme is involved in the fixation of NH₄⁺ in a glutamate molecule, producing glutamine, which is also related with the antioxidant system.

So, in the same way, it was observed that the synthesis of some **chaperones**, like Clp or GroEL, was down-regulated at pH 0.7. Clp is another Hsps chaperone related with protein folding in adaptive cellular response to many stress conditions. Both molecular chaperones have been related with the adaptative defensive mechanisms of bioleaching microorganisms under extremely acid stress. This is in the line of the RT-PCR, that showed a down-regulation of the other chaperones analysed: DnaK and DnaJ. Thus, *clp*, *dnaK*, *dnaJ* and *groEL* genes are down-regulated under extreme acid pH conditions.

On the other hand, the sliding clamp protein is a ring-shaped protein that encircles duplex DNA, binds to the DNA polymerase and tethers it to the DNA template, preventing its dissociation, and providing high processivity. This protein also plays an essential role in **DNA repair**, being crucial for cell viability, specially under stress conditions, when they play also a role in the repair of damaged DNA (Altieri & Kelman, 2018). In our study, this protein was down-regulated under extreme acid conditions.

Finally, the L7/L12 **ribosomal protein** (located in the 50S ribosomal subunit) was also down-regulated, which could mean that the protein biosynthesis levels should be lower under extreme conditions. Same result was also found in *A. ferrooxidans* under osmotic stress (Dopson *et al.*, 2017).

On the contrary, just nine of the identified proteins were **up-regulated**, six of which were defined as **hypothetical proteins**. One of the known proteins was the putative parvulin-type peptidyl-prolyl cis-trans, another **chaperone** related with folding catalysts. This could mean that the most known chaperones act in normal acid conditions (pH 3.0), while more unknown chaperones start to work in special acid conditions.

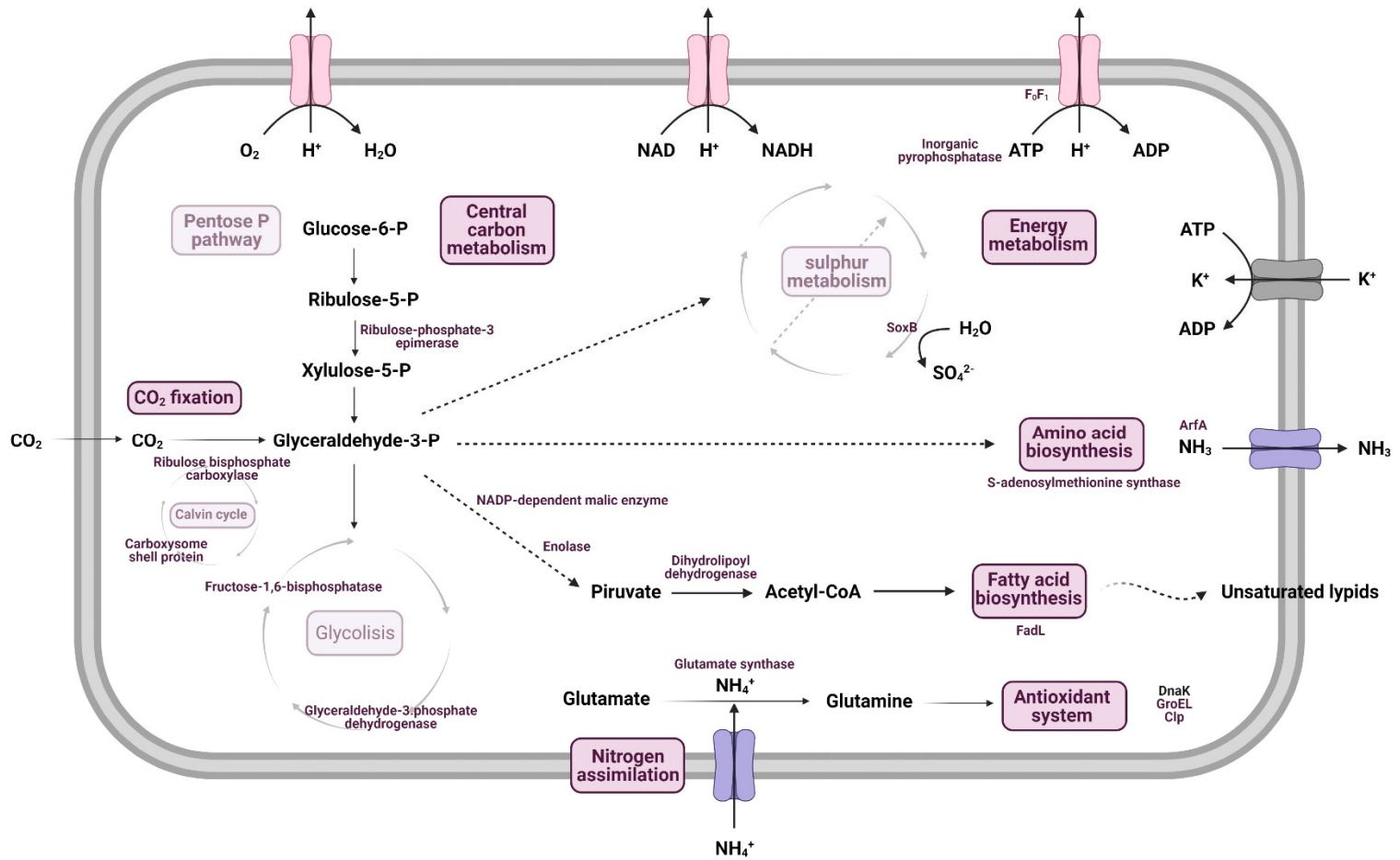


Figure 35. Model of *A. thiooxidans* metabolism and enzymes down- or up-regulated at extreme low pH conditions. Enzymes identified in the proteome analysis are represented in their respective metabolic pathway in purple colour.

Finally, the FadL protein, which is a long-chain fatty acid transporter, involved in the **translocation of long-chain acids across the outer membrane**, was also up-regulated at pH 0.7. The last identified protein up-regulated was ArfA, a peptidoglycan-binding protein, which has been related with the **ammonia secretion** in other strains, to neutralize the pH of the medium in acid environments (Guan & Liu, 2020; Song *et al.*, 2011; Yao *et al.*, 2012). Thus, two typical mechanisms related with survival in extreme acid environments would had been detected. It has been reported the changes in cell membrane fatty acids in *A. thiooxidans* during extreme acid conditions, with an increase in the unsaturated acid composition, specially the cyclopropane (C19-cyc) (Yin *et al.*, 2019). The ammonia biosynthesis has also been identified as a target of pH stress by Yin *et al.* (2019) in a transcriptomic analysis incubating *A. thiooxidans* under pH 0.8. Thus, L-glutamine can convert to L-glutamic acid and release ammonia, an alkaline substance which is secreted to the acid environment.

In conclusion, **central energetic metabolism is severely restricted in *A. thiooxidans* under extreme pH conditions as those in pH 0.7**. It has been reported that *A. ferrooxidans* growth is stopped at pHs under 1.0, which seems that at pH values below optimal, the pH gradient and the membrane potential necessary for maintained proton motive force, becomes inoperable for the bacteria, and the metabolic activity decreases. In that case, *A. ferrooxidans* shows a greater stress under extreme acid environments than under more alkaline conditions (Mykytczuk *et al.*, 2010). Same results could be observed in this study with *A. thiooxidans*, since no expression differences could be found between pH 3.0 and pH 6.0 conditions. It has even been described a drop in the growth at pH under 1.0 in *A. thiooxidans*, that could be related with this stop in the whole metabolism (Feng *et al.*, 2015). Besides, it was observed by transmission electron microscopy that, at pHs under 1.0, the capsule from *A. thiooxidans* begin to fade (Feng *et al.*, 2015). So, it could be concluded that the extreme acid stress could became an unbearable threat to cell survival.

Nevertheless, it is difficult to explain what is happening inside *A. thiooxidans* cells under extremely acid environments, since **most of the proteins could not be identified and specially those up-regulated at pH 0.7**. Thus, even when the spectra of some proteins show good quantity and quality (Figure 36) they couldn't be identified in *A. thiooxidans* SOB3 proteome. **This result reflects the problems when working with these strains and all what is unknown about them.**

However, rather than actually identify the differential expression of some proteins between different condition, this assay allowed us to verify genome sequencing quality and compare with a reference genome as *A. thiooxidans* ATCC 19377. Thus, **it would be interesting to analyse hypothetical proteins that we could find in *A. thiooxidans* SOB3 genome that could not be identified in the ATCC19377 genome** (like number 2858), or **vice versa** (such as number 1154).

Besides, **this assay enabled us to detect one-off changes in the sequence** (due to sequencing errors or due to mutations) **by proteogenomics** (Figure 37). Proteogenomics has recently emerged as a powerful technique to enhance our ability to annotate protein-coding genes. It is based on the fact that the identified peptides can provide evidence for genetic alterations, transcriptomic

alterations or helping to identify novel transcripts (Qin *et al.*, 2021; Srivastava *et al.*, 2019). In our case, numerous proteins showed some amino acid change in the protein sequence (for example proteins like numbers 923, 1804, or 2122, among others). Thus, a change in the sequence can cause that some peptide could not match in the sequence, decreasing the score and the coverage of the results. In addition, the mass of the protein can also be modified, without cutting the total length of the sequence. In this case, the numerous differences found when comparing both sequences is likely to correspond to real differences in the proteins, probably because of mutation over time. It has been reported that *Acidithiobacillus* strains could vary in phenotypic properties and cognate genetic traits due to their ecological niches. Thus, it is possible that all these differences in the protein sequences may be due to the evolution in different environmental conditions.

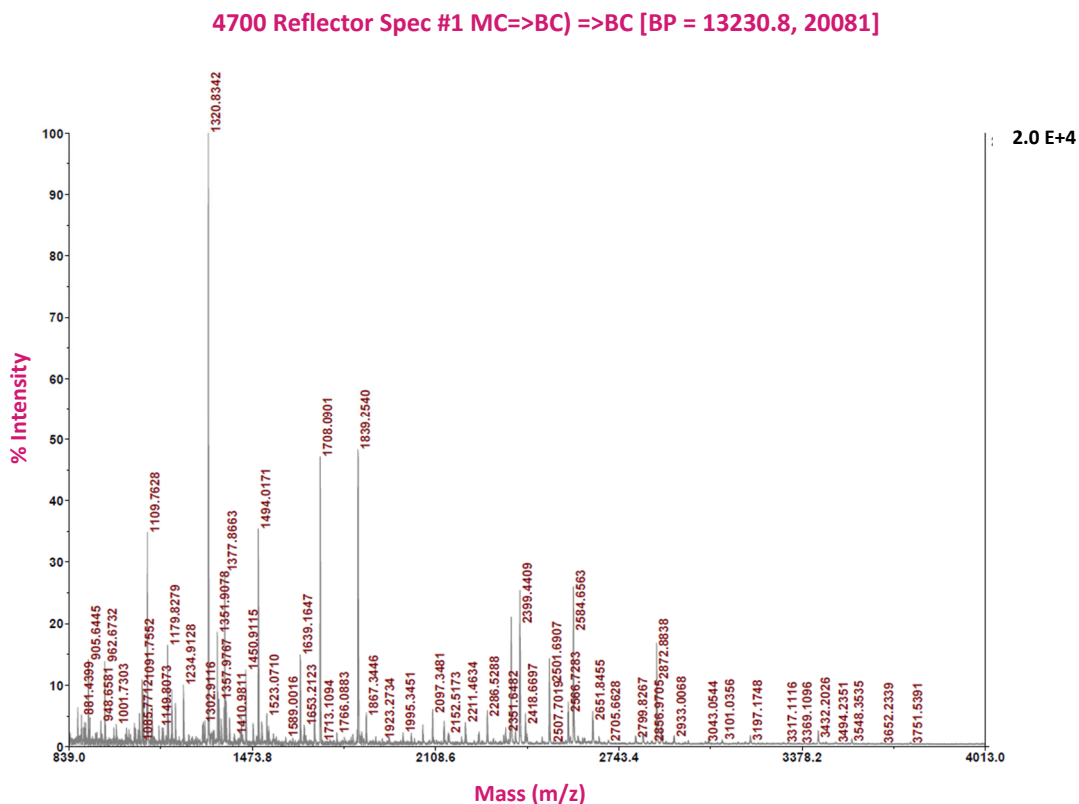


Figure 36. MALDI-ToF mass spectra of the picked and digested spot 1473. The absolute and percentage intensity of the ions are shown on the y axis, and the mass/charge ratios (m/z) of the ions are shown on the x axis.

***A. thiooxidans* ATCC 19377**

1 MSTLVCGSLA FDTIMVFQDR FKAHILPEQV HMLNVSFTVP EMRRDFGGCA
51 GNIAYNLKLK GGNPVIAGTA GQDFTPYLEH IKQQGLDTHL IRILPDHYTA
101 QAFITTDLDD NQITAFHPGA MFMAQENHLD GQIPSDVHWA IVSPDGLGAM
151 IQHLEDLTRA GIPTLFDPGQ GLPLFDAATL TRLIDMADYL TVNDYECQMV
201 QARTGLSVAE LRQRLKALIV TKGEQGSVIY HEDQETHIPT AKPRAVIDPT
251 GCGDAYRAGL LYGLEHNLGW ETSGKIASLM GAYKIETAGT QNHHTWSEF
301 KKRYQENFGS QIE

***A. thiooxidans* SOB3**

1 MSTLVCGSLA FDTIMVFQDR FKAHILPEQV HMLNVSFTVP EMRRDFGGCA
51 GNIAYNLKLK GGNPVIAGTA GQDFTPYLEH IKQQGLDTHL IRILPDHYTA
101 QAFITTDLDD NQITAFHPGA MFMAQENHLD GQIPSNVHWA IVSPDGLGAM
151 IQHLEDLTRA GIPTLFDPGQ GLPLFDAATL TRLIDMADYL TVNDYECQMV
201 QARTGLSVAE LRQRLKALIV TKGEQGSVIY HEDQETHIPT AKPRAVLDP
251 GCGDAYRAGL LYGLEHNLGW ETSGKIASLM GAYKIETAGT QNHHTWSEF
301 KKRYQENFGS QIE

Figure 37. Difference in the amino acid sequence of the adenosine kinase protein (number 1340) between *A. thiooxidans* ATCC19377 and *A. thiooxidans* SOB3. Matched peptides are shown in brown. Different amino acid between both sequences is shown in a black circle. The change of just one amino acid in the sequence makes one peptide match or not in the protein.

Table 12. List of cytoplasmic proteins picked and digested with trypsin in the *A. thiooxidans* proteome analysis under extreme acid and neutral pH conditions. Spot proteins are numbered on the figures 33 and 34. Experimental isoelectric point (pI) and molecular weight (Mw); the up- or down-regulation ratios in pH 0.7 vs 3.0, and pH 0.7 vs 6.0 conditions; the COG and KEGG numbers; and the functional classification by COG system are indicated. Those proteins up-regulated at pH 0.7 are highlighted in pink colour.

| Master No. | pI | Mw (kDa) | 0.7/3.0 Av. Ratio | 0.7/6.0 Av. Ratio | Description | COG No. | KEGG No. | EggNOG_Category |
|------------|------|----------|-------------------|-------------------|---|---------|----------|-----------------|
| 660 | 5.24 | 71.49 | -36.12 | -32.31 | 60 kDa chaperonin | COG0459 | K04077 | O |
| 668 | 5.14 | 71.49 | -37.9 | -27.45 | 60 kDa chaperonin | COG0459 | K04077 | O |
| 681 | 5.19 | 71.06 | -44.84 | -35.13 | 60 kDa chaperonin | COG0459 | K04077 | O |
| 750 | 6.18 | 67.24 | -2.58 | -3.07 | Mannosylglucosyl-3-phosphoglycerate phosphatase | COG0737 | K17224 | F |
| 813 | 5.49 | 61.36 | -26.52 | -38.25 | ATP synthase subunit α | COG0056 | K02111 | C |
| 822 | 5.02 | 61.07 | -17.07 | -19.51 | Ribulose biphosphate carboxylase large chain | COG1850 | K01601 | G |
| 873 | 5.08 | 57.17 | -43.22 | -43.35 | ATP synthase subunit beta | COG0055 | K02112 | C |
| 874 | 5.21 | 57.57 | -35.22 | -33.67 | Ribulose biphosphate carboxylase large chain | COG1850 | K01601 | G |
| 879 | 4.97 | 57.03 | -21.63 | -22.83 | ATP synthase subunit beta | COG0055 | K02112 | C |
| 880 | 5.25 | 57.03 | -30.3 | -31.65 | Ribulose biphosphate carboxylase large chain | COG1850 | K01601 | G |
| 884 | 5.15 | 57.03 | -63.29 | -67.79 | Ribulose biphosphate carboxylase large chain | COG1850 | K01601 | G |
| 885 | 5.36 | 56.64 | -33.55 | -36.18 | Glutamate synthase [NADPH] small chain | COG0493 | K00266 | E |
| 923 | 4.63 | 54.46 | -38.37 | -40.79 | Enolase | COG0148 | K01689 | G |
| 962 | 5.57 | 53.61 | -24.57 | -16.46 | Glycerol kinase | COG0554 | K00864 | C |
| 963 | 6.06 | 53.61 | -13.55 | -12.8 | soxB | COG0737 | K17224 | F |
| 964 | 6.11 | 53.73 | -8.16 | -7.66 | Dihydropolpyl dehydrogenase | COG1249 | - | C |
| 971 | 6.22 | 53.37 | -22.01 | -21.28 | soxB | COG0737 | K17224 | F |
| 974 | 5.23 | 53.49 | -6.94 | -6.62 | Metalloprotease TldD | COG0312 | K03568 | S |
| 1007 | 5.23 | 50.73 | -4.79 | -5.68 | Beta sliding clamp | COG0592 | K03629 | L |
| 1009 | 5.41 | 50.63 | -4.15 | -5.09 | Beta sliding clamp | COG0592 | K03629 | L |
| 1011 | 5.33 | 50.63 | -11.59 | -10.34 | Beta sliding clamp | COG0592 | K03629 | L |
| 1075 | 5.36 | 46.95 | -5.77 | -4.67 | S-adenosylmethionine synthase | COG0192 | K00789 | H |

Table 12. (Continued)

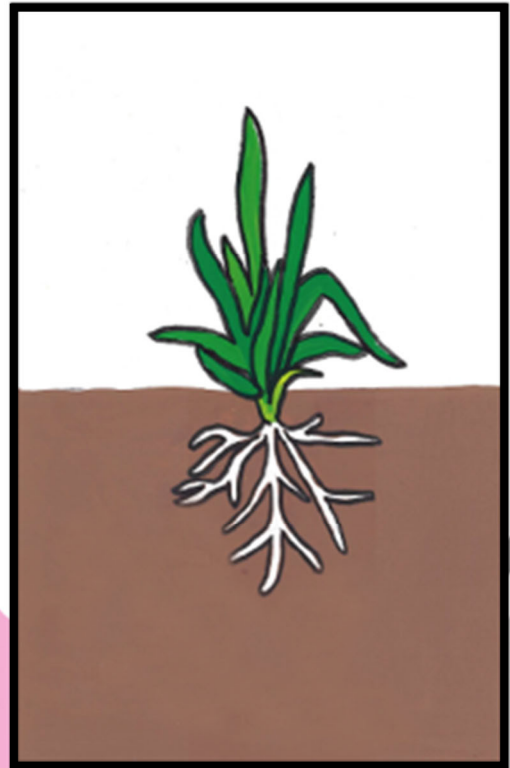
| Spot | pI | Mw (kDa) | 0.7/3.0 Av. Ratio | 0.7/6.0 Av. Ratio | Description | COG No. | KEGG No. | EggNOG Category |
|------|-------|----------|-------------------|-------------------|--|---------|----------|-----------------|
| 1131 | 5.89 | 44.377 | -2.05 | -2.07 | NADP-dependent malic enzyme | COG0281 | - | C |
| 1154 | 5.13 | 43.768 | -3.39 | -2.71 | Hypothetical protein | - | - | R |
| 1172 | 5.43 | 43.715 | 1.98 | 2.11 | Hypothetical protein | COG2067 | - | I |
| 1207 | 5.41 | 42.534 | 3.04 | 3.31 | Hypothetical protein | - | - | R |
| 1218 | 5.76 | 42.489 | -2.27 | -1.74 | Hypothetical protein | | | |
| 1234 | 5.05 | 42.005 | -5.12 | -4.66 | Hypothetical protein | | | |
| 1238 | 5.14 | 41.92 | -3.57 | -2.89 | Hypothetical protein | | | |
| 1280 | 5.06 | 41.151 | -9.53 | -11.35 | Putative membrane transport protein (Lo19II-12_873) | COG1494 | K06076 | G |
| 1316 | 4.43 | 39.966 | -16.01 | -16.52 | Hypothetical protein | COG2067 | K06076 | I |
| 1340 | 5.47 | 39.68 | -6.58 | -5.08 | Adenosine kinase | COG0524 | K00856 | G |
| 1370 | 6.42 | 39.251 | -28.15 | -26.52 | Glyceraldehyde-3-phosphate dehydrogenase | COG0057 | K00134 | G |
| 1412 | 6.64 | 38.414 | -6.75 | -7.55 | Glyceraldehyde-3-phosphate dehydrogenase | COG0057 | K00134 | G |
| 1804 | 5.53 | 28.495 | -2.29 | -2.25 | Putative metal-dependent hydrolase YcfH | COG0084 | K03424 | L |
| 1817 | 7.44 | 28.38 | 13.16 | 9.65 | Putative parvulin-type peptidyl-prolyl cis-trans | COG0760 | K03769 | O |
| 1981 | 10.06 | 25.195 | 19.4 | 15.91 | Peptidoglycan-binding protein ArfA | COG2885 | K03286 | M |
| 2005 | 5.68 | 24.617 | -5.77 | -4.86 | Ribulose-phosphate 3-epimerase | COG0036 | K01783 | G |
| 2096 | 5.35 | 23.167 | -3.65 | -4.58 | ATP-dependent Clp protease proteolytic subunit | COG0740 | K01358 | O |
| 2111 | 6.28 | 22.893 | -52.4 | -48.63 | Superoxide dismutase [Fe] | COG0605 | K04564 | P |
| 2115 | 10.06 | 22.866 | 7.18 | 10.03 | Peptidoglycan-binding protein ArfA | COG2885 | K03286 | M |
| 2122 | 5.39 | 22.625 | -8.44 | -12.35 | ATP-dependent Clp protease proteolytic subunit | COG0740 | K01358 | O |
| 2128 | 5.22 | 22.546 | -19.76 | -20.23 | Putative inorganic diphosphatase (Lo19II-12_469) | COG0221 | K01507 | C |
| 2191 | 6.00 | 21.48 | -2.01 | -2.52 | Ribosome-recycling factor | COG0233 | K02838 | J |

Table 12. (Continued)

| Spot | pI | Mw (kDa) | 0.7/3.0 Av. Ratio | 0.7/6.0 Av. Ratio | Description | COG No. | KEGG No. | EggNOG_Category |
|------|------|----------|----------------------|----------------------|--|---------|----------|-----------------|
| 2645 | 9.89 | 15.422 | 3.23 | 3.21 | hypothetical protein | cI21600 | - | R |
| 2683 | 4.31 | 15.284 | -4.16 | -6.5 | 50S ribosomal protein L7/L12 | COG0222 | K02935 | J |
| 2686 | 4.42 | 15.255 | -5.14 | -8.8 | 50S ribosomal protein L7/L12 | COG0222 | K02935 | J |
| 2731 | 6.84 | 0 | 5.33 | 2.6 | Hypothetical protein | - | - | S |
| 2767 | 5.38 | 0 | 2.1 | 1.64 | Major carboxysome shell protein 1C | COG4577 | K04027 | E |
| 2781 | 7.20 | 0 | 2.87 | 2 | Hypothetical protein | - | - | S |
| 2801 | 5.06 | 0 | -2.4 | -3.39 | Major carboxysome shell protein 1C | COG4577 | K04027 | E |
| 2815 | 5.25 | 0 | -4.79 | -5.02 | Ribulose biphosphate carboxylase small chain | COG4451 | K01602 | C |
| 2820 | 6.14 | 0 | -4.42 | -4.44 | Ribulose biphosphate carboxylase small chain | COG4451 | K01602 | C |
| 2858 | 5.64 | 0 | 2.96 | 1.26 | Hypothetical protein | COG3439 | - | S |

CHAPTER 3

Isolation, identification and selection of phosphate solubilizing bacteria and their application to barley crops



1. Introduction

Barley (*Hordeum vulgare* L.) is an annual cereal grain that was one of the first domesticated plants in the human history. Nowadays it is **the fourth most widely cultivated cereal in the world**, after wheat, rice and corn. Barley is very important in terms of production, with about 158 million tons produced during 2019, and more than 50 million hectares harvested all around the World (Figure 38). Europe is the major producer (near 60% of the world production stems from there), and Spain was the 8th producer country in the World in 2019 (<http://www.fao.org/faostat/en/#data/QC/visualize>) (Taner *et al.*, 2004; Zhou, 2009).

Barley is mainly used as feed for animals (globally, 70% of barley production is used directly or indirectly for feeding animals). In fact, the Spanish name for barley is “*cebada*”, which comes from the Latin “*cibata*”, the past participle of the verb “*cibare*”, which means “to feed”. The second most important use of barley grain is the malt production. Globally, 30% of the world’s barley production is used for malting purposes, being the amount of barley destined for beer production very important in Spain. The national production of beer in Spain in 2014 was 3.35 billion liters, making Spain the fourth largest producer in the European Union and the tenth largest in the World. In fact, barley was the most cultivated crop in Spain in 2019 (Martínez-Moreno, 2017; Taner *et al.*, 2004) (<http://www.fao.org/faostat/en/#data/QC/visualize>).

One of the main problems in the agricultural world is the excessive use of fertilizers. That cause a number of environmental and ecological problems, within and outside farmlands, such as air pollution, soil acidification and degradation, water eutrophication, crop yield reduction, and undermining of the sustainability of food and energy production from agricultural fields. Nowadays, the average of fertilizer consumption per hectare of arable land in the world is around 140 kg (<https://data.worldbank.org/indicator/AG.CON.FERT.ZS>). Besides, most of the fertilization processes nowadays are based on mineral fertilizers (mainly phosphorus, nitrogen and potassium, the so-called

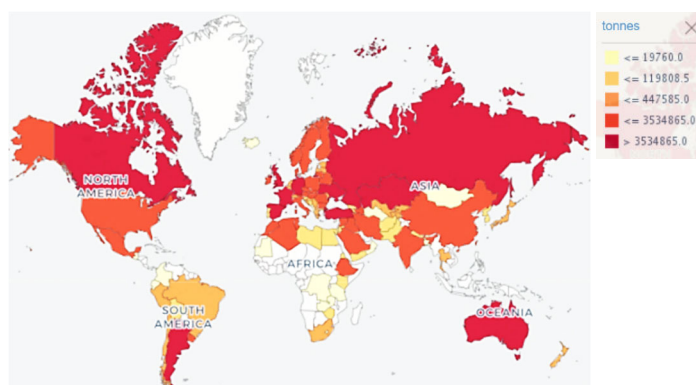


Figure 38. Production quantities of barley by country from year 2018 to 2019 by FAO (<http://www.fao.org/faostat/en/#data/QC/visualize>).

NPK-fertilizers), which are highly polluting in both production and application processes. Therefore, since the turn of the century, experts from all around the world support **the need to achieve an eco-friendly fertilization mechanism**. At first, the scientific world focused on nitrogen-fixing microorganisms as the main solution. However, some decades later, they faced **the problem of P precipitation in crop soils after fertilization. This is how phosphate solubilizing microorganisms (PSM) emerged in recent decades, as a putative solution to an environmental problem of today and tomorrow** (Giri *et al.*, 2019; Li *et al.*, 2019; Maçik *et al.*, 2020).

Although P is abundant in soil, it is a major limiting factor for plant growth as it is in an **unavailable form for root uptake. P can be found in soils in both organic** (mainly from manure and plant or animal wastes) **and inorganic** (mostly in insoluble mineral complexes with Al, Fe and Ca) **forms**. PSM are able to convert inorganic and organic soil P through various mechanisms of solubilization and mineralisation, into bioavailable forms facilitating their uptake by plant roots. Each organism can act in one or more than one way to bring about solubilization of insoluble P. Thus, **organic P solubilization is also called mineralization**, and it can occur through three different groups of enzymes: **i) phosphatases**, which are grouped into two types according to their pH of activity: acidic and alkaline, **ii) phytases**, which specifically cause release of P from phytate degradation, and, in lesser extent, **iii) phosphonatas** and C-P lyases, that cleave the C–P bond of organophosphonates. On the contrary, though it is difficult to pin point a single mechanism of **inorganic P solubilization, production of organic or inorganic acids**, with a consequent pH reduction, **appears to be of great importance**. The monovalent anion $H_2PO_4^-$ is a major soluble form of inorganic phosphate, which usually occurs at low pHs (Alori *et al.*, 2017; Sharma *et al.*, 2013).

Since 1948, when Pikovskaya suggested that microorganisms could dissolve non-readily available forms of P from soil, and play an important role in supplying P to plants, numerous methods and culture media have been developed for their study, such as Pikovskaya (PVK), bromophenol blue dye method or NBRIP medium. Most of them use **TCP (tricalcium phosphate) as insoluble P source for isolating and testing PSM** (Sharma *et al.*, 2013). Since then, numerous PSM microorganisms, from both bacteria and fungi kingdoms have been described. Nevertheless, this dissertation is focused on **PSB (phosphate solubilizing bacteria)**, since it has been reported that bacteria are usually 2 - 150 times greater solubilizer than fungi, especially in soils (Dilnashin *et al.*, 2020). In addition, another interesting skill of some PSB is endospore production, since during fertilizer production high temperatures are used, conditions that other types of microorganisms, like most of the fungus, cannot survive.

Besides, the latest research shows that all this PSB offer **other interesting skills** for crops: **plant hormone production, minerals solubilization, or even antifungal activity against crop pathogens**. Thus, in this part of the dissertation, we are focused not only on PSB isolation and characterization, but also on their analysis as **plant growth promoting rhizobacteria (PGPR)**, and their antifungal activity against some of the main pathogen fungi of barley and other cereals: *Fusarium* (species like *F. culmorum*, *F. oxysporum* or *F. graminearum*), *Alternaria spp.*, *Botrytis cinerea*, or *Rhizoctonia*

solani (González *et al.*, 2016; Hane *et al.*, 2014; Mykhalska *et al.*, 2019). *Fusarium* head blight (FHB), also known as scab, is an economically devastating disease of small grain cereal crops. It affects all small grains crops including wheat (*Triticum spp.*), barley (*Hordeum vulgare*), rye (*Secale cereale*), oats (*Avena sativa*), and triticale (*Triticosecale*). The highest economic losses occur in wheat and barley production. Symptoms are manifested as bleaching of one or more spikelets on a spike. The bleaching can start anywhere on the spike, but frequently begins in the centre of it, and can continue until the entire spike is whitened. Bleached spikes are randomly scattered in the field and appear suddenly, so that a crop that appeared healthy only a few days earlier, may show widespread symptoms (Wegulo *et al.*, 2015). *Alternaria spp.* is the main cause agent of black point disease in cereals, particularly wheat and barley. The disease consists of dark discoloration of the embryonic end of the kernel, even if the vitality of the embryo is generally not affected. Although this disease does not affect harvest yield, it can compromise grain quality and its commercial value because plants which grow from infected seeds have slow growth and development. (Fanelli *et al.*, 2013; Mykhalska *et al.*, 2019). *B. cinerea*, also known as grey mould, can infect more than 200 species of plants. The fungus is considered a typical necrotroph, co-opting the host's programmed cell death pathways to achieve infection (Dean *et al.*, 2012).

2. Material and methods

2.1. Isolation and selection of phosphate solubilizing bacteria (PSB)

Phosphate solubilizing bacteria were isolated from the ectorhizosphere (soil directly surrounding the root) of barley plants cultivated in a field located in León (Spain). Five plants were gently removed from the soil, and the soil adhered to roots was collected by introducing fragment of roots in a 50-mL tube and shaken by extensive vortexing. Next, 10-fold serial dilutions from 10^{-2} to 10^{-7} were prepared into sterile ddH₂O, by duplicate. One of the duplicates was incubated at 80°C for 10 min. Finally, 100 µL of each sample were spread on NB agar, Plate Count Agar and SCA (starch-casein agar) plates (compositions in section II in appendix) supplemented with natamycin 200 µg/mL to prevent fungal growth. Plates were incubated at 30°C up to 12 days, until growth was observed.

Bacteria representative of the predominant morphological types present on the plates were selected at random, and picked and streaked onto NBRIP agar medium (composition in section II in appendix) (Mardad *et al.*, 2013) to check for phosphate solubilization on solid media. Plates were incubated at 30°C up to 12 days. Colonies surrounded by clear zones were selected to analyse their solubilisation index.

2.2. Endospores detection

To determine endospore formation, microscopic observation after staining with malachite green and safranin is mainly used. Malachite green is a water-soluble dye, which does not adhere to the

cell wall, so heat is used to allow it to enter in the vegetative cells and the endospores. Then, the sample is washed with water, which makes the vegetative cells, but not the endospores, lose the malachite green dye. The sample is then dyed with safranin, which will stain the vegetative cells but not the endospores. Thus, the vegetative cells should appear pink/red, while the spores should be observed as green/blue.

Protocol development

- Grow the strain in NB agar medium at 30°C for 24 h, and at RT for a week.
- Add 10 µL of dH₂O onto a slide, smear a small quantity of the culture over it, and fix by heat until the sample is fully dried.
- Add several drops of malachite green⁴⁵ and heat to steam for 5 min. Keep the sample moist by adding more dye, one drop at a time, as needed. Allow the slide to cool for 2 min.
- Gently squirt a stream of dH₂O onto the top of the slide.
- Add safranin to cover the sample. And incubate at RT for 2 min.
- Gently squirt a stream of dH₂O onto the top of the slide.
- Let the sample air dry.

2.3. Determination of P solubilization in solid media

To analyse their phosphate solubilization skills, 20 µL of each bacterial culture were plated onto NB RIP agar plates (composition in section II in appendix) and incubated at 30°C up to 15 days. The halozone formed around the colony was measured every 4 days. All the experiments were carried out by triplicate. The solubilization index (SI) was determined by measuring the halo and the colony diameter according to next formula (Mardad *et al.*, 2013):

$$SI = \frac{\text{Colony diameter} + \text{Halozone diameter}}{\text{Colony diameter}}$$

According to their morphological characteristics, the strains with a SI over the average, and especially those strains showing endospores formation, were selected for later identification.

2.4. Identification of PSB

Isolates were identified by *16S rRNA* gene sequencing at Instrumental Techniques Laboratory (University of León). Genomic DNA isolation from the selected strains was carried out as described by Hopwood *et al.* (2000). Thus, cultures were grown in NB liquid medium at 30°C and 150 rpm for 24 h, and DNA was extracted as follows:

⁴⁵ **Malachite green:** 0.5% (w/v) malachite green in dH₂O.

Protocol development

- Centrifuge 10 mL of a pre-grown culture at 10,700 x g for 1 min.
- Discard the supernatant.
- Add 250 µL of lysis solution⁴⁶ and incubate 10 min at RT.
- Add 75 µL of potassium acetate buffer⁴⁷. Mix thoroughly by inversion.
- Centrifuge the samples at 17,000 x g for 2 min at RT. Transfer the supernatant to a new tube.
- Add 400 µL of isopropanol. Mix thoroughly by inversion. Incubate 5 min at RT.
- Centrifuge at 17,000 x g for 5 min at RT.
- Discard the supernatant.
- Wash the DNA adding carefully 50 µL of 70% (v/v) ethanol over the pellet.
- Discard the supernatant.
- Let the pellet dry and re-suspend in 50 µL of TE⁴⁸.

Extracted DNA was analysed by electrophoresis in a 0.7% (w/v) agarose gel in 1x TAE buffer⁴⁹ and stained with 2.0 µg/mL ethidium bromide (Sigma-Aldrich) and its concentration was measured on a *NanoDrop™ 2000 spectrophotometer* (Thermo Fisher Scientific). Genomic DNA was stored at -20°C until use.

16S rRNA genes were amplified using the 27F (5' AGAGTTTGATCCTGGCTCAG 3') and 1492R (5' TACCTTGTTACGACTT 3') primers (Peace *et al.*, 1994). Amplification reactions were developed in 1x *paq5000 DNA polymerase buffer* (Agilent Technologies) with 1 µM of each primer, 0.1 mM dNTPs (EURx), 1 U *Paq5000 DNA polymerase* (Agilent Technologies) and 15 ng template DNA. ddH₂O was used to bring the total reaction volume to 20 µL.

PCR amplification was carried out in 0.2 mL sterile tubes using a *Mastercycler Gradient Thermocycler* (Eppendorf). PCR conditions were 98°C, 3 min; 25 cycles of 98°C, 30 seg; 50°C, 1 min; 72°C, 2 min; and a final extension of 72°C 10 min. Samples were kept at 4°C until the reactions were analysed in 1% (w/v) agarose gels.

Sequence data were aligned with MEGA 7.0 software (<https://www.megasoftware.net>) and compared with available sequences of bacterial lineage in the National Centre for Biotechnology Information GenBank database (<http://www.ncbi.nlm.nih.gov>) using BLASTn software (<https://blast.ncbi.nlm.nih.gov>).

⁴⁶ **Lysis solution:** 400 mM Tris-HCl, pH 8.0; 60 mM EDTA, pH 8.0; 150 mM NaCl; 1% SDS.

⁴⁷ **Potassium acetate buffer:** 3 M potassium acetate; 11.5% (v/v) glacial acetic acid; pH 4.8.

⁴⁸ **TE buffer:** 10 mM Tris-HCl; 1 mM EDTA; pH 8.0

⁴⁹ **50x TAE buffer:** 5.71% (v/v) acetic acid; 10% (v/v) EDTA 0.5 M, pH 8.0; 24.2% (w/v) Tris base.

2.5. Determination of phosphate solubilization in liquid medium

P solubilization of the selected strains was quantified in liquid medium. Briefly, all the strains were grown in NB liquid medium at 30°C and 150 rpm for 24 h. 500-mL Erlenmeyer flasks containing 100 mL of NBRIP liquid medium (composition in section II in appendix) were inoculated at $5 \cdot 10^4$ cfu/mL and incubated at 30°C and 150 rpm for 20 days. 1 mL samples were taken every 24 h and stored at -20°C until use. pH of the cultures was determined by a *pH-meter pH526* (WTW). All experiments were carried out by triplicate. Soluble P quantification was analysed by following malachite green method (Martínez Castro, 2011) and compared with a standard curve using K_2HPO_4 (see section 2.4).

2.6. Determination of P solubilization mechanisms

2.6.1. Phosphatase activity quantification

One of the main phosphorus solubilization methods used by PSMs is the synthesis of phosphatases. The assay for phosphatases determination is based on the ability of acid and alkaline phosphatases to catalyse the hydrolysis of the *p*-nitrophenolphosphate to *p*-nitrophenol, which maximally absorbs at 405 nm. Thus, a pre-culture was grown in NB liquid medium at 30°C and 150 rpm for 24 h. Then, 25 mL of TSB (composition in section II in appendix) were inoculated at $5 \cdot 10^4$ cells/mL with the pre-culture, and incubated at 30°C and 150 rpm for 48 h. The extracellular and cytoplasmatic phosphatase activities (both acidic and alkaline) were determined as follows:

Protocol development

- Transfer 1 mL of the culture to a microtube and the rest to a 50-mL tube.
- Centrifuge the culture from the microtube at $17,000 \times g$ for 10 min and the 50-mL tube at $10,700 \times g$ for 20 min.
- Transfer the supernatant from the microtube to a new microtube and store at 4°C until use. The supernatant will be used to determine the extracellular phosphatase activity.
- Discard the supernatant from the 50-mL tube and wash the pellet twice in 0.9% NaCl.
- Resuspend the pellet in 1 mL of TE buffer⁵⁰ and sonicate with an *Ultrasonic Processor XL sonicator* (Misonix) on ice for 10 cycles of 2 s sonication and 20 s rest.
- Centrifuge at $17,000 \times g$ for 10 min, transfer the supernatant to a new microtube and store at 4°C until use. The supernatant will be used to determine the intracellular phosphatase activity.
- Place 50 μ L of each sample in each well of a 96-well microplate.

⁵⁰ **TE buffer:** 10 mM Tris-HCl; 1 mM EDTA; pH 7.0.

- Add 50 μL of substrate solution for acidic phosphatases⁵¹ or 50 μL of substrate solution for alkaline phosphatases⁵², as appropriate.
- Incubate the microplate at 37°C for 10 min on a rotary shaker at 60 rpm.
- Add 200 μL of 0.5 N NaOH to stop the reaction.
- Measure the OD at 405 nm.

A *p*-nitrophenol solution from 0 to 1 $\mu\text{mol}/\text{mL}$ was used as standard from a 5 $\mu\text{mol}/\text{mL}$ stock and run in parallel (Table 13). The blank consisted in 50 μL of buffer instead of bacterial supernatant. To determine specific activities, the total soluble protein in cell extracts and supernatants cultures was quantified by the Bradford method (see section 2.5.2).

Table 13. Preparation of the standard curve of *p*-nitrophenol for the acid and alkaline phosphatase quantification by the $\text{OD}_{405\text{ nm}}$ measurement.

| | | | | | | |
|--|-----|------|------|-----|-----|----|
| [<i>p</i> -nitrophenol] ($\mu\text{mol}/\text{mL}$) | 0 | 0.01 | 0.05 | 0.1 | 0.5 | 1 |
| V (μL) (stock) | 0 | 0.2 | 1 | 2 | 10 | 20 |
| V (μL) (ddH ₂ O) | 100 | 99.8 | 99 | 98 | 90 | 80 |

2.6.2. Phytase activity determination

a. Qualitative method: agar-plate assay

To check the ability of the isolates to hydrolyze phytate, they were plated onto PSM medium (composition in section II in appendix), and the phytase activity was assayed according to the counterstaining technique described by Kumar *et al.* (2013). Nevertheless, as a personal opinion, it is recommended to incubate only with the cobalt chloride solution to observe the halo zones.

Protocol development

- Cultures were grown into NB liquid medium at 30°C and 150 rpm for 24 h.
- Four different drops of the culture, 10 μL each, were placed in PSM medium.
- Plates were incubated at 30°C for 5 days.
- Flood the plates with 2% cobalt chloride for 5 min.
- Replace the cobalt chloride solution with freshly prepared colouring reagent containing equal volumes of 6.25% (w/v) aqueous molybdate and 0.42% (w/v) ammonium vanadate solution and incubated for 5 min at RT.

⁵¹ **Substrate solution for acidic phosphatases:** 0.1 M citric acid; 0.1 M sodium citrate; 5.5 mM *p*-nitrophenylphosphate; pH 4.8.

⁵² **Substrate solution for alkaline phosphatases:** 0.05 M glycine; 0.01% (w/v) $\text{MgCl}_2 \cdot 6\text{H}_2\text{O}$; 5.5 mM *p*-nitrophenylphosphate; pH 10.5.

b. Quantitative assay: spectrophotometric method

To quantify the phytase production, a spectrophotometric assay based on Jorquera *et al.* (2018) and Nassiri *et al.* (2015) protocols was carried out. Nevertheless, P solubilization mainly derive from the phytases secreted to the environment, so just extracellular phytases were analysed. Briefly, a pre-culture of each isolate was grown into 100 mL of LB liquid medium (composition in section II in appendix) at 30°C and 150 rpm for 24 h. 500-mL Erlenmeyer flasks containing 100 mL of LB medium were inoculated with $5 \cdot 10^4$ cells/mL and incubated at 30°C and 150 rpm for 7 days. 5 mL samples were taken and centrifugated at $6,850 \times g$ and 4°C for 5 min. Supernatants were subjected to dialysis (10 kDa) into sodium acetate buffer⁵³ at 4°C O/N.

Then, 150 µL of the crude extracellular protein extract were incubated with 600 µL of phytate solution⁵⁴ at 37°C for 30 min. The reaction was stopped by the addition of 750 µL of the stop solution (5% w/v trichloroacetic acid). Finally, 6 mL of the colour reagent⁵⁵ were added to 1.5 mL of the sample solution. Samples were centrifugated at $2675 \times g$ for 5 min. Absorbance of supernatants was measured at 700 nm.

One unit of phytase activity was defined as 1 µmol of P released in 1 min. Blanks were carried out in parallel by adding stop solution prior to substrate addition.

Lastly, soluble P standard curve was prepared using a 5 mg/mL K_2HPO_4 solution as stock as indicated in Table 14. Standard curve samples were measured spectrophotometrically at 700 nm before measuring the rest of the samples.

Table 14. Preparation of the standard curve of K_2HPO_4 for the phytase production quantification by the $OD_{700\text{ nm}}$ measurement.

| | | | | | | | |
|-----------------------------|------|-------|-------|-----|-----|-----|-----|
| [KH_2PO_4] (mg/mL) | 0 | 5 | 25 | 50 | 150 | 300 | 600 |
| V (µL) (stock) | 0 | 2.5 | 12.5 | 25 | 75 | 150 | 300 |
| V (µL) (ddH ₂ O) | 1000 | 997.5 | 987.5 | 975 | 925 | 850 | 700 |

2.6.3. Organic acid biosynthesis

To determine organic acid productions in the isolates PSB1 to PSB9, a new fermentation was carried out in modified NBRIP liquid medium. To avoid problems with the insoluble P in NBRIP medium, $Ca_3(PO_4)_2$, was replaced by 5 g/L K_2HPO_4 and 5 g/L KH_2PO_4 . Thus, 100 mL of each medium were inoculated at $5 \cdot 10^4$ cell/mL and incubated at 30°C and 150 rpm for 7 days. 2 mL samples were taken daily and cell-free culture supernatants were obtained by centrifugation at $17,000 \times g$ for 10

⁵³ **Sodium acetate buffer:** 100 mM sodium acetate, pH 5.0.

⁵⁴ **Phytate solution:** 0.2% (w/v) of sodium phytate [phytic acid sodium salt hydrate; $C_6H_{18}O_{24}P_6 \cdot xNa \cdot yH_2O$] in 100 mM sodium acetate buffer; pH 5.0.

⁵⁵ **Colour reagent:** 1.5% (w/v) ammonium molybdate, 5.5% (w/v) sulphuric acid solution and 2.7% (w/v) ferrous sulphate.

min and filtration through a 0.2 µm filter. Acetic, citric, formic, lactic, malic, oxalic, succinic and tartaric acids were measured by HPLC equipped with an Alliance 2695 refractive index detector (Waters). Isocratic elution with 0.005 M H₂SO₄ was performed using a HiPlex H (300 x 7.7 mm) column (Agilent) at 50°C and a flow rate of 0.5 mL/min.

2.6.4. Siderophore production

Siderophores are low molecular weight organic ligands, with high affinity and specificity for binding trivalent ions such as iron and aluminium (Ghosh *et al.*, 2015). Siderophore production is commonly detected by using chrome azurol sulphonate (CAS) dye, which forms a ferric complex (CAS-iron-detergent complex) of blue colour. In presence of siderophore molecules, the iron is strongly chelated, becoming the dye free in the media, and losing the blue colour.

Protocol development

- Cultures were grown into NB liquid medium at 30°C and 150 rpm for 24 h.
- Four different drops of the culture, 10 µl each, were placed in CAS agar medium.
- Plates were incubated at 30°C for 5 days.

Bacterial colonies with yellow-orange colour halo zone were selected positive for siderophore production. To avoid inconsistent results with the colour of the plates, CAS agar medium was prepared from four solutions sterilized separately before mixing following the instructions below.

a. Fe-CAS solution

The Fe-CAS solution was freshly prepared for each batch of CAS agar plates by mixing 10 mL of 1 mM FeCl₃ · 6 H₂O in 10 mM HCl with 50 mL of an aqueous solution of 1.21 mg/mL CAS. Then, 40 mL of an aqueous solution of 1.82 mg/mL hexadecyltrimethylammonium bromide (HDTMA) were prepared separately. The dark purple mixture of Fe-CAS was added slowly, with constant stirring, to the HDTMA solution, reaching a dark blue colour. The final solution was sterilized by autoclaving and stored at 50°C until use.

b. Buffer solution

The buffer solution was prepared by dissolving 0.3 g of KH₂PO₄, 0.5 g of NaCl and 1.0 g of NH₄Cl in 750 mL of dH₂O and mixing by stirring. Hereafter, 30.24 g of PIPES (1,4-Piperazinediethanesulfonic acid) were added to the solution. The pH was adjusted to 6.8 with KOH, and dH₂O was added to bring the volume up to 800 mL. Finally, 15 g of agar were added to the bottle. The final solution was sterilized by autoclaving and stored at 50°C until use. It is recommended to place a magnetic stirrer inside the bottle to homogenize all the solutions after mixing them.

c. Solution 3

The composition of solution 3 was as follows: 2 g glucose, 2 g mannitol, 493 mg $\text{MgSO}_4 \cdot 7 \text{H}_2\text{O}$, 11 mg CaCl_2 , 1.17 mg $\text{MnSO}_4 \cdot \text{H}_2\text{O}$, 1.4 mg H_3BO_3 , 0.04 mg $\text{CuSO}_4 \cdot 5 \text{H}_2\text{O}$, 1.2 mg $\text{ZnSO}_4 \cdot 7 \text{H}_2\text{O}$ and 1.0 mg $\text{Na}_2\text{MoO}_4 \cdot 2 \text{H}_2\text{O}$; in 70 mL of dH_2O . Solution 3 was autoclaved and stored at 50°C until use.

d. Casamino acids solution

Casamino acids solution consisted in 10% (w/v) casamino acids in 30 mL of dH_2O . The solution was sterilised through a 0.2 μm filter.

e. Final CAS agar medium

Solution 3 was added to the buffer solution, as was the casamino acids solution. Fe-CAS solution was added the last, with continuous stirring to mix all the solutions without forming bubbles.

2.6.5. HCN production

All the isolates were screened for the production of HCN by using the method of Lorck (1948), recently described in detail by Devi *et al.* (2018). The protocol is based on the fact that HCN is reduced to isopurpuric acid in the presence of picric acid, developing an orange-reddish colour. Thus, a pre-culture was grown into NB liquid medium at 30°C and 150 rpm for 24 h and analysed as follows:

Protocol development

- Streak the cultures onto NB solid medium supplemented with 4.4 g/L glycine.
- A Whatmann filter paper No. 1 soaked in 2% sodium carbonate in 0.5% picric acid solution was placed in the top of the plate.
- Plates were sealed with parafilm and incubated in the dark at 30°C up to 10 days.

Those isolates that developed an orange-reddish colour on the Whatmann filter paper were determined positive.

2.7. Miscellaneous plant growth promoting characters

2.7.1. Indoleacetic acid synthesis

The auxin indole-3-acetic acid (IAA) is a product of tryptophan metabolism. The quantification of the IAA synthesized by every isolate was carried out by using a colorimetric technique according the Salkowski's method (Gordon & Weber, 1951). Salkowski reagent is a mixture of ferric chloride and perchloric acid, which react with IAA yielding a pink colour solution.

Thus, flasks containing 100 mL of NB medium supplemented with 5 g/L tryptophan were inoculated at $5 \cdot 10^4$ cells/mL and incubated at 30°C and 150 rpm for 10 days. Daily, 1.5 mL samples

were taken to analyse growth (by OD₆₀₀ and by ufc count on NB agar medium) and indoleacetic acid production, which was measured spectrophotometrically by the Salkowski's method.

a. Salkowski's reagent preparation

Protocol development

- Add 2.027 g of FeCl₃ to 15 mL of dH₂O.
- Mix 49 mL of a 70% HClO₄ with 49 mL of dH₂O (final concentration of 35%).
- Add 2 mL of the FeCl₃ solution to the HClO₄.
- Autoclave at 121°C for 20 min and keep in the dark.

b. IAA standard curve

IAA standard curve was prepared using a 1 mg/mL IAA solution as stock as indicated in Table 15. Measure the standard curve samples spectrophotometrically at 530 nm before measuring the rest of the samples. Standard curve shows changes of colour since colourless (low concentration) to dark pink ones (high concentration).

Table 15. Preparation of the standard curve of IAA for the IAA quantification by the OD_{530 nm} measurement.

| | | | | | | |
|---------------|----|--------------|---------------|------------------|---------------|--------------|
| [IAA] (µg/mL) | 0 | 5 | 10 | 20 | 50 | 100 |
| V (mL) (IAA) | 0 | 1 (50 µg/mL) | 1 (100 µg/mL) | 2 mL (100 µg/mL) | 5 (100 µg/mL) | 1 mL (stock) |
| V (mL) (NB) | 10 | 9 | 9 | 8 | 5 | 9 |

c. Samples measure

Samples were mixed with the Salkowski's reagent and measured spectrophotometrically as follows:

Protocol development

- Mix 1 mL of the sample with 2 mL of Salkowski's reagent.
- Incubate the samples 25 min in the dark.
- Measure OD at 530 nm.

2.7.2. Zn solubilization

All the selected isolates were screened for their efficiency to solubilize zinc on Tris-minimal medium (composition in section II in appendix) supplemented separately with two different Zn source: tris-minimal medium supplemented with zinc oxide (ZnO) (1.244 g/L), and, on the other side, tris-minimal medium supplemented with zinc phosphate [Zn₃(PO₄)₂] (1.988 g/L). Both of them at a concentration equivalent to 0.1% Zn, following Sharma *et al.* (2011) protocol. Zn solubilization efficiency (SE) was calculated as follow:

$$SE = \frac{\text{Diameter of the halo zone}}{\text{Diameter of the colony}} \cdot 100$$

Protocol development

- Cultures were grown into NB liquid medium at 30°C and 150 rpm for 24 h.
- Four different drops of the culture, 10 µl each, were placed in Tris-minimal medium supplemented with Zn.
- Plates were incubated at 30°C up to 7 days in the dark.

Positive strains were selected according to the formation of a halo around the isolate.

2.7.3. K solubilization

The nine selected isolates were screened for their efficiency to solubilize potassium on Aleksandrov medium (composition in section II in appendix), supplemented with 0.025% (w/v) bromothymol blue, following Etesami *et al.* (2017) protocol. K solubilization efficiency (SE) was calculated as above.

Protocol development

- Cultures were grown into NB liquid medium at 30°C and 150 rpm for 24 h.
- Four different drops of the culture, 10 µl each, were placed in Aleksandrov medium supplemented with 0.25 g/L bromothymol blue.
- Plates were incubated at 30°C up to 7 days in the dark.

Positive isolates were detected by the formation of a halo around the isolate.

2.8. Greenhouse pot experiments

In order to check the effect of selected PSB on barley crop development, a greenhouse pot experiment was carried out using vermiculite as substrate, supplemented with tricalcium phosphate [Ca₃(PO₄)₂] as sole insoluble phosphorus source. Nine 10-seed replicates were carried out for each selected PSB. Cultures for seed inoculation were grown in NB liquid medium for 24 h at 30°C and 150 rpm. Every pot was irrigated with 200 mL of modified plant nutrient solution⁵⁶ without any soluble phosphorus source. Besides, the plant nutrient solution was supplemented with dextrose, as C source for the strains, and chitosan, to avoid fungal growth in the vermiculite.

⁵⁶ **Plant nutrient solution:** 0.2 g/L MgSO₄ · 7 H₂O; 0.2 g/L KCl; 0.2 g/L NaCl; 0.014 g/L EDTA; 0.0119 g/L FeSO₄; 0.018 g/L H₃BO₃; 0.02 g/L MnSO₄ · H₂O; ZnSO₄ · 7 H₂O; 0.002 g/L CuSO₄; 0.0047 g (NH₄)₆Mo₇O₂₄; 0.4 g/L Ca(NO₃)₂.

Protocol development

- Barley seeds were superficially disinfected by immersing in 70% ethanol for 1 min, and 3% sodium hypochlorite for 5 min. Rinse in sterile ddH₂O three times for 5 min.
- Place 5 L of vermiculite (washed with dH₂O and autoclaved twice at 121°C for 20 min) supplemented with 22 g of tricalcium phosphate (ratio 25:1 w/w) per pot.
- Immerse the seeds in a pre-grown culture of each individual PSB at 10⁸ cells/mL for 5 min.
- Place 10 inoculated seeds per pot.
- Inoculate each pot with 8 mL of a pre-grown culture at 10⁸ cells/mL.
- Irrigate the pots twice per week with 200 mL of modified plant nutrient solution⁵⁶ without soluble phosphate (Rigaud & Puppo, 1975) supplemented with 2 g/L chitosan and 2 g/L dextrose.

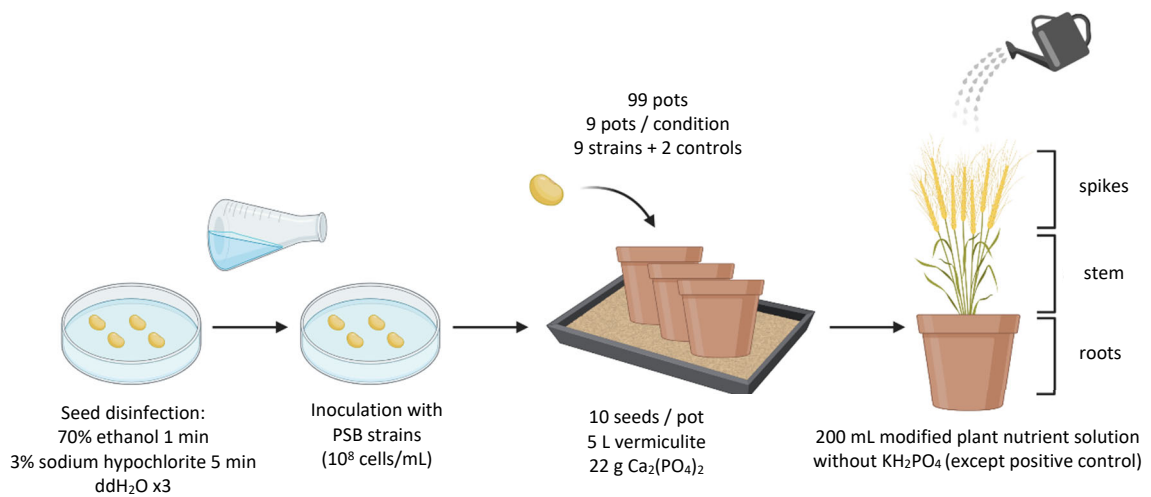


Figure 39. Diagram of the greenhouse pot experiment.

Plants were grown until maturation of the ears. Seeds for negative and positive controls were immersed into sterile NB liquid medium. Positive control pots were irrigated with plant nutrient solution supplemented with 0.2 g/L KH₂PO₄ as soluble phosphorus source.

For evaluation of the growth promotion effect of each selected PSB height, fresh and dry weight of spikes, roots and shoots were recorded. Dry weight was determined by placing the samples separately in an oven at 60°C for 72 h.

2.8.1. Phosphorus determination in root and shoot samples

Assimilated P by the plants was determined at root and shoot samples as described by Watanabe and Olsen (1965). This method is based in the reaction of orthophosphate with ammonium

molybdate under acid conditions to form molybdophosphoric acid, which reacts with vanadium to form vanadomolybdophosphoric acid, with a yellowish colour. The intensity of the yellow colour is proportional to phosphate concentration. Briefly, samples were displaced, and aerial and root parts were separated. Next, each part was grinded with an IKA MF10 Basic Grinder with an integrated 1.0 mm sieve (IKA LAbotecnik).

Protocol development

- Place 0.5 g of grinded sample in a Bloc digest 12 (Selecta) tube.
- Add 8 mL of ternary acid mixture⁵⁷.
- Digest the samples at 400°C for 30 min in a Bloc digest 12 (Selecta).
- Add ddH₂O up to 50 mL.
- Decant the samples O/N at 4°C.
- Place 5 mL of sample in a volumetric flask and add 6 mL of vanadate-molybdate reagent⁵⁸. Make up to 50 mL with ddH₂O.
- Measure absorbance at 430 nm.

Phosphoric acid (P₂O₅) was used as standard from 0 to 1% (w/v). Besides, samples were also analysed based on FAMIC (2018) by ICP-OES (iCAP 7200) (Thermo Fisher Scientific) and Qtegra 2.7 software (see section 2.3).

2.8.2. Starch determination in barley grains samples

Starch is the major component of barley kernel, and it may amount up to 70% of the seed dry weight (Asare *et al.*, 2011). Therefore, it is interesting to determine whether the presence of PGPR isolates could increase starch content in barley grains. Starch content was measured following Chow and Landhäusser (2004) protocol, which is based on starch hydrolysis to glucose, and its subsequent quantification. Thus, glucose, in presence of glucose oxidase, is converted into gluconic acid, with consequent oxygen peroxide production. This oxygen peroxide, oxidizes *O*-dianisidine, that, in acidic solution, shows a pink colour. The intensity of the pink colour measured at 540 nm is proportional to the original glucose concentration. Thus, barley grains were grinded by using a *Retsch ball mill MM200* (Fisher Scientific), and samples were filtered through a 0.7 mm sieve.

Protocol development

- Place 50 mg of grinded sample in a 15-mL tube and add 5 mL of 80% (v/v) ethanol to remove any soluble sugar. Incubate at 95°C for 10 min.

⁵⁷ **Ternary acid mixture:** 1 volume of sulphuric acid; 5 volumes of nitric acid; 2 volumes of perchloric acid.

⁵⁸ **Vanadate-molybdate reagent:** 400 mL of 0.05 M ammonium molybdate; 500 mL of 0.02 M ammonium metavanadate in 32.5% HNO₃; 100 mL ddH₂O.

- Centrifuge at 670 $\times g$ for 5 min and discard the supernatant. Repeat twice the 80% ethanol extraction.
- Let the pellet dry at 50°C for 3 - 4 h, mixing from time to time to speed desiccation.
- Place 30 mg of the washed sample in a 2-mL microtube and add 2 mL of 0.2 N KOH.
- Completely disrupt the pellet by vortexing samples for 20 s. If the pellet is not disintegrated, try to disrupt by pipetting.
- Incubate the samples 10 min at RT and 1,200 rpm in a thermomixer (*ThermoMixer F1.5*, Eppendorf).
- Boil the samples for 30 min to complete the starch solubilization process.
- Mix the samples by vortexing for 10 s.
- Centrifuge the samples 10 min at RT and 17,000 $\times g$ to remove any insoluble material.
- Transfer the supernatant to a new 1.5-mL microtube.
- Repeat the digestion with 0.2 KOH twice and mix the three basic extractions before the enzymatic digestion.
- Store the samples at 4°C until use.
- Place 200 μL samples in a new 1.5-mL microtube. Add 28 μL of 1 N HCl, 30 μL of α -amylase buffer 10x and 42 μL of fresh 0.4 U/ μL α -amylase⁵⁹ (Sigma-Aldrich, A-3176). Final concentration of α -amylase enzyme is 56 U/mL.
- Incubate at 50°C for 2 h.
- Add 50 μL of fresh 15 U/mL amyloglucosidase⁶⁰ (Sigma-Aldrich, A-7420).
- Incubate at 55°C for 2 h.
- Centrifuge 10 min at 670 $\times g$ and RT.
- Transfer the supernatant to a new 1.5-mL microtube and store the samples at 4°C until use.
- Place 200 μL samples in a 10-mL tube. Add 2 mL of fresh glucose oxidase/peroxidase reagent (Sigma-Aldrich, P 7119) and 1.6 mL of 2.5 mg/mL *O*-dianisidine (Sigma-Aldrich, D-3252).
- Incubate in the dark at 25°C for 45 min.
- Measure absorbance at 420 nm.

Final concentration was determined by comparison with a standard curve using glucose from 0 to 1 mg/mL in acetate buffer 50 mM pH 5.0, prepared from a stock solution at 10 mg/mL. Samples were diluted when needed with the same buffer and all the experiments were carried out by triplicate.

Table 16. Preparation of the standard curve of glucose for the starch quantification by the OD_{420 nm} measurement.

| | | | | | | |
|--------------------------------------|-----|-----|-----|-----|-----|-----|
| [Glucose] (mg/mL) | 0 | 0.1 | 0.2 | 0.3 | 0.4 | 0.5 |
| V (mL) (10 mg/mL stock glucose) | 0 | 0.2 | 0.4 | 0.6 | 0.8 | 1.0 |
| V (mL) (50 mM sodium acetate pH 5.0) | 2.0 | 1.8 | 1.6 | 1.4 | 1.2 | 1.0 |

⁵⁹ **α -amylase:** 25 mg 16 U/mg α -amylase (Sigma-Aldrich, A-3176); 900 μL ddH₂O; 100 μL α -amylase buffer 10x (Sigma-Aldrich, A-3176).

⁶⁰ **Amyloglucosidase:** 5 mg 30 U/mg amyloglucosidase (Sigma-Aldrich, A-7420); 1 mL 0.1 M sodium acetate, pH 5.0.

2.8.3. Statistical analysis

Plant growth (root and shoot length and dry weight), P assimilation, barley ears production, and starch richness data were tested for univariate normality using the Shapiro-Wilk test. They were subjected to univariate analysis of variance using the One-Way ANOVA (by Scheffe post-hoc test) to determine if there were significant differences between treated and untreated plants. Finally, to measure the strength of association between the variables with significant differences, a correlation analysis using Spearman's test was carried out. All the statistical analyses were carried out by using IMB SPSS Statistics 26.

2.9. *In vitro* germination assay

To analyse the effect of the isolates on seed germination, an *in vitro* germination assay was carried out with barley seeds based on Pastor-Bueis *et al.* (2017) protocol. Five 10-seed replicates were carried out with each strain. Negative control consisted in 10 seeds incubated with sterile NB liquid medium.

Protocol development

- Seeds of barley were surface-disinfected by immersion in 70% ethanol for 1 min and 3% sodium hypochlorite for 5 min. Rinse in sterile ddH₂O three times for 5 min.
- Place the seeds on a sterile 3M Whatman in 9 cm Petri dishes containing 3 mL of a 10⁸ cells/mL culture. Cover the seeds with a sterile filter paper.
- The Petri dishes were hermetically sealed and kept in a growth chamber at 25°C in the dark.
- Seeds were considered germinated when radicle has extended at least 2 mm. The number of germinated seeds was recorded daily until control reached at least 80% of germination.

Once the assay was finished, it was determined the relative germination percentage (RGP), the relative radicle growth (RRG) and the germination index (GI), as follows:

$$RGP = \frac{\text{germinated seeds at treatment}}{\text{germinated seeds at control}} \cdot 100$$

$$RRG = \frac{\text{radicle growth at treatment}}{\text{radicle growth at control}} \cdot 100$$

$$GI = \frac{RGP \cdot RRG}{100}$$

The assays were carried out with three selected strains and a co-culture of these strains in all possible combinations. Thus, it was previously discarded that some strains could inhibit the growth of the other one by co-culture in NB agar plates. Plates were incubated at 30°C for 48 h.

2.10. *In vitro* antifungal activity on agar plates

The potential to inhibit several fungal phytopathogens of all 9 selected PSB was tested on several agar media: YED, ISP1 to ISP7 and PDA (compositions in section II in appendix). The antagonism was tested by a dual culture assay as described by Álvarez-Pérez *et al.* (2017) with certain modifications. Six barley's pathogens fungi were tested in the bioassay: *Fusarium oxysporum*, *Alternaria spp.*, *Rhizoctonia solani*, *Nigrospora oryzae*, *Pleospora herbarum* and *Botrytis cinerea*. Cultures of the PSB isolates were grown on NB liquid media for 24 h at 30°C and 150 rpm. The fungi were grown on PDA agar plates at 30°C for 5 days. The bacterial culture was inoculated on the periphery of the plate and incubated at 30°C for 2 days. NB liquid media was used instead of bacterial culture at controls. A fungal disc of 6 mm diameter was placed at the centre of the petri plates and they were incubated at 30°C until control plates grew completely (Figure 40). The mycelial fungus diameter was measured. Percentage inhibition of fungal mycelium was calculated by using the following formula:

$$\% \text{ inhibition} = \frac{R_C - R_T}{R_C} \cdot 100$$

Where R_C is the radio (cm) of the fungal mycelium growing on the control plates and R_T is the mycelium radio (cm) of the fungal mycelium growing in the bacterial treated plates (Figure 40). Four measures were determined in each plate, and every assay was carried out by triplicate.



Figure 40. Diagram of the *in vitro* bioassay for the evaluation of the antifungal activity of the nine selected isolates. The PSB strains were inoculated on the periphery of the plate and the fungal pathogens were inoculated in the centre of the plate using a 6 mm agar plug. R_C was the radio of the fungal colony in the control plates, while R_T was the radio of the fungal colony in the bacterial treated plates.

3. Results and Discussion

3.1. Isolation and selection of PSB

A total of 104 morphologically distinct bacteria, based in easily observed macroscopic (size, colour, appearance and shape of the colony, and production of pigments) and microscopic traits (cellular morphology, spore production, and mobility) were obtained from rhizosphere soil of barley plants. All these strains were placed onto NBRIP agar medium, and 64 of them (61.5%) formed a clear halozone around the colony, with different degree of solubilization (Table 17). All of these 64 isolates were analysed on NBRIP agar medium to determine their solubilization index (SI) by triplicate. Thus, the SI of the isolated varies from 2.03 to 3.13 with an average of 2.30. Twenty-four of the isolated had an SI above the average and were selected for further identification.

Besides, this experiment suggested that most of the bacteria exhibited a solubilization pattern that seemed to occur in a two-step process: **i)** a rapid halo formation in the first 3 or 4 days, representing more than 85% of the final halo (and sometimes even the 100%); and **ii)** a later slow expansion of the halozone during the 11 following days.

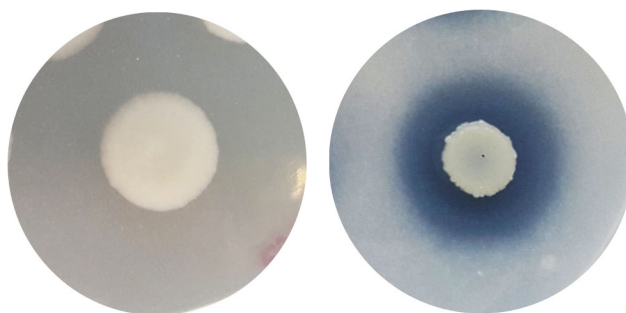


Figure 41. Phosphate solubilization analysis on NBRIP solid medium. The strain on the left does not show any solubilization capability and the strain on the right shows a solubilization halo after 3 days of incubation.

Table 17. Bacterial strains isolated from the rhizosphere of barley plants and their results for the solubilization index (SI) determination after 4 days of incubation. Selected strains have been highlighted in a pink colour box.

| Isolate | Colony diameter (cm) | Halo diameter (cm) | SI | Above average |
|---------|----------------------|--------------------|------|---------------|
| PSB1 | 1.00 | 1.30 | 2.30 | Yes |
| PSB2 | 0.90 | 1.30 | 2.44 | Yes |
| PSB3 | 0.85 | 1.35 | 2.59 | Yes |
| PSB4 | 0.80 | 1.30 | 2.63 | Yes |
| PSB5 | 0.75 | 1.50 | 3.00 | Yes |
| PSB6 | 0.75 | 1.25 | 2.67 | Yes |
| PSB7 | 0.80 | 1.20 | 2.50 | Yes |
| PSB8 | 0.80 | 1.30 | 2.63 | Yes |
| PSB9 | 0.80 | 1.20 | 2.50 | Yes |
| PSB10 | 0.70 | 1.30 | 2.86 | Yes |
| PSB11 | 0.80 | 1.10 | 2.38 | Yes |
| PSB12 | 0.70 | 1.10 | 2.57 | Yes |
| PSB13 | 0.80 | 1.45 | 2.81 | Yes |
| PSB14 | 0.95 | 1.25 | 2.32 | Yes |
| PSB15 | 0.90 | 1.70 | 2.89 | Yes |
| PSB16 | 0.85 | 1.60 | 2.88 | Yes |
| PSB17 | 0.90 | 1.45 | 2.61 | Yes |
| PSB18 | 0.90 | 1.50 | 2.67 | Yes |
| PSB19 | 0.85 | 1.35 | 2.59 | Yes |
| PSB20 | 0.90 | 1.15 | 2.28 | No |
| PSB21 | 0.80 | 1.20 | 2.50 | Yes |
| PSB22 | 0.80 | 1.70 | 3.13 | Yes |
| PSB23 | 0.75 | 1.40 | 2.87 | Yes |
| PSB24 | 0.80 | 1.30 | 2.63 | Yes |
| PSB25 | 0.90 | 1.10 | 2.22 | No |
| PSB26 | 1.00 | 1.20 | 2.20 | No |
| PSB27 | 0.80 | 0.95 | 2.19 | No |
| PSB28 | 0.80 | 0.95 | 2.19 | No |
| PSB29 | 0.70 | 0.83 | 2.19 | No |
| PSB30 | 1.00 | 1.15 | 2.15 | No |
| PSB31 | 1.00 | 1.15 | 2.15 | No |
| PSB32 | 0.70 | 0.80 | 2.14 | No |
| PSB33 | 1.10 | 1.25 | 2.14 | No |
| PSB34 | 0.75 | 0.85 | 2.13 | No |
| PSB35 | 0.75 | 0.85 | 2.13 | No |
| PSB36 | 0.75 | 0.85 | 2.13 | No |
| PSB37 | 0.85 | 0.95 | 2.12 | No |
| PSB38 | 0.90 | 1.00 | 2.11 | No |
| PSB39 | 0.90 | 1.00 | 2.11 | No |
| PSB40 | 0.90 | 1.00 | 2.11 | No |
| PSB41 | 0.90 | 1.00 | 2.11 | No |
| PSB42 | 0.77 | 0.85 | 2.10 | No |
| PSB43 | 0.70 | 0.77 | 2.10 | No |
| PSB44 | 0.70 | 0.75 | 2.07 | No |
| PSB45 | 0.70 | 0.75 | 2.07 | No |
| PSB46 | 0.70 | 0.75 | 2.07 | No |
| PSB47 | 0.75 | 0.80 | 2.07 | No |
| PSB48 | 0.75 | 0.80 | 2.07 | No |
| PSB49 | 0.75 | 0.80 | 2.07 | No |
| PSB50 | 0.75 | 0.80 | 2.07 | No |
| PSB51 | 0.75 | 0.80 | 2.07 | No |
| PSB52 | 0.75 | 0.80 | 2.07 | No |

Table 17. (Continued)

| Isolate | Colony diameter (cm) | Halo diameter (cm) | SI | Above average |
|---------|----------------------|--------------------|------|---------------|
| PSB53 | 0.75 | 0.80 | 2.07 | No |
| PSB54 | 0.80 | 0.85 | 2.06 | No |
| PSB55 | 0.80 | 0.85 | 2.06 | No |
| PSB56 | 0.80 | 0.85 | 2.06 | No |
| PSB57 | 0.85 | 0.90 | 2.06 | No |
| PSB58 | 0.85 | 0.90 | 2.06 | No |
| PSB59 | 0.85 | 0.90 | 2.06 | No |
| PSB60 | 1.00 | 1.05 | 2.05 | No |
| PSB61 | 0.96 | 1.00 | 2.04 | No |
| PSB62 | 0.77 | 0.80 | 2.04 | No |
| PSB63 | 0.75 | 0.77 | 2.03 | No |
| PSB64 | 0.75 | 0.77 | 2.03 | No |
| PSB65 | 0.75 | - | | |
| PSB66 | 0.70 | - | | |
| PSB67 | - | - | | |
| PSB68 | 0.90 | - | | |
| PSB69 | - | - | | |
| PSB70 | 0.70 | - | | |
| PSB71 | 0.70 | - | | |
| PSB72 | 0.70 | - | | |
| PSB73 | - | - | | |
| PSB74 | 0.70 | - | | |
| PSB75 | 0.80 | - | | |
| PSB76 | 0.85 | - | | |
| PSB77 | - | - | | |
| PSB78 | 0.90 | - | | |
| PSB79 | 0.80 | - | | |
| PSB80 | 0.70 | - | | |
| PSB81 | 0.70 | - | | |
| PSB82 | 0.80 | - | | |
| PSB83 | 0.80 | - | | |
| PSB84 | 0.90 | - | | |
| PSB85 | - | - | | |
| PSB86 | - | - | | |
| PSB87 | - | - | | |
| PSB88 | 0.70 | - | | |
| PSB89 | 0.90 | - | | |
| PSB90 | 0.70 | - | | |
| PSB91 | 0.70 | - | | |
| PSB92 | 0.80 | - | | |
| PSB93 | - | - | | |
| PSB94 | 0.80 | - | | |
| PSB95 | 0.85 | - | | |
| PSB96 | 0.80 | - | | |
| PSB97 | 0.74 | - | | |
| PSB98 | 0.60 | - | | |
| PSB99 | 0.60 | - | | |
| PSB100 | 0.95 | - | | |
| PSB101 | 0.75 | - | | |
| PSB102 | 0.75 | - | | |
| PSB103 | 0.80 | - | | |
| PSB104 | 0.80 | - | | |

3.1. Identification of PSB

Those 24 isolates showing higher SI values were identified by *16s rRNA* gene sequencing. Thus, 14 different species (9 isolates were identified as *Burkholderia fungorum*, 2 isolates as *Pseudomonas fluorescens*, and 2 isolates as *Pseudomonas brassicacearum*), that belonged to 7 different genera were identified (Table 18).

Table 18. Twenty-four selected bacterial strains based on their higher than average phosphate SI in solid NBRIP medium and their molecular identification by *rRNA 16S* gene sequencing. Selected strains for further assays are highlighted by pink colour.

| Isolate | 16S rRNA sequence similarity (%) | Solubilization index (SI) | Standard deviation (SD) |
|--|----------------------------------|---------------------------|-------------------------|
| <i>Burkholderia fungorum</i> PSB7 | 100.00% | 3.125 | 0.12 |
| <i>Achromobacter xylooxidans</i> PSB5 | 99.63% | 3.000 | 0.22 |
| <i>Burkholderia fungorum</i> PSB22 | 99.91% | 2.888 | 0.16 |
| <i>Burkholderia fungorum</i> PSB16 | 99.91% | 2.882 | 0.09 |
| <i>Pseudomonas fluorescens</i> PSB23 | 99.81% | 2.866 | 0.09 |
| <i>Pseudomonas brassicacearum</i> PSB10 | 100.00% | 2.857 | 0.09 |
| <i>Pseudomonas</i> sp. PSB17 | 99.90% | 2.812 | 0.07 |
| <i>Burkholderia fungorum</i> PSB18 | 99.71% | 2.666 | 0.12 |
| <i>Pseudomonas koreensis</i> PSB6 | 100.00% | 2.666 | 0.08 |
| <i>Pseudomonas brassicacearum</i> PSB24 | 100.00% | 2.625 | 0.06 |
| <i>Pantoea eucrina</i> PSB4 | 99.71% | 2.625 | 0.09 |
| <i>Enterobacter cloacae</i> PSB8 | 99.90% | 2.625 | 0.21 |
| <i>Burkholderia fungorum</i> PSB13 | 100.00% | 2.611 | 0.20 |
| <i>Burkholderia fungorum</i> PSB19 | 100.00% | 2.588 | 0.08 |
| <i>Bacillus</i> sp. PSB3 | 99.91% | 2.588 | 0.03 |
| <i>Pseudomonas oryzihabitans</i> PSB12 | 100.00% | 2.571 | 0.02 |
| <i>Burkholderia fungorum</i> PSB21 | 99.91% | 2.500 | 0.03 |
| <i>Burkholderia fungorum</i> PSB15 | 99.91% | 2.500 | 0.20 |
| <i>Advenella mimigardefordensis</i> PSB9 | 99.51% | 2.500 | 0.06 |
| <i>Pseudomonas plecoglossicida</i> PSB2 | 99.90% | 2.440 | 0.14 |
| <i>Pseudomonas fluorescens</i> PSB11 | 99.90% | 2.375 | 0.10 |
| <i>Pseudomonas aeruginosa</i> PSB14 | 99.80% | 2.315 | 0.13 |
| <i>Bacillus megaterium</i> PSB1 | 100.00% | 2.300 | 0.06 |
| <i>Burkholderia fungorum</i> PSB20 | 100.00% | 2.277 | 0.15 |

There were three isolates whose *16S rRNA* gene sequences matched with several strains. In those cases, their sequences were manually aligned to determine the species they belonged. Thus, PSB9 nBLAST analysis showed the same similarity to *A. mimigardefordensis* and *A. kashmirensis* strains. Nevertheless, the manual alignment showed five differences in the 1,430 nt sequence characterized, so **PSB9 could be classified as *A. mimigardefordensis*** (Figure 42a). In the case of strain PSB17, there

was no different nucleotide with *P. putida*, *P. fluorescens* and *P. plecoglossicida* sequences in the 1,047 nt sequence characterized, so it was impossible to determine the strain which PSB17 belonged at that moment (Figure 42b). Finally, strain PSB3 nBLAST analysis showed 99.91% of similarity with *Bacillus cereus*, *B. toyonensis* and *B. thuringiensis*, and no differences were found in the 1,091 nt sequence characterized (Figure 42c). With these 3 species, in spite of the incomplete identification, that did not suppose a problem at this stage of the study, since none of them had been reported as pathogen. Currently, *B. thuringiensis* is a well-known bio-insecticide (Azizoglu, 2019), and *B. toyonensis* has been used as feed additive for piglets, due to its protective activity against enteric pathogens (Kantas *et al.*, 2015), so, in any case, PSB3 could be a strain of interest.

After a bibliographic research, seven strains were discarded due to its possible pathogenicity for plants, humans or animals. For example, *P. brassicacearum*, despite it has long been studied for its beneficial plant growth-promoting and biocontrol properties, it has also been reported as minor pathogen that blur the boundaries between saprophytism and parasitism and, under certain conditions can cause disease in some crops (such as tomato), causing chlorosis and necrotic lesions (Belimov *et al.*, 2007; M. Yang *et al.*, 2020). Thus, it was decided to discard that strain to avoid future possible problems. Other problematic strain is *P. fluorescens*, which has been described as pathogen for bulb plants and co-pathogen in various plant diseases (Stoyanova & Bogaevska, 2015). Finally, *P. aeruginosa* represses *Arabidopsis* seed germination and is able to infect the roots of *Arabidopsis* and sweet basil (*Ocimum basilicum*), causing plant mortality after 7 days of inoculation (Chahtane *et al.*, 2018; Walker *et al.*, 2004).

On the other hand, *P. oryzihabitans* was discarded due to its human and animal pathogenicity, since it has been considered as nosocomial pathogen, involved in infections in immunocompromised hosts (Woo *et al.*, 2014).

Taking into account all these facts, the isolates selected for the following assays were: *Bacillus megaterium* PSB1 (recently re-named *Pristia megaterium*), *Pseudomonas plecoglossicida* PSB2, *Bacillus* sp. PSB3, *Pantoea eucrina* PSB4, *Achromobacter xylosoxidans* PSB5, *Pseudomonas koreensis* PSB6, *Burkholderia fungorum* PSB7, *Enterobacter cloacae* PSB8, and *Advenella mimigardefordensis* PSB9.

Some of the selected strains are well-known PSB strains: *Bacillus* sp., for example, have already shown antifungal capabilities and plant hormone production (Astriani *et al.*, 2020; Etesami *et al.*, 2017; Kang *et al.*, 2014; S. C. Wu *et al.*, 2005); *B. fungorum* have been deeply described as PSM before, and it has been reported that it is one of the PSB described so far, that reaches the lowest pH values, due to its high organic acid production (de Amaral Leite *et al.*, 2020; Martins da Costa *et al.*, 2015); *E. cloacae* has also been described as PSM, mainly due to its phytase production (Kalsi *et al.*, 2016); and last but not least, *Pseudomonas* sp. are also well-known PSM, since *P. koreensis* has already been reported as phosphate solubilizer in NBRIP medium (and also as PGPR in *Medicago* plants or as nitrogen-fixator) (Álvarez *et al.*, 2012; Ben Zineb *et al.*, 2020), and *P. plecoglossicida* strain, isolated

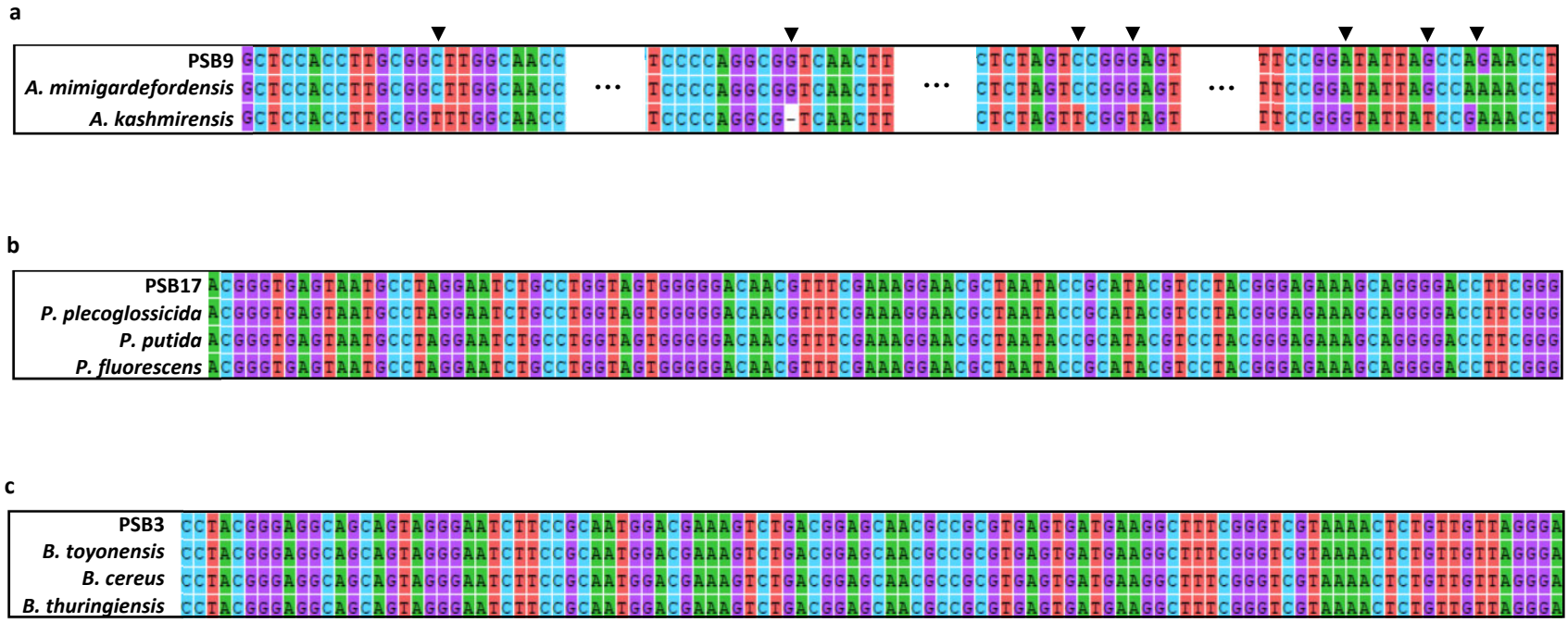


Figure 42. Alignment of the 16s rRNA gene sequence characterized of (a) the isolate PSB9 with *A. mimigardefordensis* and *A. kashmirensis*, (b) the isolate PSB17 with *P. plecoglossida*, *P. putida* and *P. fluorescens*, and (c) the isolate PSB3 with *B. toyonensis*, *B. cereus* and *B. thuringiensis*. Arrows indicate the sites with different sequences between the analysed strains.

from soybean rhizospheric soils, has recently been described as phosphate solubilizer and indoleacetic acid producer (Astriani *et al.*, 2020).

On the other hand, *A. xylooxidans* is a lesser-known strain, but has also been previously described as PSB, after being isolated from wheat root by Jha and Kumar (2009). Finally, we could not find any report about *A. mimigardefordensis* and *P. eucrina* as PSB. Nevertheless, it has been reported that some close strains showed phosphate solubilizing capabilities: for example, *Advenella incenata* showed P-solubilization skills into NBRIP solid medium. This may indicate that *A. mimigardefordensis* could also show similar skills (Espinosa-Victoria *et al.*, 2009). There have also been described some *Pantoea* strains that synthesize phytases, so they could act as phosphate solubilizers (Suleimanova, Toymentseva, *et al.*, 2015). As far as we know, the present study is the first time that both strains (*A. mimigardefordensis* and *P. eucrina*) are reported as phosphate solubilizing microorganisms, since it has been shown that they are able to solubilize tricalcium phosphate in NBRIP solid medium.

3.2. Endospores formation

After the assay, just two isolates showed endospore formation skills: *B. megaterium* PSB1 and *Bacillus* sp. PSB3. It is not a surprise since *Bacillus* sp. are well known endospore producers (Vos *et al.*, 2011).

3.3. Analysis of the phosphate solubilization capabilities in liquid medium

The phosphorus solubilization assay in solid medium showed, qualitatively, which strains were able to solubilize P. Thus, to quantify this P solubilization, the nine isolates were grown into NBRIP liquid medium with tricalcium phosphate as sole P source.

The growth of each strain is shown in Figure 43, whereas pH evolution is represented in Figure 44. The maximum soluble orthophosphate concentration was detected for *E. cloacae* (2.04 mM), after 17 days of growth, followed by *B. fungorum* (1.92 mM, at day 10 of incubation) and *P. koreensis* and *P. plecoglossicida* (1.68 mM and 1.59 mM, respectively) after 17 and 11 days growing (Figure 45). It can be observed that the pH of *B. fungorum* and *P. plecoglossicida* assays decreased until day 11, when both reached their maximum solubilization levels (Figure 43 and 44). Regarding the drop in pH observed for these strains, it has been proposed that it could be related to organic acid synthesis, which has been described as one of the main mechanisms of P solubilization (Wei, Zhao, *et al.*, 2018). On the contrary, *B. fungorum* should exhibit other complementary mechanisms, since it was the second greatest solubilizing strain, but showed the fourth lowest pH. Therefore, it seemed interesting to deep into the analysis of the mechanisms that could be using the different strains to solubilize P. In addition, it is interesting to note how the amount of soluble P in the medium decreased after reaching the highest level in the case of *B. fungorum*. That could be explained as auto-consumption by the bacteria, or as a change in its metabolism, since a very marked increase in

the pH of the medium could be observed only 24 h before this consumption started. Furthermore, *Bacillus* sp. and *B. megaterium* showed the poorest P solubilization values. In fact, *Bacillus* sp. hardly solubilized P during the first 12 days of the experiment. This could be explained by their poor growth in NBRIP medium (between 10^3 and 10^5 cells/mL) (Figure 43), since we know that both strains are able to grow up to 10^8 cells/mL in NB liquid medium (data not shown). In both cases, a rather slow decrease in pH values was observed, compared to the rest of the strains, taking more than 13 days to reach values close to 5 - 5.5. On the contrary, it has been reported that *P. eucrina* is able to decrease the pH of the medium from 7.0 up to 3.91 in 24 h (Suleimanova, Beinhauer, *et al.*, 2015).

Remarkably, no significant positive correlation was found between P solubilization in liquid media and the halozone produced in solid media, since *A. xylosoxidans* showed the second highest levels in the solid medium assay and was the third lowest solubilizer in liquid medium. This result is concomitant with that described by Alam *et al.* (2013), who states that a halozone production on solid medium let recognize a PSM, but it does not provide a good quantitative estimation of P solubilizing capabilities.

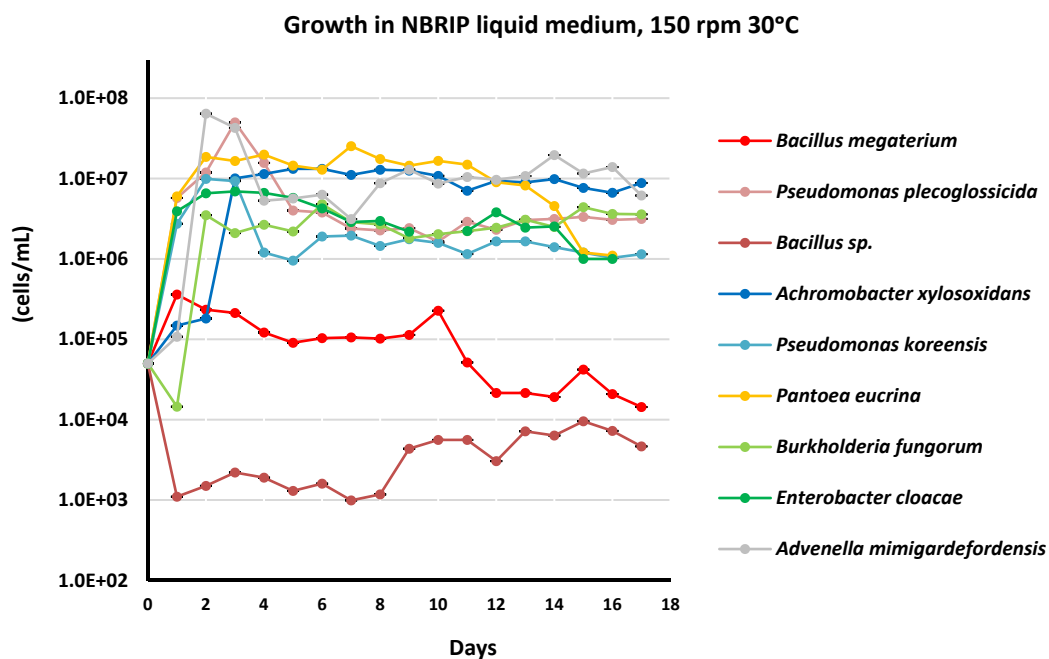


Figure 43. Growth of isolates PSB1 to PSB9 in NBRIP liquid medium. Data shown (with SD) are the average of three independent experiments.

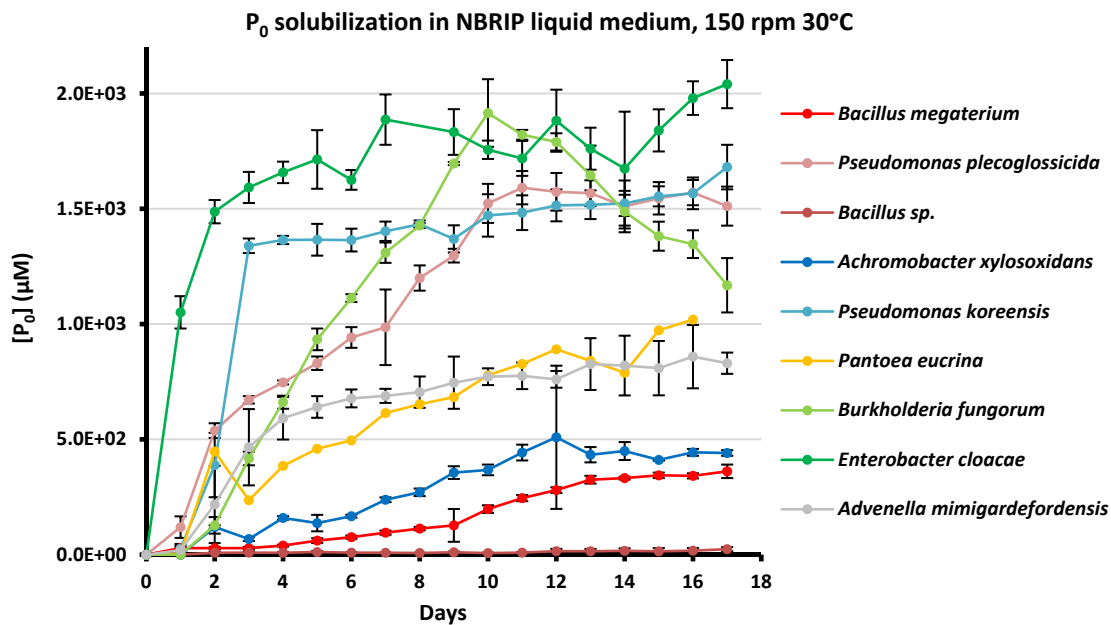


Figure 44. Evolution of phosphate solubilization in NBRIP liquid medium by bacterial isolates PSB1 to PSB9. Data shown (with SD) are the average of three independent experiments.

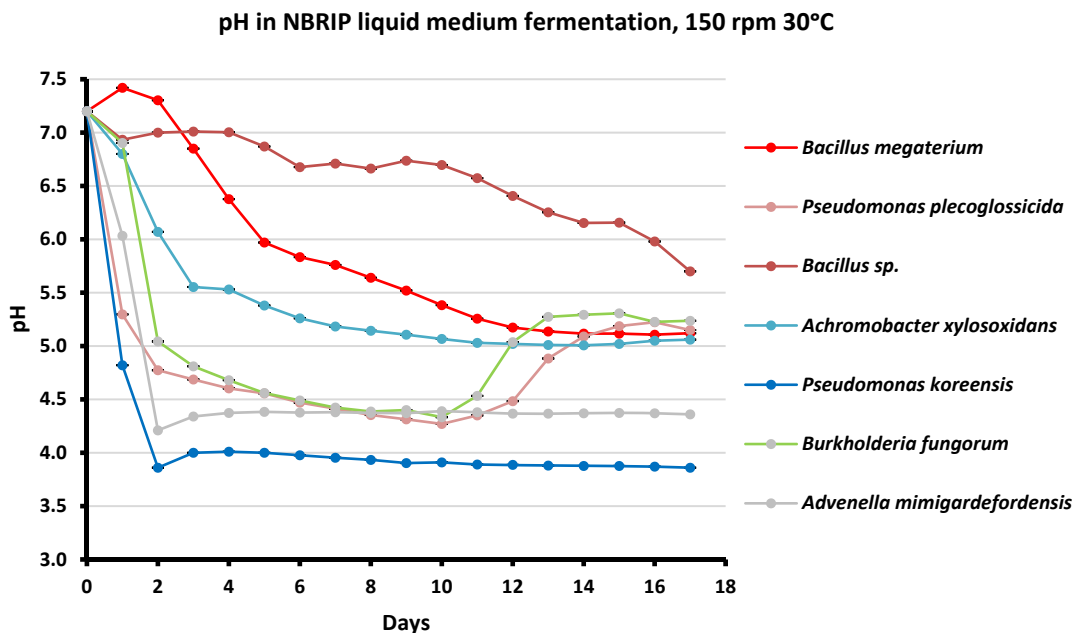


Figure 45. pH of the supernatant in the fermentation for phosphate solubilization quantification in NBRIP liquid medium. Data shown (with SD) are the average of three independent experiments.

3.4. Analysis of different P solubilization mechanisms

3.4.1. Acidic and alkaline phosphatase activity determination

The first P solubilization mechanism that was analysed was the production of both intracellular and extracellular acid and alkaline phosphatases. *B. megaterium* PSB1 exhibited the highest levels of both acidic and alkaline extracellular phosphatase, with *Bacillus* sp. PSB3 and *P. eucriina* PSB6 also showed moderate levels of both activities (Figure 46). The rest of the strains showed relatively low extracellular phosphatase levels. In general, intracellular phosphatase levels are not remarkable, except in the case of *B. fungorum*. P solubilization is mainly carried out by extracellular phosphatase activities, and accordingly, it made sense to detect the highest levels of extracellular phosphatase activity for both acid and alkaline phosphatases. Similar results had been reported in *Bacillus thuringiensis* (Ambreen *et al.*, 2020). Finally, most of the isolated did not exhibited significant levels of acidic intracellular phosphatases.

Curiously, it has been previously reported the production of acid and alkaline phosphatase in *Enterobacter* sp. and *Pseudomonas* sp., but, in our case, these two strains showed relatively low extracellular phosphatase levels (Krey *et al.*, 2011; S. Srivastava & Srivastava, 2020).

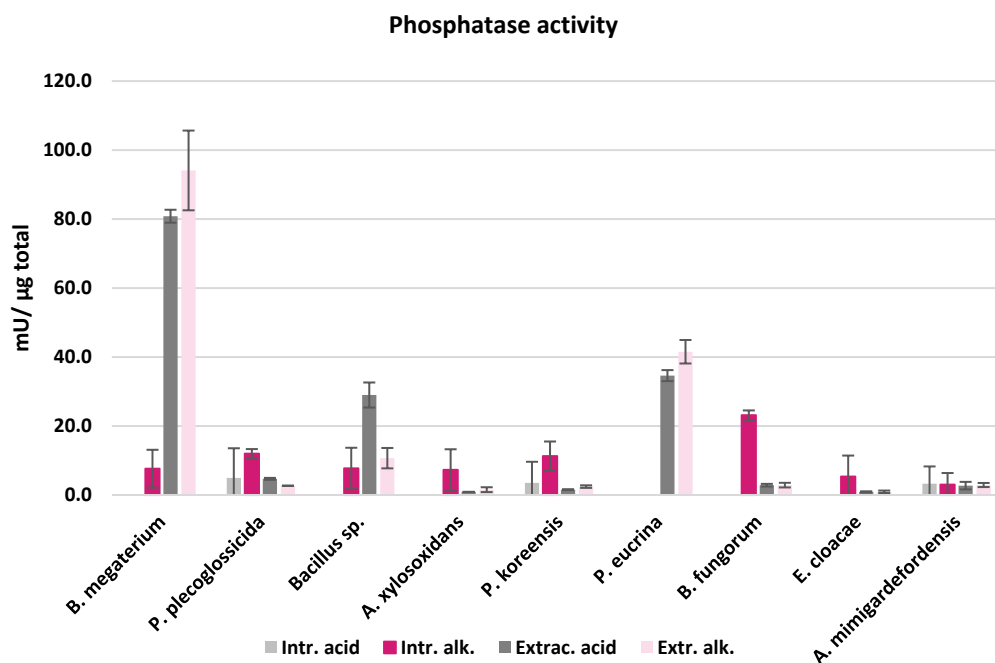


Figure 46. Intracellular and extracellular, acid and alkaline phosphatase determination in the nine selected PSB strains in TSB liquid medium after 48 h of incubation at 30°C and 150 rpm. Data shown (with SD) are the average of three independent experiments.

On the contrary, *B. megaterium* was the strain showing the highest acid and alkaline extracellular phosphatase activities, but it is the second lowest P solubilizer strain in the NBRIP liquid medium assay. This result could be explained if we take into account that phosphatases are mainly involved in the solubilization of P from organic matter of soil (organic P), and the assay carried out in NBRIP medium use inorganic P.

Otherwise, these results lead us to think that it was possible that both *Bacillus* strains were consuming part of the solubilized P, since in view of these data, solubilization values higher than those shown in the P solubilization test in NBRIP liquid medium would had been expected.

Finally, we would speculate that strains such as *B. fungorum* or *E. cloacae* can use other solubilization mechanisms to achieve such high solubilization rates in the NBRIP liquid medium assay.

3.4.2. Phytase production

Phytase activity was detected in all the isolates in liquid medium, although activity levels ranged between 40.59 to 142.98 mU/mL, being *A. mimigardefordensis* the strain exhibiting the highest level of phytase biosynthesis and *E. cloacae* the lowest one (Figure 48). Interestingly, *E. cloacae*, *Bacillus* sp., *P. koreensis* and *P. eucrina* had not shown halozone in PSM solid medium. Thus, it could be concluded that phytase production was not detected in solid medium when production is below 65 mU/mL.

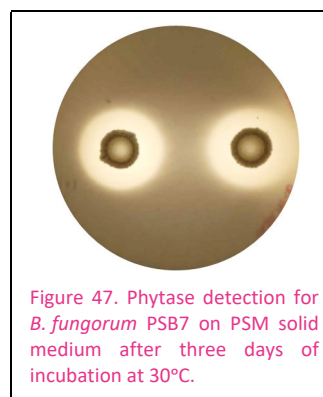


Figure 47. Phytase detection for *B. fungorum* PSB7 on PSM solid medium after three days of incubation at 30°C.

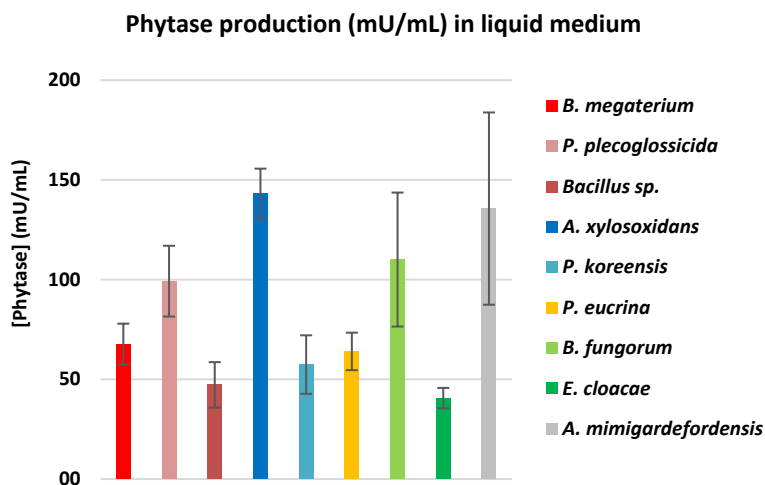


Figure 48. Phytase production in PSM liquid medium for the nine selected PSB strains after 7 days growing at 30°C and 150 rpm. Data shown (with SD) are the average of three independent experiments.

Phytase production has been reported in several strains related with the nine assayed isolates: *Bacillus* sp., *Klebsiella terrigena*, *Pseudomonas* sp., *Enterobacter* sp., *Burkholderia* sp. and *Advenella* sp. (Ramírez & Kloepper, 2010; B. Singh & Satyanarayana, 2011; P. Singh *et al.*, 2014; Suleimanova, Beinhauer, *et al.*, 2015). Nevertheless, it can be reported that phytase activity is inherent to each strain, since after characterizing four different isolates, identified as *Advenella* sp., Singh *et al.* (2014) described that all of them showed large production differences (from 0.076 to 0.174 U/mL).

Interestingly, some of these low-phosphatase activity strains like *A. xylosoxidans*, *A. mimigardefordensis*, *B. fungorum*, and *P. plecoglossicida* exhibited the highest levels of phytase activity. Nevertheless, *E. cloacae* was the strain with the lowest capability to produce both phytase and phosphatase activities (Table 18).

Table 19. Extracellular phosphatase and phytase activities of PSB isolates. Values showed are the means (with SD) of two independent experiments made by triplicate.

| Isolate | Acidic phosphatase (mU/μg protein) | Alkaline phosphatase (mU/μg protein) | Phytase (mU/ml) |
|-----------------------------------|---------------------------------------|---|--------------------|
| <i>B. megaterium</i> PSB1 | 80.83 (± 1.9) | 94.10 (± 11.6) | 67.70 (± 10.2) |
| <i>P. plecoglossicida</i> PSB2 | 4.70 (± 0.3) | 2.70 (± 0.1) | 99.20 (± 17.7) |
| <i>Bacillus</i> sp. PSB3 | 29.00 (± 3.6) | 10.70 (± 2.9) | 47.20 (± 11.4) |
| <i>P. eucrina</i> PSB4 | 34.62 (± 1.6) | 41.54 (± 3.4) | 64.00 (± 12.6) |
| <i>A. xylosoxidans</i> PSB5 | 0.91 (± 0.1) | 1.56 (± 0.7) | 143.00 (± 14.7) |
| <i>P. koreensis</i> PSB6 | 1.55 (± 0.2) | 2.45 (± 0.4) | 57.40 (± 9.4) |
| <i>B. fungorum</i> PSB7 | 2.86 (± 0.4) | 2.88 (± 0.7) | 110.10 (± 33.6) |
| <i>E. cloacae</i> PSB8 | 0.91 (± 0.2) | 0.95 (± 0.3) | 40.60 (± 5.1) |
| <i>A. mimigardefordensis</i> PSB9 | 2.72 (± 1.1) | 2.91 (± 0.6) | 135.60 (± 48.2) |

3.4.3. Organic acid biosynthesis

The detection of some of the most organic acids involved in phosphorus solubilization was carried out in NBRIP liquid medium. After replacing the P source with potassium phosphate, *P. eucrina* could not grow in the NBRIP medium.

HPLC always indicated that a first peak close to 17.5 min retention time (peak 1, Figure 49) is observed in all the samples. It probably corresponds to some compound of the NBRIP medium, since it also appeared in the blank (non-inoculated NBRIP) samples. In addition, a peak was observed close to 25.0 min at every sample. It corresponds to the glucose present in the NBRIP medium (Figure 49).

All the strain produced formic acid during the first 48 h (Table 21), which seemed to be metabolized, since it disappeared at larger fermentation times. Its disappearance seemed to be

related to the subsequent appearance of peaks 6 (retention time 39.3 min) and 7 (retention time 40.7 min), which could suggest that these peaks might correspond to compounds related to the metabolism or modifications of formic acid, although, unfortunately, they could not be identified.

Some of the strains (*P. plecoglossicida*, *P. koreensis*, *B. Fungorum*, *E. cloacae* and *A. mimgardfordensis*), produced citric acid after 72 hours of fermentation (Peak 2 in Figure 49b). All of them produced a compound with a very similar retention time (21.5 min) during the previous hours. It is very possible that this compound is related to the metabolism of citric acid, although, again, it could not be identified. Interestingly, the pH-drop during the P solubilization assay in NBRIP liquid medium occurred during the first 48 hours (Figure 45). Thus, a relation between the production of citric acid (and its derivatives), with the drastic decrease in pH, and the beginning of phosphorus solubilization could be observed. It has already been reported that citric acid is one of the main acids in the P solubilization from PSM. Acidity has a significant influence on the P solubilizing capacity of PSM. Thus, citric acid has a very high acidity constant, so it has an important effect on extracellular pH (Wei, Zhao, *et al.*, 2018; Zúñiga-Silgado *et al.*, 2020). The three strains that showed the highest levels of citric acid production were *B. fungorum*, *P. plecoglossicida* and *P. koreensis* (Table 20), which are three of the strains that reached more acidic pH in the P solubilization in NBRIP liquid medium assay.

Finally, only *P. plecoglossicida* showed production of tartaric acid, and *E. cloacae* was the only one producing a compound with a retention time of 43.9 min (peak 8 in Table 21), which could not be identified.

Table 20. Retention time of the organic acids analysed by HPLC using 0.005 M H₂SO₄ as mobile phase.

| Compound | Retention time (min) |
|---------------|----------------------|
| Citric acid | 22.360 |
| Tartaric acid | 23.188 |
| Oxalic acid | 24.376 |
| Glucose | 25.232 |
| Malic acid | 26.099 |
| Succinic acid | 31.367 |
| Lactic acid | 33.084 |
| Formic acid | 34.600 |
| Acetic acid | 37.368 |

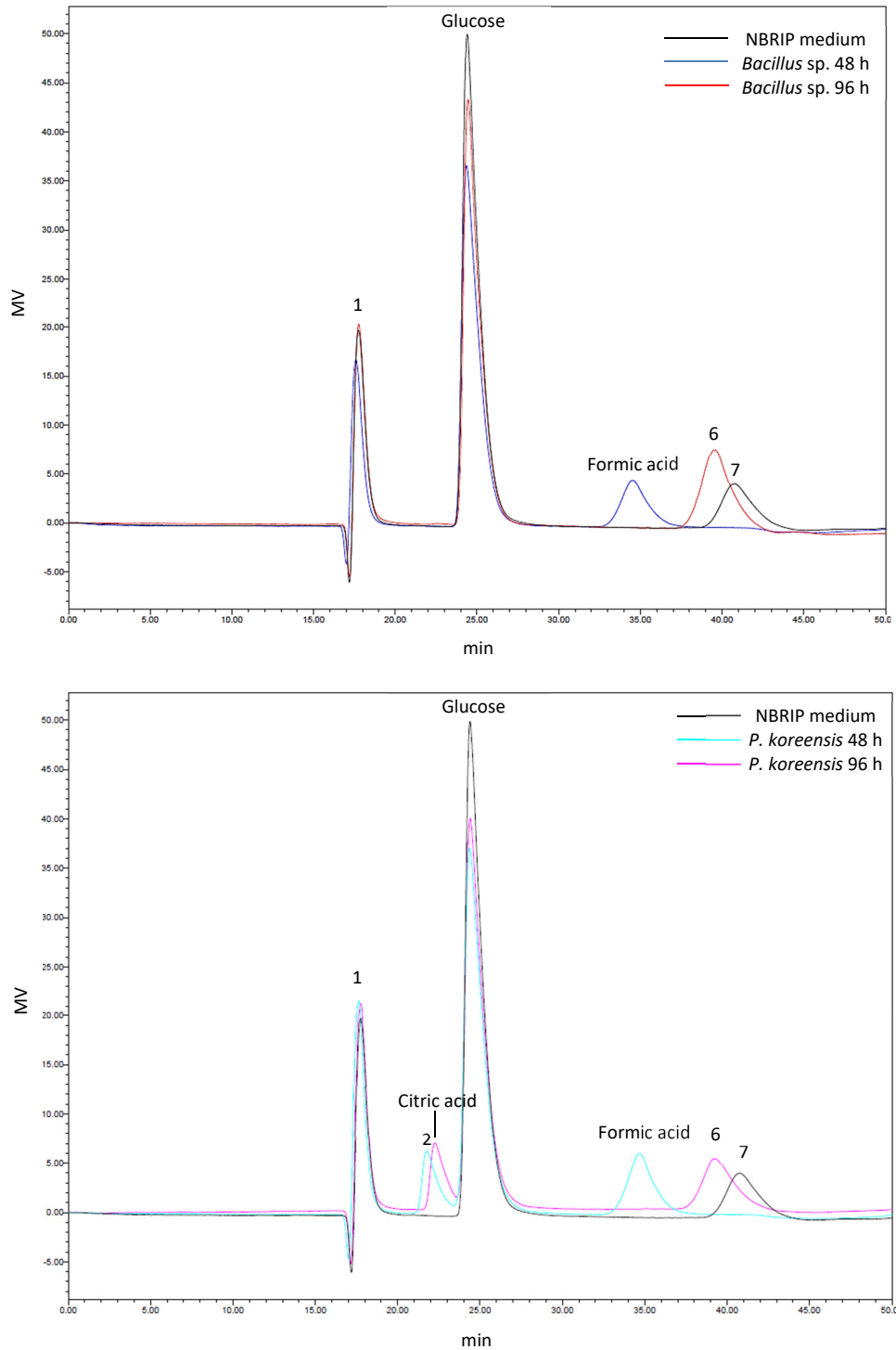


Figure 49. HPLC analysis of *Bacillus sp.* (up) and *P. koreensis* (down) extract in modified NBRIP liquid medium at 48 and 96 h of fermentation.

Table 21. Determination of the organic acid production by the PSB analysed. The concentration of the compounds identified was quantified (mg/mL) while the secretion of the rest of the compounds is indicated by their peak area.

| | | Peak 2 (cm ²) | Citric acid (mg/mL) | Tartaric acid (mg/L) | Glucose (mg/mL) | Formic acid (mg/mL) | Peak 6 (cm ²) | Peak 7 (cm ²) | Peak 8 (cm ²) |
|----------------------------------|--------------|------------------------------|------------------------|-------------------------|--------------------|------------------------|------------------------------|------------------------------|------------------------------|
| Retention time | | 21.521 | 22.360 | 23.188 | 24.376 | 34.600 | 39.272 | 40.722 | 43.898 |
| NBRIP medium | | | | | 3.468 | | | 489769.5 | |
| <i>B. megaterium</i> | 24 h | | | | 2.946 | 0.492 | | | |
| | 48 h | | | | 2.837 | 0.468 | | | |
| | 72 h | 30.746 | | | 2.894 | | | 421.811 | |
| | 96 h | 43.211 | | | 2.900 | | | 396.753 | |
| | 120 h | 55.384 | | | 2.803 | | 438.444 | | |
| | 144 h | 51.689 | | | 2.896 | | 408.966 | | |
| <i>P. plecoglossicida</i> | 24 h | 215.689 | | | 2.366 | 0.408 | | | |
| | 48 h | 37.199 | | 0.040 | 2.526 | 0.474 | | | |
| | 72 h | | 0.220 | | 2.374 | | | 449.289 | |
| | 96 h | 13.472 | 0.418 | | 2.098 | | | 429.359 | |
| | 120 h | | 0.484 | | 1.704 | | 380.040 | | |
| | 144 h | | 0.655 | | 1.753 | | 423.837 | | |
| <i>Bacillus</i> sp. | 24 h | | | | 2.761 | 0.448 | | | |
| | 48 h | | | | 2.938 | 0.813 | | | |
| | 72 h | | | | 2.795 | | | 685.351 | |
| | 96 h | | | | 2.830 | | 734.257 | 196.202 | |
| | 120 h | | | | 2.747 | | 621.095 | | |
| | 144 h | | | | 2.398 | | 521.372 | | |

Table 21. (Continued)

| | | Peak 2 (cm ²) | Citric acid (mg/mL) | Tartaric acid (mg/L) | Glucose (mg/mL) | Formic acid (mg/mL) | Peak 6 (cm ²) | Peak 7 (cm ²) | Peak 8 (cm ²) |
|------------------------|-------|------------------------------|------------------------|-------------------------|-----------------|------------------------|------------------------------|------------------------------|------------------------------|
| Retention time | | 21.521 | 22.36 | 23.188 | 24.376 | 34.600 | 39.272 | 40.722 | 43.898 |
| <i>A. xylosoxidans</i> | 24 h | | | | 2.753 | 0.443 | | | |
| | 48 h | | | | 2.859 | 0.467 | | | |
| | 72 h | | | | 2.843 | | | 386.575 | |
| | 96 h | | | | 3.368 | | 524.727 | | |
| | 120 h | | | | 3.026 | | 420.209 | | |
| | 144 h | | | | 2.452 | | 378.242 | | |
| <i>P. koreensis</i> | 24 h | 228.662 | | | 2.701 | 0.520 | | | |
| | 48 h | 344.200 | | | 2.503 | 0.517 | | | |
| | 72 h | | 0.353 | | 2.621 | | | 443.673 | |
| | 96 h | | 0.364 | | 2.626 | | 461.570 | | |
| | 120 h | | 0.340 | | 2.467 | | 424.944 | | |
| | 144 h | | 0.284 | | 2.049 | | 443.103 | | |
| <i>B. fungorum</i> | 24 h | | | | 2.749 | 0.500 | | | |
| | 48 h | 136.594 | | | 2.605 | 0.513 | | | |
| | 72 h | | 0.502 | | 2.196 | | | 455.946 | |
| | 96 h | | 0.748 | | 1.938 | | 475.903 | | |
| | 120 h | | 0.796 | | 1.525 | | 398.473 | | |
| | 144 h | | 0.935 | | 1.520 | | 465.784 | | |

Table 21. (Continued)

| | | Peak 2 (cm ²) | Citric acid (mg/mL) | Tartaric acid (mg/L) | Glucose (mg/mL) | Formic acid (mg/mL) | Peak 6 (cm ²) | Peak 7 (cm ²) | Peak 8 (cm ²) |
|------------------------------|-------|------------------------------|------------------------|-------------------------|--------------------|------------------------|------------------------------|------------------------------|------------------------------|
| Retention time | | 21.521 | 22.36 | 23.188 | 24.376 | 34.600 | 39.272 | 40.722 | 43.898 |
| <i>E. cloacae</i> | 24 h | 35.530 | | | 2.682 | 0.478 | | | |
| | 48 h | 37.638 | | | 2.681 | 0.501 | | | |
| | 72 h | | 0.015 | | 2.644 | | | 418.479 | |
| | 96 h | | 0.028 | | 2.421 | | 453.667 | | 35.560 |
| | 120 h | | 0.022 | | 2.500 | | 429.238 | | |
| | 144 h | | 0.022 | | 2.497 | | 450.979 | | 48.688 |
| <i>A. mimigardefordensis</i> | 24 h | | | | 2.926 | 0.489 | | | |
| | 48 h | 20.048 | | | 3.066 | 0.520 | | | |
| | 72 h | | 0.021 | | 3.063 | | | 421.903 | |
| | 96 h | | 0.027 | | 3.083 | | 448.643 | | |
| | 120 h | | 0.033 | | 3.054 | | 468.907 | | |
| | 144 h | | 0.029 | | 3.039 | | 443.916 | | |

3.4.4. Siderophore production

As detailed in the introduction, siderophore production is an important skill of PGPR. On the one hand, the production of siderophores favours P solubilization, since the siderophores react mainly with trivalent cations like iron and aluminium present in acidic and neutral soils, respectively, preventing them from binding to free phosphorus. Thus, the synthesis of siderophores is one of the indirect mechanisms of P solubilization used by several microorganisms. On the other hand, iron sequestration has been related to the prevention of phytopathogen infections in crops (Gu *et al.*, 2020).

For these reasons, siderophore production was determined by plating the nine isolates onto CAS agar medium containing chrome azurol (CAS) and hexadecyltrimethylammonium bromide (HDTMA), also known as CTAB, as indicators. Only *B. megaterium* PSB1 and *B. fungorum* PSB7 strains showed positive results, by forming a halozone surrounding the colony on CAS agar medium. Nevertheless, it was not possible to determine if, as in the case of phytase detection in agar plates, the rest of the strains could exhibit a lower siderophore production than the necessary one for its detection in agar plates.

Thus, some members from *Pseudomonas* genera have been described as siderophore producers. Nevertheless, none of the two *Pseudomonas* isolates produced halozone on CAS agar plates (Sasirekha & Srividya, 2016; Vindeirinho *et al.*, 2021).

3.4.5. HCN production

HCN (hydrogen cyanide) has been commonly described as a biocontrol factor against phytopathogens. Nevertheless, it has been reported that it does not intervene in the toxicity against microorganisms per se, but HCN sequesters the iron present in the soil, as occurs with siderophores. Phytopathogen biocontrol by iron competition has been described in siderophore producers, which are able to inhibit phytopathogen infections (Gu *et al.*, 2020). Moreover, HCN production could be an indirect mechanism of phosphorus solubilization in soil, in the same way that siderophore production is: iron sequestration could prevent it from binding free phosphate, which remains available in solution for its assimilation by plants (Backer *et al.*, 2018; Rijavec & Lapanje, 2016).

After 7 days of incubation, the only HCN producer was *B. fungorum* PSB7. Nevertheless, it has been previously reported that *B. megaterium* and *Pseudomonas* sp. can produce HCN when grown onto King's B broth (Abd El-Rahman *et al.*, 2019; N. Khan *et al.*, 2020). Thus, despite *Pseudomonas* and *Bacillus* species did not show HCN production onto NB agar plates, it is possible that the production of HCN could depend in some strains on the culture media used in the assay (Ahmad *et al.*, 2008), or, alternatively, is a strain-dependent trait.

3.5. Miscellaneous plant growth-promoting traits

3.5.1. Indoleacetic acid production

Under natural conditions, plant roots excrete several organic compounds, including tryptophan, which can be used by the rhizobacteria for IAA biosynthesis. The IAA production by rhizobacteria can help to activate the non-native plant response to resist biotic and abiotic stress conditions. IAA is considered one of the most important phytohormones, and its production by PGPRs can vary between different species and strains and it is greatly influenced by culture conditions (Lebrazi *et al.*, 2020). In this case, all the tested isolates, with the exception of *A. mimigardefordensis*, which could not grow in these conditions, were able to produce IAA at different levels, being *E. cloacae* the strain showing the higher production of this phytohormone (88.52 µg/mL) well above the rest (Figure 50). IAA is related to the development, directly or indirectly, of roots and leaves (lateral root elongation, leaf growth, etc.). Thus, it is expected that those strains that produce higher levels of IAA will enhance crop development.

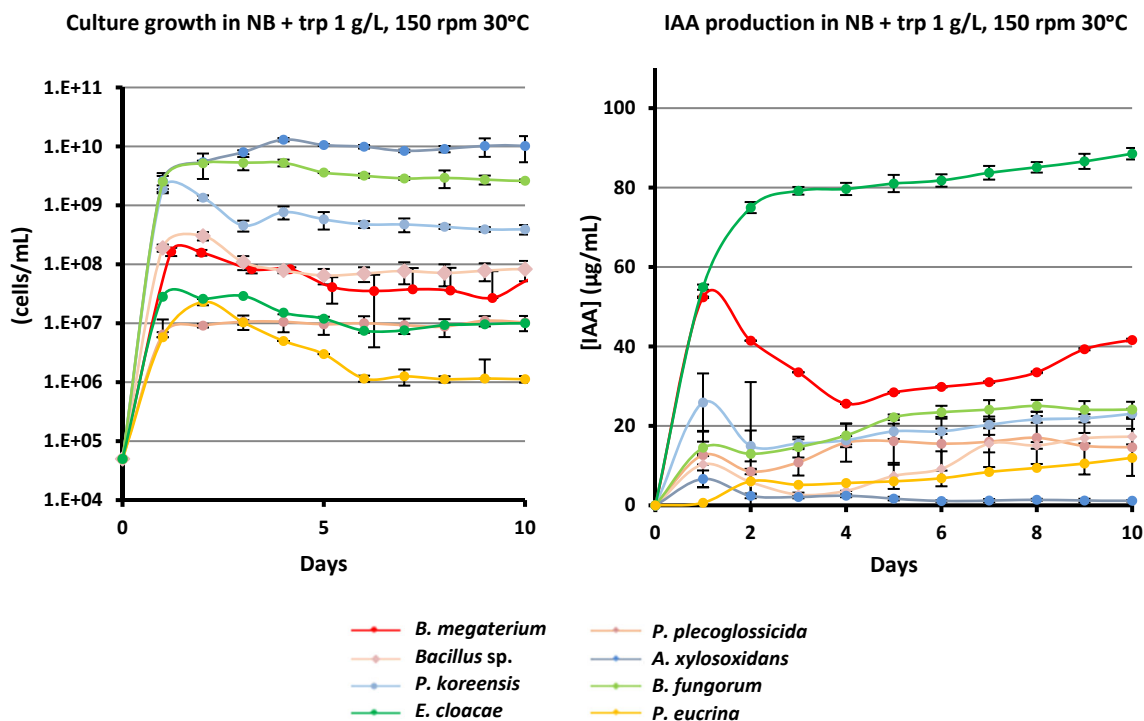


Figure 50. Growth of PSB1 to PSB9 isolates (left) and evolution of IAA production (right) in NB liquid medium, supplemented with 1 g/L trp. Data shown (with SD) are the average of three independent experiments.

3.5.2. Zn solubilization

About almost 50% of the world's soils used for cereal production have low available Zn, which causes reduction in yield and nutritional quality of grains (Mumtaz *et al.*, 2017). For this reason, the ability to solubilize Zn from $Zn(PO_4)_2$ and ZnO was analysed for isolates PSB1 to PSB9. None of the strains solubilized ZnO, and just three of them could solubilize $Zn(PO_4)_2$, showing *P. koreensis* the higher solubilization efficiency (SE) (Figure 51).

Some *Bacillus* strains have been already described as good Zn solubilizers onto tris-minimal medium, but none of our *Bacillus* isolates showed Zn-solubilization skills (Mumtaz *et al.*, 2017). However, it seems that Zn solubilization is more related with the composition of the soil sample from the isolation, than the isolate strain per se, since only 20 of 115 *Bacillus* isolates showed Zn solubilization skills as reported by Khande *et al.* (2017). These strains were isolated from a soil rich in soluble Zn, so those microorganisms did not need to solubilize Zn. Besides, in our assay, it can be observed that the strains showed huge SD, so the Zn-solubilization skills were not homogeneous.

3.5.3. K solubilization

It has been reported that between 1 and 10% of K soil is precipitated and non-disposable for crops. Thus, it could be also interesting to analyse the K-solubilization skills of the isolates as an asset for biofertilizers formulation. Besides, inoculation with potassium solubilizing bacteria (KSB) has been related with the enhance of seed germination, seedling vigour, and root and plant growth (Etesami *et al.*, 2017).

Thus, five of our isolates showed K-solubilization skills on agar plate, reaching *E. cloacae* the highest values (Figure 51). This strain had already been described as high K-solubilizer, as well as *B. fungorum* and *Pseudomonas* sp. (Dong *et al.*, 2019; Sun *et al.*, 2020). However, K solubilization can vary depending on different mineral K sources (trisilicate, feldspar, biotite, mica, bentonite...), so *in silico* results could be different than *in vivo* results, since these results are just for potassium-feldspar assay (Etesami *et al.*, 2017). This is due to the fact that the main mechanism for K solubilization is the biosynthesis and secretion of organic acids, which production strongly depends on the growth medium. Different organic acids are involved in the solubilization of insoluble K, but tartaric acid, citric acid, succinic acid, α -ketogluconic acid, and oxalic acid are the most prominent acids involved (Etesami *et al.*, 2017; Sun *et al.*, 2020)

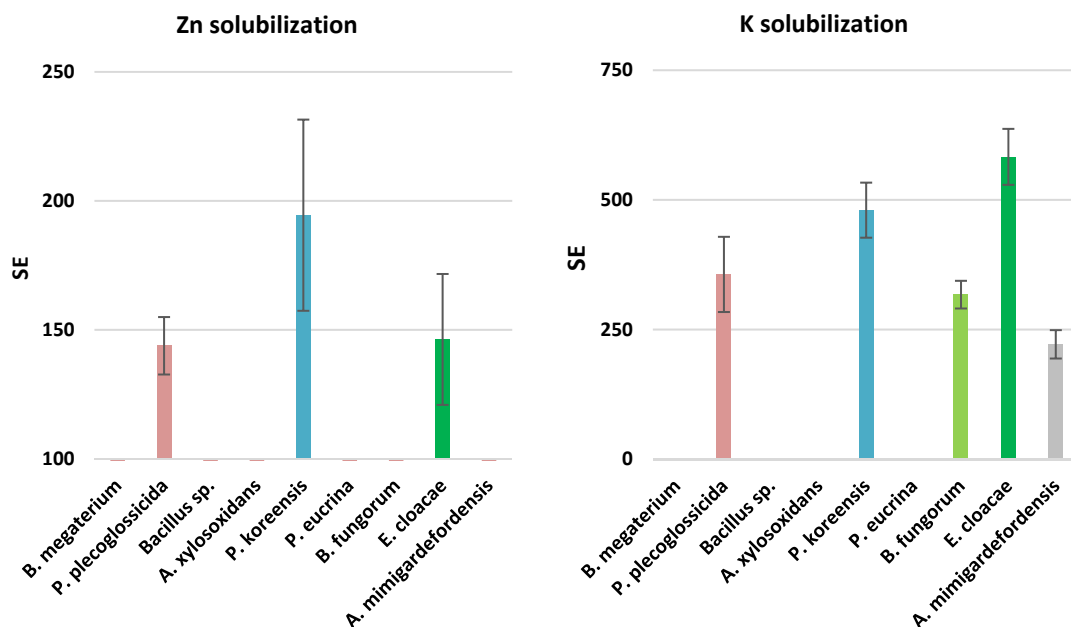


Figure 51. Zn solubilization efficiency (SE) in Tris minimal solid medium for the nine selected PSB strains (left), and K solubilization efficiency (SE) in Aleksandrov solid (right) after 7 days growing at 30°C. Data shown (with SD) are the average of three independent experiments.

3.6. Greenhouse pot experiment

The main objective of a biofertilizer is to improve the development of the crop. Therefore, the effect of the nine isolates on barley crops was analysed in a greenhouse pot experiment. In this case, pots were provided with all the necessary nutrients, except phosphorus, which was supplied as tricalcium phosphate, an insoluble source of P. A positive control was supplemented with soluble phosphorus, to determine the growth of barley under normal conditions. Besides, to analyse the real effect of the isolates, an uninoculated negative control without any other P source was also used.

The average number of plants developed per pot, ranged between 7.33 (73.3% of seeds germinated for *Bacillus sp.* treatment) and 8.67, for both negative and positive controls, although no significant differences were observed between treatments (Table 22). In a similar way, no significant differences were detected for the ear number obtained per pot, with values ranging from 10.67 (negative control) to 11.78 (positive control). Once the plants had completed their growth cycle they were uprooted and dry weight was determined for both roots and shoots. Again, no significant differences were observed in the root dry weight.

After the analysis, the average height of the negative control barley plants was significantly lower than in the rest of the treatments (Figure 52). In fact, some of the isolates (*B. megaterium*, *A. xylosoxidans*, *P. koreensis*, *B. fungorum* and *A. mimigardefordensis*) were even able to cause a greater height growth than that observed in the positive control plants (Figure 53a). Negative control also showed the lowest average stems dry weight, although significant differences were only observed in the treatments with *B. megaterium*, *Bacillus* sp., *A. xylosoxidans* and *A. mimigardefordensis*, which exhibited the highest values for dry weight and height stems (Figure 53b).

P assimilation was much higher in stems than in roots (Figures 53c and 54a). The highest values were obtained in plants from the positive control and *A. mimigardefordensis* treatment, respectively. Besides, the mean P-assimilation for the negative control plants, in both root and shoot, was lower than for the rest of the conditions. This poor P-assimilation caused a negative effect on the maturation of the plants and spikes in the negative control plants. As a result, they showed a high rate of green or immature ears, as well as purple stems (Figure 52). All the treatments were able to reverse this deficiency in plant growth and maturation of the ears, with significant differences between all the isolates regarding negative control. In that sense, again, negative control plants



Figure 52. Pots of barley inoculated with *B. fungorum* (left) and negative control in the greenhouse pot assay after 3 months. Note the great difference regarding the development in height of the plants, how the ears of the negative control are not able to reach a correct maturity, and how its stems have a purple colour the base of the plant.

showed the lowest mean ears dry weight values, being significant differences detected regarding treatments of *B. megaterium*, *Bacillus* sp., *P. eucrina*, *P. koreensis*, *B. fungorum* and *A. mimigardefordensis* (Figure 53d). We could also observe that the total starch / glucose content of the negative control spikes was the lowest of all the treatments, and significant differences were detected with all treatments, except *A. xylosoxidans* and *E. cloacae* (Figure 54b).

Therefore, higher levels of P assimilation in both roots and stems may be strongly associated with a greater crop development, although it was not the only factor involved. The statistical analysis showed that there was no correlation between the assimilation of P in the stems and the general growth of the plant (Table 22). However, it appears that there was a correlation between the P assimilated in the roots and the plant development.

On the other hand, we did not find any correlation between the levels of P solubilization in NBRIP liquid medium and the P assimilation in crops. Plants are known to exert some control over their rhizospheric microbiome by synthesizing and exuding some compounds to recruit specific species, which generate some species-specific microbial communities (Backer *et al.*, 2018; T. Lu *et al.*, 2018; Qu *et al.*, 2020). Therefore, it should be expected that some species with low P solubilization capacity could be effectively integrated into the rhizosphere biome, while others, that showed higher levels of solubilization, did not

In conclusion, in a general way, the two strains that showed the greatest effects promoting the growth of barley crops in the greenhouse pots assay were *A. mimigardefordensis* and *B. megaterium*.

Table 22. Different parameters of barley plants inoculated with different PSB strains in greenhouse pot experiment. The results showed are the means (with SD) of two independent experiments made by triplicate.

| Isolate | Number of plants per pot | Number of ears per pot |
|--|--------------------------|------------------------|
| <i>Bacillus megaterium</i> PSB1 | 8.22 (± 0.67) | 11.67 (± 1.22) |
| <i>Pseudomonas plecoglossicida</i> PSB2 | 8.56 (± 1.01) | 11.44 (± 1.13) |
| <i>Bacillus</i> sp. PSB3 | 7.33 (± 1.12) | 11.00 (± 0.87) |
| <i>Pantoea eucrina</i> PSB4 | 7.89 (± 0.78) | 11.56 (± 1.42) |
| <i>Achromobacter xylosoxidans</i> PSB5 | 8.22 (± 0.87) | 11.56 (± 1.81) |
| <i>Pseudomonas koreensis</i> PSB6 | 8.33 (± 1.22) | 11.11 (± 0.78) |
| <i>Burkholderia fungorum</i> PSB7 | 8.11 (± 1.27) | 10.33 (± 0.87) |
| <i>Enterobacter cloacae</i> PSB8 | 9.00 (± 1.22) | 11.67 (± 1.66) |
| <i>Advenella mimigardefordensis</i> PSB9 | 8.22 (± 1.09) | 11.67 (± 1.00) |
| Control (+) | 8.67 (± 0.71) | 11.78 (± 1.09) |
| Control (-) | 8.67 (± 0.87) | 10.67 (± 1.32) |

Table 23. Study of the statistical correlation between some of the study variables in the greenhouse pot experiment. The results showed correspond to the Spearman's correlation coefficient. Those data with statistical significance (p -value <0.05) are highlighted in pink.

| | Strain | Stem height | Stem dry weight | Stem P ₀ assimilated | Root dry weight | Root P ₀ assimilated | Spike dry weight | Glucose in spikes |
|---------------------------------|--------|-------------|-----------------|---------------------------------|-----------------|---------------------------------|------------------|-------------------|
| Strain | 1 | | | | | | | |
| Stem height | 0.009 | 1 | | | | | | |
| Stem dry weight | 0 | 0 | 1 | | | | | |
| Stem P ₀ assimilated | 0.324 | 0.249 | 0.491 | 1 | | | | |
| Root dry weight | 0.016 | 0.000 | 0 | 0.394 | 1 | | | |
| Root P ₀ assimilated | 0.939 | 0.004 | 0.351 | 0.163 | 0.116 | 1 | | |
| Spike dry weight | 0 | 0 | 0 | 0.61 | 0 | 0.016 | 1 | |
| Glucose in spikes | 0.738 | 0.937 | 0.231 | 0.931 | 0.251 | 0.985 | 0.010 | 1 |

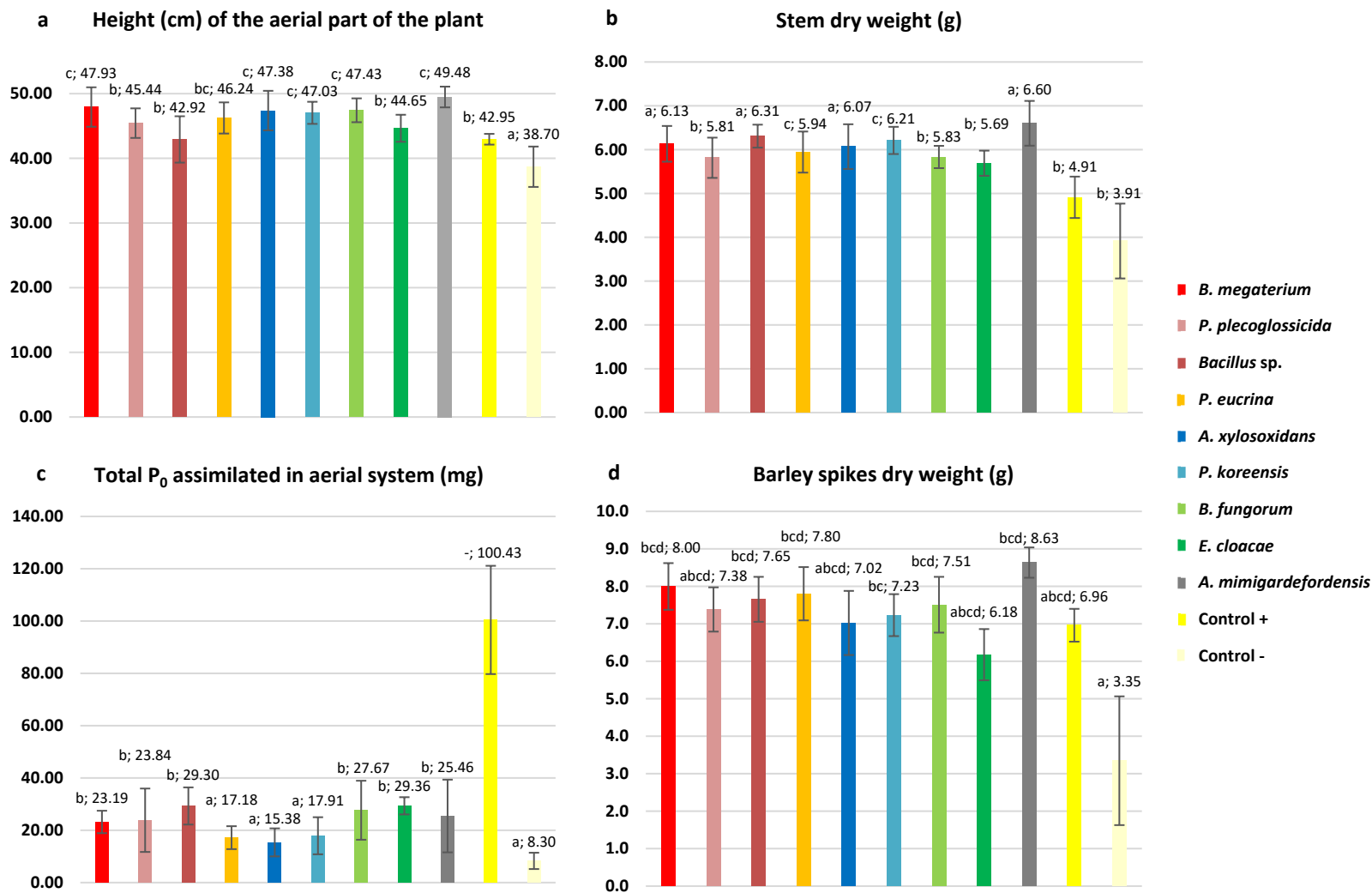


Figure 53. Effect on barley plants inoculated with different PSB strains at the end of the experiment: height of the aerial part of the plant (A), stem dry weight (B), total phosphorus assimilated in aerial system (C) and dry weight of ears (D). The data shown correspond to the average of 9 replicates and each replica corresponded to 10 plants sown per pot. Bars marked with the same letter are not significantly different ($P \geq 0.05$).

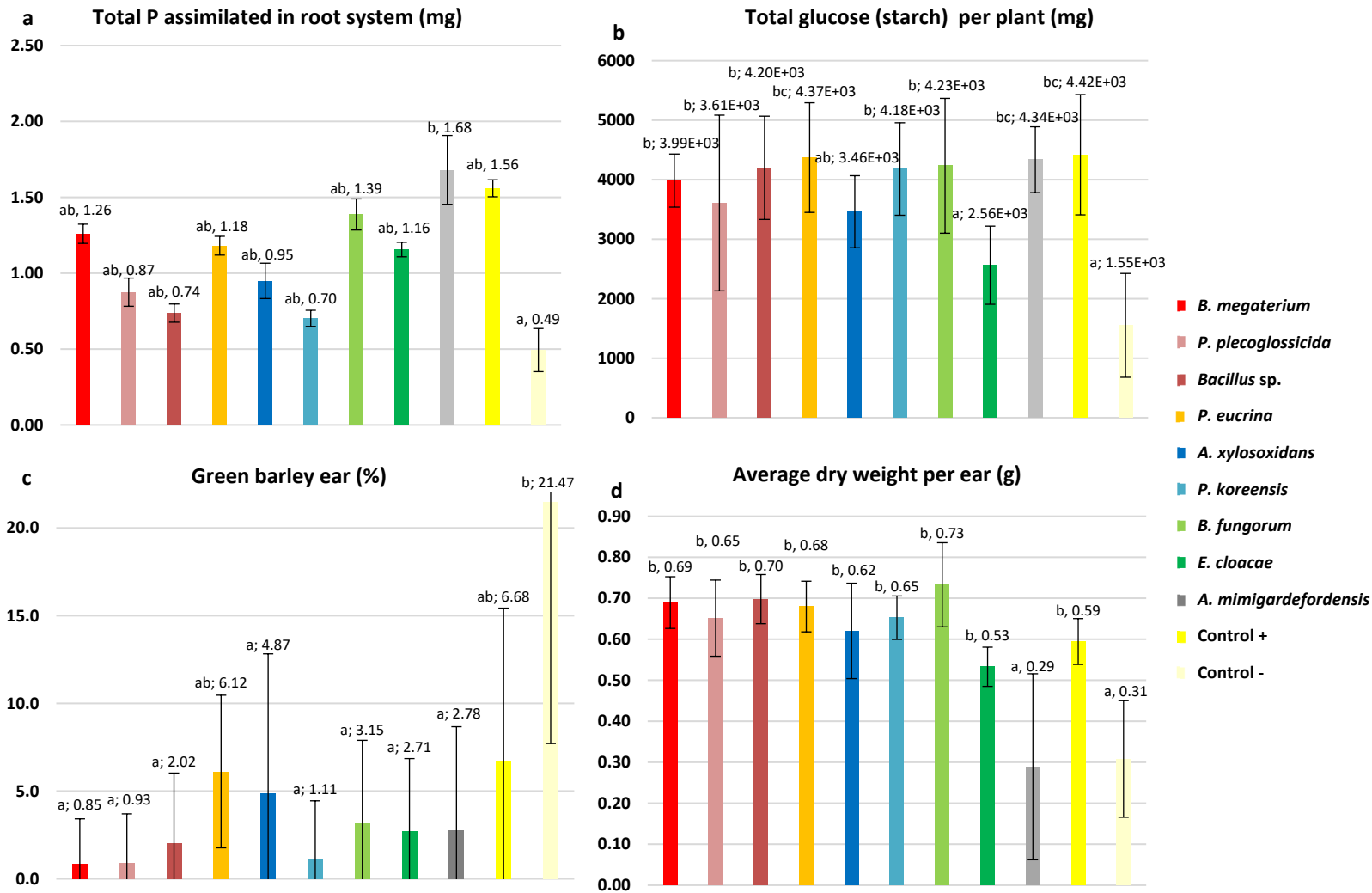


Figure 54. Effect on barley plants inoculated with different PSB strains at the end of the experiment: phosphorus assimilated in the root system (A), total glucose in the ears (B), percentage of immature green barley ears at the end of the experiment (C) and average of the dry weight of each ear (D). The data shown correspond to the average of 9 replicates and each replica corresponded to 10 plants sown per pot. Bars marked with the same letter are not significantly different ($P \geq 0.05$).

3.7. *In vitro* germination assay

Although the number of plants per pot in the greenhouse pot experiment did not show significant differences, an in-depth assay was carried out to determine the putative effect of three PSB selected strains on the germination process. Data were analyzed once the control had reached 80% of germinated seeds, which occurred after four days of incubation. The results suggested that *A. mimigardefordensis* and, especially, the co-inoculation of *A. mimigardefordensis* with *B. megaterium*, seemed to stimulate the growth and development of roots and stems (Figure 55). However, the statistical study did not show significant differences when comparing inoculated seeds and negative controls. This may be due to the high standard deviations that existed in these two treatments. These deviations were a consequence of those seeds with late germination, which although had roots with more than 2 mm (and therefore they were quantified in the study), those were much shorter than those exhibited by the rest of the seeds in the plate (Figure 56c). In general, *A. mimigardefordensis* when inoculated alone, or in combination with *B. megaterium* showed improved stem and root elongation, and even greater development of adventitious roots (Figures 56a and 56b).

Some potassium-solubilizer strains have been related with germination enhancement and seedling vigor improvement (Etesami *et al.*, 2017). In this case, it was not detected an increase at germination ratio, but the seeds inoculated with *A. mimigardefordensis* showed higher plant growth and longer roots with further development of secondary roots.

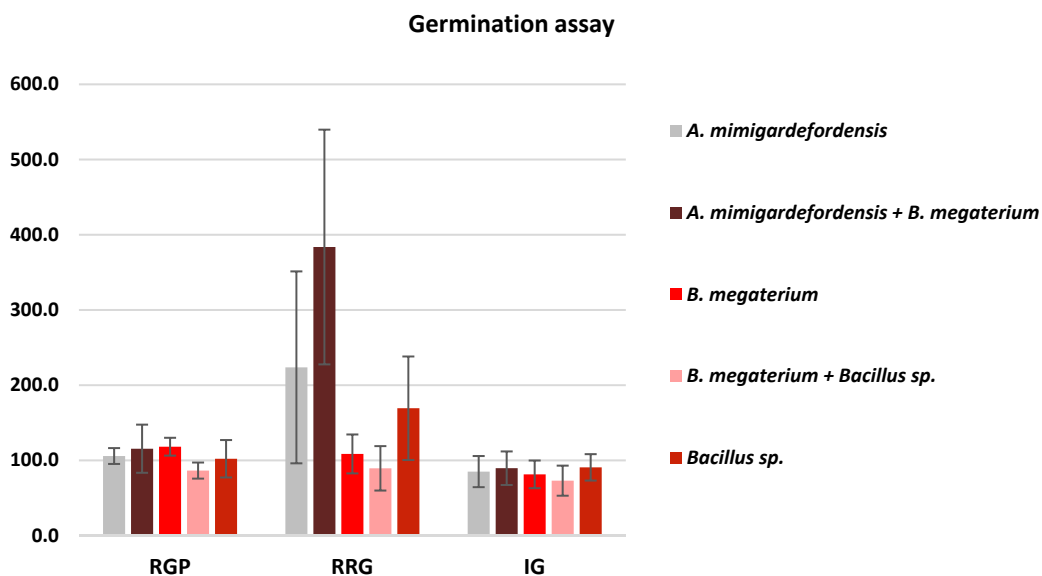


Figure 55. *In vitro* germination assay for three selected strains and their combination for Relative Germination Percentage (RGP), the Relative Radicle Growth (RRG) and the Germination Index (GI) results. Data shown (with SD) are the average of three independent experiments.

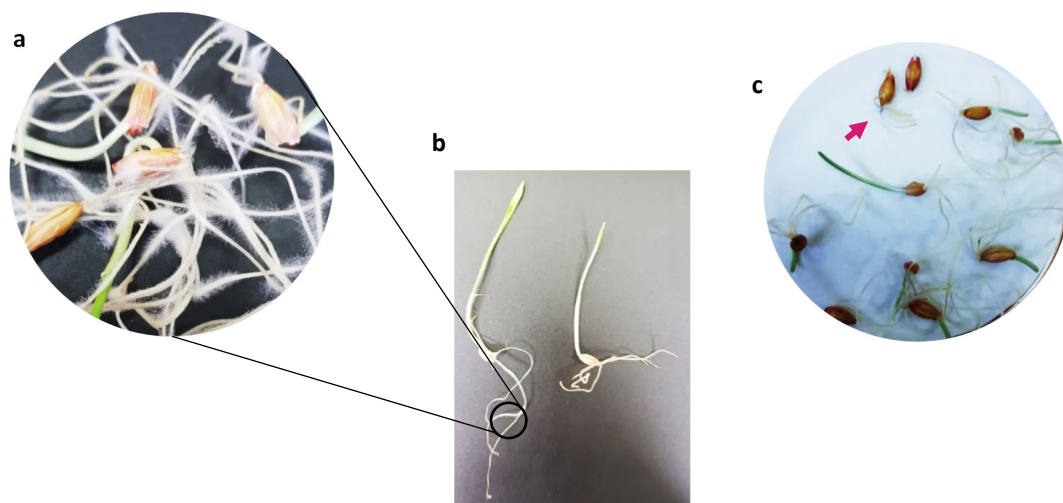


Figure 56. (a) Picture slowing the root development in the germination assay of a sample co-inoculated with *A. mimigardefordensis* and *B. megaterium* after four days of incubation. (b) Comparison of barley seeds development inoculated with *A. mimigardefordensis* + *B. megaterium* (left), and the negative control (right) in the germination assay after 4 days of incubation. (c) Picture of one plate inoculated with *A. mimigardefordensis* in the germination assay after 3 days of incubation. The arrow indicates one of the seeds with late germination, which had a much shorter root development than the rest in the treatment, which generates very large standard deviations in the statistical study.

3.8. *In vitro* antifungal activity on agar plates

The antifungal activity of the isolates PSB1 to PSB9 was bioassayed against some well-known fungal pathogens, which affect several crops, including barley, like *Alternaria* sp., *Botrytis cinerea*, *Fusarium oxysporum*, *Pleospora herbarum*, *Nigrospora oyzae*, and *Rhizoctonia solani*. Bioassays were carried out in nine different agar media, but ISP5 and ISP7 were the only ones that supported the growth of all fungal and bacterial strains tested in the bioassay. Differences in the inhibition index of one strain against the same pathogen were detected depending on the culture medium.

A radar graph was made with all the results obtained from the inhibition index of each strain in each medium, and the total area for each PSB-fungal strain was calculated. In this way, it was possible to determine, in a general way, the strains that exhibited the highest antifungal activity in each medium. In general, *A. xylosoxidans* and *P. koreensis* showed the highest antifungal inhibition capacities, followed by *B. fungorum*, *P. plecoglossicida* and *B. megaterium* (Figures 57 and 58). On the contrary, *P. eucrina* did not show any type of antifungal activity in ISP5 medium, and poor antagonistic effect on ISP7.

Two strains showed the best antifungal activity in general terms, *A. xylosoxidans* and *P. koreensis*. It has been previously reported that both strains exhibit antibacterial or antifungal activity against crop pathogens, reducing or even inhibiting the growth of fungus like *F. oxysporum* or *Alternaria* sp. (Dhaouadi *et al.*, 2019; Kaur *et al.*, 2019; Rafikova *et al.*, 2016).

It is interesting to note that, in most cases, some strains showed hardly any antifungal activity against one of the fungi in one medium, and exhibited very high growth inhibition against the same pathogen in another medium. This fact made us think that the isolates can exhibit different antifungal mechanisms against the different fungi, and therefore the activity could depend on the culture medium composition. For example, *B. megaterium* PSB1 exhibited a total inhibition of *B. cinerea* and *Alternaria* sp. growth, and also a good antifungal activity against *F. oxysporum* (inhibition index of 96,5%) and *N. oryzae* (94.9%) in ISP5 agar medium. On the contrary, *B. megaterium* did not show any antifungal activity against *P. herbarum* in the same medium. However, the inhibition rate on ISP7 against *P. herbarum* was, on average, 71.9%. Another clear example is *A. xylooxidans*, which showed almost total inhibition percentages for all fungi except *P. herbarum* on ISP5 medium. On the contrary, the inhibition rate on ISP7 was 87.2% against *P. herbarum*, while it did not show any effect against *R. solani*.

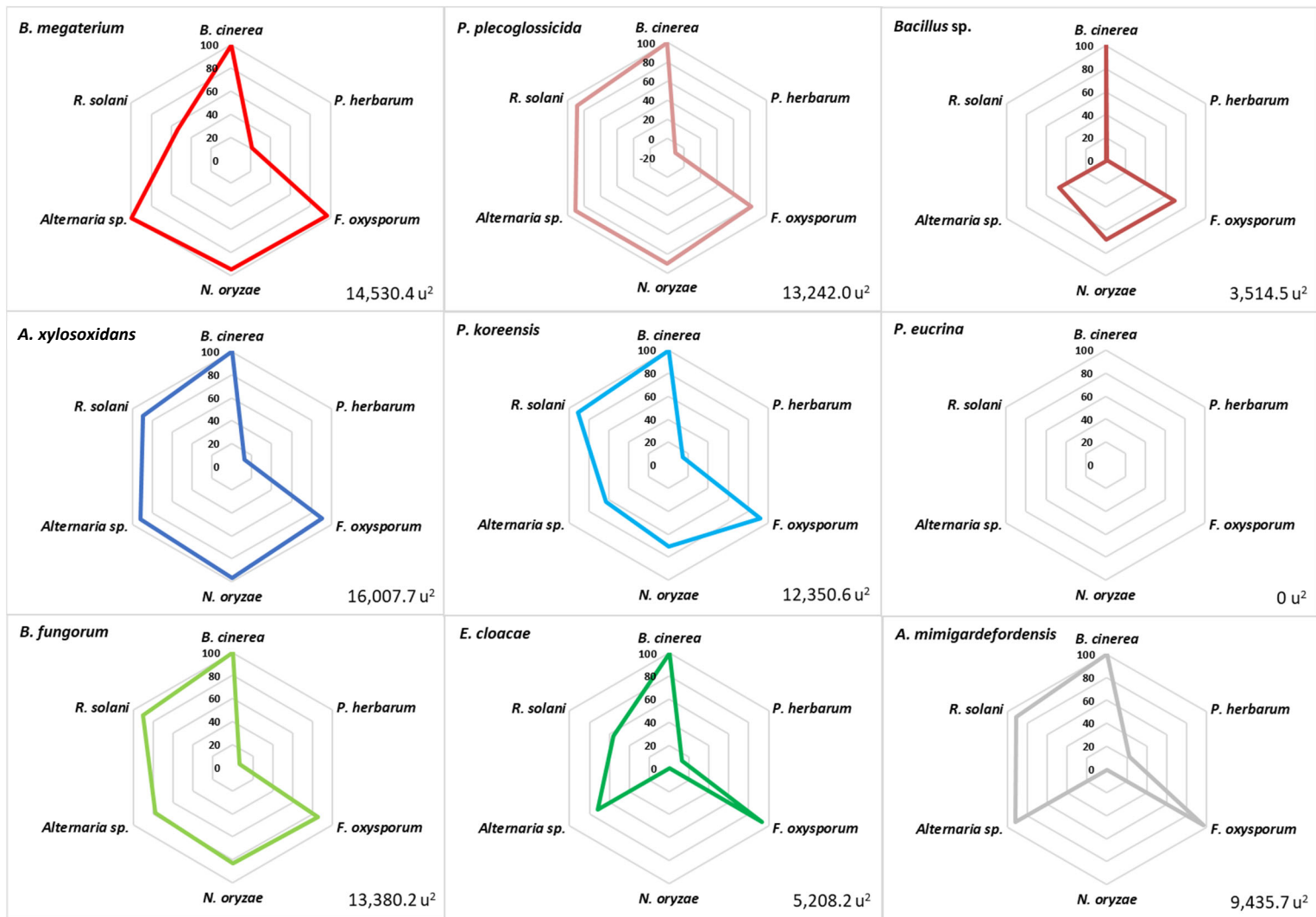


Figure 57. Antifungal activity of isolates PSB1 to PSB9 determined by an *in vitro* bioassay (dual culture technique) on ISP5 medium. Average Inhibition index (I index) from three independent experiments are shown in a 0-100 scale. Data shown were measured for each pathogen at different times when the pathogen growth in absence of antagonist PSB isolate (control) was 4.5 cm.

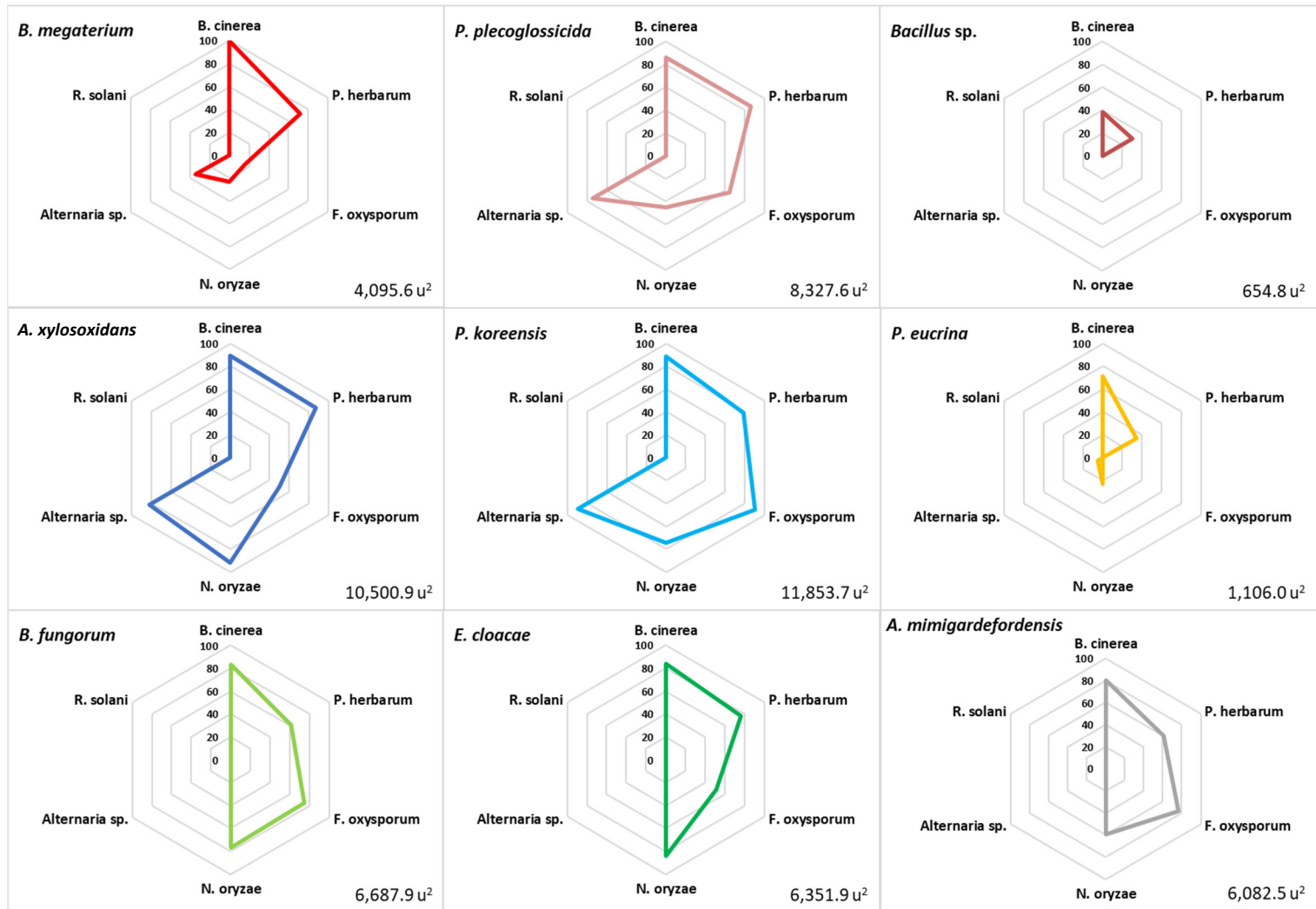
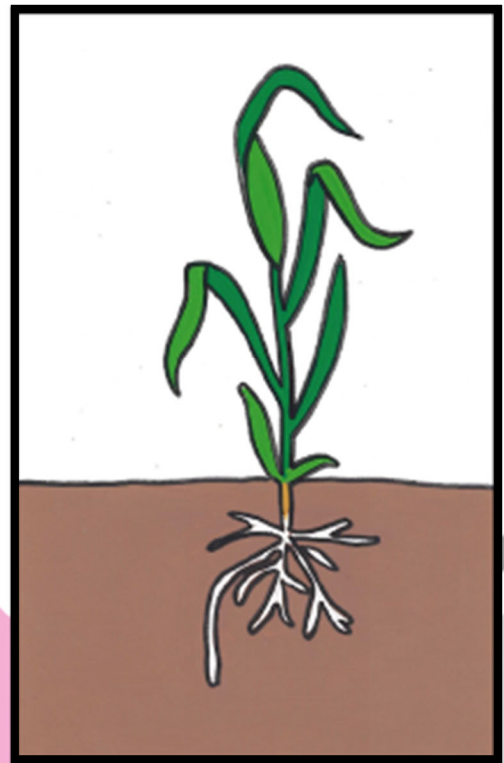


Figure 58. Antifungal activity of isolates PSB1 to PSB9 determined by an *in vitro* bioassay (dual culture technique) on ISP7 medium. Average I index from three independent experiments are shown in a 0-100 scale. Data shown were measured for each pathogen at different times when the pathogen growth in absence of antagonist PSB isolate (control) was 4.5 cm.

GENERAL DISCUSSION



CONFIDENTIAL

II. Improving the phosphorus performance in soils.

The use of biofertilizers has been addressed for decades and they seem to be the future of the agriculture industry. For some time now, P-solubilizing microorganisms have been aiming to be a solution to the problem of the legacy P in crop soils. Thus, nine P-solubilizing bacteria were isolated and selected: *B. megaterium*, *P. plecoglossicida*, *Bacillus* sp., *P. eucrina*, *A. xylosoxidans*, *P. koreensis*, *B. fungorum*, *E. cloacae* and *A. mimigardefordensis*.

It is well-known that most of the P solubilizing strains show other plant-growth promoting skills: mineral solubilization, plant hormones production, antimicrobial activity, and siderophore production, among others. Thus, the skills of the nine isolates were analysed for some of these plant-growth promoting skills. To sum up, among the nine strains tested, *B. fungorum* showed the best *in vitro* P solubilization skills (both in solid and in liquid assays). In addition, *B. fungorum* was the one that generated the highest values of assimilated P in barley plants in the greenhouse pot assay, being able to solubilize P through all the direct and indirect mechanisms analysed: phytases and phosphatases production, organic acid secretion, and siderophore and HCN production. Therefore, after verifying that all the tested P-solubilizing strains were able to reverse the P deficiency in the absence of soluble P, there are other skills to consider when choosing a strain as a biofertilizer.

Hence, the main purpose of biofertilizers is to improve crop development. In this sense, despite the assimilation of P has been widely related to plant growth, we could observe that, for barley crops, *B. fungorum* was the one that got the higher P assimilated values, but not the one that showed the best results in the barley assay. On the contrary, *B. megaterium* and *A. mimigardefordensis* were the strains that most improved the development of the barley crop in the greenhouse pot experiment.

Thus, it is needed something else to be a good PGPR. The skills that an ideal PGPR for biofertilizer application should fulfill have been described (Basu *et al.*, 2021; Vejan *et al.*, 2016):

- It should be highly rhizosphere-competent and eco-friendly.
- It should colonize the plant roots in significant numbers upon inoculation.
- It should be compatible with other bacteria in the rhizosphere.
- It should be able to promote plant growth.
- It should exhibit a broad spectrum of action.
- It should be tolerant of physicochemical factors like heat, desiccation, radiations and oxidants.
- It should demonstrate better competitive skills over the existing rhizobacterial communities.

Therefore, *Bacillus megaterium* is a good candidate as PGPR for biofertilizer formulations. The term rhizosphere competence was first coined by Ahmad and Baker in 1987, and was defined as “*the ability of some strain to grow and function in the developing rhizosphere*” (Gupta *et al.*, 2014). Diverse species of *Bacillus* have been isolated from the rhizosphere of some crops as maize or rice.

It is no new that it is able to colonize plant roots. In fact, they have been previously isolated from the roots of numerous plants, so they should be compatible with other bacteria in the rhizosphere (Dahmani *et al.*, 2020; Z. L. Liu & Sinclair, 1993; Trivedi & Pandey, 2008; Zheng & Sinclair, 2000).

Besides, *Bacillus megaterium* has already shown plant-growth promoting activity for *Retama monosperma*, tomato plants, and *Arabidopsis thaliana* (Dahmani *et al.*, 2020; Nascimento *et al.*, 2020; Ortíz-Castro *et al.*, 2008; Zou *et al.*, 2010). Thus, in view of the chapter 3 results, it can be concluded that *B. megaterium* PSB1 can also improve barley's growth, since higher stem length and dry weight, barley ears dry weight and assimilated P in stem were obtained in the greenhouse pots experiments. However, it is necessary to carry out more studies to affirm that it has a broad spectrum of action, since it has not been deeply studied yet.

In addition, it is known that *B. megaterium* is an endospore producer. Species from *Bacillus* genera are well-known producer of endospores, an interesting ability for a biofertilizer strain, not only due to the high temperatures that are reached in the fertilizer production process, but also because of the different climatic conditions they must face in soil. Thus, endospores are a good solution to resist physicochemical factors, since they are highly resistant to chemical and physical stresses, even heat, radiation, oxidative damage and chemical compounds (Vos *et al.*, 2011).

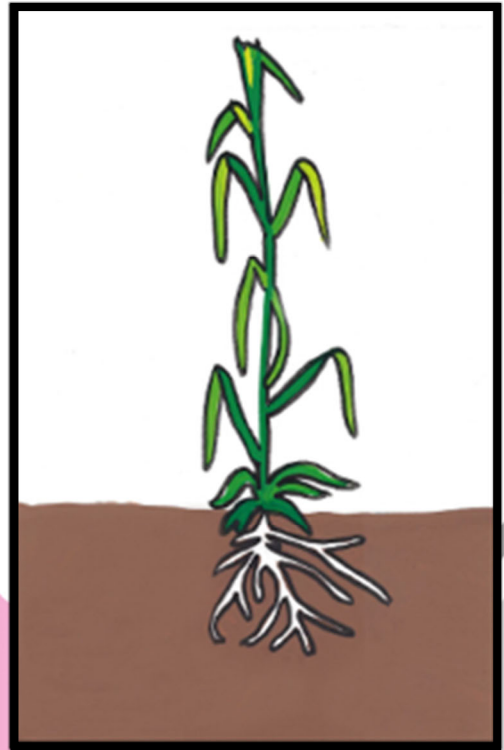
And last but not least, it has been demonstrated that *B. megaterium* PSB3 shows good skills as PGPR when compared to other strains all along chapter 3. Besides, *B. megaterium* showed high antifungal skills. It is not the first time that the *B. megaterium* skills as biocontrol agent against crop pathogenic fungi has been studied, since it had been previously reported that it was capable of inhibiting *F. oxysporum* and *A. alternata* growth (Trivedi & Pandey, 2008). It is well known that several *Bacillus* strains are able to produce antimicrobial agents, lytic enzymes against fungal cell walls, or even endotoxins against a large group of insects (Azizoglu, 2019; Lastochkina *et al.*, 2020; Saxena *et al.*, 2019). Regarding its antimicrobial activity, the ability of *Bacillus* to induce systemic resistance of the plant through the production of compounds such as salicylic acid, ethylene or jasmonic acid, which induce systemic resistance in plants, is also interesting. Thus, it would be interesting to analyse the response of cultures to infection with different pathogens after inoculation with *B. megaterium* (Beris *et al.*, 2018).

All these skills make *B. megaterium* one of the perfect candidates for biofertilizer production (Chen *et al.*, 2020; Khan *et al.*, 2020; Saxena *et al.*, 2019). In fact, some important companies such, as Bayer Crop Science, Syngenta or Certis, have already commercial *Bacillus*-based bioformulations in agriculture, mainly with *B. subtilis*, *B. pumilus* and *B. amyloliquefaciens* (Borriss, 2020).

On the other hand, *A. mimigardefordensis* has not been described as PGPR until now. This strain is known for its ability to synthesize polythioester homopolymers (PTEs), widely used in several industries (Wübbeler *et al.*, 2014). However, in view of the results obtained in the greenhouse pot assay with barley seeds, it appears to be a very promising PGPR strain.

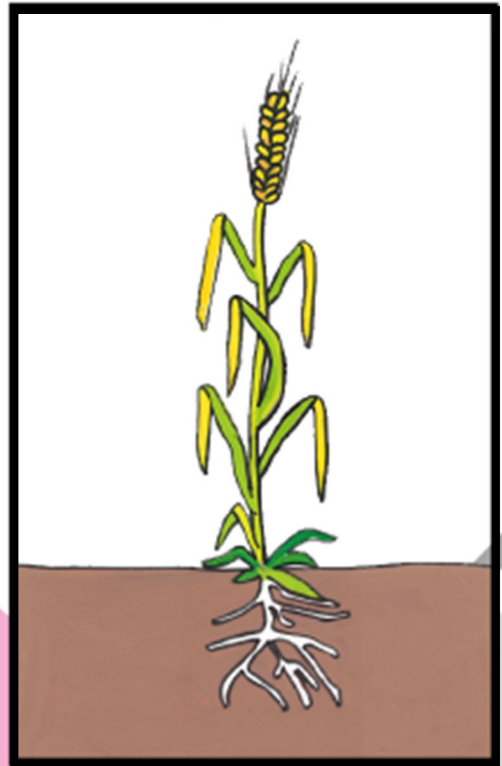
However, it is still necessary its study as rhizobacterial strain and determine if it is able to colonize the rhizosphere of the plant, if it has a broad spectrum of action, and shows a similar effect on other crops, or if it is compatible with other bacteria present in the plant rhizosphere. We know that it is compatible with the nine isolates in this dissertation (data not shown), and that it exhibits better competitive skills over well-known PGPR strains such as *B. fungorum* or *Pseudomonas* sp.

FUTURE PERSPECTIVES



CONFIDENTIAL

CONCLUSIONS



CONFIDENTIAL

BIBLIOGRAPHY



A

Abd El-Rahman, A. F., Shaheen, H. A., Abd El-Aziz, R. M., & Ibrahim, D. S. S. (2019). Influence of hydrogen cyanide-producing rhizobacteria in controlling the crown gall and root-knot nematode, *Meloidogyne incognita*. *Egyptian Journal of Biological Pest Control*, 29(1), 41. <https://doi.org/10.1186/s41938-019-0143-7>

Abdallah, A. R., Safwat, M. S. A., Moharram, T. M., Ahmed, S., & Soliman, H. (2009). Biofertilizers and their importance in environmental and sustainable agriculture. *Journal of Agricultural Chemistry and Biotechnology*, 34(2), 769–779. <https://doi.org/10.21608/jacb.2009.90281>

Aeron, A., Khare, E., Kumar, C., Vijay, J., Meena, S., Mohammed, S., & Aziz, A. (2019). Revisiting the plant growth - promoting rhizobacteria: lessons from the past and objectives for the future. *Archives of Microbiology*, 3. <https://doi.org/10.1007/s00203-019-01779-w>

Ahmad, F., Ahmad, I., & Khan, M. S. (2008). Screening of free-living rhizospheric bacteria for their multiple plant growth promoting activities. *Microbiological Research*, 163(2), 173–181. <https://doi.org/10.1016/j.micres.2006.04.001>

Alam, S. (2013). In vitro solubilization of inorganic phosphates by phosphate solubilizing microorganisms. *African Journal of Microbiology Research*, September, 1–6. <https://doi.org/10.5897/AJMR2013.5861>

Alori, E. T., Glick, B. R., & Babalola, O. O. (2017). Microbial Phosphorus Solubilization and Its Potential for Use in Sustainable Agriculture. *Frontiers in Microbiology*, 8. <https://doi.org/10.3389/fmicb.2017.00971>

Altieri, A. S., & Kelman, Z. (2018). DNA Sliding Clamps as Therapeutic Targets. *Frontiers in Molecular Biosciences*, 5. <https://doi.org/10.3389/fmolb.2018.00087>

Álvarez-Pérez, J. M., González-García, S., Cobos, R., Olego, M. Á., Ibañez, A., Díez-Galán, A., Garzón-Jimeno, E., & Coque, J. J. R. (2017). Use of endophytic and rhizosphere actinobacteria from grapevine plants to reduce nursery fungal graft infections that lead to young grapevine decline. *Applied and Environmental Microbiology*, 83(24). <https://doi.org/10.1128/AEM.01564-17>

Álvarez, C. L., Marín, M., Díez, M. C., & Osorio, N. W. (2012). Molecular identification of microorganisms associated to the rhizosphere of vanilla and their potential use as biofertilizers. *Acta Horticulturae*, 964, 107–114. <https://doi.org/10.17660/ActaHortic.2012.964.13>

Ambreen, S., Yasmin, A., & Aziz, S. (2020). Isolation and characterization of organophosphorus phosphatases from *Bacillus thuringiensis* MB497 capable of degrading Chlorpyrifos, Triazophos and Dimethoate. *Heliyon*, 6(7), e04221. <https://doi.org/10.1016/j.heliyon.2020.e04221>

Asare, E. K., Jaiswal, S., Maley, J., Båga, M., Sammynaiken, R., Rossnagel, B. G., & Chibbar, R. N. (2011). Barley Grain Constituents, Starch Composition, and Structure Affect Starch in Vitro Enzymatic Hydrolysis. *Journal of Agricultural and Food Chemistry*, 59(9), 4743–4754. <https://doi.org/10.1021/jf200054e>

Astriani, M., Zubaidah, S., Abadi, A. L., & Suarsini, E. (2020). *Pseudomonas plecoglossicida* as a novel bacterium for phosphate solubilizing and indole-3-acetic acid-producing from soybean rhizospheric soils of East Java, Indonesia. *Biodiversitas Journal of Biological Diversity*, 21(2). <https://doi.org/10.13057/biodiv/d210220>

Atlas, R. M. (2010). *Handbook of Microbiological Media* (T. and F. Group (Ed.); 4th edition). Press, CRC. <https://doi.org/10.1201/EBK1439804063>

Avdalović, J., Beškoski, V., Gojgić-Cvijović, G., Mattinen, M. L., Stojanović, M., Zildžović, S., & Vrvic, M. M. (2015). Microbial solubilization of phosphorus from phosphate rock by iron-oxidizing *Acidithiobacillus* sp. B2. *Minerals Engineering*, *72*, 17–22. <https://doi.org/10.1016/j.mineng.2014.12.010>

Aziz, R. K., Bartels, D., Best, A. A., DeJongh, M., Disz, T., Edwards, R. A., Formsmma, K., Gerdes, S., Glass, E. M., Kubal, M., Meyer, F., Olsen, G. J., Olson, R., Osterman, A. L., Overbeek, R. A., McNeil, L. K., Paarmann, D., Paczian, T., Parrello, B., ... Zagnitko, O. (2008). The RAST Server: Rapid Annotations using Subsystems Technology. *BMC Genomics*, *9*(1), 75. <https://doi.org/10.1186/1471-2164-9-75>

Azizoglu, U. (2019). *Bacillus thuringiensis* as a Biofertilizer and Biostimulator: a Mini-Review of the Little-Known Plant Growth-Promoting Properties of Bt. *Current Microbiology*, *76*(11), 1379–1385. <https://doi.org/10.1007/s00284-019-01705-9>

B

Backer, R., Rokem, J. S., Ilangumaran, G., Lamont, J., Praslickova, D., Ricci, E., Subramanian, S., & Smith, D. L. (2018). Plant Growth-Promoting Rhizobacteria: Context, Mechanisms of Action, and Roadmap to Commercialization of Biostimulants for Sustainable Agriculture. *Frontiers in Plant Science*, *9*. <https://doi.org/10.3389/fpls.2018.01473>

Baker-Austin, C., & Dopson, M. (2007). Life in acid: pH homeostasis in acidophiles. *Trends in Microbiology*, *15*(4), 165–171. <https://doi.org/10.1016/j.tim.2007.02.005>

Barber, S. A. (1995). *Soil Nutrient Bioavailability: A Mechanistic Approach* (John Wiley & Sons (Ed.); 2nd editio).

Barreiro, C. (2004). Respuesta al choque térmico en la bacteria productora de aminoácidos *Corynebacterium glutamicum* ATCC 13032: caracterización de promotores inducibles por calor. Tesis Doctoral. Universidad de León.

Barreiro, C., González-Lavado, E., Brand, S., Tauch, A., & Martín, J. F. (2005). Heat shock proteome analysis of wild-type *Corynebacterium glutamicum* ATCC 13032 and a spontaneous mutant lacking GroEL1, a dispensable chaperone. *Journal of Bacteriology*, *187*(3), 884–889. <https://doi.org/10.1128/JB.187.3.884-889.2005>

Barreiro, C., & Martínez-Castro, M. (2019). Regulation of the phosphate metabolism in *Streptomyces* genus: impact on the secondary metabolites. *Applied Microbiology and Biotechnology*, *103*(4), 1643–1658. <https://doi.org/10.1007/s00253-018-09600-2>

Barreiro, C., Morales, A., Vázquez-Iglesias, I., & Sola-Landa, A. (2017). Intra- and extra-cellular proteome analyses of steroid-producer *Mycobacteria*. In J. L. Barredo & I. Herráiz (Eds.), *Microbial steroids: methods and protocols*. (1st edition). Springer Science. https://doi.org/10.1007/978-1-4939-7183-1_6

Basu, A., Prasad, P., Das, S. N., Kalam, S., Sayyed, R. Z., Reddy, M. S., & El Enshasy, H. (2021). Plant Growth Promoting Rhizobacteria (PGPR) as Green Bioinoculants: Recent Developments, Constraints, and Prospects. *Sustainability*, *13*(3), 1140. <https://doi.org/10.3390/su13031140>

Belimov, A., Dodd, I., Safronova, V., Hontzeas, N., & Davies, W. (2007). *Pseudomonas brassicacearum* strain Am3 containing 1-aminocyclopropane-1-carboxylate deaminase can show both pathogenic and growth-promoting properties in its interaction with tomato. *Journal of Experimental Botany*, *58*(6), 1485–1495. <https://doi.org/10.1093/jxb/erm010>

Bellenberg, S., Huynh, D., Poetsch, A., Sand, W., & Vera, M. (2019). Proteomics Reveal Enhanced Oxidative Stress Responses and Metabolic Adaptation in *Acidithiobacillus ferrooxidans* Biofilm Cells on Pyrite. *Frontiers in Microbiology*, 10. <https://doi.org/10.3389/fmicb.2019.00592>

Ben Zineb, A., Trabelsi, D., Ayachi, I., Barhoumi, F., Aroca, R., & Mhamdi, R. (2020). Inoculation with Elite Strains of Phosphate-Solubilizing Bacteria Enhances the Effectiveness of Fertilization with Rock Phosphates. *Geomicrobiology Journal*, 37(1), 22–30. <https://doi.org/10.1080/01490451.2019.1658826>

Bergamo, R. F., Teresa, M., Novo, M., Veríssimo, R. V., Paulino, L. C., Stoppe, N. C., Inês, M., Sato, Z., Manfio, G. P., Inácio, P., Garcia, O., & Ottoboni, L. M. M. (2004). Differentiation of *Acidithiobacillus ferrooxidans* and *A. thiooxidans* strains based on 16S – 23S rDNA spacer polymorphism analysis. 155, 559–567. <https://doi.org/10.1016/j.resmic.2004.03.009>

Beris, D., Theologidis, I., Skandalis, N., & Vassilakos, N. (2018). *Bacillus amyloliquefaciens* strain MBI600 induces salicylic acid dependent resistance in tomato plants against Tomato spotted wilt virus and Potato virus Y. *Scientific Reports*, 8(1), 10320. <https://doi.org/10.1038/s41598-018-28677-3>

Bhatti, T. M., & Yawar, W. (2010). Bacterial solubilization of phosphorus from phosphate rock containing sulfur-mud. *Hydrometallurgy*, 103(1–4), 54–59. <https://doi.org/10.1016/j.hydromet.2010.02.019>

Booth, I. R. (1985). Regulation of cytoplasmic pH in bacteria. *Microbiological Reviews*, 49(4), 359–378. <https://doi.org/10.1128/mr.49.4.359-378.1985>

Borriss, R. (2020). Phytostimulation and Biocontrol by the Plant-Associated *Bacillus amyloliquefaciens* FZB42: An Update (pp. 1–20). https://doi.org/10.1007/978-981-15-2576-6_1

Bradford, M. M. (1976). A rapid and sensitive method for the quantitation of microgram quantities of protein utilizing the principle of protein-dye binding. *Analytical Biochemistry*, 72, 248–254. [https://doi.org/10.1016/0003-2697\(76\)90527-3](https://doi.org/10.1016/0003-2697(76)90527-3)

Brierley, C. L. (2008). How will biomining be applied in future? *Transactions of Nonferrous Metals Society of China*, 18(6), 1302–1310. [https://doi.org/10.1016/S1003-6326\(09\)60002-9](https://doi.org/10.1016/S1003-6326(09)60002-9)

Brito, L. F., López, M. G., Straube, L., Passaglia, L. M. P., & Wendisch, V. F. (2020). Inorganic Phosphate Solubilization by Rhizosphere Bacterium *Paenibacillus sonchi*: Gene Expression and Physiological Functions. *Frontiers in Microbiology*, 11. <https://doi.org/10.3389/fmicb.2020.588605>

Bucher, M., Rausch, C., & Daram, P. (2001). Molecular and biochemical mechanisms of phosphorus uptake into plants. *Journal of Plant Nutrition and Soil Science*, 164(2), 209–217. [https://doi.org/10.1002/1522-2624\(200104\)164:2<209::AID-JPLN209>3.0.CO;2-F](https://doi.org/10.1002/1522-2624(200104)164:2<209::AID-JPLN209>3.0.CO;2-F)

C

Calle-Castañeda, S.M., Márquez-Godoy, M.A., & Hernández-Ortiz, J. P. (2018a). Phosphorus recovery from high concentrations of low-grade phosphate rocks using the biogenic acid produced by the acidophilic bacteria *Acidithiobacillus thiooxidans*. *Minerals Engineering*, 115, 97–105. <https://doi.org/10.1016/j.mineng.2017.10.014>

Calle-Castañeda, S. M., Márquez-Godoy, M. A., & Hernández-Ortiz, J. P. (2018b). Solubilization of phosphorus from phosphate rocks with *Acidithiobacillus thiooxidans* following a growing-then-recovery process. *World Journal of Microbiology and Biotechnology*, 34(1), 17. <https://doi.org/10.1007/s11274-017-2390-7>

Camacho, D., Frazao, R., Fouillen, A., Nanci, A., Lang, B. F., Apte, S. C., Baron, C., & Warren, L. A. (2020). New Insights Into *Acidithiobacillus thiooxidans* Sulfur Metabolism Through Coupled Gene Expression, Solution Chemistry, Microscopy, and Spectroscopy Analyses. *Frontiers in Microbiology*, *11*. <https://doi.org/10.3389/fmicb.2020.00411>

Candiano, G., Bruschi, M., Musante, L., Santucci, L., Ghiggeri, G. M., Carnemolla, B., Orecchia, P., Zardi, L., & Righetti, P. G. (2004). Blue silver: A very sensitive colloidal Coomassie G-250 staining for proteome analysis. *Electrophoresis*, *25*(9), 1327–1333. <https://doi.org/10.1002/elps.200305844>

Carstensen, A., Herdean, A., Schmidt, S. B., Sharma, A., Spetea, C., Pribil, M., & Husted, S. (2018). The Impacts of Phosphorus Deficiency on the Photosynthetic Electron Transport Chain. *Plant Physiology*, *177*(1), 271–284. <https://doi.org/10.1104/pp.17.01624>

Ceccotti, S. P., Morris, R. J., & Messick, D. L. (1998). A Global Overview of the Sulphur Situation: Industry'S Background, Market Trends, and Commercial Aspects of Sulphur Fertilizers. In *Nutrients in Ecosystems* (pp. 175–202). Springer. https://doi.org/10.1007/978-94-011-5100-9_6

Chahtane, H., Nogueira Füller, T., Allard, P.-M., Marcourt, L., Ferreira Queiroz, E., Shanmugabalaji, V., Falquet, J., Wolfender, J.-L., & Lopez-Molina, L. (2018). The plant pathogen *Pseudomonas aeruginosa* triggers a DELLA-dependent seed germination arrest in *Arabidopsis*. *ELife*, *7*. <https://doi.org/10.7554/eLife.37082>

Chang, C.-Y., Chen, S.-Y., Klipkhayai, P., & Chiemchaisri, C. (2019). Bioleaching of heavy metals from harbor sediment using sulfur-oxidizing microflora acclimated from native sediment and exogenous soil. *Environmental Science and Pollution Research*, *26*(7), 6818–6828. <https://doi.org/10.1007/s11356-019-04137-x>

Chatzipavlidis, I., Kefalogianni, I., Venieraki, A., & Holzapfel, W. (2013). *Status and trends of the Conservation and Sustainable use of microorganisms in agroindustrial processes*. www.fao.org

Chen, H., Yang, B., & Chen, X. (2009). Identification and characterization of four strains of *Acidithiobacillus ferrooxidans* isolated from different sites in China. *Microbiological Research*, *164*(6), 613–623. <https://doi.org/10.1016/j.micres.2007.09.002>

Chen, K., Tian, Z., He, H., Long, C., & Jiang, F. (2020). *Bacillus* species as potential biocontrol agents against citrus diseases. *Biological Control*, *151*, 104419. <https://doi.org/10.1016/j.biocontrol.2020.104419>

Chen, W., Yin, S., Wu, A., Wang, L., & Chen, X. (2020). Bioleaching of copper sulfides using mixed microorganisms and its community structure succession in the presence of seawater. *Bioresource Technology*, *297*, 122453. <https://doi.org/10.1016/j.biortech.2019.122453>

Chen, Yang, F., Zhang, L., & Wang, J. (2016). Organic Acid Secretion and Phosphate Solubilizing Efficiency of *Pseudomonas* sp. PSB12: Effects of Phosphorus Forms and Carbon Sources. *Geomicrobiology Journal*, *33*(10), 870–877. <https://doi.org/10.1080/01490451.2015.1123329>

Chi, A., Valenzuela, L., Beard, S., Mackey, A. J., Shabanowitz, J., Hunt, D. F., & Jerez, C. A. (2007). Periplasmic Proteins of the Extremophile *Acidithiobacillus ferrooxidans*. *Molecular & Cellular Proteomics*, *6*(12), 2239–2251. <https://doi.org/10.1074/mcp.M700042-MCP200>

Chi, Huang, X., Xiao, C., Wu, Y., & Zhang, W. (2009). Bioleaching of soluble phosphorus from rock phosphate containing pyrite with DES-induced *Acidithiobacillus ferrooxidans*. *Journal of Central South University of Technology*, *16*(5), 758–762. <https://doi.org/10.1007/s11771-009-0126-z>

Chi, Xiao, C., & Gao, H. (2006). Bioleaching of phosphorus from rock phosphate containing pyrites by *Acidithiobacillus ferrooxidans*. *Minerals Engineering*, *19*(9), 979–981. <https://doi.org/10.1016/j.mineng.2005.10.003>

Chow, P. S., & Landhäusser, S. M. (2004). A method for routine measurements of total sugar and starch content in woody plant tissues. *Tree Physiology*, *24*(10), 1129–1136. <https://doi.org/10.1093/treephys/24.10.1129>

Cobos, R., Barreiro, C., Mateos, R., & Coque, J.-J. R. (2010). Cytoplasmic- and extracellular-proteome analysis of *Diplodia seriata*: a phytopathogenic fungus involved in grapevine decline. *Proteome Science*, *8*(1), 46. <https://doi.org/10.1186/1477-5956-8-46>

Cortés, M. P., Acuña, V., Travisany, D., Siegel, A., Maass, A., & Latorre, M. (2020). Integration of Biological Networks for *Acidithiobacillus thiooxidans* Describes a Modular Gene Regulatory Organization of Bioleaching Pathways. *Frontiers in Molecular Biosciences*, *6*. <https://doi.org/10.3389/fmolb.2019.00155>

D

Dahmani, M. A., Desrut, A., Moumen, B., Verdon, J., Mermouri, L., Kacem, M., Coutos-Thévenot, P., Kaid-Harche, M., Bergès, T., & Vriet, C. (2020). Unearthing the Plant Growth-Promoting Traits of *Bacillus megaterium* RmBm31, an Endophytic Bacterium Isolated From Root Nodules of *Retama monosperma*. *Frontiers in Plant Science*, *11*. <https://doi.org/10.3389/fpls.2020.00124>

de Amaral Leite, A., de Souza Cardoso, A. A., de Almeida Leite, R., de Oliveira-Longatti, S. M., Filho, J. F. L., de Souza Moreira, F. M., & Melo, L. C. A. (2020). Selected bacterial strains enhance phosphorus availability from biochar-based rock phosphate fertilizer. *Annals of Microbiology*, *70*(1), 6. <https://doi.org/10.1186/s13213-020-01550-3>

de Boer, M. A., Wolzak, L., & Slootweg, J. C. (2019). Phosphorus: Reserves, Production, and Applications. In H. Ohtake & S. Tsuneda (Eds.), *Phosphorus Recovery and Recycling* (1st edition). Springer Singapore.

Dean, R., Van Kan, J. A. L., Pretorius, Z. A. ., Hammond-Kosack, K. E., Di Pietro, A., Spanu, P. D., Rudd, J. J., Dickman, M., Kahmann, R., Ellis, J., & Foster, G. D. (2012). The Top 10 fungal pathogens in molecular plant pathology. *Molecular Plant Pathology*, *13*(4), 414–430. <https://doi.org/10.1111/j.1364-3703.2011.00783.x>

Deng, S., Gu, G., Wu, Z., & Xu, X. (2017). Bioleaching of arsenopyrite by mixed cultures of iron-oxidizing and sulfur-oxidizing microorganisms. *Chemosphere*, *185*, 403–411. <https://doi.org/10.1016/j.chemosphere.2017.07.037>

Devi, R., Thakur, R., & Rajni Devi, C. (2018). Screening and identification of bacteria for plant growth promoting traits from termite mound soil. *Journal of Pharmacognosy and Phytochemistry*, *7*(2), 1681–1686.

Dhaouadi, S., Rouissi, W., Mougou-Hamdane, A., & Nasraoui, B. (2019). Evaluation of biocontrol potential of *Achromobacter xylosoxidans* against *Fusarium* wilt of melon. *European Journal of Plant Pathology*, *154*(2), 179–188. <https://doi.org/10.1007/s10658-018-01646-2>

Díaz, M., Castro, M., Copaja, S., & Guiliani, N. (2018). Biofilm Formation by the Acidophile Bacterium *Acidithiobacillus thiooxidans* Involves c-di-GMP Pathway and Pel exopolysaccharide. *Genes*, *9*(2), 113. <https://doi.org/10.3390/genes9020113>

Dilnashin, H., Birla, H., Hoat, T. X., Singh, H. B., Singh, S. P., & Keswani, C. (2020). Applications of agriculturally important microorganisms for sustainable crop production. In *Molecular Aspects of Plant Beneficial Microbes in Agriculture* (pp. 403–415). Elsevier. <https://doi.org/10.1016/B978-0-12-818469-1.00033-X>

Dong, X., Lv, L., Wang, W., Liu, Y., Yin, C., Xu, Q., Yan, H., Fu, J., & Liu, X. (2019). Differences in Distribution of Potassium-Solubilizing Bacteria in Forest and Plantation Soils in Myanmar. *International Journal of Environmental Research and Public Health*, *16*(5), 700. <https://doi.org/10.3390/ijerph16050700>

Dopson, M., Holmes, D. S., Lazcano, M., McCredden, T. J., Bryan, C. G., Mulroney, K. T., Steuart, R., Jackaman, C., & Watkin, E. L. J. (2017). Multiple Osmotic Stress Responses in *Acidihalobacter prosperus* Result in Tolerance to Chloride Ions. *Frontiers in Microbiology*, *7*. <https://doi.org/10.3389/fmicb.2016.02132>

Du, Q., Zhang, S., Antonietti, M., & Yang, F. (2020). Sustainable Leaching Process of Phosphates from Animal Bones To Alleviate the World Phosphate Crisis. *ACS Sustainable Chemistry & Engineering*, *8*(26), 9775–9782. <https://doi.org/10.1021/acssuschemeng.0c02233>

Duquesne, K., Lieutaud, A., Ratouchniak, J., Muller, D., Lett, M.-C., & Bonnefoy, V. (2008). Arsenite oxidation by a chemoautotrophic moderately acidophilic *Thiomonas* sp.: from the strain isolation to the gene study. *Environmental Microbiology*, *10*(1), 228–237. <https://doi.org/10.1111/j.1462-2920.2007.01447.x>

E

Espinosa-Victoria, D., López-Reyes, L., & De La Cruz-Benítez, A. (2009). Use of *16S rRNA* gene for characterization of phosphate-solubilizing bacteria associated with corn. *Revista Fitotecnia Mexicana*, *32*(1), 31–37. <https://doi.org/10.35196/rfm.2009.1.31-37>

Etesami, H., Emami, S., & Alikhani, H. A. (2017). Potassium solubilizing bacteria (KSB): Mechanisms, promotion of plant growth, and future prospects - A review. *Journal of Soil Science and Plant Nutrition*, *17*(4), 897–911. <https://doi.org/10.4067/S0718-95162017000400005>

F

Fageria, N. K. (2008). *The Use of Nutrients in Crop Plants* (1st ed.). CRC Press.

Falagán, C., & Johnson, D. B. (2016). *Acidithiobacillus ferriphilus* sp. nov., a facultatively anaerobic iron- and sulfur-metabolizing extreme acidophile. *International Journal of Systematic and Evolutionary Microbiology*, *66*(1), 206–211. <https://doi.org/10.1099/ijsem.0.000698>

Falkowski, P. G. (2001). Biogeochemical Cycles. In *Encyclopedia of Biodiversity* (pp. 552–564). Elsevier. <https://doi.org/10.1016/B978-0-12-384719-5.00013-7>

Fanelli, F., Amatuli, M. T., Moretti, A., Mulè, G., & Logrieco, A. F. (2013). *Alternaria* Black point of cereals as emerging mycotoxin problem in climate change. *JSM Mycotoxins*, *63*(1), 39–46.

Fang, L., Wang, Q., Li, J., Poon, C. S., Cheeseman, C. R., Donatello, S., & Tsang, D. C. W. (2020). Feasibility of wet-extraction of phosphorus from incinerated sewage sludge ash (ISSA) for phosphate fertilizer production: A critical review. *Critical Reviews in Environmental Science and Technology*, 1–33. <https://doi.org/10.1080/10643389.2020.1740545>

FAO (2020).

<http://www.fao.org/3/y4252e/y4252e06.htm>

Fasim, F., Ahmed, N., Parsons, R., & Gadd, G. M. (2002). Solubilization of zinc salts by a bacterium isolated from the air environment of a tannery. *FEMS Microbiology Letters*, *213*(1), 1–6. <https://doi.org/10.1111/j.1574-6968.2002.tb11277.x>

Feng, Yang, H., & Wang, W. (2015). System-level understanding of the potential acid-tolerance components of *Acidithiobacillus thiooxidans* ZJJN-3 under extreme acid stress. *Extremophiles*, *19*(5), 1029–1039. <https://doi.org/10.1007/s00792-015-0780-z>

Filippelli, G. M. (2008). The Global Phosphorus Cycle: Past, Present, and Future. *Elements*, 4(2), 89–95.

<https://doi.org/10.2113/GSELEMENTS.4.2.89>

Fu, B., Zhou, H., Zhang, R., & Qiu, G. (2008). Bioleaching of chalcopyrite by pure and mixed cultures of *Acidithiobacillus* spp. and *Leptospirillum ferriphilum*. *International Biodeterioration & Biodegradation*, 62(2), 109–115. <https://doi.org/10.1016/j.ibiod.2007.06.018>

G

García-Calvo, L., Ullán, R. V., Fernández-Aguado, M., García-Lino, A. M., Balaña-Fouce, R., & Barreiro, C. (2018). Secreted protein extract analyses present the plant pathogen *Alternaria alternata* as a suitable industrial enzyme toolbox. *Journal of Proteomics*, 177, 48–64. <https://doi.org/10.1016/j.jprot.2018.02.012>

Garrity, G. M., Brenner, D. J., Krieg, N. R., & Staley, J. (2005a). Bergey's Manual of Systematic Bacteriology, vol 2 part C. The alpha-, beta-, delta-, and epsilonproteobacteria. In *Human Factors: The Journal of Human Factors and Ergonomics Society* (2nd edition, Vol. 2, Issue 1). Springer US. <https://doi.org/10.1177/001872086000200109>

Garrity, G. M., Brenner, D. J., Krieg, N. R., & Staley, J. T. (2005b). Bergey's Manual of Systematic Bacteriology, vol 2 part B. The gammaproteobacteria. In D. J. Brenner, N. R. Krieg, & J. T. Staley (Eds.), *Bergey's Manual of Systematic Bacteriology, vol 2 part B. The gammaproteobacteria*. (2nd edition). <https://doi.org/10.1245/s10434-010-1229-3>

Ghosh, P., Rathinasabapathi, B., & Ma, L. Q. (2015). Phosphorus solubilization and plant growth enhancement by arsenic-resistant bacteria. *Chemosphere*, 134, 1–6. <https://doi.org/10.1016/j.chemosphere.2015.03.048>

Giri, B., Prasad, R., Wu, Q.-S., & Varma, A. (Eds.). (2019). *Biofertilizers for Sustainable Agriculture and Environment* (1st edition, Vol. 55). Springer International Publishing. <https://doi.org/10.1007/978-3-030-18933-4>

Glick, B. R. (2012). Plant Growth-Promoting Bacteria: Mechanisms and Applications. *Scientifica*, 2012, 1–15. <https://doi.org/10.6064/2012/963401>

Godio Fernandez, R. P. (2007). Clonación y caracterización de los genes involucrados en la ruta biosintética del ácido clavárico, un anticancerígeno producido por *Hypholoma sublateritium*. Tesis Doctoral. Universidad de León.

González, C., Brito, N., & Sharon, A. (2016). Infection process and fungal virulence factors. In S. Fillinger & Y. Elad (Eds.), *Botrytis – the Fungus, the Pathogen and its Management in Agricultural Systems* (1st edition). Springer International Publishing. <https://doi.org/10.1007/978-3-319-23371-0>

Gordon, S. A., & Weber, R. P. (1951). Colorimetric estimation of indoleacetic acid. *Plant Physiology*, 26(1), 192–195.

Gorg, A. (2004). 2-D Electrophoresis. Principles and Methods. In *Handbook*.

Gu, S., Wei, Z., Shao, Z., Friman, V.-P., Cao, K., Yang, T., Kramer, J., Wang, X., Li, M., Mei, X., Xu, Y., Shen, Q., Kümmerli, R., & Jousset, A. (2020). Competition for iron drives phytopathogen control by natural rhizosphere microbiomes. *Nature Microbiology*, 5(8), 1002–1010. <https://doi.org/10.1038/s41564-020-0719-8>

Guan, N., & Liu, L. (2020). Microbial response to acid stress: mechanisms and applications. *Applied Microbiology and Biotechnology*, 104(1), 51–65. <https://doi.org/10.1007/s00253-019-10226-1>

Gumulya, Y., Boxall, N., Khaleque, H., Santala, V., Carlson, R., & Kaksonen, A. (2018). In a quest for engineering acidophiles for biomining applications: challenges and opportunities. *Genes*, *9*(2), 116.

<https://doi.org/10.3390/genes9020116>

Gupta, V. K., Schmoll, M., Herrera-Estrella, A., Upadhyay, R. S., Druzhinina, I., & Tuohy, M.-G. (Eds.). (2014). *Biotechnology and Biology of Trichoderma* (1st edition). Elsevier.

<https://doi.org/10.1016/C2012-0-00434-6>

H

Han, Y., Ma, X., Zhao, W., Chang, Y., Zhang, X., Wang, X., Wang, J., & Huang, Z. (2013). Sulfur-oxidizing bacteria dominate the microbial diversity shift during the pyrite and low-grade pyrolusite bioleaching process. *Journal of Bioscience and Bioengineering*, *116*(4), 465–471. <https://doi.org/10.1016/j.jbiosc.2013.04.012>

Hane, J. K., Anderson, J. P., Williams, A. H., Sperschneider, J., & Singh, K. B. (2014). Genome Sequencing and Comparative Genomics of the Broad Host-Range Pathogen *Rhizoctonia solani* AG8. *PLoS Genetics*, *10*(5), e1004281. <https://doi.org/10.1371/journal.pgen.1004281>

Haneklaus, N., Bayok, A., & Fedchenko, V. (2017). Phosphate Rocks and Nuclear Proliferation. *Science & Global Security*, *25*(3), 143–158.

<https://doi.org/10.1080/08929882.2017.1394061>

Havliš, J., Thomas, H., Šebela, M., & Shevchenko, A. (2003). Fast-response proteomics by accelerated in-gel digestion of proteins. *Analytical Chemistry*, *75*(6), 1300–1306. <https://doi.org/10.1021/ac026136s>

Hopwood, D. ., Kieser, T., Bibb, M. J., Buttner, M. J., & Chater, K. F. (2000). *Practical Streptomyces genetics* (1st edition). John Innes Foundation.

Horeh, N. B., Mousavi, S. M., & Shojaosadati, S. A. (2016). Bioleaching of valuable metals from spent lithium-ion mobile phone batteries using *Aspergillus niger*. *Journal of Power Sources*, *320*, 257–266.

<https://doi.org/10.1016/j.jpowsour.2016.04.104>

Huang, Z., Cheng, C., Liu, Z., Zeng, H., Feng, B., Zhong, H., Luo, W., Hu, Y., Guo, Z., He, G., & Fu, W. (2019). Utilization of a new Gemini surfactant as the collector for the reverse froth flotation of phosphate ore in sustainable production of phosphate fertilizer. *Journal of Cleaner Production*, *221*, 108–112. <https://doi.org/10.1016/j.jclepro.2019.02.251>

Huber, B., Herzog, B., Drewes, J. E., Koch, K., & Müller, E. (2016). Characterization of sulfur oxidizing bacteria related to biogenic sulfuric acid corrosion in sludge digesters. *BMC Microbiology*, *16*(1), 153. <https://doi.org/10.1186/s12866-016-0767-7>

I

IHS market:

<https://ihsmarkit.com/products/sulphur-chemical-economics-handbook.html>

J

Jami, M.-S., Barreiro, C., García-Estrada, C., & Martín, J.-F. (2010). Proteome Analysis of the Penicillin Producer *Penicillium chrysogenum*. *Molecular & Cellular Proteomics*, *9*(6), 1182–1198. <https://doi.org/10.1074/mcp.M900327-MCP200>

Jerez, C. A. (2017a). Bioleaching and Biomining for the Industrial Recovery of Metals. In *Reference Module in Life Sciences*. Elsevier. <https://doi.org/10.1016/B978-0-12-809633-8.09185-8>

Jerez, C. A. (2017b). Biomining of metals: how to access and exploit natural resource sustainably. *Microbial Biotechnology*, *10*(5), 1191–1193. <https://doi.org/10.1111/1751-7915.12792>

- Jha, P., & Kumar, A. (2009). Characterization of Novel Plant Growth Promoting Endophytic Bacterium *Achromobacter xylosoxidans* from Wheat Plant. *Microbial Ecology*, 58(1), 179–188. <https://doi.org/10.1007/s00248-009-9485-0>
- Johnson. (2009). Extremophiles: Acidic Environments. In M. Schaechter (Ed.), *Encyclopedia of Microbiology* (3rd edition). Elsevier. <https://doi.org/10.1016/B978-012373944-5.00278-9>
- Johnson. (2014). Biomining—biotechnologies for extracting and recovering metals from ores and waste materials. *Current Opinion in Biotechnology*, 30, 24–31. <https://doi.org/10.1016/j.copbio.2014.04.008>
- Johnson, D. B. (1995). Selective solid media for isolating and enumerating acidophilic bacteria. *Journal of Microbiological Methods*, 23(2), 205–218. [https://doi.org/10.1016/0167-7012\(95\)00015-D](https://doi.org/10.1016/0167-7012(95)00015-D)
- Johnson, & Quatrini, R. (2016). Acidophile Microbiology in Space and Time. In *Acidophiles: Life in Extremely Acidic Environments* (pp. 3–16). Caister Academic Press. <https://doi.org/10.21775/9781910190333.01>
- Jönander, C., & Dahllöf, I. (2020). Short and long-term effects of low-sulphur fuels on marine zooplankton communities. *Aquatic Toxicology (Amsterdam, Netherlands)*, 227, 105592. <https://doi.org/10.1016/j.aquatox.2020.105592>
- Jorquera, M. A., Gabler, S., Inostroza, N. G., Acuña, J. J., Campos, M. A., Menezes-blackburn, D., & Greiner, R. (2018). Screening and Characterization of Phytases from Bacteria Isolated from Chilean Hydrothermal Environments. *Microbial Ecology* 387–399. <https://doi.org/10.1007/s00248-017-1057-0>
- Kalsi, H. K., Singh, R., Dhaliwal, H. S., & Kumar, V. (2016). Phytases from Enterobacter and Serratia species with desirable characteristics for food and feed applications. *Biotech*, 6(1), 64. <https://doi.org/10.1007/s13205-016-0378-x>
- Kang, S. M., Radhakrishnan, R., You, Y. H., Joo, G. J., Lee, I. J., Lee, K. E., & Kim, J. H. (2014). Phosphate Solubilizing *Bacillus megaterium* mj1212 Regulates Endogenous Plant Carbohydrates and Amino Acids Contents to Promote Mustard Plant Growth. *Indian Journal of Microbiology*, 54(4), 427–433. <https://doi.org/10.1007/s12088-014-0476-6>
- Kantas, D., Papatsiros, V. G., Tassis, P. D., Giavasis, I., Bouki, P., & Tzika, E. D. (2015). A feed additive containing *Bacillus toyonensis* (Toyocerin) protects against enteric pathogens in postweaning piglets. *Journal of Applied Microbiology*, 118(3), 727–738. <https://doi.org/10.1111/jam.12729>
- Kaur, M., Jangra, M., Singh, H., Tambat, R., Singh, N., Jachak, S. M., Mishra, S., Sharma, C., Nandanwar, H., & Pinnaka, A. K. (2019). Pseudomonas koreensis Recovered From Raw Yak Milk Synthesizes a β -Carboline Derivative With Antimicrobial Properties. *Frontiers in Microbiology*, 10. <https://doi.org/10.3389/fmicb.2019.01728>
- Keckler, K. P., Corma, A., Knox, T., Greenough, P., & Hodges, M. G. (2009). *Process for removal of sulfur from components for blending of transportation fuels* (Patent No. US 7,473,349 B2).
- Khan, M. S., Zaidi, A., & Wani, P. A. (2007). Role of phosphate-solubilizing microorganisms in sustainable agriculture — A review. *Agronomy for Sustainable Development*, 27(1), 29–43. <https://doi.org/10.1051/agro:2006011>

Khan, N., Bano, A. M. D., & Babar, A. (2020). Impacts of plant growth promoters and plant growth regulators on rainfed agriculture. In *PLoS ONE* (Vol. 15, Issue 4). <https://doi.org/10.1371/journal.pone.0231426>

Khande, R., Sharma, S. K., Ramesh, A., & Sharma, M. P. (2017). Zinc solubilizing *Bacillus* strains that modulate growth, yield and zinc biofortification of soybean and wheat. *Rhizosphere*, 4, 126–138. <https://doi.org/10.1016/j.rhisph.2017.09.002>

Kogel, J. E., Trivedi, N. C., Barker, J. M., & Krukowski, S. T. (Eds.). (2009). *Industrial minerals and rocks: commodities, markets, and uses*. (7th edition). Society for Mining, Metallurgy, and Exploration, Inc.

Konishi, Y., Asai, S., & Yoshida, N. (1995). Growth Kinetics of *Thiobacillus thiooxidans* on the Surface of Elemental Sulfur. *Applied and Environmental Microbiology*, 61(10), 3617–3622. <https://doi.org/10.1128/aem.61.10.3617-3622.1995>

Krey, T., Caus, M., Baum, C., Ruppel, S., & Eichler-Löbermann, B. (2011). Interactive effects of plant growth-promoting rhizobacteria and organic fertilization on P nutrition of *Zea mays* L. and *Brassica napus* L. *Journal of Plant Nutrition and Soil Science*, 174(4), 602–613. <https://doi.org/10.1002/jpln.200900349>

Krulwich, T. A., Sachs, G., & Padan, E. (2011). Molecular aspects of bacterial pH sensing and homeostasis. *Nature Reviews Microbiology*, 9(5), 330–343. <https://doi.org/10.1038/nrmicro2549>

Kumar, P., Chamoli, S., & Agrawal, S. (2012). Enhanced phytase production from *Achromobacter* sp. PB-01 using wheat bran as substrate: prospective application for animal feed. *Biotechnology Progress*, 28(6), 1432–1442. <https://doi.org/10.1002/btpr.1622>

Kumar, V., Singh, P., Jorquera, M. A., Sangwan, P., Kumar, P., Verma, A. K., & Agrawal, S. (2013). Isolation of phytase-producing bacteria from Himalayan soils and their effect on growth and phosphorus uptake of Indian mustard (*Brassica juncea*). *World Journal of Microbiology and Biotechnology*, 29(8), 1361–1369. <https://doi.org/10.1007/s11274-013-1299-z>

Ľ

Laemmli, U. K. (1970). Cleavage of structural proteins during the assembly of the head of bacteriophage T4. *Nature*, 227(5259), 680–685. <https://doi.org/10.1038/227680a0>

Lastochkina, O., Baymiev, A., Shayahmetova, A., Garshina, D., Koryakov, I., Shpirnaya, I., Pusenkova, L., Mardanshin, I., Kasnak, C., & Palamutoglu, R. (2020). Effects of Endophytic *Bacillus Subtilis* and Salicylic Acid on Postharvest Diseases (*Phytophthora infestans*, *Fusarium oxysporum*) Development in Stored Potato Tubers. *Plants*, 9(1), 76. <https://doi.org/10.3390/plants9010076>

Lebrazi, S., Niehaus, K., Bednarz, H., Fadil, M., Chraibi, M., & Fikri-Benbrahim, K. (2020). Screening and optimization of indole-3-acetic acid production and phosphate solubilization by rhizobacterial strains isolated from *Acacia cyanophylla* root nodules and their effects on its plant growth. *Journal of Genetic Engineering and Biotechnology*, 18(1), 71. <https://doi.org/10.1186/s43141-020-00090-2>

Lehtovirta-Morley, L. E., Ge, C., Ross, J., Yao, H., Nicol, G. W., & Prosser, J. I. (2014). Characterisation of terrestrial acidophilic archaeal ammonia oxidisers and their inhibition and stimulation by organic compounds. *FEMS Microbiology Ecology*, 89(3), 542–552. <https://doi.org/10.1111/1574-6941.12353>

Li, J., & Marschner, P. (2019). Phosphorus Pools and Plant Uptake in Manure-Amended Soil. *Journal of Soil Science and Plant Nutrition*, 19(1), 175–186. <https://doi.org/10.1007/s42729-019-00025-y>

Li, Li, Q., Wang, Z., Ji, G., Zhao, H., Gao, F., Su, M., Jiao, J., Li, Z., & Li, H. (2019). Environmental fungi and bacteria facilitate lecithin decomposition and the transformation of phosphorus to apatite. *Scientific Reports*, 9(1), 15291. <https://doi.org/10.1038/s41598-019-51804-7>

Li, X., Mercado, R., Kernan, T., West, A. C., & Banta, S. (2014). Addition of citrate to *Acidithiobacillus ferrooxidans* cultures enables precipitate-free growth at elevated pH and reduces ferric inhibition. *Biotechnology and Bioengineering*, 111(10), 1940–1948. <https://doi.org/10.1002/bit.25268>

Liska, A. J., & Shevchenko, A. (2003). Expanding the organismal scope of proteomics: Cross-species protein identification by mass spectrometry and its implications. *PROTEOMICS*, 3(1), 19–28. <https://doi.org/10.1002/pmic.200390004>

Liu, J., Wu, W., Zhang, X., Zhu, M., & Tan, W. (2017). Adhesion properties of and factors influencing *Leptospirillum ferriphilum* in the biooxidation of refractory gold-bearing pyrite. *International Journal of Mineral Processing*, 160, 39–46. <https://doi.org/10.1016/j.minpro.2017.01.001>

Liu, Y., Wang, J., Hou, H., Chen, G., Liu, H., Liu, X., & Shen, L. (2020). Effect of Introduction of Exogenous Strain *Acidithiobacillus thiooxidans* A01 on Structure and Function of Adsorbed and Planktonic Microbial Consortia During Bioleaching of Low-Grade Copper Sulfide. *Frontiers in Microbiology*, 10. <https://doi.org/10.3389/fmicb.2019.03034>

Liu, Z. L., & Sinclair, B. (1993). Colonization of soybean roots by *Bacillus megaterium* B153-2-2. *Soil Biology and Biochemistry*, 25(7), 849–855.

Lorck, H. (1948). Production of Hydrocyanic Acid by Bacteria. *Physiologia Plantarum*, 1(2), 142–146. <https://doi.org/10.1111/j.1399-3054.1948.tb07118.x>

Lu, C., & Tian, H. (2017). Global nitrogen and phosphorus fertilizer use for agriculture production in the past half century: shifted hot spots and nutrient imbalance. *Earth System Science Data*, 9(1), 181–192. <https://doi.org/10.5194/essd-9-181-2017>

Lu, T., Ke, M., Peijnenburg, W. J. G. M., Zhu, Y., Zhang, M., Sun, L., Fu, Z., & Qian, H. (2018). Investigation of Rhizospheric Microbial Communities in Wheat, Barley, and Two Rice Varieties at the Seedling Stage. *Journal of Agricultural and Food Chemistry*, 66(11), 2645–2653. <https://doi.org/10.1021/acs.jafc.7b06155>

Lutgens, F. K., & Tarbuck, E. J. (2014). *Essentials of geology* (12th ed.). Pearson College Div.

M

Mączik, M., Gryta, A., & Frąc, M. (2020). Biofertilizers in agriculture: An overview on concepts, strategies and effects on soil microorganisms. *Advances in Agronomy*, 31–87. <https://doi.org/10.1016/bs.agron.2020.02.001>

Mardad, I., Serrano, A., & Soukri, A. (2013). Solubilization of inorganic phosphate and production of organic acids by bacteria isolated from a Moroccan mineral phosphate deposit. *African Journal of Microbiology Research*, 7(8), 626–635. <https://doi.org/10.5897/AJMR12.1431>

Marlenne, G.-R., Fernanda, M.-V., & Norma G, R.-A. (2020). *Acidithiobacillus thiooxidans* DSM 26636: An Alternative for the Bioleaching of Metallic Burrs. *Catalysts*, 10(11), 1230. <https://doi.org/10.3390/catal10111230>

- Marsulex Environmental Technologies. (2010). *Sulphur & petroleum coke markets: More important than you might think!* 20. <https://refiningcommunity.com/wp-content/uploads/2017/06/Sulphur-Petroleum-Coke-Markets-More-important-than-you-might-think-Marsulex-DCU-Calgary-2010.pdf>
- Martínez-Moreno, F. (2017). Barley Types and Varieties in Spain: A Historical Overview. *Ciencia e Investigación Agraria*, 44(1), 1–12. <https://doi.org/10.7764/rcia.v44i1.1638>
- Martínez Castro, M. (2011). *Phosphate control of the immunosuppressant tacrolimus biosynthesis in two species of Streptomyces genus*. Tesis Doctoral. Universidad de León.
- Martins da Costa, E., de Lima, W., Oliveira-Longatti, S. M., & de Souza, F. M. (2015). Phosphate-solubilizing bacteria enhance *Oryza sativa* growth and nutrient accumulation in an oxisol fertilized with rock phosphate. *Ecological Engineering*, 83, 380–385. <https://doi.org/10.1016/j.ecoleng.2015.06.045>
- Matin, A. (1990). Keeping a neutral cytoplasm; the bioenergetics of obligate acidophiles. *FEMS Microbiology Letters*, 75(2–3), 307–318. [https://doi.org/10.1016/0378-1097\(90\)90541-W](https://doi.org/10.1016/0378-1097(90)90541-W)
- Méndez-Tovar, M., García-Meza, J. V., & González, I. (2019). Electrochemical monitoring of *Acidithiobacillus thiooxidans* biofilm formation on graphite surface with elemental sulfur. *Bioelectrochemistry*, 128, 30–38. <https://doi.org/10.1016/j.bioelechem.2019.03.004>
- Mihelcic, J. R., Fry, L. M., & Shaw, R. (2011). Global potential of phosphorus recovery from human urine and feces. *Chemosphere*, 84(6), 832–839. <https://doi.org/10.1016/j.chemosphere.2011.02.046>
- Mirete, S., Morgante, V., & González-Pastor, J. E. (2017). Acidophiles: Diversity and mechanisms of adaptation to acidic environments. In H. Stan-Lotter & S. Fendrihan (Eds.), *Adaption of Microbial Life to Environmental Extremes* (2nd edition). Springer International Publishing. <https://doi.org/10.1007/978-3-319-48327-6>
- Mukhtar, S., Shahid, I., Mehnaz, S., & Malik, K.A. (2017). Assessment of two carrier materials for phosphate solubilizing biofertilizers and their effect on growth of wheat (*Triticum aestivum* L.). *Microbiological Research*, 205(May), 107–117. <https://doi.org/10.1016/j.micres.2017.08.011>
- Mumtaz, M. Z., Ahmad, M., Jamil, M., & Hussain, T. (2017). Zinc solubilizing *Bacillus* spp. potential candidates for biofortification in maize. *Microbiological Research*, 202, 51–60. <https://doi.org/10.1016/j.micres.2017.06.001>
- Mykhalska, L. M., Zozulia, O. L., Hrytsev, O. A., Sanin, O. Y., & Schwartau, V. V. (2019). Distribution of species of *Fusarium* and *Alternaria* genera on cereals in Ukraine. *Biosystems Diversity*, 27(2), 186–191. <https://doi.org/10.15421/011925>
- Mykytczuk, N. C. S., Trevors, J. T., Ferroni, G. D., & Leduc, L. G. (2010). Cytoplasmic membrane fluidity and fatty acid composition of *Acidithiobacillus ferrooxidans* in response to pH stress. *Extremophiles*, 14(5), 427–441. <https://doi.org/10.1007/s00792-010-0319-2>
- Mykytczuk, N. C. S., Trevors, J. T., Ferroni, G. D., & Leduc, L. G. (2011). Cytoplasmic membrane response to copper and nickel in *Acidithiobacillus ferrooxidans*. *Microbiological Research*, 166(3), 186–206. <https://doi.org/10.1016/j.micres.2010.03.004>

Nascimento, F. X., Hernández, A. G., Glick, B. R., & Rossi, M. J. (2020). Plant growth-promoting activities and genomic analysis of the stress-resistant *Bacillus megaterium* STB1, a bacterium of agricultural and biotechnological interest. *Biotechnology Reports*, 25, e00406. <https://doi.org/10.1016/j.btre.2019.e00406>

Naseri, T., Bahaloo-Horeh, N., & Mousavi, S. M. (2019). Environmentally friendly recovery of valuable metals from spent coin cells through two-step bioleaching using *Acidithiobacillus thiooxidans*. *Journal of Environmental Management*, 235, 357–367. <https://doi.org/10.1016/j.jenvman.2019.01.086>

Nassiri, M., & Ariannejad, H. (2015). Comparative Analysis of Peripheral Alkaline Phytase Protein Structures Expressed in *E. coli*. *Reports of Biochemistry & Molecular Biology*, 4(1), 10–18. <http://www.ncbi.nlm.nih.gov/pubmed/26989745>

Negishi, A., Muraoka, T., Maeda, T., Takeuchi, F., Kanao, T., Kamimura, K., & Sugio, T. (2005). Growth inhibition by tungsten in the sulfur-oxidizing bacterium *Acidithiobacillus thiooxidans*. *Bioscience, Biotechnology and Biochemistry*, 69(11), 2073–2080. <https://doi.org/10.1271/bbb.69.2073>

Ngatia, L., & Taylor, R. (2019). Phosphorus Eutrophication and Mitigation Strategies. *Phosphorus - Recovery and Recycling*. <https://doi.org/10.5772/intechopen.79173>

Nguyen, Ha, M.-G., Shin, S., Seo, M., Jang, J., Jo, S., Kim, D., Lee, S., Jung, Y., Kang, P., Shin, C., & Ahn, Y. (2018). Electrochemical effect on bioleaching of arsenic and manganese from tungsten mine wastes using *Acidithiobacillus* spp. *Journal of Environmental Management*, 223, 852–859. <https://doi.org/10.1016/j.jenvman.2018.06.040>

Nguyen, T. A., Fu, C. C., & Juang, R. S. (2016). Biosorption and biodegradation of a sulfur dye in high-strength dyeing wastewater by *Acidithiobacillus thiooxidans*. *Journal of Environmental Management*, 182, 265–271. <https://doi.org/10.1016/j.jenvman.2016.07.083>

Nuñez, H., Moya-Beltrán, A., Covarrubias, P. C., Issotta, F., Cárdenas, J. P., González, M., Atavales, J., Acuña, L. G., Johnson, D. B., & Quatrini, R. (2017). Molecular Systematics of the Genus *Acidithiobacillus*: Insights into the Phylogenetic Structure and Diversification of the Taxon. *Frontiers in Microbiology*, 8. <https://doi.org/10.3389/fmicb.2017.00030>

O

Ohtake, H., & Tsuneda, S. (Eds.). (2019). *Phosphorus Recovery and Recycling*. Springer Singapore. <https://doi.org/10.1007/978-981-10-8031-9>

Okibe, N., & Johnson, D. B. (2004). Biooxidation of pyrite by defined mixed cultures of moderately thermophilic acidophiles in pH-controlled bioreactors: Significance of microbial interactions. *Biotechnology and Bioengineering*, 87(5), 574–583. <https://doi.org/10.1002/bit.20138>

Ortíz-Castro, R., Valencia-Cantero, E., & López-Bucio, J. (2008). Plant growth promotion by *Bacillus megaterium* involves cytokinin signaling. *Plant Signaling & Behavior*, 3(4), 263–265. <https://doi.org/10.4161/psb.3.4.5204>

Overbeek, R., Olson, R., Pusch, G. D., Olsen, G. J., Davis, J. J., Disz, T., Edwards, R. A., Gerdes, S., Parrello, B., Shukla, M., Vonstein, V., Wattam, A. R., Xia, F., & Stevens, R. (2014). The SEED and the Rapid Annotation of microbial genomes using Subsystems Technology (RAST). *Nucleic Acids Research*, 42(D1), D206–D214. <https://doi.org/10.1093/nar/gkt1226>

P

Pastor-Bueis, R., Mulas, R., Gómez, X., & González-Andrés, F. (2017). Innovative liquid formulation of digestates for producing a biofertilizer based on *Bacillus siamensis*: Field testing on sweet pepper. *Journal of Plant Nutrition and Soil Science*, *180*(6), 748–758. <https://doi.org/10.1002/jpln.201700200>

Peace, T. A., Brock, K. V., & Stills, H. F. (1994). Comparative analysis of the 16S rRNA gene sequence of the putative agent of proliferative ileitis of hamsters. *International Journal of Systematic Bacteriology*, *44*(4), 832–835. <https://doi.org/10.1099/00207713-44-4-832>

Penn, C., & Camberato, J. (2019). A Critical Review on Soil Chemical Processes that Control How Soil pH Affects Phosphorus Availability to Plants. *Agriculture*, *9*(6), 120. <https://doi.org/10.3390/agriculture9060120>

Q

Qin, G., Liu, Z., & Xie, L. (2021). Multiple Omics Data Integration. In *Systems Medicine* (pp. 103–115). Elsevier. <https://doi.org/10.1016/B978-0-12-801238-3.11508-9>

Qu, Q., Zhang, Z., Peijnenburg, W. J. G. M., Liu, W., Lu, T., Hu, B., Chen, J., Chen, J., Lin, Z., & Qian, H. (2020). Rhizosphere Microbiome Assembly and Its Impact on Plant Growth. *Journal of Agricultural and Food Chemistry*, *68*(18), 5024–5038. <https://doi.org/10.1021/acs.jafc.0c00073>

Quatrini, R., & Johnson, D. B. (2018). Microbiomes in extremely acidic environments: functionalities and interactions that allow survival and growth of prokaryotes at low pH. *Current Opinion in Microbiology*, *43*, 139–147. <https://doi.org/10.1016/j.mib.2018.01.011>

R

Rafikova, G. F., Korshunova, T. Y., Minnebaev, L. F., Chetverikov, S. P., & Loginov, O. N. (2016). A new bacterial strain, *Pseudomonas koreensis* IB-4, as a promising agent for plant pathogen biological control. *Microbiology*, *85*(3), 333–341. <https://doi.org/10.1134/S0026261716030115>

Ramírez, C. A., & Kloepper, J. W. (2010). Plant growth promotion by *Bacillus amyloliquefaciens* FZB45 depends on inoculum rate and P-related soil properties. *Biology and Fertility of Soils*, *46*(8), 835–844. <https://doi.org/10.1007/s00374-010-0488-2>

Rana, K., Rana, N., & Singh, B. (2020). Applications of sulfur oxidizing bacteria. In *Physiological and Biotechnological Aspects of Extremophiles* (pp. 131–136). Elsevier. <https://doi.org/10.1016/B978-0-12-818322-9.00010-1>

Reta, G., Dong, X., Li, Z., Su, B., Hu, X., Bo, H., Yu, D., Wan, H., Liu, J., Li, Y., Xu, G., Wang, K., & Xu, S. (2018). Environmental impact of phosphate mining and beneficiation: review. *International Journal of Hydrology*, *2*(4). <https://doi.org/10.15406/ijh.2018.02.00106>

Rigaud, J., & Puppo, A. (1975). Indole-3-acetic acid catabolism by soybean bacteroids. *Journal of General Microbiology*, *88*(2), 223–228. <https://doi.org/10.1099/00221287-88-2-223>

Rijavec, T., & Lapanje, A. (2016). Hydrogen Cyanide in the Rhizosphere: Not Suppressing Plant Pathogens, but Rather Regulating Availability of Phosphate. *Frontiers in Microbiology*, *7*. <https://doi.org/10.3389/fmicb.2016.01785>

Roncarati, D., & Scarlato, V. (2017). Regulation of heat-shock genes in bacteria: from signal sensing to gene expression output. *FEMS Microbiology Reviews*, *41*(4), 549–574. <https://doi.org/10.1093/femsre/fux015>

Ruttenberg, K. C. (2003). The Global Phosphorus Cycle. In *Treatise on Geochemistry* (pp. 585–643). Elsevier. <https://doi.org/10.1016/B0-08-043751-6/08153-6>

S

Salwan, R., & Sharma, V. (2020). Overview of extremophiles. In *Physiological and Biotechnological Aspects of Extremophiles* (pp. 3–11). Elsevier. <https://doi.org/10.1016/B978-0-12-818322-9.00001-0>

Sambrook, J., Rusell, D. W., & Joseph Sambrook, D. W. R. (2001). *Molecular cloning: a laboratory manual* (3th ed.). Cold Spring Harbor Laboratory Press.

Santos, M. S., Nogueira, M. A., & Hungria, M. (2019). Microbial inoculants: reviewing the past, discussing the present and previewing an outstanding future for the use of beneficial bacteria in agriculture. *AMB Express*, *9*(1). <https://doi.org/10.1186/s13568-019-0932-0>

Sasirekha, B., & Srividya, S. (2016). Siderophore production by *Pseudomonas aeruginosa* FP6, a biocontrol strain for *Rhizoctonia solani* and *Colletotrichum gloeosporioides* causing diseases in chilli. *Agriculture and Natural Resources*, *50*(4), 250–256. <https://doi.org/10.1016/j.anres.2016.02.003>

Saxena, A. K., Kumar, M., Chakdar, H., Anuroopa, N., & Bagyaraj, D. J. (2019). *Bacillus* species in soil as a natural resource for plant health and nutrition. *Journal of Applied Microbiology*, 1–12. <https://doi.org/10.1111/jam.14506>

Schachtman, D. P., Reid, R. J., & Ayling, S. M. (1998). Phosphorus Uptake by Plants: From Soil to Cell. *Plant Physiology*, *116*(2), 447–453. <https://doi.org/10.1104/pp.116.2.447>

Schippers, A., Hedrich, S., Vasters, J., Drobe, M., Sand, W., & Willscher, S. (2013). *Bio-mining: Metal Recovery from Ores with Microorganisms* (pp. 1–47). https://doi.org/10.1007/10_2013_216

Sharma, P., K. C. Kumawat, K. C. K., Kaur, S., & Kaur, N. (2011). Assessment of Zinc solubilization by Endophytic Bacteria in Legume Rhizosphere. *Indian Journal of Applied Research*, *4*(6), 439–441. <https://doi.org/10.15373/2249555X/June2014/137>

Sharma, Sayyed, R. Z., Trivedi, M. H., & Gobi, T. A. (2013). Phosphate solubilizing microbes: sustainable approach for managing phosphorus deficiency in agricultural soils. *SpringerPlus*, *2*, 587. <https://doi.org/10.1186/2193-1801-2-587>

Shirling, E. B., & Gottlieb, D. (1966). Methods for characterization of *Streptomyces* species. *International Journal of Systematic Bacteriology*, *16*(3), 313–340. <https://doi.org/10.1099/00207713-16-3-313>

Singh, B., & Satyanarayana, T. (2011). Microbial phytases in phosphorus acquisition and plant growth promotion. *Physiology and Molecular Biology of Plants*, *17*(2), 93–103. <https://doi.org/10.1007/s12298-011-0062-x>

Singh, P., Kumar, V., & Agrawal, S. (2014). Evaluation of phytase producing bacteria for their plant growth promoting activities. *International Journal of Microbiology*, *2014*, 1–7. <https://doi.org/10.1155/2014/426483>

Smith, F. W. (2002). The phosphate uptake mechanism. *Plant and Soil*, *245*(1), 105–114. <https://doi.org/10.1023/A:1020660023284>

Song, H., Huff, J., Janik, K., Walter, K., Keller, C., Ehlers, S., Bossmann, S. H., & Niederweis, M. (2011). Expression of the ompATb operon accelerates ammonia secretion and adaptation of *Mycobacterium tuberculosis* to acidic environments. *Molecular Microbiology*, *80*(4), 900–918. <https://doi.org/10.1111/j.1365-2958.2011.07619.x>

Southern, E. M. (1975). Detection of specific sequences among DNA fragments separated by gel electrophoresis. *Journal of Molecular Biology*, *98*(3), 503–517.

Srivastava, N., Gupta, B., Gupta, S., Danquah, M. K., & Sarethy, I. P. (2019). Analyzing Functional Microbial Diversity. In *Microbial Diversity in the Genomic Era* (pp. 79–102). Elsevier. <https://doi.org/10.1016/B978-0-12-814849-5.00006-X>

Srivastava, S., & Srivastava, S. (2020). Prescience of endogenous regulation in *Arabidopsis thaliana* by *Pseudomonas putida* MTCC 5279 under phosphate starved salinity stress condition. *Scientific Reports*, *10*(1), 5855. <https://doi.org/10.1038/s41598-020-62725-1>

Starosvetsky, J., Zukerman, U., & Armon, R. H. (2013). A simple medium modification for isolation, growth and enumeration of *Acidithiobacillus thiooxidans* (syn. *Thiobacillus thiooxidans*) from water samples. *Journal of Microbiological Methods*, *92*(2), 178–182. <https://doi.org/10.1016/j.mimet.2012.11.009>

Steinberg, T. H. (2009). Protein Gel Staining Methods. In R. R. Burgess & M. P. Deutscher (Eds.), *Methods Enzymol* (1st edition). Elsevier Inc. [https://doi.org/10.1016/S0076-6879\(09\)63031-7](https://doi.org/10.1016/S0076-6879(09)63031-7)

Steiner, G., Geissler, B., Watson, I., & Mew, M. C. (2015). Efficiency developments in phosphate rock mining over the last three decades. *Resources, Conservation and Recycling*, *105*, 235–245. <https://doi.org/10.1016/j.resconrec.2015.10.004>

Stoyanova, M., & Bogaevska, N. (2015). *Pseudomonas fluorescens* – a primary and secondary pathogen of bulbous plants. *Science and Technologies*, *6*.

Suleimanova, A. D., Beinhauer, A., Valeeva, L. R., Chastukhina, I. B., Balaban, N. P., Shakirov, E. V., Greiner, R., & Sharipova, M. R. (2015). Novel Glucose-1-Phosphatase with High Phytase Activity and Unusual Metal Ion Activation from Soil Bacterium *Pantoea* sp. Strain 3.5.1. *Applied and Environmental Microbiology*, *81*(19), 6790–6799. <https://doi.org/10.1128/AEM.01384-15>

Suleimanova, A. D., Toymontseva, A. A., Boulygina, E. A., Kazakov, S. V., Mardanova, A. M., Balaban, N. P., & Sharipova, M. R. (2015). High-quality draft genome sequence of a new phytase-producing microorganism *Pantoea* sp. 3.5.1. *Standards in Genomic Sciences*, *10*(1), 95. <https://doi.org/10.1186/s40793-015-0093-y>

Sun, F., Ou, Q., Wang, N., Guo, Z. xuan, Ou, Y., Li, N., & Peng, C. (2020). Isolation and identification of potassium-solubilizing bacteria from *Mikania micrantha* rhizospheric soil and their effect on *M. micrantha* plants. *Global Ecology and Conservation*, *23*, e01141. <https://doi.org/10.1016/j.gecco.2020.e01141>

T

Taner, A., Muzaffer, A., & Fazil, D. (2004). Barley: Post-harvest Operations. In *Food and Agriculture Organization of the United Nations*. <http://www.fao.org/3/a-au997e.pdf>

Tang, D.-J., He, Y.-Q., Feng, J.-X., He, B.-R., Jiang, B.-L., Lu, G.-T., Chen, B., & Tang, J.-L. (2005). *Xanthomonas campestris* pv. *campestris* Possesses a Single Gluconeogenic Pathway That Is Required for Virulence. *Journal of Bacteriology*, *187*(17), 6231–6237. <https://doi.org/10.1128/JB.187.17.6231-6237.2005>

Thuynsma, R., Kleinert, A., Kossmann, J., Valentine, A. J., & Hills, P. N. (2016). The effects of limiting phosphate on photosynthesis and growth of *Lotus japonicus*. *South African Journal of Botany*, *104*, 244–248. <https://doi.org/10.1016/j.sajb.2016.03.001>

Travisany, D., Cortés, M. P., Latorre, M., Di Genova, A., Budinich, M., Bobadilla-Fazzini, R. A., Parada, P., González, M., & Maass, A. (2014). A new genome of *Acidithiobacillus thiooxidans* provides insights into adaptation to a bioleaching environment. *Research in Microbiology*, 165(9), 743–752. <https://doi.org/10.1016/j.resmic.2014.08.004>

Trivedi, P., & Pandey, A. (2008). Plant growth promotion abilities and formulation of *Bacillus megaterium* strain B 388 (MTCC6521) isolated from a temperate Himalayan location. *Indian Journal of Microbiology*, 48(3), 342–347. <https://doi.org/10.1007/s12088-008-0042-1>

V

U.S. Geological Survey. (2020). *Mineral Commodity Summaries*. <https://doi.org/10.3133/mcs2020>

V

Vejan, P., Abdullah, R., Khadiran, T., Ismail, S., & Nasrulhaq Boyce, A. (2016). Role of Plant Growth Promoting Rhizobacteria in Agricultural Sustainability—A Review. *Molecules*, 21(5), 573. <https://doi.org/10.3390/molecules21050573>

Vindeirinho, J. M., Soares, H. M. V. M., & Soares, E. V. (2021). Modulation of Siderophore Production by *Pseudomonas fluorescens* Through the Manipulation of the Culture Medium Composition. *Applied Biochemistry and Biotechnology*, 193(3), 607–618. <https://doi.org/10.1007/s12010-020-03349-z>

Vos, P. de, Garrity, G. M., Jones, D., Krieg, N. R., Ludwig, W., Rainey, F., Schleifer, K.-H., & Whitman, W. B. (2011). *Bergey's manual of Systematic Bacteriology: Volume Three. The Firmicutes*. In W. B. Whitman (Ed.), *International Journal of Pediatric Otorhinolaryngology* (2nd edition, Vol. 75, Issue 9). <https://doi.org/10.1016/j.ijporl.2011.05.009>

W

Waksman, S. A., & Joffe, J. S. (1922). Microorganisms concerned in the oxidation of sulfur in the soil II. *Thiobacillus thiooxidans*, a new sulfur-oxidizing organism isolated from the soil. *Journal of Bacteriology*, 7(2), 239–256. <https://doi.org/10.1128/JB.7.2.239-256.1922>

Walker, T. S., Bais, H. P., Déziel, E., Schweizer, H. P., Rahme, L. G., Fall, R., & Vivanco, J. M. (2004). *Pseudomonas aeruginosa* -Plant Root Interactions. Pathogenicity, Biofilm Formation, and Root Exudation. *Plant Physiology*, 134(1), 320–331. <https://doi.org/10.1104/pp.103.027888>

Wang, H., Zhang, X., Zhu, M., & Tan, W. (2015). Effects of dissolved oxygen and carbon dioxide under oxygen-rich conditions on the biooxidation process of refractory gold concentrate and the microbial community. *Minerals Engineering*, 80, 37–44. <https://doi.org/10.1016/j.mineng.2015.06.016>

Wang, Lin, J.-Q., Liu, X.-M., Pang, X., Zhang, C.-J., Yang, C.-L., Gao, X.-Y., Lin, C.-M., Li, Y.-Q., Li, Y., Lin, J.-Q., & Chen, L.-X. (2019). Sulfur Oxidation in the Acidophilic Autotrophic *Acidithiobacillus* spp. *Frontiers in Microbiology*, 9. <https://doi.org/10.3389/fmicb.2018.03290>

Wang, X., Ma, L., Wu, J., Xiao, Y., Tao, J., & Liu, X. (2020). Effective bioleaching of low-grade copper ores: Insights from microbial cross experiments. *Bioresource Technology*, 308, 123273. <https://doi.org/10.1016/j.biortech.2020.123273>

Warren, J. K. (2016). *Evaporites: A Geological Compendium* (2nd ed.). Springer International Publishing. <https://doi.org/10.1007/978-3-319-13512-0>

Watanabe, F. S., & Olsen, S. R. (1965). Test of an ascorbic acid method for determining phosphorus in water and NaHCO₃ extracts from soil. *Soil Science Society of America Journal*, 29(6), 677. <https://doi.org/10.2136/sssaj1965.03615995002900060025x>

Wegulo, S. N., Baenziger, P. S., Hernandez Nopsa, J., Bockus, W. W., & Hallen-Adams, H. (2015). Management of *Fusarium* head blight of wheat and barley. *Crop Protection*, *73*, 100–107. <https://doi.org/10.1016/j.cropro.2015.02.025>

Wei, X., Liu, D., Liao, L., Wang, Z., Li, W., & Huang, W. (2018). Bioleaching of heavy metals from pig manure with indigenous sulfur-oxidizing bacteria: effects of sulfur concentration. *Heliyon*, *4*(9), e00778. <https://doi.org/10.1016/j.heliyon.2018.e00778>

Wei, Zhao, Y., Shi, M., Cao, Z., Lu, Q., Yang, T., Fan, Y., & Wei, Z. (2018). Effect of organic acids production and bacterial community on the possible mechanism of phosphorus solubilization during composting with enriched phosphate-solubilizing bacteria inoculation. *Bioresource Technology*, *247*(September 2017), 190–199. <https://doi.org/10.1016/j.biortech.2017.09.092>

Wilhelm, J., Pingoud, A., & Hahn, M. (2003). Real-time PCR-based method for the estimation of genome sizes. *Nucleic Acids Research*, *31*(10), e56. <https://doi.org/10.1093/nar/gng056>

Williams, K. P., Gillespie, J. J., Sobral, B. W. S., Nordberg, E. K., Snyder, E. E., Shallom, J. M., & Dickerman, A. W. (2010). Phylogeny of Gammaproteobacteria. *Journal of Bacteriology*, *192*(9), 2305–2314. <https://doi.org/10.1128/JB.01480-09>

Williams, K. P., & Kelly, D. P. (2013). Proposal for a new class within the phylum Proteobacteria, *Acidithiobacillia* classis nov., with the type order *Acidithiobacillales*, and emended description of the class Gammaproteobacteria. *International Journal of Systematic and Evolutionary Microbiology*, *63*(Pt_8), 2901–2906. <https://doi.org/10.1099/ijs.0.049270-0>

Woo, K.-S., Choi, J.-L., Kim, B.-R., Kim, J.-E., Kim, K.-H., Kim, J.-M., & Han, J.-Y. (2014). Outbreak of *Pseudomonas oryzae* Pseudobacteremia Related to Contaminated Equipment in an Emergency Room of a Tertiary Hospital in Korea. *Infection & Chemotherapy*, *46*(1), 42. <https://doi.org/10.3947/ic.2014.46.1.42>

Wu, S. C., Cao, Z. H., Li, Z. G., Cheung, K. C., & Wong, M. H. (2005). Effects of biofertilizer containing N-fixer, P and K solubilizers and AM fungi on maize growth: a greenhouse trial. *Geoderma*, *125*(1–2), 155–166. <https://doi.org/10.1016/j.geoderma.2004.07.003>

Wu, W., Liu, X., Zhang, X., Li, X., Qiu, Y., Zhu, M., & Tan, W. (2019). Mechanism underlying the bioleaching process of LiCoO₂ by sulfur-oxidizing and iron-oxidizing bacteria. *Journal of Bioscience and Bioengineering*, *128*(3), 344–354. <https://doi.org/10.1016/j.jbiosc.2019.03.007>

Wübbeler, J. H., Hiessl, S., Schuldes, J., Thürmer, A., Daniel, R., & Steinbüchel, A. (2014). Unravelling the complete genome sequence of *Advenella mimigardefordensis* strain DPN7T and novel insights in the catabolism of the xenobiotic polythioester precursor 3,3'-dithiodipropionate. *Microbiology*, *160*(7), 1401–1416. <https://doi.org/10.1099/mic.0.078279-0>

γ

Yang, M., Mavrodi, D. V., Mavrodi, O. V., Thomashow, L. S., & Weller, D. M. (2020). Exploring the Pathogenicity of *Pseudomonas brassicacearum* Q8r1-96 and Other Strains of the *Pseudomonas fluorescens* Complex on Tomato. *Plant Disease*, *104*(4), 1026–1031. <https://doi.org/10.1094/PDIS-09-19-1989-RE>

Yang, X., Post, W. M., Thornton, P. E., & Jain, A. (2012). The distribution of soil phosphorus for global biogeochemical modeling. *Biogeosciences Discussions*, *9*(11), 16347–16380. <https://doi.org/10.5194/bgd-9-16347-2012>

Yao, Y., Barghava, N., Kim, J., Niederweis, M., & Marassi, F. M. (2012). Molecular Structure and Peptidoglycan Recognition of *Mycobacterium tuberculosis* ArfA (Rv0899). *Journal of Molecular Biology*, *416*(2), 208–220. <https://doi.org/10.1016/j.jmb.2011.12.030>

Ye, Y., Ngo, H. H., Guo, W., Liu, Y., Li, J., Liu, Y., Zhang, X., & Jia, H. (2017). Insight into chemical phosphate recovery from municipal wastewater. *Science of The Total Environment*, *576*, 159–171. <https://doi.org/10.1016/j.scitotenv.2016.10.078>

Yin, Z., Feng, S., Tong, Y., & Yang, H. (2019). Adaptive mechanism of *Acidithiobacillus thiooxidans* CCTCC M 2012104 under stress during bioleaching of low-grade chalcopyrite based on physiological and comparative transcriptomic analysis. *Journal of Industrial Microbiology and Biotechnology*, *46*(12), 1643–1656. <https://doi.org/10.1007/s10295-019-02224-z>

Z

Zangarini, S., Pepè Sciarria, T., Tambone, F., & Adani, F. (2020). Phosphorus removal from livestock effluents: recent technologies and new perspectives on low-cost strategies. *Environmental Science and Pollution Research*. <https://doi.org/10.1007/s11356-019-07542-4>

Zeng, J., Gou, M., Tang, Y.-Q., Li, G.-Y., Sun, Z.-Y., & Kida, K. (2016). Effective bioleaching of chromium in tannery sludge with an enriched sulfur-oxidizing bacterial community. *Bioresource Technology*, *218*, 859–866. <https://doi.org/10.1016/j.biortech.2016.07.051>

Zhang, Jiaen, Feng, L., Ouyang, Y., Hu, R., Xu, H., & Wang, J. (2020). Phosphate-solubilizing bacteria and fungi in relation to phosphorus availability under different land uses for some latosols from Guangdong, China. *CATENA*, *195*, 104686. <https://doi.org/10.1016/j.catena.2020.104686>

Zhang, Jing, Liu, R., Xi, S., Cai, R., Zhang, X., & Sun, C. (2020). A novel bacterial thiosulfate oxidation pathway provides a new clue about the formation of zero-valent sulfur in deep sea. *The ISME Journal*, *14*(9), 2261–2274. <https://doi.org/10.1038/s41396-020-0684-5>

Zhang, X., Liu, Z., Wei, G., Yang, F., & Liu, X. (2018). In Silico Genome-Wide Analysis Reveals the Potential Links Between Core Genome of *Acidithiobacillus thiooxidans* and Its Autotrophic Lifestyle. *Frontiers in Microbiology*, *9*. <https://doi.org/10.3389/fmicb.2018.01255>

Zhang, Y., Yang, Y., Liu, J., & Qiu, G. (2013). Isolation and characterization of *Acidithiobacillus ferrooxidans* strain QXS-1 capable of unusual ferrous iron and sulfur utilization. *Hydrometallurgy*, *136*, 51–57. <https://doi.org/10.1016/j.hydromet.2013.03.005>

Zheng, & Li. (2016). Synergy between *Rhizobium phaseoli* and *Acidithiobacillus ferrooxidans* in the Bioleaching Process of Copper. *BioMed Research International*, *2016*, 1–7. <https://doi.org/10.1155/2016/9384767>

Zheng, X. Y., & Sinclair, B. (2000). The effects of traits of *Bacillus megaterium* on seed and root colonization and their correlation with the suppression of *Rhizoctonia* root rot of soybean. *BioControl*, *45*, 223–243. <https://doi.org/10.1023/a:1009998304177>

Zhou, M. X. (2009). *Barley Production and Consumption* (pp. 1–17). https://doi.org/10.1007/978-3-642-01279-2_1

Zhou, Q., Gao, J., Li, Y., Zhu, S., He, L., Nie, W., & Zhang, R. (2017). Bioleaching in batch tests for improving sludge dewaterability and metal removal using *Acidithiobacillus ferrooxidans* and *Acidithiobacillus thiooxidans* after cold acclimation. *Water Science and Technology*, *76*(6), 1347–1359. <https://doi.org/10.2166/wst.2017.244>

Zhu, Li, M., & Whelan, M. (2018). Phosphorus activators contribute to legacy phosphorus availability in agricultural soils: A review. *Science of the Total Environment*, *612*, 522–537. <https://doi.org/10.1016/j.scitotenv.2017.08.095>

Zou, C., Li, Z., & Yu, D. (2010). *Bacillus megaterium* strain XTBG34 promotes plant growth by producing 2-pentylfuran. *The Journal of Microbiology*, *48*(4), 460–466. <https://doi.org/10.1007/s12275-010-0068-z>

Zúñiga-Silgado, D., Rivera-Leyva, J. C., Coleman, J. J., Sánchez-Reyez, A., Valencia-Díaz, S., Serrano, M., De-Bashan, L. E., & Folch-Mallol, J. L. (2020). Soil Type Affects Organic Acid Production and Phosphorus Solubilization Efficiency Mediated by Several Native Fungal Strains from Mexico. *Microorganisms*, *8*(9), 1337. <https://doi.org/10.3390/microorganisms8091337>

APPENDIX



I. Abbreviations

| | |
|--|--|
| °C: Centigrade degrees | P ₀ : Total soluble phosphorus |
| Abs: Spectrophotometer absorbance | PCR: Polymerase Chain Reaction |
| ACN: Acetonitrile | PGPR: Plant Growth Promoting Rhizobacteria |
| AMBI: Ammonium Bicarbonate | pI: Isoelectric point |
| APS: Ammonium Persulphate | pK _a : acid dissociation constant |
| bp: Base pair | PR: Phosphate Rock |
| cfu: Colony-Forming Unit | PSB: Phosphate Solubilizer Bacteria |
| COG: Cluster of Orthologous Groups | PSM: Phosphate Solubilizer Microorganisms |
| Da, kDa: dalton, kilodalton | qPCR: Quantitative Polymerase Chain Reaction |
| DIGE: Differential in Gel Electrophoresis | RISCs: Reduced Inorganic Sulphur Compounds |
| dH ₂ O: Deionized water | RT: Room Temperature |
| ddH ₂ O: Double-deionized water (ultrapure) | RT-PCR: Reverse Transcription Polymerase Chain Reaction |
| DTT: Dithiothreitol | S: Sulphur |
| FAO: Food and Agriculture Organization of the United Nations | SD: Standard Deviation |
| g, mg, µg: Grams, milligrams, micrograms. | SDS: Sodium Dodecyl Sulphate |
| h, min, seg: Hours, minutes, seconds | SDS-PAGE: Sodium Dodecyl Sulphate Polyacrylamide Gel Electrophoresis |
| HPLC: High Performance Liquid Chromatography | SI: Solubilization Index |
| IAA: Indole-3 acetic acid | SOB: Sulphur-Oxidize Bacteria |
| IAM: Iodoacetamide | TCP: Tricalcium Phosphate |
| IEF: First-dimension isoelectric focusing | TFA: Trifluoroacetic Acid |
| L, mL, µ: liter, milliliter, microliter | Trp: Tryptophan |
| M, mM, µM, nM: molar, millimolar, micromolar, nanomolar | Vh: Volts/hour |
| N: Normal | v/v: Volume/volume |
| nt: Nucleotides | w/v: Weight/volume |
| OD: Optical Density | w/w: Weight/weight |
| O/N: Over Night | |
| ORF: Open Reading Frame | |
| P: Phosphorus | |

II. Culture media

* Every media was autoclaved at 121°C for 20 min unless otherwise is indicated.

9K-Fe

Solution A

Composition per 500 mL (2X) (Bhatti & Yawar, 2010):

| | |
|---|--------|
| (NH ₄) ₂ SO ₄ | 3.00 g |
| MgSO ₄ · 7 H ₂ O | 0.50 g |
| KCl | 0.10 g |
| K ₂ HPO ₄ | 0.50 g |
| Ca(NO ₃) ₂ | 0.01 g |
| pH 2.0 ± 0.2 at 25°C | |

Solution B

Composition per 500 mL (2X):

| | |
|--|---------|
| FeSO ₄ · 7 H ₂ O | 44.30 g |
| pH 2.0 ± 0.2 at 25°C | |

* Sterilize solution A and filter solution B through a 0.45 µm membrane and mix 1:1 (v/v) both solutions prior to use.

9K-Na₂S₂O₃

Solution A

Composition per 500 mL (2X) (based on 9K-Fe from Bhatti & Yawar, 2010):

| | |
|---|--------|
| (NH ₄) ₂ SO ₄ | 3.00 g |
| MgSO ₄ · 7 H ₂ O | 0.50 g |
| KCl | 0.10 g |
| K ₂ HPO ₄ | 0.50 g |
| Ca(NO ₃) ₂ | 0.01 g |
| pH 4.0 ± 0.2 at 25°C | |

Solution B

Composition per 500 mL (2X):

| | |
|--|---------|
| Na ₂ S ₂ O ₃ · 5 H ₂ O | 10.00 g |
| pH 4.0 ± 0.2 at 25°C | |

* Sterilize solution A and filter solution B through a 0.45 µm membrane and mix 1:1 (v/v) both solutions prior to use.

Aleksandrov medium

Composition per litter (Etesami *et al.*, 2017):

| | |
|---|---------|
| Glucose | 5.00 g |
| MgSO ₄ · 7 H ₂ O | 0.50 g |
| CaCO ₃ | 0.10 g |
| FeCl ₃ | 0.006 g |
| Ca ₃ (PO ₄) ₂ | 2.00 g |
| Potassium feldespate | 3.00 g |

pH 7.2 ± 0.2 at 25°C

AT: *Acidithiobacillus* medium (DSMZ 35)

Composition per litter:

| | |
|--|--------|
| NH ₄ Cl | 0.10 g |
| KH ₂ PO ₄ | 3.00 g |
| MgCl ₂ · 6 H ₂ O | 0.10 g |
| CaCl ₂ · 2 H ₂ O | 0.14 g |

pH 4.2 ± 0.2 at 25°C

| | |
|---------------|--------|
| Sulphur | 10.0 g |
|---------------|--------|

* Sterilize the medium by autoclave at 121°C for 20 min. For sulphur sterilization, place the sulphur in screw-capped tubes or bottles, wet with a few drops of water and heat for 3 hours to 90 - 100°C in a water bath on each of three successive days. Add sulphur prior to use.

ATCC 172

The N-Z amine type A from the original media was replace for tryptone. **Composition** per litter:

| | |
|-------------------------|--------|
| Glucose | 10.0 g |
| Soluble starch | 20.0 g |
| Yeast extract | 5.0 g |
| Tryptone | 5.0 g |
| CaCO ₃ | 1.0 g |
| Agar | 15.0 g |

pH 4.5 ± 0.2 at 25°C

ATT: *Acidithiobacillus thiooxidans* medium (DSMZ 71)**Composition** per liter:

| | |
|--|--------|
| KH ₂ PO ₄ | 3.00 g |
| MgSO ₄ · 7 H ₂ O | 0.50 g |
| (NH ₄) ₂ SO ₄ | 3.00 g |
| CaCl ₂ · 2 H ₂ O | 0.25 g |
| Na ₂ S ₂ O ₃ · 5 H ₂ O | 5.00 g |

pH 4.5 ± 0.2 at 25°C

ISP1 (Tryptone - yeast Extract Broth)Commonly known as ISP1 from the international *Streptomyces* Project, based on Shirling and Gottlieb (1966). **Composition** per liter:

| | |
|---------------------------------|-------|
| Casein enzymic hydrolysate..... | 5.0 g |
| Yeast extract | 3.0 g |
| Agar | 20 g |

pH 7.2 ± 0.2 at 25°C

ISP2 (Yeast extract – malt extract agar)Commonly known as ISP2 from the international *Streptomyces* Project, based on Shirling and Gottlieb (1966). **Composition** per liter:

| | |
|---------------------|--------|
| Yeast extract | 4.0 g |
| Malt extract | 10.0 g |
| Dextrose | 4.0 g |
| Agar | 20 g |

pH 7.2 ± 0.2 at 25°C

IPS3 (Oatmeal agar)Commonly known as ISP3 from the international *Streptomyces* Project, based on Shirling and Gottlieb (1966). **Composition** per liter:

| | |
|----------------------------------|--------|
| Oatmeal (Quaker White Oats)..... | 20.0 g |
| Agar | 18 g |

pH 7.2 ± 0.2 at 25°C

ISP trace salt solution (see below).....1 mL

ISP4 (Inorganic salts-starch agar)

Commonly known as ISP4 from the international *Streptomyces* Project, based on Shirling and Gottlieb (1966). **Composition** per liter:

| | |
|---|--------|
| Soluble starch | 10.0 g |
| K ₂ HPO ₄ | 1.0 g |
| MgSO ₄ · 7 H ₂ O | 1.0 g |
| NaCl | 1.0 g |
| (NH ₄) ₂ SO ₄ | 2.0 g |
| CaCO ₃ | 2.0 g |
| Agar | 20 g |

pH 7.2 ± 0.2 at 25°C

ISP trace salt solution (see below).....1 mL

ISP5 (Glycerol – asparagine agar)

Commonly known as ISP5 from the international *Streptomyces* Project, based on Shirling and Gottlieb (1966). **Composition** per liter:

| | |
|---------------------------------------|--------|
| L-asparagine (anhydrous basis) | 1.0 g |
| Glycerol..... | 10.0 g |
| K ₂ HPO ₄ | 1.0 g |
| Agar | 20 g |

pH 7.2 ± 0.2 at 25°C

ISP trace salt solution (see below).....1 mL

ISP6 (Peptone – iron agar)

Commonly known as ISP6 from the international *Streptomyces* Project, based on Shirling and Gottlieb (1966). **Composition** per liter:

| | |
|---|---------|
| Peptone | 15.00 g |
| Proteose peptone | 5.00 g |
| Ferric Ammonium Citrate | 0.50 g |
| K ₂ HPO ₄ | 1.00 g |
| Na ₂ S ₂ O ₃ | 0.08 g |
| Yeast extract | 1.00 g |
| Agar | 20 g |

pH 6.7 ± 0.2 at 25°C

ISP7 (Tyrosine agar)

Commonly known as ISP7 from the international *Streptomyces* Project, based on Shirling and Gottlieb (1966). **Composition** per liter:

| | |
|--|---------|
| L-asparagine | 1.00 g |
| L-tyrosine | 0.50 g |
| Glycerol..... | 15.00 g |
| K ₂ HPO ₄ | 0.50 g |
| MgSO ₄ · 7 H ₂ O | 0.50 g |
| NaCl | 0.50 g |
| FeSO ₄ · 7 H ₂ O | 0.01 g |
| Agar | 20 g |

pH 7.2 ± 0.2 at 25°C

ISP trace salt solution (see below).....1 mL

ISP Trace salt solution

Composition per liter:

| | |
|--|-------|
| FeSO ₄ · 7 H ₂ O | 0.1 g |
| MnCl ₂ · 4 H ₂ O | 0.1 g |
| ZnSO ₄ · 7 H ₂ O | 0.1 g |

NB (Nutrient Broth)

This medium is commonly available as a premixed powder. **Composition** per liter (Atlas, 2010):

| | |
|---------------------|-------|
| Peptone | 5.0 g |
| NaCl | 5.0 g |
| Yeast extract | 2.0 g |
| Beef extract | 1.0 g |

pH 7.4 ± 0.2 at 25°C

NBRIP (National Botanical Research Institute's Phosphate)

Composition per liter (Mardad *et al.*, 2013):

| | |
|---|---------|
| Glucose | 10.00 g |
| MgCl ₂ · 6 H ₂ O | 5.00 g |
| MgSO ₄ · 7 H ₂ O..... | 0.25 g |
| KCl..... | 0.20 g |
| (NH ₄) ₂ SO ₄ | 0.10 g |
| Ca ₃ (PO ₄) ₂ | 5.00 g |
| Agar | 20 g |

pH 7.0 ± 0.2 at 25°C

NYG (peptone yeast extract glycerol medium)

Composition per liter (Tang *et al.*, 2005):

| | |
|---------------------|--------|
| Peptone | 5.0 g |
| Yeast extract | 3.0 g |
| Glycerol..... | 20.0 g |
| Agar | 20 g |

pH 7.0 ± 0.2 at 25°C

LB (Luria-Bertani broth)

Composition per liter (Atlas, 2010):

| | |
|-----------------------------------|--------|
| NaCl | 10.0 g |
| Yeast extract | 5.0 g |
| Pancreatic digest of casein | 10.0 g |

pH 7.0 ± 0.2 at 25°C

Leptospirillum (HH) (DSMZ 882)

Solution A

| | |
|---|----------|
| (NH ₄) ₂ SO ₄ | 132.0 mg |
| MgCl ₂ · 6 H ₂ O | 53.0 mg |
| KH ₂ PO ₄ | 27.0 mg |
| CaCl ₂ · 2 H ₂ O | 147.0 mg |
| ddH ₂ O | 950 mL |

pH 1.8 (use 10N H₂SO₄)

Solution B

| | |
|--|--------|
| FeSO ₄ · 7 H ₂ O | 20.0 g |
| 0.25 N H ₂ SO ₄ | 50 mL |

pH 1.2 ± 0.2 at 25°C

Solution C (Trace elements solution)

Composition per litter:

| | |
|--|---------|
| MnCl ₂ · 4 H ₂ O | 76.0 mg |
| ZnCl ₂ | 68.0 mg |
| CoCl ₂ · 6 H ₂ O | 64.0 mg |
| H ₃ BO ₃ | 31.0 mg |
| Na ₂ MoO ₄ | 10.0 mg |
| CuCl ₂ · 2 H ₂ O | 67.0 mg |

* Sterilize solutions separately and mix 950 mL of solution A with 50 mL of solution B. Finally, add 1 mL of solution C prior to use. The final pH of the medium should be 1.8.

PDA (Potato Dextrose Agar)

Composition per litter (Atlas, 2010):

| | |
|-------------------------------|--------|
| Glucose | 20.0 g |
| Potatoes, infusion from | 15.0 g |
| Agar | 15 g |

pH 5.6 ± 0.2 at 25°C

This medium is available as a premixed powder from Conda Laboratories.

Plate Count Agar

Composition per litter (Atlas, 2010):

| | |
|-----------------------------------|-------|
| Glucose | 1.0 g |
| Yeast extract | 2.5 g |
| Pancreatic digest of casein | 5.0 g |
| Agar | 15 g |

pH 7.0 ± 0.2 at 25°C

This medium is available as a premixed powder from Pronadinsa S.A.

PSM (Phytase Screening Medium)

Composition per liter (P. Kumar *et al.*, 2012):

| | |
|--|---------|
| D-glucose | 20.00 g |
| Sodium phytate | 4.00 g |
| CaCl ₂ | 2.00 g |
| NH ₄ NO ₃ | 5.00 g |
| KCl..... | 0.50 g |
| MgSO ₄ · 7 H ₂ O..... | 0.50 g |
| FeSO ₄ · 7 H ₂ O | 0.01 g |
| MnSO ₄ · H ₂ O..... | 0.01 g |
| Agar | 20 g |

pH 6.0 ± 0.2 at 25°C

SCA (Starch Casein Agar)

Modified from Atlas *et al.* (2010). Composition per liter:

| | |
|--|--------|
| Starch | 2.00 g |
| Casein | 0.30 g |
| KNO ₃ | 2.00 g |
| NaCl | 2.00 g |
| K ₂ HPO ₄ | 2.00 g |
| MgSO ₄ · 7 H ₂ O..... | 0.05 g |
| CaCO ₃ | 0.02 g |
| FeSO ₄ · 7 H ₂ O | 0.01 g |
| Agar | 20 g |

pH 7.0 ± 0.1 at 25°C

SOC (super optimal broth with catabolite repression)

SOC medium is based on SOB (super optimal broth) and is a rich medium mainly used in the recovery steps of *E. coli* competent cells transformation because it maximizes the transformation efficiency. **Composition** per liter (Sambrook *et al.*, 2001):

| | |
|-------------------------|--------|
| Tryptone | 20.0 g |
| Yeast extract | 5.00 g |
| NaCl..... | 0.58 g |
| KCl | 0.19 g |
| MgCl ₂ | 0.95 g |
| MgSO ₄ | 1.20 g |

pH 7.0 ± 0.1 at 25°C

Add 20 mL of a sterile 1 M solution of glucose (18 g of glucose in 100 mL of ddH₂O) after autoclaving the previous solution and letting it cool to 60°C or less. After the sugar has dissolved, adjust the volume and sterilize by passing it through a 0.22 µm filter.

Thiobacillus agar (TA)

Composition per liter (Starosvetsky *et al.*, 2013):

| | |
|---|--------|
| (NH ₄) ₂ SO ₄ | 0.40 g |
| MgSO ₄ · 7 H ₂ O..... | 0.50 g |
| CaCl ₂ | 0.25 g |
| KH ₂ PO ₄ | 4.00 g |
| FeSO ₄ | 0.01 g |
| Na ₂ S ₂ O ₃ | 5.00 g |
| Bromocresol green 0.4% (w/v) | 2 ml |

pH 4.0 ± 0.2 at 25°C

TSB (Tryptic soy broth)

This medium is commonly available as a premixed powder. **Composition** per liter (Atlas, 2010):

| | |
|-------------------------------------|--------|
| Pancreatic digest of casein | 18.0 g |
| Papaic digest of soybean meal | 6.00 g |
| NaCl | 6.00 g |

pH 7.3 ± 0.2 at 25°C

Tris-minimal medium

Composition per litter (Fasim *et al.*, 2002):

| | |
|--|--------|
| Tris base..... | 6.06 g |
| NaCl | 4.68 g |
| KCl..... | 1.49 g |
| NH ₄ Cl..... | 1.07 g |
| Na ₂ SO ₄ | 0.43 g |
| MgCl ₂ · 2 H ₂ O | 0.20 g |
| CaCl ₂ · 2 H ₂ O | 0.03 g |
| Agar | 15 g |

pH 7.0 ± 0.2 at 25°C

TY (Tryptone-Yeast)

Composition per litter (Sambrook *et al.*, 2001):

| | |
|---------------------|---------|
| Tryptone | 16.00 g |
| Yeast extract | 10.00 g |
| NaCl..... | 2.50 g |

pH 7.0 ± 0.1 at 25°C

YED (Yeast Dextrose Agar)

Composition per litter (Atlas, 2010):

| | |
|---------------------|--------|
| Glucose | 10.0 g |
| Yeast extract | 10.0 g |
| Agar | 20 g |

pH 7.0 ± 0.2 at 25°C

Hanzeplein 1, P.O. Box 30001, HPC EB80

9700 RB Groningen, the Netherlands

University Medical Center Groningen

Department of Medical Microbiology
Molecular Bacteriology

Prof. Dr. J.M. van Dijk

Telephone +31 (0)50-3615187
Telefax +31 (0)50-3619105
E-mail j.m.van.dijk01@umcg.nl

Enclosures

Our ref.

Cc.

Date 30 November 2020

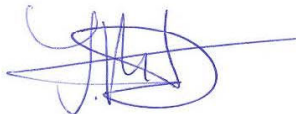
Subject

To whom this may concern,

Herewith, I CERTIFY that Miss Ana María Ibáñez Sanchez (DNI:71171864-C) has completed a pre-doctoral secondment in my laboratory of Molecular Bacteriology at the Dept. of Medical Microbiology of the University Medical Center Groningen from September 1, 2020 to November 30, 2020.

The purpose of her secondment has been to perform research on the expression of a gene cluster from *Bacillus megaterium*, which encodes a lasso peptide with antimicrobial activity, in different chassis strains of *Bacillus* sp. in order to investigate its biological function. It has been a pleasure to host Ms. Ibáñez Sanchez in my laboratory and she has been a credit to her home institute at the Universidad de León in every relevant aspect.

Sincerely,



Jan Maarten van Dijk



External PhD Thesis referee report

Ms. Ana María Ibáñez Sánchez submitted the PhD thesis entitled “Development of microbial technologies for the soluble phosphorus production by phosphate rock solubilization”, developed at the Instituto de Investigación de la Viña y el Vino, under the supervision of Dr. Juan José Rubio Coque and Dr. Carlos Barreiro Méndez, from the University of León. I hereby present my comments on the document.

Phosphorus (P) is the second most limiting nutrient for agricultural crops. Given its reduced bioavailability, the probable mid-term future depletion of the main current phosphorous source (phosphate rock reserves), as well as the difficulties to exploit phosphorous reservoirs in soils, novel solutions must be explored. The PhD work conducted by Ms. Ibáñez Sánchez adds to the field of biomining and biofertilizers based on the use of phosphate solubilizing microorganisms, as promising answers to the phosphate problem.

The structure of the thesis includes a general Introduction, a presentation of the general and specific Objectives of the PhD thesis, three Results chapters (each with their corresponding Material and Methods, Results and Discussion sections), a General Discussion section referring to all the PhD thesis results, further work and Future Perspectives and, finally, the obtained relevant Conclusions.

The manuscript is easy to follow, very well written and well organized. The industrial applicability of the results can be directly inferred from the relevance of the conclusions, as well as the fact that the thesis is linked to a private industrial project with a clear aim. I discuss the different sections in further detail below.

The thesis manuscript presents first an Introduction containing an overview of the problems surrounding the utilization and extraction of phosphorous, as well as its biological implications and the importance of phosphorous for life. I found the Introduction to be well-thought, relevant, thorough, and up to date. Ms. Ibáñez Sánchez demonstrates good knowledge of the state of the art in her field, as well as most recent work and current challenges. As for the Objectives of the PhD thesis, they are well designed and presented. They are also clearly addressed along this thesis.

The first Results chapter (Chapter 1) focuses on the isolation of eight strains of sulphur-oxidizing bacteria to solubilize phosphorous from phosphate rock schlams, as well as the characterization of the ability to solubilize phosphorous of different selected isolated strains. A particular *Acidithiobacillus thiooxidans* strain stood out from the rest when it comes to phosphorous solubilization in mini-dump assays.

The second Results chapter (Chapter 2) revolves around the molecular study of the strain *A. thiooxidans* SOB3. Its genome was sequenced to carry out proteomic studies and evaluate

the strain responses under pH stress conditions. Chapter 2 demonstrates the hardships usually encountered when working with poorly studied, fastidious extremophiles, and presents a good and thorough description of the necessary optimization and troubleshooting. Ms. Ibáñez Sánchez also presents interesting ideas for future work to complement the results obtained during her work.

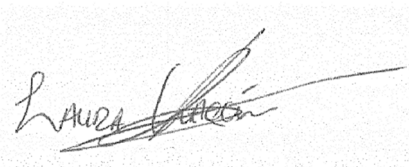
Chapter 3 is entitled “Isolation, identification and selection of phosphate solubilizing bacteria and their application to barley crop”. Along the chapter, Ms. Ibáñez Sánchez describes the isolation of phosphate solubilizing bacteria from the ectorrhizosphere of locally obtained barley plants. Isolates were identified and their phosphate solubilization ability and mechanisms were studied. The results are complemented with a greenhouse pot experiment to check the effects of the isolates on barley crop development.

The thesis work is finalized with a General Discussion, a reflection on Future Perspectives and recommendations for further work and, finally, Conclusions. The General Discussion presents interesting observations that help put the results of the thesis in context and demonstrates the applicability of said results. As for the Future Perspectives and Conclusions sections, I found them to be relevant and clearly presented.

In conclusion, it is my impression that the PhD thesis carried out by Ms. Ibáñez Sánchez and presented in this manuscript includes novel, high quality, interdisciplinary scientific work. The thesis work answers current challenges and scientific questions that are of great importance from a sustainability point of view, and that have inherent value considering possible industrial applications in the fields of biofertilizers and biomining. They also constitute relevant groundwork that will serve as a basis for further knowledge of isolated strains as novel biosolutions to the problem of phosphorous.

I consider the thesis work presented by Ms. Ibáñez Sánchez entirely suitable for public reading and defense, and I strongly recommend its acceptance by the PhD thesis commission.

Trondheim, 5th June 2021



Dr. Laura Garcia Calvo

Postdoctoral Researcher

*Department of Biotechnology and Food Science (IBT),
Norwegian University of Science and Technology (NTNU)*

External PhD thesis referee report

The experimental work described in the PhD dissertation submitted by Ms. Ana María Ibáñez Sánchez with the title “Development of microbial technologies for the soluble phosphorus production by phosphate rock solubilization” was performed at the Instituto de Investigación de la Viña y el Vino under the supervision of Prof. dr. Juan José Rubio Coque who is affiliated at the University of León. The work described in the PhD Thesis of Ms. Ibáñez Sánchez address the current phosphate rock solubilization problems and she proposes two solutions to it.

Her thesis is divided into eight sections as follows: a general introduction, objectives, three experimental chapters, a general discussion, future perspectives and final conclusions. To note, each experimental chapter includes its own independent introduction, material and methods, results and discussion sections. The dissertation is well organized and it is clearly written to be accessible to scientists with different backgrounds. The originality and quality of the research presented in this dissertation contributes positively to deal with topics of global relevance and industrial application. Furthermore, the present dissertation is part of a private project, fact that highlight its immediate industrial application.

In the **Introduction**, Ms. Ibáñez Sánchez gives an overview about the current problems of phosphorus in nature covering its easy precipitation in soils after the fertilization and the imminent depletion of its mining reserves. She also reviews the current measurements and proposes new solutions, such as the use of biomining processes to improve the performance of the current mining wastes. Her literature review shows that she is knowledgeable and highly skillful in her field. The specific **objectives** of the dissertation are well designed and are in line with the main objective. Importantly, the objectives are accomplished throughout the thesis.

The research described in **Chapter 1** focus on the isolation and characterization of the sulphur-oxidizing bacteria for the phosphorus solubilization from phosphate rock. To this end, an assay was designed to determine the solubilization capabilities of bacteria during a biomining process with phosphate rock wastes and sulphur as only energy source. The results allowed to identified one strain that overperformed in terms of solubilization of phosphorus in mini-dumps assays. Remarkably, in Chapter 1, Ms. Ibáñez Sánchez describes the procedure and results of her first scaling-up process in a 25-tonnes dump.

The study in **Chapter 2** described the response of *Acidithiobacillus thiooxidans* under extreme acid conditions by means of genome sequencing, RT-PCR and a proteome analysis by DIGE. The obtained results are especially valuable since *A. thiooxidans* is an extremophiles microorganism which is complicated to handle and few information is available. Thus, the results obtained by Ms. Ibáñez Sánchez are an appreciable contribution to the scientific community.

Chapter 3 describes the isolation and characterization of phosphate solubilizing bacteria with potential use as biofertilizers. In addition, some studies and bioassays have allowed to analyze some of their characteristics as plant growth-promoting bacteria. Chapter 3 also describes the antifungal capacity of some of these strains against a selection of the most important pathogenic barley fungi. Notably, her assay performed on barley crops made possible to observe the effects of these isolates on the plants, and the effect of solubilization of insoluble phosphorus in the crops.

The experimental work described in the PhD dissertation of Ms. Ibáñez Sánchez involves a set of different technics. Her approach, includes microbiological assays, bioassays, development of new protocols for biomining assay at laboratory scale, genome analysis, proteomic studies, determination of organic acids by HPLC, q-PCR and RT-PCR assays and statistical analysis just to mention some of them. The diversity in her approach allowed her to get answer from different perspectives to have a complete study.

In conclusion, considering the quality of research described in Ms. Ibáñez Sánchez's dissertation and the demonstrated potential application of her studies, I would like to recommend to the PhD commission Ms. Ibáñez Sánchez's thesis to accept her thesis for defense for obtaining her PhD degree. I am confident that she will excel in her PhD defense.

Dr. Rocío Aguilar Suárez

Postdoctoral Researcher
FGen, Basel, Switzerland, 5th June 2021

A handwritten signature in black ink, appearing to read 'R. Aguilar', enclosed within a circular scribble.

“There will come a time when you believe everything is finished. That will be the beginning”

“Llegará un momento en que creas que todo ha terminado. Ese será el principio”

Epicuro de Samos (341 a.C. - 270 a.C.)